ASSESSING REGIONAL HYDRO-CLIMATE IMPACTS USING HIGH RESOLUTION CLIMATE MODELLING: A STUDY OVER VIETNAM

VU MINH TUE

NATIONAL UNIVERSITY OF SINGAPORE

2012

ASSESSING REGIONAL HYDRO-CLIMATE IMPACTS USING HIGH RESOLUTION CLIMATE MODELLING: A STUDY OVER VIETNAM

VU MINH TUE

(M.Sc., Nanyang Technological University, Singapore)

A THESIS SUBMITTED

FOR THE DEGREE OF DOCTOR OF PHILOSOPHY

DEPARTMENT OF CIVIL AND ENVIRONMENTAL ENGINEERING

NATIONAL UNIVERSITY OF SINGAPORE

2012

DECLARATION

I hereby declare that this thesis is my original work and it has been written by me in its entirety. I have duly acknowledged all the sources of information which have been used in the thesis.

This thesis has also not been submitted for any degree in any university previously.

VU MINH TUE

(15 September 2012)

ACKNOWLEDGEMENTS

Although the list of the individuals I wish to thank extends beyond the limits of this page, I would like to sincerely thank some of them here for their help and support in manifold ways.

First and foremost, I would like to express my wholehearted thanks to my supervisor, Assoc. Prof. Dr. Liong Shie-Yui, for his wisdom, knowledge and enthusiasm in guiding me throughout this research study. Without him, I would definitely be lost groping for the research direction. He is not only a great supervisor, but a great mentor who has directed me in numerous ways, both academically and professionally.

I am grateful to Dr.Vijayaraghavan Srivatsan, a strict vegetarian and a bosom friend, for introducing the climate science and modelling. With his devoted spirit, his inspiration and his great efforts to explain things clearly and simply, he helped in bringing climate science closer to me. I wish to thank my good friends and colleagues, Dr. Nguyen Ngoc Son for initializing model runs and assisting with linux operations, Ms. Liew San Chuin and Mr. Ethan Nguyen Duc Trung, also colleagues at TMSI, for their support and help. I extend my thanks to intern students Liew Mengjie, Phey Giap Seng and Chong Wee Pin for their kind support.

Let me also accord my thanks to the Tropical Marine Science Institute for this research opportunity that has made this PhD, a reality. I also thank the National University of Singapore, Dept. of Civil and Environmental Engineering, for the scholarship that made this PhD possible. I also thank the Tianjin Supercomputer Center, Tianjin, China, that enabled me to run high resolution climate simulations on Tianhe-1A, one of the fastest supercomputers in the world and for their technical support. I thank the Center for Hazards Research, Dept. of Civil and Environmental Engineering at NUS and the Center for Environmental Sensing and Modeling, Singapore-MIT Alliance for Research and Technology, for their support in providing computational resources. Lastly and most importantly, I owe a special gratitude to my parents for their continuous and strong support. To them, I dedicate this thesis proposal.

TABLE OF CONTENTS

SUMMARY

The Intergovernmental Panel on Climate Change (IPCC) estimates that global surface temperatures may rise to about 1-2 °C by the year 2050 and to about 2-5 °C by the end of the 21st century, depending on how much of the anthropogenic Green House Gases (GHG) will be emitted to the atmosphere in the coming decades. Latest findings from the IPCC show many evidences that climate change has already affected many sectors in Southeast Asia, one of the highly climate vulnerable regions in the world. It is high time that more research into climate science is necessary as far as Southeast Asia is concerned, not just in understanding the climate and its change but also be able to understand the climate impacts and its severity so that all countries in Southeast Asia can prepare themselves adequately to adapt to such changes. In such a perspective of Southeast Asian climate change, this thesis focused on Vietnam as the main study region.

A systematic ensemble high resolution climate modelling study over Vietnam has been performed. Applying two widely used regional climate models, WRF and PRECIS, future climate change over the period 2071-2100 has been ascertained with respect to the present day baseline conditions over the period 1961-1990. The results indicate that the surface temperature over Vietnam could increase up to 4 °C by the end of the century, while rainfall shows primarily increases of more than 20 % in many regions suggesting wetter and possibly flooding conditions, and slight decrease in some regions suggesting drier and drought conditions. A hydrological impact study using the results of the climate models was also done over a catchment in central Vietnam to assess future stream flow conditions. The results largely indicate that the peak and the post-peak rainfall seasons could experience a strong increase in stream flow, suggesting risks of flooding. All these results have implications for water resources, agriculture, bio diversity and economy and serve as some useful findings for the policy makers. This study, by itself, is one of the first of its kind studies done over Vietnam.

ACRONYMS AND ABBREVIATIONS

ADB	Asian Development Bank
AOGCM	Atmospheric Ocean General Circulation Model
APHRODITE	Asian Precipitation Highly Resolved Observation Data Integration Towards the Evaluation of water resources
AR4	Fourth Assessment Report
CCSM	Community Climate System Model
CFC	Chloro Fluoro Carbon
CPC	Climate Prediction Center
CRU	Climatic Research Unit
CSIRO	Commonwealth Scientific and Industrial Research Organization
ECHAM	European Centre HAMburg Model
ECMWF	European Centre for Medium range Weather Forecasts
EEPSEA	Economic and Environment Program for SouthEast Asia
ERA40	European ReAnalysis 40 years
GHCN	Global Historical Climatology Network
GHG	GreenHouse Gases
GISS	Goddard Institute for Space Studies
HRU	Hydrological Response Unit
IMHEN	Institute of Meteorology, Hydrology and ENvironment
IPCC	Intergovernmental Panel on Climate Change
LMB	Lower Mekong Basin
MM5	Mesoscale Model version 5
MMD	Multi-Model Dataset
MPI	Max Planck Institute
NASA	National Aeronautics and Space Administration
NCAR	National Center for Atmospheric Research
NCEP	National Centers for Environment Prediction
NOAA	National Oceanic and Atmospheric Administration
NWP	Numerical Weather Prediction
PCM	Parallel Climate Model
PRECIS	Providing REgional Climate for Impact Studies
PRUDENCE	Prediction of Regional scenarios and Uncertainty for Defining EuropeaN Climate change risk and Effects
SWAT	Soil and Water Assessment Tool
TAR	Third Assessment Report
UDEL	University of DELaware
UKMO	United Kingdom Meteorology Office
USDA	United State Department of Agriculture
USGS	United States Geological Survey
WCRP	World Climate Research Program
WMO	World Meteorological Organization
WRF	Weather Research and Forecasting

LIST OF TABLES

LIST OF FIGURES

CHAPTER 1 INTRODUCTION

1.1 THE CLIMATE CHANGE ISSUE

Climate Change is real. It is happening at an alarming rate that it has already become a hot topic of discussion in our daily life. There is a strong scientific consensus that the rapid rise in anthropogenic (human induced) greenhouse gas (GHG) emissions over the past two centuries has been a major contributor to the global warming that we experience now. The Intergovernmental Panel on Climate Change (IPCC) estimates that global surface temperatures may rise to about 1-2 °C by the year 2050 and to about 2-5 °C by the end of the 21st century, depending on how much of the anthropogenic GHG will be emitted to the atmosphere in the coming decades (IPCC, 2007a). Whilst there is much uncertainty on these GHG emissions, the issue right now is, even if the future warming is limited to about 2°C, the natural and human systems are still likely to experience significant impacts (United Nations Framework Convention on Climate Change, UNFCCC, 2010). The nature and the intensity of such climate change impacts are expected to be mostly negative and the developing countries are likely to suffer greater impacts than the developed ones, due to lack of adequate adaptive measures. The National Aeronautics and Space Administration (NASA), has released evidences of recent climate change, mainly coming from available three major global surface temperature reconstructions (tree rings, ice cores and coral records). These show that the Earth has warmed up since 1880 and most of this warming has occurred since the 1970s, with 20 warmest years having occurred since 1981 and all 10 of the warmest years occurring in the past 12 years. The mean global sea level has risen by 17cm (6.7 inches) over the last century and the oceans have taken in much of the increased warming, with the top 700 meters showing a warming of about 0.302 °F. Shrinking ice sheets over Arctic and Antarctic regions, glacial retreats, varied rainfall changes and increases in specific humidity in the atmosphere have also been reported that add to the evidences of changing climate (http://climate.nasa.gov/evidence/). Most of the current research studies suggest that the impact of a global temperature rise of 1-2 °C is unlikely to be equal everywhere on earth. Such changes are expected to be non-linear that a

temperature increase of 2-3 °C may have a greater impact than the 1-2 °C increase. There are also likely to be certain thresholds and critical points beyond which changes either to the extent of a collapse of an eco-system or changes in ocean circulation patterns could be seen. Other existing or emerging environmental problems such as land degradation, threat to hydrological systems and pollution may also likely to be amplified due to climate change impacts (Dawson and Spannagle, 2009). The climate sensitivity, which is the equilibrium global surface temperature change that would result due to a doubling $CO_{2,}$ is likely to be between 1.5 °C to 11 °C, but its exact value is still unknown (Stainforth, 2005). In its Fourth Assessment Report (AR4), the IPCC has mentioned that this climate sensitivity is likely to be between 1 to 6 °C with a most likely value of 3 °C by the end of the century. This climate sensitivity parameter is not only related to the concentrations of CO_2 in the atmosphere but also to other GHG quantities, but also related to CO_2e (known as carbon-dioxide equivalent) which accounts for all other anthropogenic GHG emissions such as methane, nitrous oxide, sulphur dioxides and chloro-fluoro carbons. It has been noted by the National Oceanic and Atmospheric Administration (NOAA), that, as of August 2012, the global atmospheric CO_2 concentrations have risen to nearly 392.41 ppmv (parts per million volume) and CO_2e have risen to levels of nearly 500 ppmv. These CO_2e concentrations are also rising rapidly and this is likely to bring forward the date of concentrations reaching double the values of pre-industrial levels (280 ppmv). Given these substantial uncertainties associated with CO_2 and CO_2e concentrations, arriving at a specific figure for the climate sensitivity has become impossible at this stage.

It has also been established that the relationship between CO_2 concentrations versus surface temperature is non-linear (Figure 1-1). Since the CO_2 residual time is longer (50-100 years) in the atmosphere, the surface temperature is also likely to increase non-linearly. Due to this warming, the global sea-level rise is also expected to continue with concomitant thermal expansion of oceans. It is for this reason the concentrations of GHGs and their stabilization in the atmosphere need to be acted upon immediately. The IPCC mentions that if no major

actions are taken, the GHG concentrations could double pre-industrial levels as early as 2040 and levels of up to 1000 ppmv could be seen by 2100 (IPCC, 2007a).

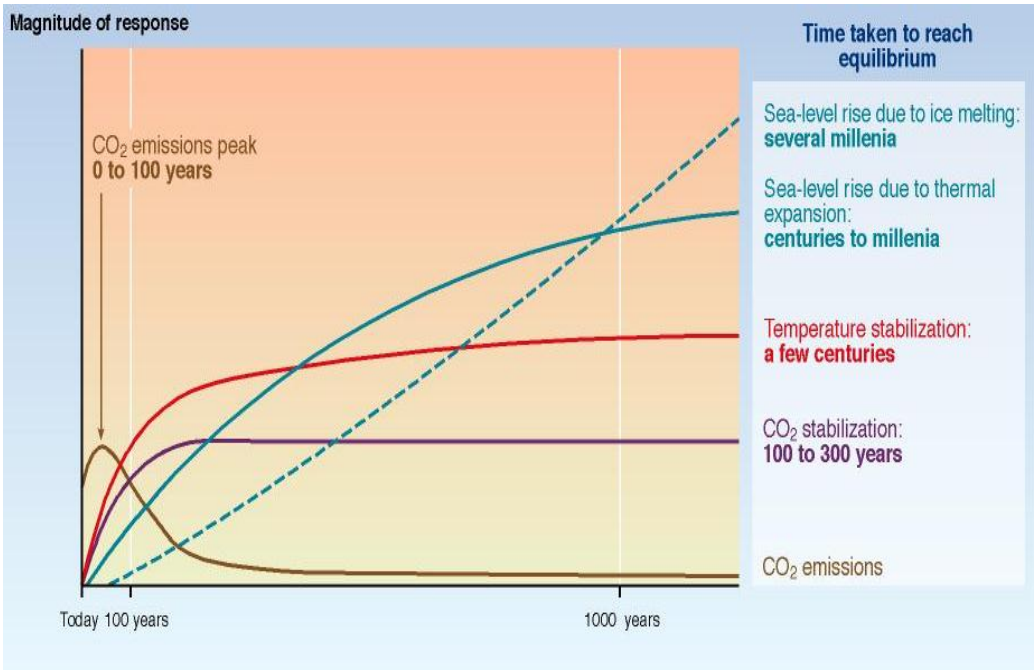

Figure 1-1: Relationship between CO_2 concentrations vs Temperature increase
[Adapted from the IPCC, 2007]

Since the degree of climate sensitivity has a direct impact on the costs associated with stabilization of GHG concentrations, the international community is struggling to devise suitable mitigation measures. Therefore, reducing emissions and striving for early stabilization becomes a priority. The mitigation costs in combating climate change and its impacts are something many goverments are finding difficult to cope up with. Hence, the economically weaker nations are more burdened and their resilience to act against climate change impacts reduces. This burden is augmented when some geographical locations such as regions of Africa and Southeast Asia remain naturally vulnerable to climate change. Some existing impacts related to hydrological changes to natural water systems, health, agriculture, landslides, floods, drought and extreme events such as tropical cyclones may see aggravation with changing climate and advanced adaptation and mitigation strategies need to be developed for these regions with support from developed nations and other international community. The

latest findings from the Goddard Institute of Space Studies (GISS) in the USA also suggest that the temperature anomaly (long term change in normal values) has risen more than 0.6 °C higher than long term records since 1880 (Figure 1-2).

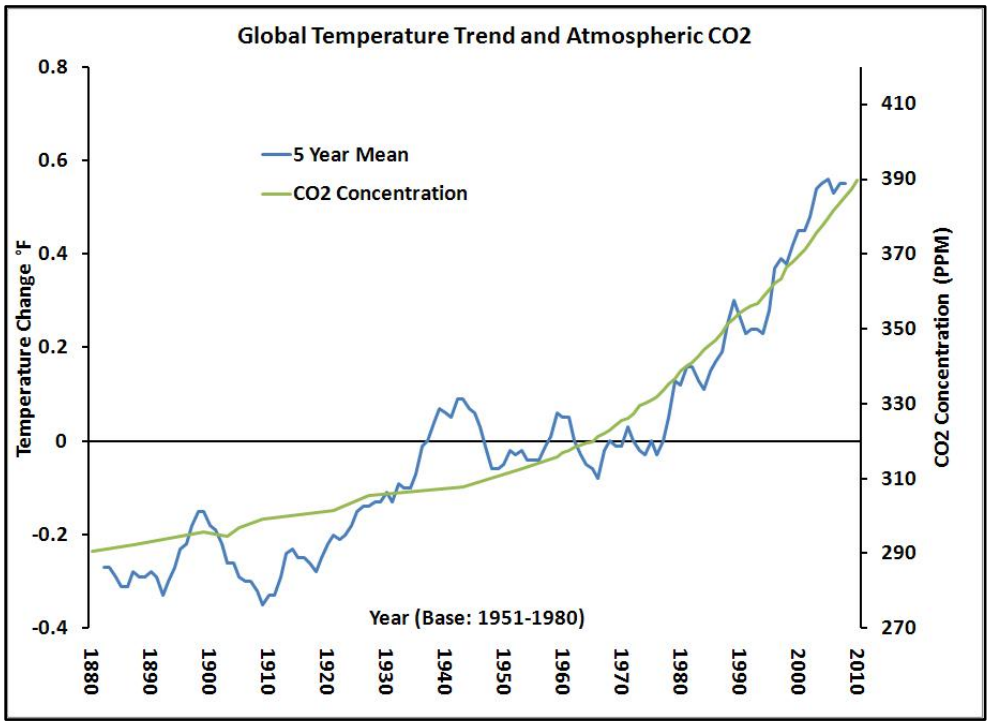

Figure 1-2: Temperature anomaly since 1880
[Adapted from http://www.c2es.org/facts-figures/trends/co2-temp]

These evidences of temperature increases have also come from direct measurements of rising surface air temperatures and subsurface ocean temperatures and from phenomena such as increases in average global sea levels, retreating glaciers and changes to many other physical and biological systems. Therefore, it is obvious that we, as humans, need to act against this anthropogenic climate change. Although our scientific knowledge in the observation of climate change has increased, there is still much uncertainty in understanding the different physical processes that are involved in the climate system.

Figure 1-3 shows the different elements of natural and anthropogenic radiative forcings that contribute to climate change. The graph also highlights that the net radiative forcing is largely positive, primarily due to CO_2. The last column highlights the level of scientific understanding (LOSU) we have with these different radiative forcing terms, especially anthropogenic. This

remains a fundamental challenge to the scientific community to model and predict climate change with lesser uncertainties. But, at the outset, how do we predict climate?

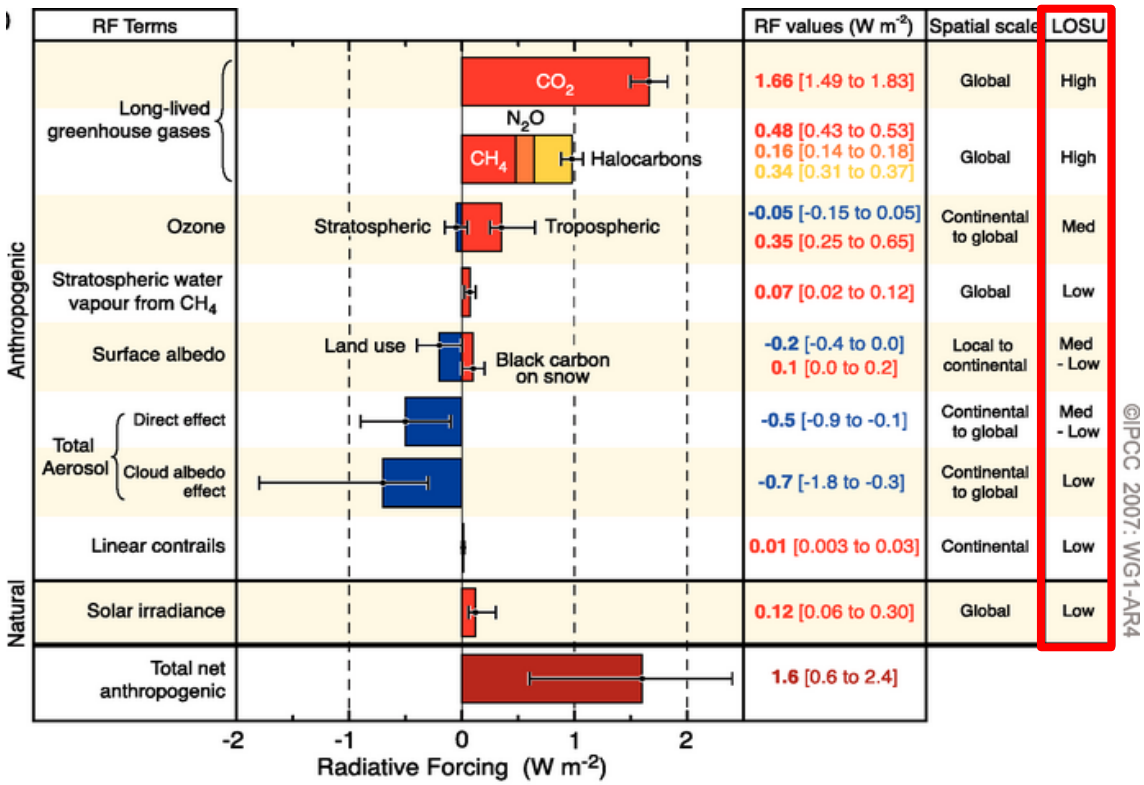

Figure 1-3: Radiative forcings and Level of scientific understanding
[Adapted from IPCC, 2007]

1.2 PREDICTION OF CLIMATE

In the process of climate prediction there are several stages of uncertainties and addressing these uncertainties in impact studies presents difficulties because only a small subset of the potential pathways through these stages would have been explicitly modelled (Mearns et al., 2001). These several stages in climate prediction have been referred to as 'a cascade of uncertainties' that is shown in Figure 1-4. Along with the uncertainties involved in the different plausible emission scenarios for the future, the carbon and vegetation cycles, the socio-economic changes and the atmospheric CO_2 concentrations, the main sources of uncertainties come from the climate models, especially the Global Climate Models (also called General Circulation Models, in short and hereafter in this thesis, referred to as **'GCMs'**).

These are physical numerical models that incorporate and represent a 'mini-earth' that simulate the earth's climate.

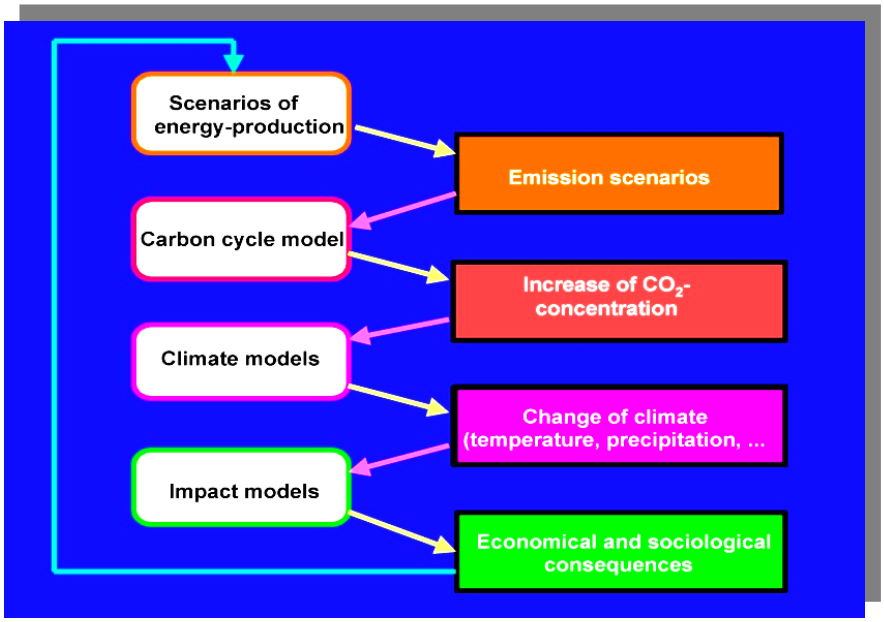

Figure 1-4: A 'cascade of uncertainties' in the process of climate prediction
[Adapted from Mearns et al., 2001]

These GCMs are generally categorized into coupled Atmosphere-Ocean General Circulation Models (AOGCMs), which resolve both the atmosphere and ocean components of the earth and Atmospheric General Circulation Models (AGCMs), which consist only of the atmospheric component. These GCMs are the common and primary modelling tools used for climate simulations and are run at typical horizontal spatial resolutions of about 150-400 km i.e., about 1.5° - 4° on a latitude/longitude grid. The range of the spatial resolutions of the AOGCMs that were used in the Multi Model Dataset (MMD) of the IPCC varies from 1° to 5° (IPCC, 2007a). This MMD is a set of IPCC coordinated GCM simulations of future climate projections described by Meehl et al. (2007), used for the Fourth Assessment Report of the IPCC. A list of these GCMs is shown in Appendix A.

Several research studies have mentioned that although GCMs represent the main features of the global atmospheric circulation reasonably well, their performance in reproducing regional climatic details is rather poor, due to their coarse spatial resolutions. Over the past few years, the numerical simulations have grown to greater heights – thanks to the advent of improved

technology and availability of super computers. This has fundamentally made possible, simulating global climate at far higher resolutions (between ~20 km to 100 km). Since the GCMs still remain as primary tools in understanding climate and climate change at a global scale, improvements in GCM modelling are still being pursued by the climate research community. However, some of the regional and local scale climate forcings due to land use characteristics, complex topography, land-ocean contrasts, aerosols, radiatively active gases, snow, sea ice and ocean currents are not resolved well by GCMs. Hence, it has been strongly realized that to study sub-global scales, i.e., continental, regional or sub-regional scales, the GCMs do not provide detailed information of climate as it is observed in reality, largely attributable to the coarse resolution of the GCMs, that makes them unsuitable for regional impact studies. This is important because the regional and sub-regional climates are often affected by forcings and circulations such as cyclones, mesoscale convective systems and land/sea breezes that occur at a sub-grid scale of the GCM. The need for regional scale information is also emphasized by the fact that GCM climate projections do not allow regional examinations such as water balances or trends of extreme precipitation due to their coarse grid resolution. This clearly applies to impact studies, say, in the case of studying the hydrological impacts over a river basin, as most of the river basins of the world are smaller than the typical resolutions (~300 km) of the GCM and such hydrological models need to be driven by high resolution data for better assessments of regional scale impacts. The GCMs do not simulate precipitation, one of the most important and sensitive climate parameter highly variable in space and time, with adequate fine scale details to be applied for regional scale impact studies. Hence, when impact studies are done, like those of hydrology, regional scale impact studies warrant high resolution climate information. It is therefore obvious that the GCMs cannot explicitly capture the fine scale structure that characterizes climate variables in many regions of the world that is required to run impact models. Therefore, before the GCM derived outputs such as precipitation and temperature can be used to drive the impact models at a regional or a local scale, there is an intermediate step which requires a 'downscaling' of this large scale GCM information to regional scales.

1.3 CLIMATE DOWNSCALING

The IPCC defines a 'regional scale' between 10^4 to 10^7 km^2 and a 'local scale' less than 10^4 km^2. The concept of downscaling implies there is an 'added value' expected when downscaling such large scale information to a regional or a local scale (IPCC, 2001). Some of the areas where this technique can enhance large scale information are: simulation of the spatial structure of temperature and precipitation in complex topography, land use distribution, regional and local atmospheric circulations that include jet cores, mesoscale convective systems, sea and land breeze effects and tropical storms (Giorgi, 1990). Some processes at high temporal frequencies include precipitation frequencies, surface wind variability, monsoon front onset and withdrawal and occurrences of extreme weather events (IPCC, 2001).

There are two fundamental approaches that exist for downscaling of large scale information to a regional or a local scale. The first is a statistical method, called 'Statistical Downscaling', which establishes empirical relationships between large scale climate variables and local climate and the other is a method where a higher resolution climate model, widely known as a Regional Climate Model, hereafter referred to in this thesis as **'RCM'**, is driven using the GCM output. This technique is called as the 'Dynamical Downscaling' or commonly, regional climate modelling.

The main assumptions for the statistical downscaling are that: (i) high quality large scale and local data will be available for a sufficiently long period to establish robust relationships of the current climate and (ii) relationships which are derived from recent climate will be relevant in a future climate. Many papers have dealt with statistical downscaling concepts, their prospects and their limitations (Von Storch (1995); Hewitson and Crane (1996), Wilby and Wigley (1997); Zorita and von Storch (1997); Gyalistras et al., (1994); Murphy (1999, 2000); Widmann and Bretherton, 2000). The advantages of using this technique are that they are computationally inexpensive and can easily be applied to analyze the output data from different GCM experiments. The applications of this downscaling technique vary widely with respect to regions, spatial and temporal scales, type of predictors (those climate variables

which are used to predict) and predictands (those climate variables which are predicted) and their climate statistics (Jones et al., 2004). However, the major theoretical weakness of the statistical downscaling methods is their basic assumption that the statistical relationships developed for present day climate also hold good under the different forcing conditions of possible future climates, is not verifiable (IPCC, 2001). In addition, data with which to develop the empirical relationships are not readily available in remote regions or regions with complex topography. Robust station data are also required for validation of the method, which are not always available everywhere and this is one of the key limitation. Besides these limitations, these empirically based techniques do not account for possible systematic changes in regional forcing conditions or feedback processes.

In contrast to statistical downscaling, the main principles of dynamical downscaling is that this technique uses comprehensive numerical and physical models of the climate system and allows direct modelling of the dynamics of these physical systems that characterize the climate of a region. This technique employs the earlier mentioned regional climate models which are run at high spatial resolutions over a chosen limited area of the globe. The minimum horizontal spatial resolution that is commonly used for a RCM is around 10-20 km though lower and higher resolutions of RCMs are now widely used for climate modelling experiments (IPCC, 2007a). The general approach is to drive the RCM using the large scale climate fields provided by the GCM so that the high resolution model simulates the climate features and physical processes in greater detail for a chosen limited area of the globe, whilst drawing information about initial conditions, time-dependent lateral and surface boundary conditions from the GCM. The main advantages of the dynamical downscaling techniques are that they provide high resolution information of climate variables derived from mesoscale (100-1000 km) atmospheric processes not resolved by GCMs. These RCMs generate multiple climate variables in a self-consistent manner, take into account physical feedback processes in atmospheric circulations, do not assume a fixed relationship between the variable of interest

and the large scale circulation and provide consistency with the large scale information of their driving GCMs.

This regional climate modelling technique originated from numerical weather prediction and the use of RCMs for climate application was pioneered by Dickinson et al. (1989) and Giorgi (1990). Many studies have mentioned the use of RCMs in climate research basically owing to their higher spatial resolutions and their ability to include fine scale topography. They have been used to realistically simulate regional climate features such as orographic precipitation (Frei et al., 2003), extreme climate events (Fowler et al., 2005a; Frei et al., 2006) and regional scale climate anomalies or non-linear effects, such as those associated with the El Nino Southern Oscillation (ENSO) (Leung et al., 2003a). Some research studies within the western U.S., Europe and New Zealand, where topographic effects on temperature and precipitation are prominent, have reported more skill in dynamical downscaling than in regions such the Great Plains of the U.S. and China where regional forcings are weaker (Wang et al., 2004). This regional climate modelling technique also remains an excellent tool in improving our understanding of key climate processes such as cloud-radiation forcing, cumulus convection and land surface processes (Pan et al., (1995); Paegle et al., (1996); Dudek et al., (1996); Bosilovich and Sun (1999); Schar et al., (1999); Sen et al., (2004); Wang et al., (2004)).

However, as mentioned earlier, the model skill depends strongly on the quality of the driving GCM and the presence and strength of regional scale forcings such as orography, land-sea contrast and vegetation cover. It has also been observed that the application of RCMs to geographically diverse regions and model inter-comparison studies have allowed the strengths and weaknesses of dynamical downscaling to be better understood (Wang et al., 2004; Leung et al., 2004). It has been noted that dynamical downscaling can also provide improved simulations of mesoscale precipitation processes useful for producing more plausible climate change scenarios for extreme events and climate variability at regional scales (Schmidli et al., 2006).

In the recent years, RCMs are also used widely to address issues such as urban air quality and heat island effects (Leung et al., 2003a), and of course, there exists a plethora of related climate change studies.

In the light of this brief overview to the downscaling techniques, it must be noted here that this thesis discusses climate modelling using the dynamical downscaling approach only. Although it is a relatively computationally demanding exercise (compared to statistical downscaling), this method was chosen to study climate and climate change to gain a better physical understanding of the climate system and to make full use of the 'added value' this technique will bring in order to apply these results for further impact studies.

At this point of discussions, the region that is chosen for this research study and the rationale for doing so also need to be elucidated.

1.4 REGIONAL CLIMATE CHANGE – SOUTHEAST ASIA

In its Fourth Assessment Report, the IPCC has given regional climate change projections for several regions of the world, including Asia and Southeast Asia (Chapter 11, AR4, 2007). Most of the economically weaker countries, next to Africa, in Southeast Asia happen to be highly vulnerable to climate change and are in need of both scientific expertise and the economic strength to combat climate change. Latest findings from the IPCC's Third Assessment Report (TAR), released in 2001, and that of the Fourth Assessment Report released in 2007, show many evidences that climate change has already affected many sectors in Southeast Asia. The mean surface air temperature over Southeast Asia has increased by 0.1-0.3 °C per decade from 1950-2000. Decreasing trends in precipitation as well as rising trends in sea level (1-3 mm/year) have also been noted. The number of extreme weather events such as hot days/warm nights and the number of heavy storm events and tropical cyclones has also increased. These climate changes have impacts on other physical systems - increasing temperatures and increasing extreme weather events also lead to the decline of crop yield in many Southeast Asian countries (Thailand, Vietnam, Indonesia), massive flooding in Hanoi and Hue (Vietnam), Bangkok (Thailand), Jakarta (Indonesia), Vientiane (Laos), landslides in

the Philippines and droughts in many other parts of the Mekong river basin. Water shortage, agriculture constrains, food security, infectious diseases, forest fires and degradation of coastal and marine resources have also been increasing (IPCC, 2007b).

Furthermore, the results from the MMD models of the IPCC (Table 1-1) have also projected an increase in annual precipitation over Southeast Asia with a median rate of +7 % with extremes between -2 % to +15 % for all seasons. The strongest and most consistent increases are seen over northern Indonesia, Singapore and Malaysia in June, July, August (JJA) and over southern Indonesia and Papua New Guinea in December, January, February (DJF). The annual temperature change for the whole of Southeast Asia is expected to be around 3 °C by the end of this century.

Table 1-1: Southeast Asia climate change projections of temperature and precipitation from a set of 21 global models in the MMD for the A1B scenario
[Adapted from IPCC AR4 (2007)]

		Temperature Response (°C)						Precipitation Response (%)						Extreme Seasons (%)		
Region[a]	Season	Min	25	50	75	Max	T yrs	Min	25	50	75	Max	T yrs	Warm	Wet	Dry
SEA	DJF	1.6	2.1	2.5	2.9	3.6	10	-4	3	6	10	12	80	99	23	2
	MAM	1.5	2.2	2.7	3.1	3.9	10	-4	2	7	9	17	75	100	27	1
11S,95E	JJA	1.5	2.2	2.4	2.9	3.8	10	-3	3	7	9	17	70	100	24	2
to	SON	1.6	2.2	2.4	2.9	3.6	10	-2	2	6	10	21	85	99	26	3
20N,115E	Annual	1.5	2.2	2.5	3.0	3.7	10	-2	3	7	8	15	40	100	44	1

The United Nations Climate Change Conference held in Bali, Indonesia, in December 2007, recognized the need for an enhanced action on adaptation and the provision of financial resources for such adaptation measures (Yusuf and Francisco, 2009). It was also noted that most developing countries in Asia have the least capacity to adapt to climate change and are therefore in need of whatever external support they can get to build their adaptive capacity (Francisco, 2008).

Under the auspices of the EEPSEA (Economy and Environment Program for Southeast Asia), an assessment of climate vulnerability was made by Yusuf and Francisco (2009), who constructed an index of the climate change vulnerability of subnational administrative areas in

seven countries of Southeast Asia - Vietnam, Laos, Cambodia, Thailand, Malaysia, the Philippines and Indonesia. Climate hazards comprising floods, droughts, tropical cyclones, sea level rise and landslides were considered and mapped for the entire Southeast Asian region and a multi-climate hazard index was developed that highlighted the vulnerability of several regions over Southeast Asia. This is shown in Figure 1-5. Detailed documentation of this study can be found in the relevant literature citation mentioned above.

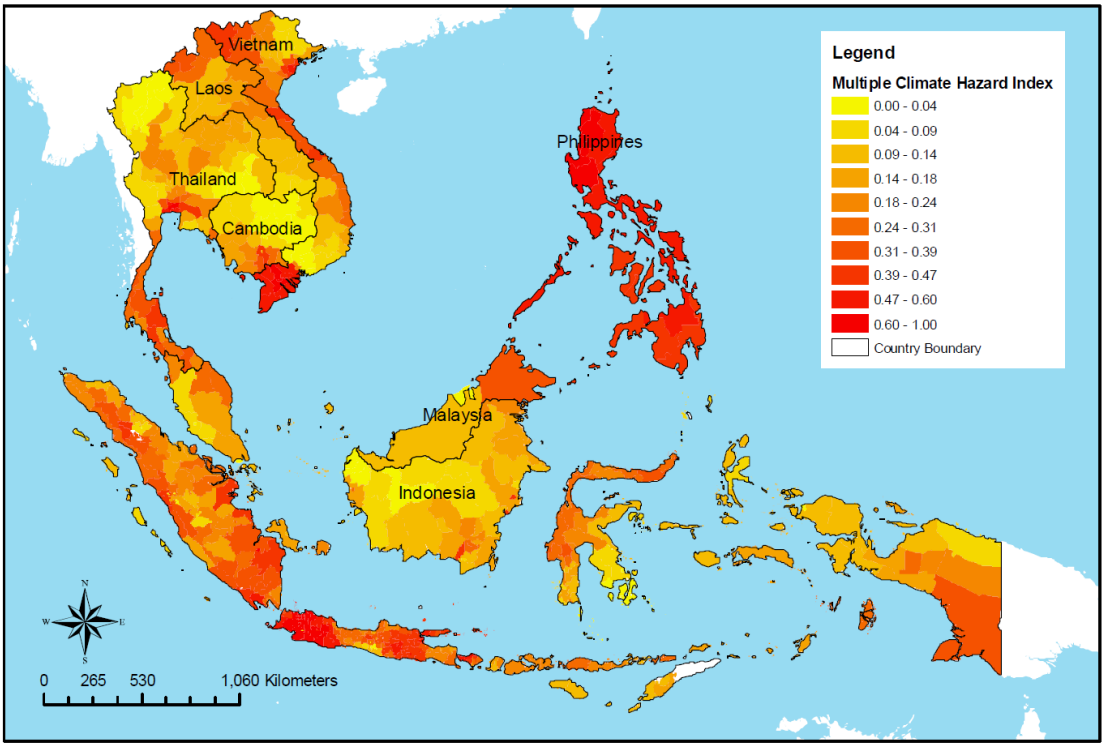

Figure 1-5: Climate Change Vulnerability Map of Southeast Asia
[Adapted from Yusuf and Francisco, 2009]

The Asian Development Bank (ADB) has also released its study of the economics of climate change over Southeast Asia (ADB, 2009) and has called for more adaptive measures and strategies to mitigate climate change impacts. This study has mostly taken into account the findings of the IPCC. These recent studies of the IPCC, ADB and EEPSEA have indicated that much more detailed research is needed for the Southeast Asian countries to better understand climate change and its long and short term impacts over the region. This includes not just refinements in data collection, analyses and modelling, but also a new look at the archipelagic and insular land and seascapes unique to Southeast Asia. There is a lot of scientific and

technical know-how amongst countries like the USA, UK, Australia and New Zealand, from where the contributions to climate science has poured into in the form of extensive research and collaborations that eventually have made a scientific volume, such as the AR4, possible. Like in continental Africa where climate research studies are few and far between, Southeast Asia suffers from similar challenges. In addition to lack of sufficient scientific contribution, Southeast Asia has limitations in available climate data, dense and robust observational networks and technology that support such an intricate science as that of climate. Invariably, the datasets and models are all derived from European or American research, and in more recent years, from China, Japan and Australia. It is high time that much more research into climate science is necessary as far as Southeast Asia is concerned, not just in understanding the climate and its change but also be able to understand the climate impacts and its severity so that all countries in Southeast Asia prepare themselves adequately to adapt to such changes.

Within such a perspective of Southeast Asian climate change, this thesis aims to focus on Vietnam as the main study region. The following sections provide a description of the geography and climate of Vietnam, the rationale in choosing this region for study and an introduction to a particular hydrological catchment in Vietnam over which future hydro climatological changes shall be ascertained.

1.5 STUDY REGION – VIETNAM

Vietnam is located in Southeast Asia, bounded between the latitudes of 8 °N to 23 °N and longitudes of 102 °E to 109 °E. The total land area occupies 330,992 km^2. Vietnam has a 1400 km borderline to the North with China, 2067 km with Laos and Cambodia to the West. The coast line of 3260 km covers the East and the South. Apart from 2 offshore archipelagos, Hoang Sa (Da Nang province) and Truong Sa (Khanh Hoa Province), Vietnam also has a system of coast 3000 big and small islands with total area of more than 1600 km^2. Three-fourths of Vietnam's territory is covered by mountains and hills with highest peaks of more than 3000 m. There are two typical types of climate over Vietnam, identified by separation of the country into nearly two equal segments by the Hai Van pass at latitude 16 °N (black circle

in Figure 1-6a). Based on the topography and geography, Nguyen and Nguyen (2004) characterized Vietnam into 7 climate sub-regions from North to South of Vietnam that has been widely accepted by the Vietnam climatological community and also acknowledged by some literatures (MONRE, 2009; Ho et al., 2011 and Phan et al., 2009). In this research, we apply the same 7 climate sub-regions named from S1 through to S7 (Sub-region 1 to 7). These are mentioned in Table 1-2 and shown in Figure 1-6a. The topographical feature over Vietnam, taken from the SRTM (Shuttle Radar Topography Mission) dataset, is displayed in Figure 1-6b.

Table 1-2: Climate sub-region of Vietnam

Sub-Region Climate	Name
Northwest	S1
Northeast	S2
Red River Delta	S3
North Central	S4
South Central	S5
Central Highland	S6
South	S7

(a)

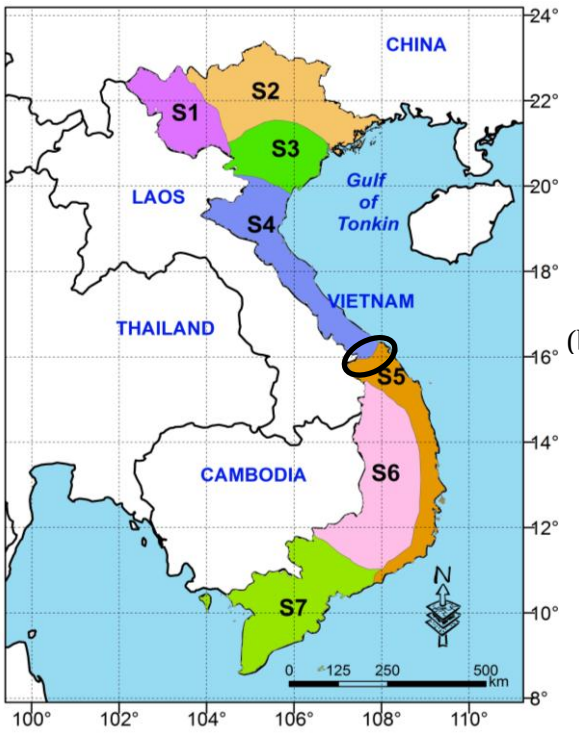

(b)

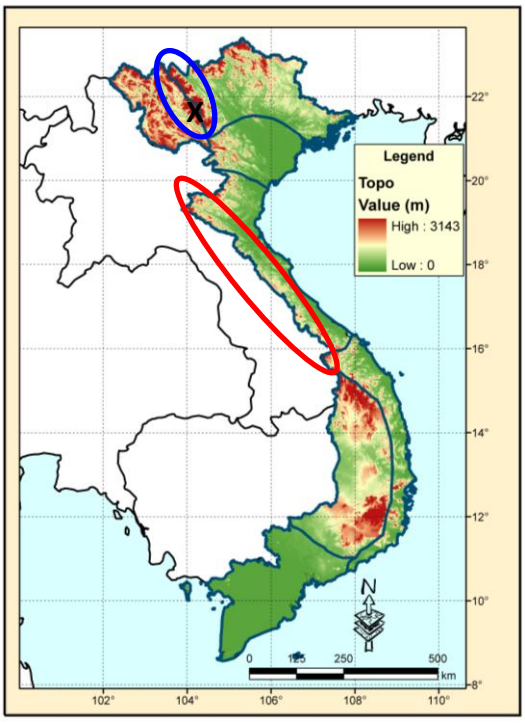

Figure 1-6: Vietnam climate zones and river basin geography
(a) Seven climatic sub-regions (b) Topography of Vietnam

Due to the differences in latitudes and the distinguished variety of topography, the climate of Vietnam tends to vary considerably from place to place. The Northwest (S1) and Northeast (S2) are the two mountainous areas separated by the Hoang Lien Son mountain range (blue circle in Figure 1-6b). Hoang Lien Son has a length of 180 km and is a south eastern part of the Himalayan range, in which lies the Fansipan peak (shown as 'X' in Figure 1-6b) – the highest peak of Vietnam at 3143 m. Because of the Hoang Lien Son, the S2 region bears the direct effect of the Northeast monsoon season while the S1 region does not. S3 is the delta region with low topography over which lies Hanoi, the capital of Vietnam. During the winter or dry season, extending roughly from November to April, the northeast monsoon winds usually blow from the northeast along the China coast and across the Gulf of Tonkin. Regions S4 and S5 are located along the coastal central area of Vietnam, but because of the high mountain ranges at Hai Van pass, the climates of S4 and S5 are different: S4 has all 4 seasons, summer, winter, autumn and spring and S5 has only 2 seasons: dry and wet (rainy), but no cold winters. The Annamite range, also called Truong Son mountain range in Vietnamese, (red circle in Figure 1-6b) is a mountain range of western Vietnam that extends about 1100 km along the border of Laos, Vietnam and a part of Northeast Cambodia.

Together with the high topography of Central Highland S6, this range acts like a barrier that blocks the Northeast monsoon wind passing across Gulf of Tonkin and causes heavy rain over the eastern side of it. The Central Highland area S6 is situated over high topography and thus it has distinct climate compared to the low land area over the southern region S7. The average annual temperature is generally higher in the plains than in the mountains and plateaus and in the south than in the north. Temperatures in the southern plains vary less, ranging between 21 °C and 28 °C in a year. The seasons in the mountains and plateaus and in the north experience temperature ranges from 5°C in December/January and about 37 °C in July/August.

Vietnam is located in the area affected by typhoon and tropical cyclones in the North West Pacific Ocean. On an average, annually, there are 4-5 typhoons/tropical cyclones affecting Vietnam. Annual rainfalls are very different in different regions, ranging between 600 mm to

5000 mm. About 80-90 % of the rainfall concentrates during the rainy season. Several regions are prone to floods during the rainy season but during dry seasons, drought is often recorded. It is also such that some regions of Vietnam experience more (less) rainfall leading to floods (droughts).

Vietnam is located in the downstream of two big rivers: Mekong and Red Rivers. The Mekong river basin area is about 795,000 km^2 (including Tonle Sap and its delta) with an annual water runoff to the South China Sea (called East Sea or "Biển Đông" in Vietnam) about 505 billion m^3. The Red river basin has an area of 169,000 km^2 and annually it transports 138 billion m^3 of water to the South China Sea. Hence, as a whole, the total runoff reaches 835 billion m^3. The spatial and temporal distribution of runoff is very uneven. More than 80 % of the runoff concentrates in summer (5-6 months) and the remaining 20 % of runoff, in winter (6-7 months).

Vietnam is one of the twenty five countries that has a high level of biodiversity and is ranked 16^{th} in biological diversity (having 16 % of world's species). Vietnam is also a major exporter of agricultural products. Currently, it is the world's largest producer of cashew nuts, with a one-third global share, the largest producer of black pepper that counts for one-third of the world's market and the second-largest rice exporter in the world, Thailand being the first. Vietnam has the highest proportion of land use for permanent crops, about 6.93 %, of any nation in the Greater Mekong sub-region. Other primary exports include coffee, tea, rubber, and fishery products. However, the agricultural share of Vietnam's Gross Domestic Product (GDP) has fallen in recent decades, declining from 42 % in 1989 to 21 % in 2010, as production in other sectors of the economy has increased – all these having implications in a changing climate.

1.6 DAKBLA CATCHMENT

This section describes the Dakbla catchment, which is the hydrological study region of this thesis. The Dakbla river is a small tributary of the Mekong river located over the Lower Mekong Basin (LMB). The catchment has a total area of 2560 km^2 from upstream to Kon Tum

station and lies over the Central Highland region of Vietnam. The watershed is covered mostly by tropical forests which are classified as: tropical evergreen forest, young forest, mixed forest, planned forest and shrub. The climate of this region follows the pattern of Central Highland in Vietnam with an annual average temperature of about 20-25 °C and total annual average rainfall of about 1500-3000 mm with high evapotranspiration rate of about 1000-1500 mm per annum.

There are 2 main seasons for the Central Highland region: a rainy season from May through to October (referred to, in short, as MJJASO) and dry season from November through to April (referred to, in short, as NDJFMA). March and April are the two hottest months of the year often relating to severe drought conditions in this region. Flood season is around one month after the rainy season because it needs some buffer time to fill up the groundwater for basalt soil in this region after an earlier long 6 month dry period. Due to the steep slope topography and heavy rainfall concentrations, stream flow in this region acquires a high velocity that creates massive damage to people and property. For easy reference, the location of the catchment is shown in Chapter 3, Figure 3-1 along with technical descriptions of the catchment.

The local economy is based heavily on rubber and coffee plantations on typical red basalt soil in which, by the end of 2010, coffee was accounted for 10 % of Vietnam's annual export earnings (Ha and Shively, 2007). With the advantage of topography of this Central Highland region, there is a very high potential of constructing hydropower dams in this region to store surface water for multipurpose needs: irrigation, electric generation and flood control. Upper Kon Tum hydropower, with an installed capacity of 210 MW, has been under construction since 2009 (to be completed in 2014) in the upstream region of Dakbla river and at 110 km downstream, the Yaly hydropower plan has been constructed (installed capacity 720 MW – second biggest hydropower project in Vietnam) which has been in operation since 2001. Forecasting stream flow from rainfall is therefore quite an important task in this region in order to operate the hydropower dam as well as for irrigation. This description of the Dakbla catchment brings the scientific discussion of this chapter to a closure.

1.7 THESIS OBJECTIVES

In a research objective, this thesis represents one of the first study dealing with climate change impacts in this region (Vietnam). Using two RCMs (WRF and PRECIS, described in Chapter 3), the study focuses on high resolution dynamical downscaling over Vietnam and use the results for further impact studies using the SWAT model (described in Chapter 3). Some of these results will be published in leading journals and attempts will be made to liaise with local governmental agencies and research institutes/organizations to further research initiatives. It is believed that this will lead a way to directly reach the stake holders and policy makers to involve in more research and collaborative exercises of a larger framework.

The main objectives of this thesis are:

(i) To provide ensemble high resolution future regional climate projections over Vietnam

(ii) To assess future hydrological changes over a catchment in Vietnam, using the results of the ensemble high resolution regional climate projections

As further reading unfolds ahead,

- Chapter 2 articulates on the added value of dynamical downscaling and provides a literature review of some latest climate change studies and some hydrological research.
- Chapter 3 discusses the models used in this study, its overall methodology, the different data used and some performance metrics applied for model evaluations.
- Chapter 4 discusses the results of the regional climate models over Vietnam and summarizes the main findings of future climate change projections.
- Chapter 5 describes the hydrological modelling study over the Dakbla catchment and summarizes the main findings of the future hydro-climatological changes ascertained.
- Chapter 6, after an overall summary, highlights the main findings from the entire study, its usefulness for adaptation and policy making and concludes the thesis with some recommendations and possible future work.

CHAPTER 2 LITERATURE REVIEW

2.1 INTRODUCTION

As mentioned in Chapter 1, this research work focuses on climate modelling using dynamic downscaling method to study the change and variability of the climate system. The results of this climate modelling will then be used for further impact studies; in the case of this thesis, assessing future hydrological climate response over a catchment in Vietnam. This chapter, therefore, is dedicated to a review of various literatures in the research community that have applied these methods for different aspects of studying climate change. The limitation that global climate models are not suited for small scale regional climate impact studies was already cited in Chapter 1. Hence, it is of paramount significance to define and establish why dynamical downscaling is widely followed and what 'added value' it imparts as a key method by itself. This chapter begins with its first section, Section 2.2, which will take the readers through some case studies and arguments that would answer this question. The use of the regional climate model output for hydrological impact studies are discussed in Section 2.5 along with some case studies that have employed the hydrological model (these models are described in Chapter 3). To keep the chapter concise, selected recent research work from regional climate research and hydrological impact studies are considered and reviewed.

2.2 WHAT IS THE 'ADDED VALUE' OF RCMs?

This section cites some examples from some key regional climate research that primarily suggest the "added value" of RCMs. It was mentioned in Chapter 1 that one of the main advantages of using regional climate models is their ability to include fine scale topographic details. This enables to improve climate simulations to a great extent as the high resolution simulations incorporate local climate features and circulations due to enhanced topographic details. It can be recalled here that this is something the global models lack due to their relatively coarser spatial resolution. As shown in Figure 2-1, a RCM with a spatial resolution of 50 km is able to resolve the topographic features in great detail compared to a GCM having a spatial resolution of about 300 km. The figure shows the detailed topography over the

European domain, the study done as a part of the PRUDENCE (Prediction of Regional scenarios and Uncertainty for Defining EuropeaN Climate change risk and Effects) project (Christensen, 2001). It is obvious from this figure that the GCM fails to resolve fine topographic details which influence regional climate simulations while the improvement the high resolution RCM makes is evident. This was one of the major RCM experiments done about a decade ago ever since the 'added value' of downscaling due to high resolution topography was strongly realized.

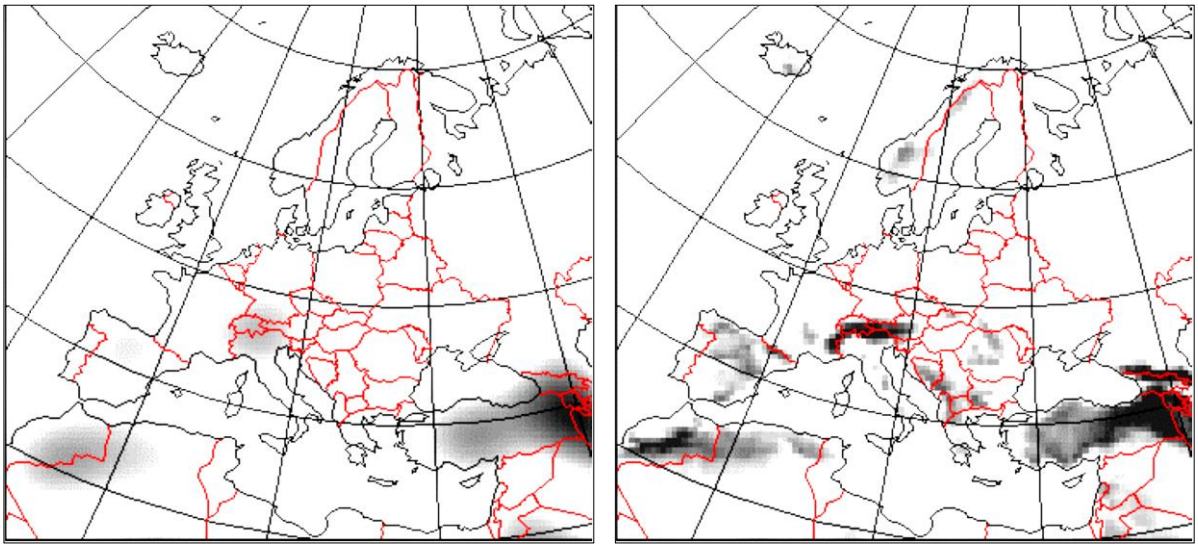

(a) **(b)**

Figure 2-1: Topographic details over Europe
(a) GCM - 300 km (b) RCM – 50 km
[Adapted from Christensen O.B., 2001]

Jones et al. (2004) compared the GCM and RCM simulated winter precipitation over Great Britain to observations (Figure 2-2). The GCM HadCM3 and RCM HadRM3P, both developed at the Hadley Centre, UK, were used in this study where the RCM HadRM3P was driven by the global model HadCM3. The figure shows that the observations clearly exhibit enhanced rainfall over the mountains of the western part of the country, particularly the northwest while the east-west gradients in rainfall are also clearly resolved. This feature was missing in the GCM simulation which showed only an overall north–south gradient with no detailed rainfall distributions as seen in the observations. In contrast to the GCM, the 50 km RCM represented the observed rainfall pattern much more closely. Since the terrain at this higher resolution was

resolved well in an RCM, it was reported that the RCM was able to simulate precipitation with reasonable accuracy.

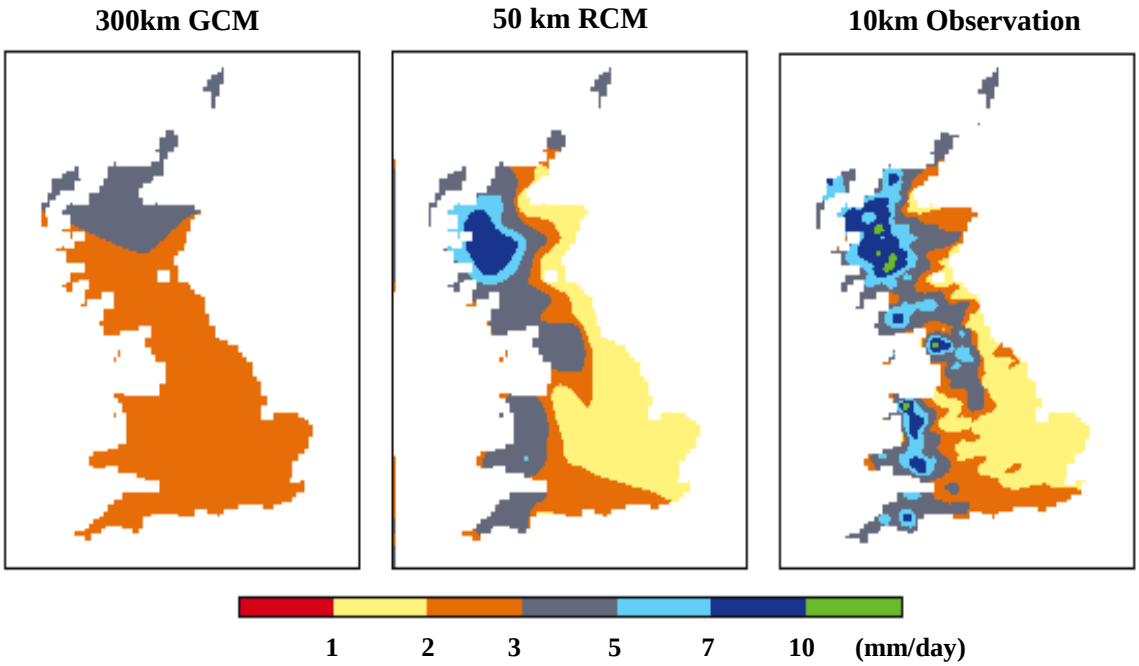

Figure 2-2: Precipitation over Great Britain simulated by GCM and RCM vs observations
[Adapted from Jones et al., 2004]

The mean winter DJF surface temperature change in the western United States, simulated by the GCM PCM and RCM MM5 driven by the GCM PCM, is shown in Figure 2-3. The Parallel Climate Model (PCM) developed by the National Center for Atmospheric Research (NCAR)/Dept. of Energy, USA) and the Mesoscale Model version 5 (MM5) was developed by both Pennsylvania State University & NCAR, USA. Temperature changes were calculated as the difference between the ensemble simulation of the future climate (2040–2060) following a "business as usual" emission scenario and the control climate (without CO_2). The authors reported that as the global model did not resolve well the coastal mountain ranges at a 2.8° × 2.8° spatial resolution, larger warming was found over the Rocky Mountains centered at 114°W (indicated in the figure for clarity), where snow pack was reduced in the future climate. In the RCM simulations, larger warming was seen along the coastal range where snow pack reduction was the highest. These results suggested that the snow-albedo feedback effects were important and they can cause an additional warming of about 1 °C (Leung et al., 2004). Such a feedback mechanism was resolved well in the RCM than in the GCM.

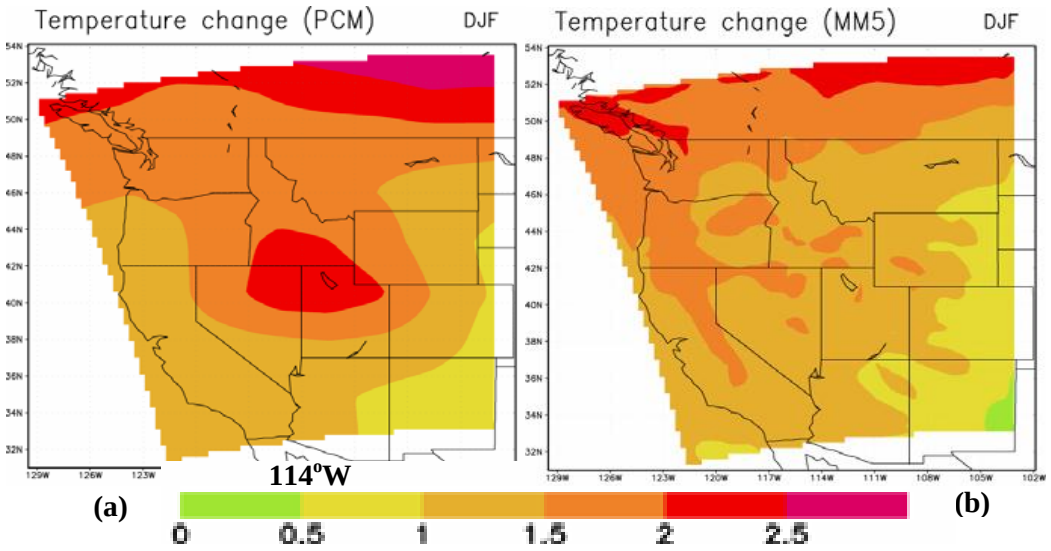

Figure 2-3: Mean DJF Temperature change
(a) GCM PCM (b) RCM MM5 *[Adapted from Leung et al., 2004]*

Not only in climate change studies do the RCMs provide the 'added value'. The coarse resolution of GCMs does not allow them to resolve cyclones, but RCMs, with their higher resolution, are able to resolve such mesoscale weather events. This is clearly seen in Figure 2-4 which shows the low pressure (shown as 'L' in the figure) pattern for a particular day simulated by both a GCM (HadAM3H, Hadley Centre) and the corresponding RCM (HadRM3H, Hadley Centre). The cyclone in the Mozambique Channel between Madagascar island and eastern southern African coast is well resolved by the RCM which is absent in the driving GCM. This study was documented by Jones et al. (2004).

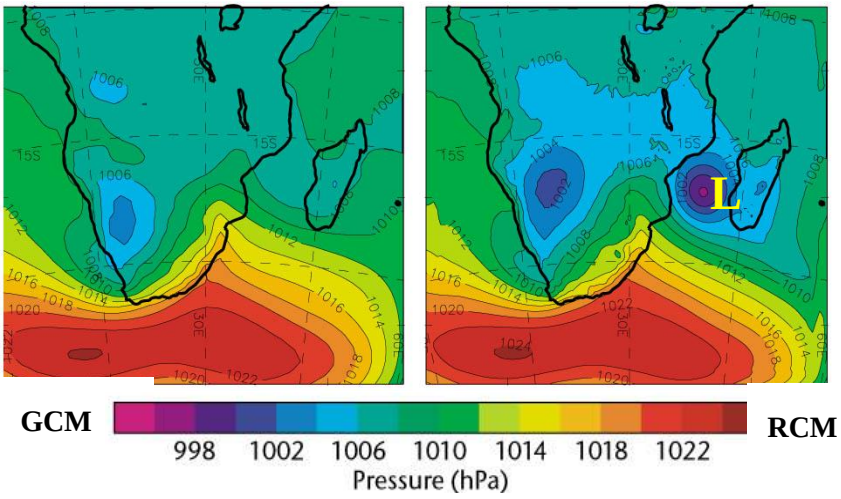

Figure 2-4: Simulation of a cyclone in the Mozambique Channel by GCM and RCM
[Adapted from Jones et al., 2004]

An Indian monsoon climate change study was done by the Hadley Centre, which projected changes in monsoon behaviour over the future. Shown in the Figure 2-5 are the GCM and RCM simulations that look similar, but the added value of RCM is highly explicit. This is because, the rainfall changes over the Western Ghats mountain regions along the west coast of India is decreased in the GCM whilst an increase of up to 3 mm/day in the RCM is seen. In addition, the south central regions seem to have an increase in rainfall simulated by the GCM but a decrease in the RCM. As the RCM resolves the topography and the sub-seasonal variations in the monsoon rainfall, the projections of the RCM were reported to be credible.

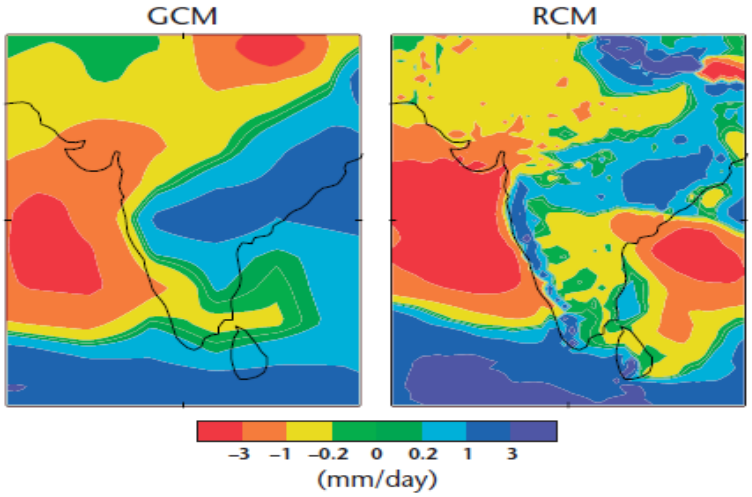

Figure 2-5: Future Changes in monsoon rainfall over India simulated by GCM and RCM
[Adapted from Jones et al., 2004]

From the few examples cited above, it is clear that right from studying mesoscale events through to climate change projections, the use of RCMs certainly do 'add value' over GCM simulations. These examples are, by all means, not the final list of literature that supports regional climate simulations using RCMs but are merely some random snap shots of cited literature to bolster the 'added value' of RCMs. This serves as an overview of the comparisons between GCMs and RCMs in climate simulations and how/why dynamical downscaling is considered robust for climate studies. To this end, this is also a good start for some literature review, leading to an appreciation of the 'added value' of downscaling. In a continuation of this discussion, the following section describes more of similar studies, focusing on regional climate modelling and assessing climate change.

2.3 APPLICATIONS OF RCMs IN CLIMATE RESEARCH

Several RCMs have been developed by many climate research centres in the world and are being used for a wide range of studies right from numerical weather prediction through to climate change projections. Some of those recent research studies that have focused on regional climate simulations and regional climate projections are discussed here. A few illustrations have been added for some case studies for a better appreciation of the science.

Chotamonsak et al. (2011) performed regional climate simulations over Southeast Asia using the RCM WRF model driven by the GCM ECHAM5 forced by the A1B future emission scenario. Dynamical downscaling of the GCM ECHAM5 was done at a 60 km horizontal resolution to project changes from 1990–1999 to 2045–2054 and compared against observations. The authors stated that the regional climate model reproduced the spatial distribution of temperature reasonably well, although with a cold bias for maximum temperature (Tmax) over Southeast Asia. It was also reported that the model simulations exhibited a warm bias for minimum temperatures (Tmin). The wet-season (rainy) precipitation was simulated with lesser skill than the dry-season precipitation. Future changes in precipitation showed increases on an average but with local decreases during the dry season. These results are shown in Figure 2-6.

Bukovsky and Karoly (2011) downscaled the global NCEP (National Centers for Environmental Prediction) reanalyses and the GCM CCSM3.0 using the WRF model, where the reanalyses were used for the evaluation of present day climate and the GCM CCSM3.0 was used to derive future projections of climate under the A2 emission scenario. The results showed that the WRF was able to produce more realistic precipitation than that of its driving systems (GCM CCSM3.0 and NCEP reanalyses). The authors mainly reported that the magnitude of heavy and average precipitation events, the frequency distribution and the diurnal cycle of precipitation over the central United States were greatly improved. As to climate change impacts, the projections from this study also suggested an increase in frequency of both floods and droughts during warm seasons in the future.

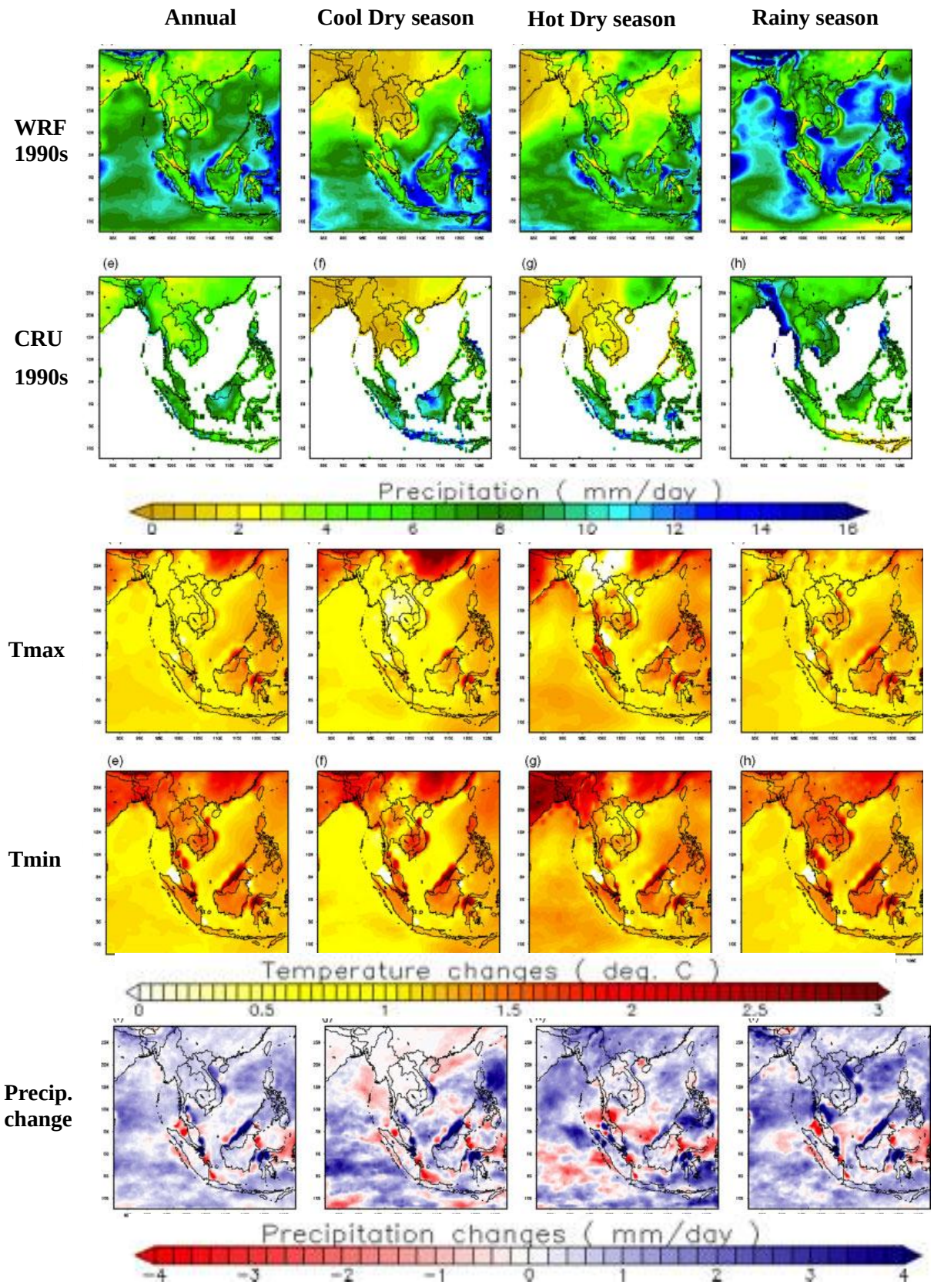

Figure 2-6: WRF simulations over Southeast Asia
[Adapted from Chotamonsak et al., 2011]

Hong et al. (2010) studied the East Asian monsoon system and future climate change scenarios over Korea using the WRF model driven by the global NCEP reanalyses and GCM ECHAM5 at a 12 km horizontal resolution. The authors mentioned that the WRF model was able to reproduce large scale circulation features of the East Asian Monsoon system and its associated hydro climate very well. Their goal was to provide meteorological data for hydrology and air pollution models that require spatial resolutions of 10 km or higher and their study suggested the usefulness of the RCM WRF for such a purpose.

In a study over a Norwegian domain, Heikkila et al. (2010) showed that the RCM WRF model was able to add significant detail to the representation of precipitation and surface temperature when the model was driven by the global ERA40 reanalysis. It was reported that the geographical distribution, the wet day frequencies and the extreme values of precipitation were highly improved due to the better representation of orography. They reported that the refining the resolution from 30 km to 10 km further increased the skill of the model, in the simulation of precipitation. Their results suggested that the use of 10 km resolution was advantageous for producing future regional climate projections.

A 40 year dynamical downscaling study using the WRF model (12 km horizontal resolution) for the present day climate was performed by Caldwell et al. (2009) over California. The WRF model was driven by the 1°×1.25° GCM NCAR CCSM3.0. Detailed comparisons between modelled and observed regional averaged precipitation, surface temperature and snowpack were performed. The authors reported that the regional model reproduced the spatial distribution of precipitation quite well, but substantially overestimated rainfall along the windward slopes. Additionally, they indicated that the coastal temperatures appeared to be too warm due to a coastal sea surface temperature bias inherited from the driving model. It was also reported that the WRF modelled snowfall/snowmelt agreed quite well with observations, but snow water equivalent was found to be much too low due to monthly re-initialization of all regional model fields from CCSM3.0 values.

Tapidor (2010) presented an analysis of the precipitation climate signal in Europe emerging

from a simulation of eight RCMs with five observational datasets as the reference for present day climate conditions. The study also included simulations from the IPCC A2 family of scenarios from eight different RCMs that were involved in the PRUDENCE project over Europe. After accounting for the differences between observed and simulated precipitation in the present climate, the analysis of results showed significant agreement in the future climate signal for most of the European regions. The author reported that, primarily, the RCMs were able to simulate the state of the present day climate very well and that precipitation was reasonably well simulated.

Salathe et al. (2008) performed simulations of future climate scenarios using a high-resolution climate model (MM5) which showed markedly different trends in temperature and precipitation over the Pacific Northwest than in the global model (ECHAM5) in which it was nested, apparently due to the mesoscale processes not resolved at coarse resolution. Present day (1990-1999) and future (2020-2029, 2045-2054 and 2090-2099) climates were simulated at high resolution (15 km grid spacing) using the RCM MM5. The robustness of the model results in simulating present day climate was established through comparisons with the observed and simulated seasonal variability and the study showcased the 'added value' in downscaling.

Done et al. (2005) performed some simulations of the cold season regional climate of the Western United States using the RCM WRF with initial and boundary conditions derived from the NCEP reanalysis data for the winter period of 1990. The simulated cold season accumulated precipitation agreed well with observations in terms of the spatial distribution. The model captured the double band of precipitation along the coast of the northwest United States associated with the coastal hills and the Cascade Range which produced enhanced precipitation over the higher terrain of the Rocky Mountains, establishing the robustness of RCM in resolving terrain and its associated climate features. The mean surface temperature also compared well with observations in terms of spatial distribution and magnitudes.

Alves and Marengo (2010) used the RCM PRECIS to evaluate the accuracy and skill in describing the seasonal variability of the main climatological features over South America and adjacent oceans, in long-term simulations (30 years, 1961–1990). The analysis was performed using seasonal averages from observed and simulated precipitation, temperature and lower and upper level atmospheric circulations. It was reported by the authors that precipitation and temperature patterns as well as the main general circulation features were well simulated by the model. They also reported that in the regional model, there were still systematic errors which might be related to the physics of the model (convective schemes, topography and land surface processes) and the lateral boundary conditions and possible biases inherited from the global model. This simulation is shown in Figure 2-7.

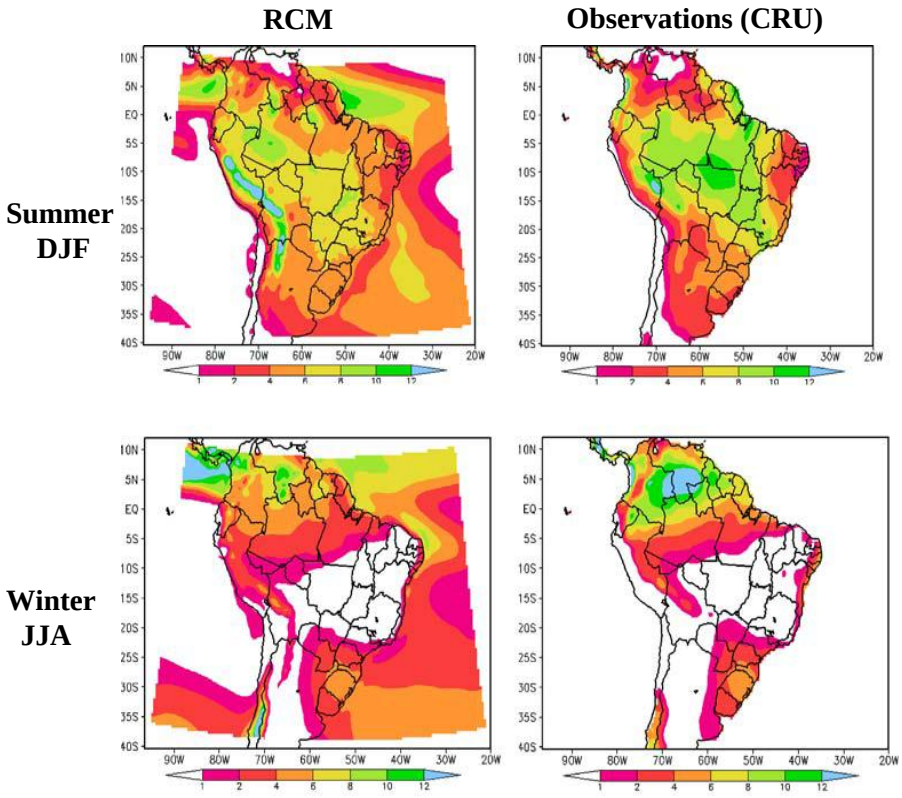

Figure 2-7: PRECIS climate simulations for the present-day climate
Comparisons of RCM vs Observations (CRU)
[Adapted from Alves and Marengo, 2010]

Kumar et al. (2011) performed simulations from a 17-member perturbed physics ensemble generated using the Hadley Centre Coupled Model (HadCM3) for the 'Quantifying Uncertainty in Model Predictions' (QUMP) project which were used to drive the RCM PRECIS. The PRECIS simulations were carried out for a continuous period of 1961–2098. The

model showed reasonable skill in simulating the monsoon climate over India. The climate projections were examined over three future time slices, 2011–2040, 2041–2070 and 2071–2098. The authors reported that the model projections indicated significant warming over India towards the end of the 21st century and that the summer monsoon precipitation over India was likely to be 9–16% more during the last 30 years of the 21st century compared to the baseline 1961–1990.

Campbell et al. (2010) studied changes of rainfall and temperature for the period 2071–2100 under the IPCC A2 and B2 scenarios using the PRECIS regional climate model. They reported that the model simulated the present-day (1979–1990) rainfall and temperature climatologies reasonably well, capturing the characteristic bimodal nature of the Caribbean rainfall and the boreal summer maximum and winter minimum temperatures. For the period 2071–2100, temperatures were projected to increase across the region by 1–4 °C for all months irrespective of the scenario. The rainfall response varied with season with one of the more robust changes being an intensification of a gradient pattern in November–January, in which the northern Caribbean (i.e., north of 22 °N) gets wetter and the southern Caribbean gets drier. There was also a strong June–October drying signal. These results pointed to changes in the regional circulation patterns due to the human-induced climate change and suggested further investigations.

In another study, Marengo et al. (2009) also used the PRECIS regional climate modelling system to analyze the distribution of extremes of temperature and precipitation in South America over the past (1961–1990) and in the future (2071–2100) climate under the IPCC A2 and B2 emissions scenarios. When model results were compared with observations, it was seen that, for the present climate, the model simulated the spatial distribution of extreme temperature and rainfall events well enough although temperature distributions were more realistic than rainfall. This study also highlighted that precipitation is a difficult variable to be simulated well while temperature is rather easy to be simulated.

Further, studies of Soares et al. (2012), Flaounas et al.(2011), Leung and Qian (2009), Zhang et al. (2009), Lo et al. (2008), Liang et al. (2005), have shown the WRF model as an effective RCM in climate studies and its usefulness for dynamical downscaling research. Similar studies using the PRECIS model have also been documented by Karmalkar et al. (2011), Duliere et al. (2011), Yadav et al. (2010), Mileham et al. (2009), Islam et al. (2009), Bloom et al. (2008), Buonomo et al. (2007) and Kumar et al. (2006), to name a few.

Although the aforementioned studies are only a few of many dynamical downscaling research works, they serve as some selected highlights of this research over the recent past. These studies strongly indicate that regional climate models are highly useful tools to achieve high resolution climate data from coarsely resolved global climate models. Regional models show higher detail for mountain ranges or coastal zones, more numerous and differing vegetation and soil characteristics and description of smaller-scale atmospheric processes which lead to the formation of mesoscale weather phenomena. These RCM characteristics are believed to produce model output that is closer to reality than the more coarsely resolved global model data, both for reanalyses for hindcast studies and for global scenario simulations. This added variability occurred mainly on those spatial scales that are best resolved by the regional model, indicating added value from the RCM. In addition, these studies also suggest that temperature simulations are largely realistic as they are more homogeneous rather than rainfall simulations; rainfall is known to be highly variable in space and time and hence the most difficult and sensitive climate variable to simulate, be it numerical weather forecast or long term climate. Dynamical downscaling, therefore, shows high potential to improve climate forecasts/projections towards users' need, to understand physical climate system in detail and to obtain realistic climate simulations for both present day and future climates. This, in turn, helps the downstream impact studies to make use of the results obtained from dynamical downscaling for further research, i.e., in mitigation, adaptation and policy making in climate change applications. What should also be placed as a caution are not only these advantages of RCMs in 'adding value', but also their limitations. Some research studies (Wang et al., 2004;

Leung et al., 2003; Christensen and Christensen, 2004; Bader et al., 2008) have considered the strengths, limitations and challenges in the RCMs. However, it is not within the scope of this thesis to evaluate the advantages and limitations of RCMs. Rather, the usefulness of RCMs as dynamical downscaling tool is recognized from numerous studies done by the climate modelling community around the world and from the vast amount of literature available that bolsters this cause. It is also to be noted that improvement in the quality of RCMs to yield more realistic simulations are a continuing processes of model development. In addition to the knowledge gained from a vast literature, it is also noted here that this research work has been done at the Tropical Marine Science Institute (TMSI), NUS, where one of the main research foci is climate modelling and dynamical downscaling. Therefore, the research experience gained during this PhD thesis research working on several climate change projects at TMSI also adds to the confidence in undertaking this research study.

2.4 EXISTING MODELLING STUDIES OVER INDOCHINA PENINSULA AND VIETNAM

In a continuation of the literature review, this short section outlines some of the few regional climate modelling studies have been done exclusively over the Indochina Peninsula (which encapsulates Vietnam as such) and over Vietnam. This information lays yet another strong rationale to the work done in this thesis study, since very few studies exist in climate research over this region. To that end, this study is certainly a contributor to more of such efforts.

Ho et al. (2011) used the regional climate model RegCM3 to assess future climate changes over the mid-century driven by the GCM CCSM3.0, forced under the IPCC future A1B and A2 emission scenarios over Vietnam. Their study revealed an increase in the hot summer days and a decrease in number of colder nights over Vietnam as a consequence of global warming. The study also suggested that heavy rainfall events in rainy season may decrease for all sub-regions, except northwest and south centre of Vietnam. This is notable that although Vietnam is small compared to the larger Indochina region, sub-regional differences within Vietnam are not unusual.

Takahashi et al. (2010) performed a control simulation using the WRF model driven by ERA40 reanalysis data combined with land use and predicted soil moisture data over Indochina. The purpose of this study was to examine the impact of changes in land surface conditions on regional climate over this study region, because of the fast deforestation that has occurred within this part of tropical Southeast Asia. Two additional experiments assuming wetter and drier land surface condition were performed and compared against the control simulation. The authors concluded that there was a significant effect of land use and land cover changes to the diurnal precipitation cycle over the Indochina region.

In another study, Takahashi et al. (2009) performed a 25 km simulation using the WRF model to address changes in the September month rainfall over the Indochina peninsula over a 30 year period, 1966-1995. The authors reported that the WRF model successfully simulated the observed long-term decrease in rainfall and concluded that the weakening tropical-cyclone activity over the Indochina Peninsula region was the likely reason for the decrease in rainfall.

The regional climate model RegCM3 (Regional Climate Model version 3.0) was used to address the seasonal and interannual variations of rainfall and temperature over Vietnam by Phan et al. (2009), the model been driven by the ERA40 reanalyses. The study reported that the model reproduced the observed annual cycle and interannual variability of rainfall and temperature relatively well. However, it was reported that the model still underestimated the surface temperature distributions over most of the sub-regions. During rainy and dry seasons, the model underestimated and overestimated precipitation, respectively.

In a different study, the Ministry of Natural Resources and Environment (MONRE) of Vietnam conducted a study using MAGICC/SCENGEN, a climate Scenario Generator (Wigley, 2008). This is a user-friendly interactive software that allows users to investigate future climate change and its uncertainties at both global and regional levels. Using this tool, MONRE (2009) projected annual and seasonal changes in future climate using 3 emission scenarios (B1, B2 and A2) over the future period 2020-2100 relative to the 1980-1999. The Table 2-1 shows the projections for the 7 climatic zones over Vietnam from the results of this

study for the year 2100 under the high emission scenario A2, the more concerning emission scenario of the three. Results show a mixed response of changes, mainly precipitation (P), that greatly differ from region to region, while temperature (T) changes are relatively narrow. Although this MAGICC/SCENGEN is not a sophisticated regional climate modelling tool such as any RCM, the findings from this study give some preliminary ideas of possible changes in the future climate.

Table 2-1: Seasonal Changes in Temperature and Precipitation in 2100 in Vietnam climate zones relative to the period 1980-1999, high scenario (A2)
[Adapted from MONRE (2009)]

Climate zones	Periods	T (°C)	P (%)	Climate zones	Periods	T (°C)	P (%)
North West	Ann	3.3	9.3	South Central	Ann	2.4	4.1
	DJF	4.0	7.2		DJF	2.5	-13.0
	MAM	3.8	-7.1		MAM	2.2	-18.1
	JJA	2.1	15.1		JJA	2.8	5.0
	SON	3.3	2.8		SON	1.8	15.3
North East	Ann	3.2	9.3	Central Highlands	Ann	2.1	1.8
	DJF	3.8	4.9		DJF	2.6	-18.5
	MAM	3.5	-5.6		MAM	2.4	-22.2
	JJA	2.1	16.1		JJA	1.9	0.3
	SON	3.4	3.8		SON	1.9	18.5
North Delta	Ann	3.1	10.1	South	Ann	2.6	1.9
	DJF	3.5	5.5		DJF	2.1	-19.6
	MAM	3.9	-8.6		MAM	2.7	-18.2
	JJA	2.2	19.1		JJA	2.9	2.1
	SON	2.7	6.1		SON	2.9	16.5
North Central	Ann	3.6	9.7				
	DJF	3.7	3.8				
	MAM	4.1	-12.6				
	JJA	3.3	18.5				
	SON	3.4	10.8				

The UK Hadley Centre performed a 17-member perturbed physics ensemble using the QUMP Hadley Centre Coupled Model HadCM3 for Monsoon Asia and Indochina/Vietnam using the PRECIS regional climate model. Their results suggested an overall decrease in rainfall

projections by 1 to 2 mm/day and increases in temperatures of about 3 °C, towards the end of the 21st century.

All these studies above indicate continuing uncertainties in climate projections over this region and that much more detailed assessments of future changes over is needed not only over the Indochina region as such, but over Vietnam. Yet again, the objective of this thesis in pronouncing high resolution climate projection can be stressed here for this very reason, as this study serves to contribute to one such detailed high resolution regional climate modelling study over Vietnam.

2.5 USE OF GLOBAL AND REGIONAL CLIMATE MODEL OUTPUTS FOR HYDROLOGICAL SIMULATIONS

The issue of the 'added value' of using RCMs has been mentioned several times earlier, owing primarily for the reason that GCM derived climate estimates are not useful for impact studies due to their coarse resolutions. When it comes to studying climate impacts, GCM projections are subject to substantial uncertainties in the modelling process so that climate projections are not easy to be incorporated as in the case of hydrological impact studies (Mearns et al., 2001; Allen and Ingram, 2002; Forest et al., 2002). It has been noted that such uncertainties have produced biases in the simulation of river flows when using direct GCM outputs for hydrological impact studies. Some studies have found that uncertainties in climate change impacts on water resources are primarily due to the uncertainty in precipitation inputs and less due to the uncertainties in greenhouse gas emissions, in climate sensitivities or in hydrological models themselves (IPCC, 2007b). Most climate change impact studies consider only changes in precipitation and temperature, based on changes in the averages of long-term monthly values. A major problem in the use of GCM outputs for impact studies is the mismatch of spatial grid scales between GCMs (typically a few hundred kilometers) and the hydrological processes. Water is managed at the catchment scale and adaptation is local, while GCMs work on large spatial grids. Generally, precipitation projections are less consistent than those of temperature due to its high variability, spatially and temporally, with large inter-model ranges

for seasonal mean rainfall responses. These inconsistencies are explained partly by the inability of GCMs to reproduce the mechanisms responsible for precipitation such as the convection processes and the hydrological cycle or to account for orography (IPCC, 2007b). With uncertainties in such climate projections, impacts studies are very challenging and difficult. While temperatures are expected to increase everywhere over land and during all seasons of the year, at different increments, precipitation is expected to increase in many river basins, and to decrease in many others (IPCC, 2007a). However, it has been long noted that quantitative projections of changes in precipitation, river discharges and water levels at the river-basin scale remain uncertain (IPCC, 2001). Precipitation, a principal input signal to water systems, is not reliably simulated in these global climate models due to their coarse resolutions (IPCC, 2007b). As in the case of studying climate change projections using high resolution models, the use of outputs from such high resolution models for studies such as hydrological impacts are far more appropriate. In this context, this section reviews some case studies using GCMs and RCMs for hydrological studies, to once again highlight the merits and the 'added value' in downscaling.

Arnell (2004) conducted a study assessing future runoff changes on some river basins in the world, using GCM outputs for estimating river flows under both present and future climates. The results of this study are shown in Figure 2-8 which provide an indication of the effects of future climate change on long-term average annual river runoff by the 2050s across the world, under the IPCC A2 emission scenario, estimated by different climate models.

It was reported that climate change is likely to increase water resources stresses in some parts of the world where runoff decreases, including around the Mediterranean, in parts of Europe, central and southern America and southern Africa. In other water-stressed parts of the world, particularly in southern and eastern Asia, climate change is likely to increase runoff. It was also reported by the author that there were differences in the magnitude and direction of climate change over some parts of the world, including Asia. It was seen that even for large river basins, climate change scenarios from different climate models resulted in very different

projections of future runoff change, such as in Australia, South America and Southern Africa. This strongly highlighted the uncertainties in the output of climate estimates derived from different GCMs and called for a robust study to constrain these uncertainties.

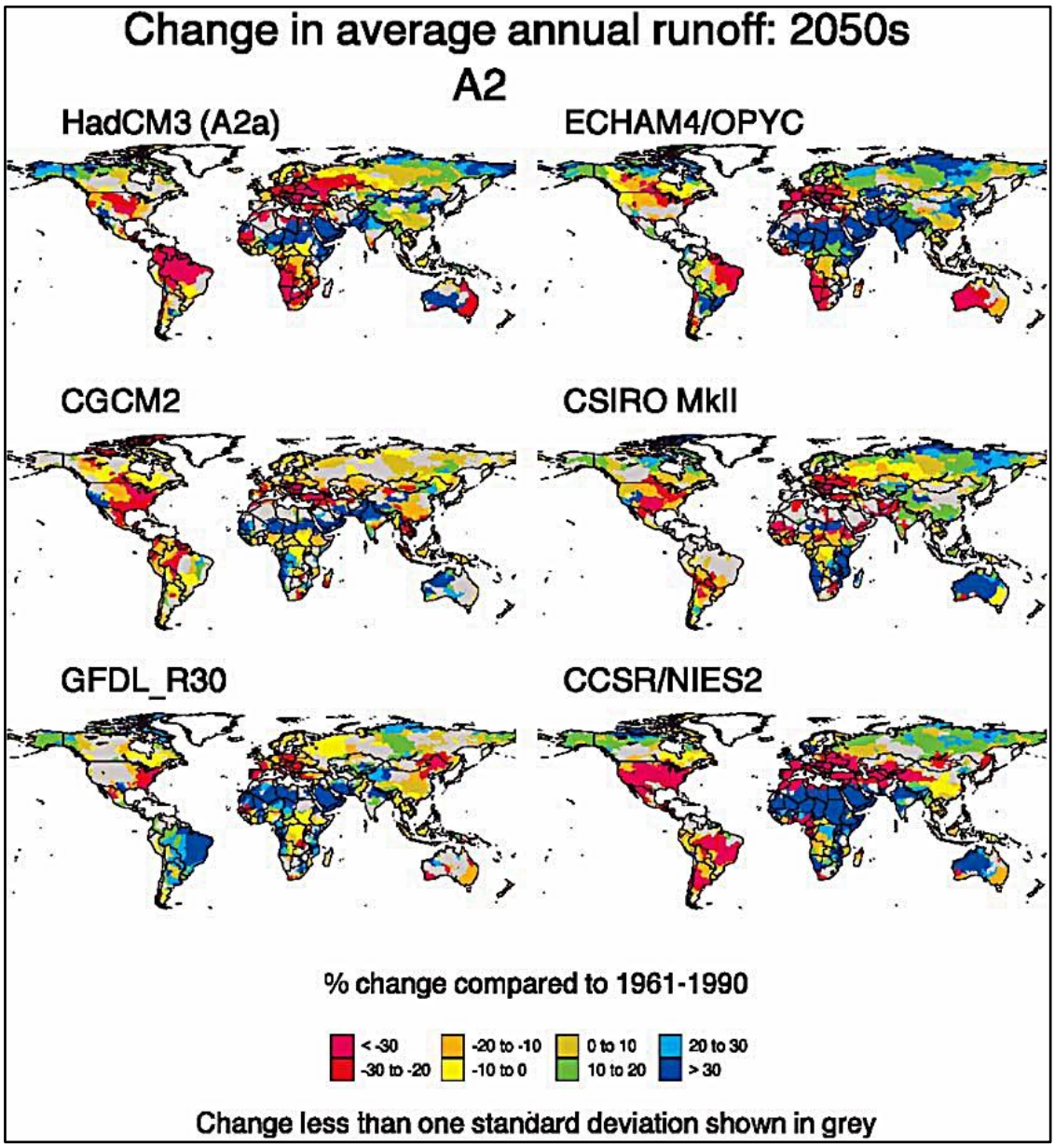

Figure 2-8: Changes in average annual runoff for 2050 using A2 IPCC Emission scenario shown by different GCMs. Percentage change compared to 1961-1990. (GCMs HadCM3, ECHAM4, CGCM2, CSIRO, GFDL and CCSR/NIES)
[Adapted from Arnell (2004)]

In a hydrological modelling study of the Okavango River basin and Okavango delta in Southern Africa, Andersson et al. (2006) applied scenario modelling as a tool for integrated water resource management in the Okavango River basin. The Pitman hydrological model

(Pitman, 1973) was used to assess the impact of various climate change scenarios on downstream river flow. Pitman model of the river basin was applied to both present day historical conditions and future climate change scenarios to assess the impact of climate change on river flows. Four GCMs (HadCM3, CCSR/NIES, CCCMA and GFDL) with present day conditions and future A2 IPCC emission scenario were applied in the study (Figure 2-9).

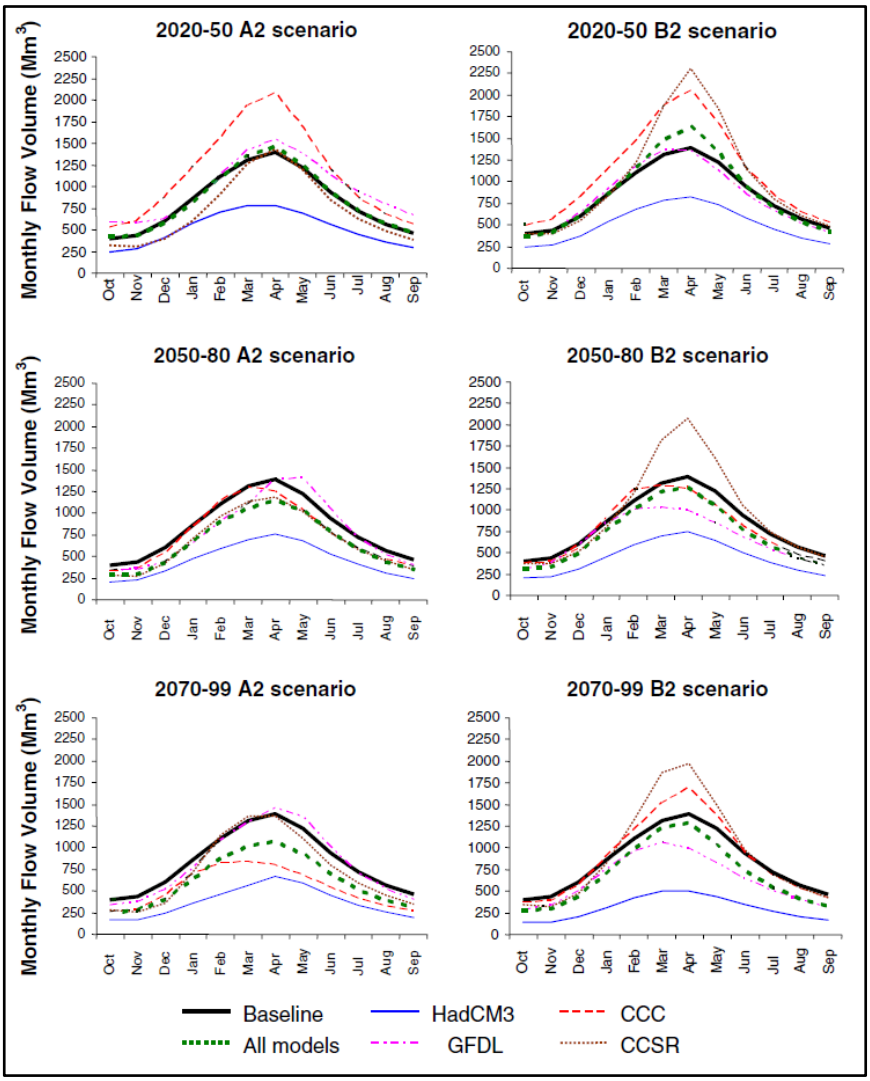

Figure 2-9: Mean monthly flow at Mukwe
Showing baseline simulations and with assessment of changes of precipitation and evaporation derived from various GCMs, driven by the A2 and B2 greenhouse gas emission scenarios.
[Adapted from Andersson et al. (2006)

Their results showed that there was considerable uncertainty about the magnitude and trend of any future discharge response associated with both the GCM and the IPCC emission scenarios. Results of this study showed that the modelled experiments indicated a reduction in future flow after about 2050, for both the A2 and B2 GHG scenarios, that reduces more over time.

This is seen in Figure 2-9 which shows the mean monthly flow at a particular station (Mukwe) in the Okavango River basin, simulated by the SWAT hydrological model. The key conclusion from the study was that, different GCMs predicted future conditions in the Okavango Basin ranging from drier than present to wetter than present and there were differences in both the degree of change and the trend of change between the Okavango river catchment area and the Okavango Delta.

The above cited studies are examples of how hydrological impact studies are done using the outputs of GCMs. The studies also highlighted the limitations in the use of the results due to large uncertainties in the estimated future runoff. It has therefore emphasized that changes in future precipitation may be more adequately specified on the sub-basin scale by downscaling the coarse GCM data using RCMs allowing for more detailed assessments of spatial heterogeneities in climate change impacts on water resources since these are limited area models run at a higher resolution compared to GCMs (Andersson et al., 2006). The IPCC also reported that during recent years many studies have focused on diverse applications of RCMs for impact studies which include downscaling from the climate model scale to the catchment scale, using regional climate models to create scenarios to drive hydrological models and quantifying the effect of hydrological model uncertainties on estimated impacts of climate change (IPCC, 2007b). Modelling is an inherently probabilistic exercise, with uncertainty amplified at each stage of the process, from scenario generation to simulation of hydrological processes and management impacts (Praskievicz and Chang, 2009). At the basin scale, significant factors affecting hydrological impacts of climate change include latitude, topography, geology and land use. Under scenarios of future climate change, many basins are likely to experience changes not only in their mean hydrological state, but also in their frequency and magnitude of extremes. In order to provide the policy makers with the best possible information on future climate changes, reliable information on climate variables, mainly, precipitation, temperature & evapotranspiration are needed. As information obtained from the GCMs are rather too coarse, information from high resolution RCMs are used as inputs to hydrological models for impact studies (Teutschbein and Seibert, 2010).

Akin to the dynamical downscaling method that was reviewed in the earlier section, some reviews on studies that have used regional climate model outputs for hydrological impact studies are done further in this section. This places an emphasis on the science and technique where the dynamically downscaled outputs are used for hydrological impacts studies, as the one done in this thesis.

González-Zeas et al. (2012) applied the results from the European regional climate model project PRUDENCE for the period 1961-1990 in a hydrological study using a distributed hydrological model SIMPA (Spanish acronym meaning 'integrated system for rainfall-runoff modelling') over 338 basins in Spain. The authors used four different interpolation methods for downscaling runoff to the basin scale from 10 RCMs. The objective was to find the best choice to obtain bias corrected, monthly runoff time series from the RCM outputs. The authors opined that they introduced a simple methodology in this study which could be used for studies where properly calibrated hydrologic model is not available. Their simulated results compared well with their counterparts from observations and that this had implications for understanding future climate change since the results for the present day climate were credible.

Im et al. (2010) dynamically downscaled the GCM ECHO-G using the RCM RegCM3 whose outputs were applied to determine the hydrological response over three Korean basins. Two sets of multi-decadal simulations were performed over a reference period (1971–2000) and a future period (2021–2050). The authors reported increases in future runoff due to increases in future rainfall derived from the RCM and indicated the usefulness of the application of RCM derived information for use in impact assessments.

Ma et al. (2010) studied the hydrological response to future climate change over the Agano river basin in Japan using the output of the regional climate model, WRF. The performance of the one dimensional hydrological model SVAT & HYCY (Ma and Fukushima, 2002), was validated using a 20-year hindcast for the baseline period between 1980 and 1999 where the hydrological model showed a rather high correlation, of about 0.79, for the monthly mean discharge in the winter season of model results compared to station records.

The future changes in discharges, shown in Figure 2-10, indicated increases in some months and decreases in the other, with reference to the baseline period of the 1990s.

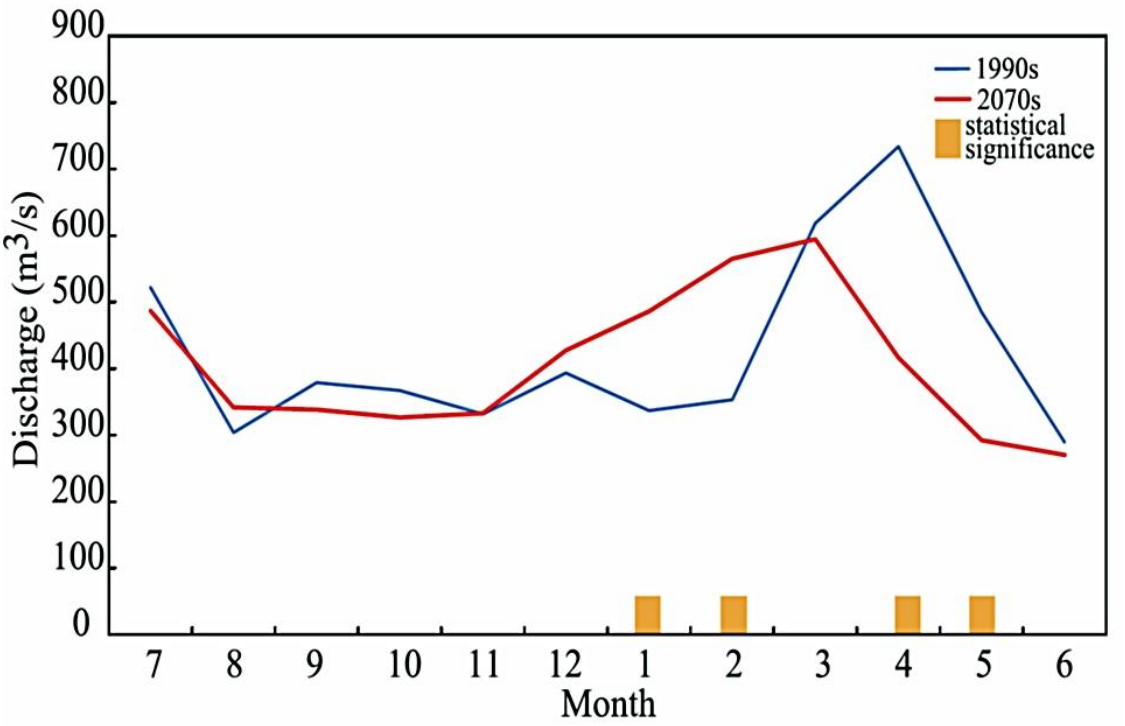

Figure 2-10: Hydrological simulation of Agano river basin discharge: Present day vs Future
[Adapted from Ma et al. (2010)]

Akhtar et al. (2008) used the PRECIS model at 25km resolution to estimate the changes in water resources in three river basins in the Hindukush-Karakorum-Himalaya (HKH) over the northern Indian region. Two study periods were considered, present day (1961-1990) and future (2071-2100) under the A2 emission scenario. A hydrological model HBV (Hydrologiska Byråns Vattenbalansavdelning), developed by Bergström (1976,1992), was applied to quantify the future discharge based on different inputs: one, HBV-Met, which took the input from observed meteorological data while the other, HBV-PRECIS, was calibrated with inputs from PRECIS in addition to using the actual output from PRECIS without any calibration. Future rainfall and temperature were constructed through the delta change approach in HBV-Met, whilst in HBV-PRECIS, the actual PRECIS RCM output was directly used. Based on the increases in temperature and precipitation from the RCM, the authors reported an increase in discharge based on 100 % and 50 % glacier scenarios whilst it showed drastic decrease in 0 % glaciers. The HBV-PRECIS posed a higher risk of flood over the future

climate. An important finding from authors was that the transfer of climate change signals into the hydrological changes was more consistent in HBV-PRECIS than in HBV-MET.

Another application of RCM outputs was conducted by Fowler and Kilsby (2007) in simulating river flows in northwest England. The output data from RCM HadRM3H were used as input to hydrological models that were calibrated for eight catchments. The authors reported that the simulated daily flow distributions were reasonable and hence could be used with some confidence to examine future changes in flow regimes.

Climate change inputs from different RCMs produced from the PRUDENCE experiment (Christensen and Christensen, 2007) were used in a study by Graham et al. (2007) to address how differences in the climate models affect estimates of projected hydrological change over the Baltic Basin, the Bothnian Bay Basin and the Rhine Basin, in Europe. The application of the delta factor method (that takes the difference between the future and present day climate estimates as the change factor) for assessing future changes was deemed robust and the authors concluded that the hydrological simulations were more dependent on the choice of the GCM that was downscaled and not the RCM which was used to downscale the GCMs.

Salathe (2005) applied the downscaled RCM results to simulate stream flow in the Yakima River, a mountainous river basin in Washington, USA, to illustrate how model differences affect stream flow simulations. The downscaling was applied to the output of three models (ECHAM4, HADCM3 and PCM) for simulations of historic conditions (1900–2000), denoted as 'HST' in Figure 2-11 and two future emissions scenarios (A2 and B2 for 2000–2100). The author reported that the ECHAM4 simulation closely reproduced the observed statistics of temperature and precipitation for the 42 year period 1949–90. Stream flow computed from this climate simulation likewise produced similar statistics to stream flow computed from the observed data. The downscaled climate change scenarios from these models were examined in the light of the differences in the present day simulations. Stream flows simulated from the ECHAM4 results showed the greatest sensitivity to climate change, with the peak in summer time flow occurring 2 months earlier by the end of the 21st century.

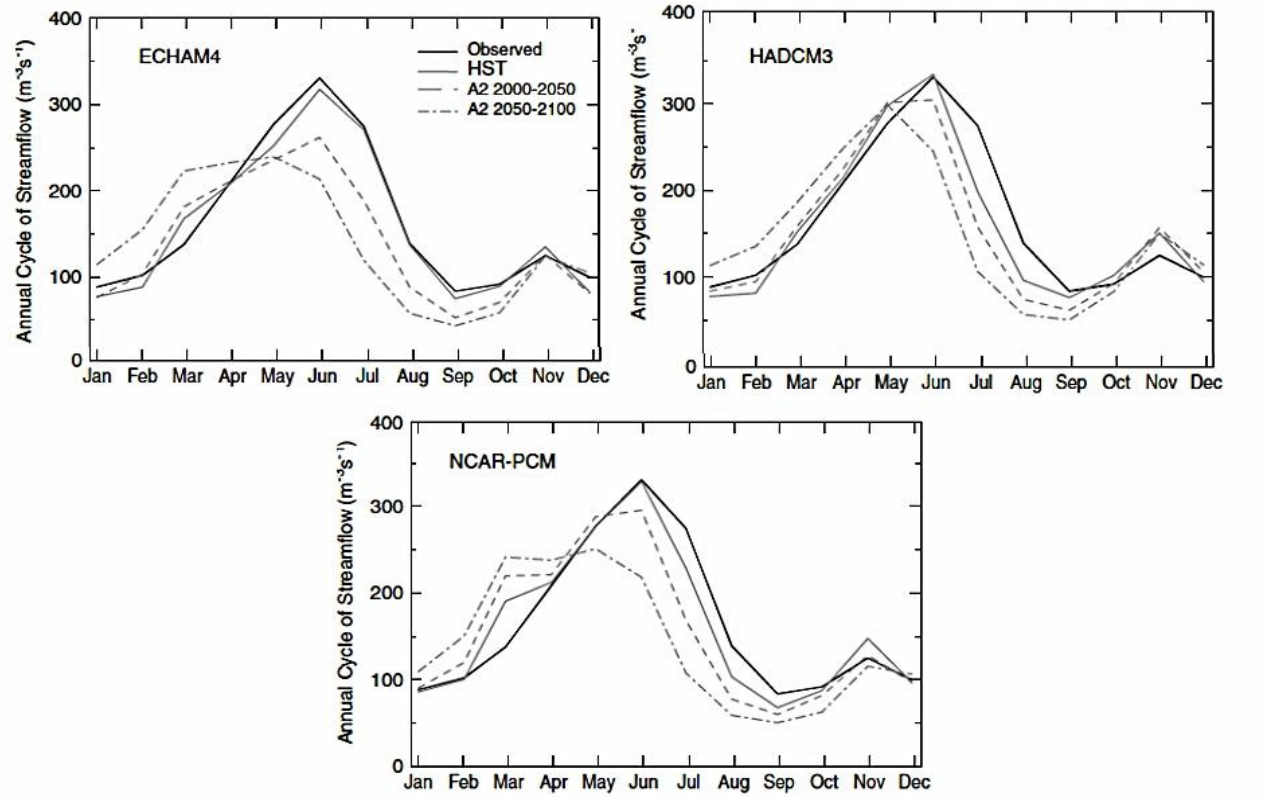

Figure 2-11: Annual Cycle of stream flow changes over Yakima river
[Adapted from Salathe (2005)]

Kotlarski et al. (2005) applied RCM output driven by the ERA15 reanalyses as input to a hydrological model and evaluated their uncertainties. Although they indicated that no model (RCM) is best, more uncertainties lie in observations, model parameterizations and internal model variability and suggested the use of ensembles – to use more RCMs driven by different large scale models so as to get a range of possible outcomes.

Wood et al. (2004) undertook an approach where six different downscaled climate model outputs for use in hydrologic simulation were evaluated, with particular emphasis on each method's ability to produce precipitation and other variables used to drive a macro scale hydrology model applied at a higher spatial resolution than the climate model. Comparisons were made on the basis of a twenty-year (1975–1995) climate simulation produced by the GCM PCM. The implications of the comparison for a future (2040–2060) PCM climate scenario were also explored and the results suggested that application of some bias-corrections could improve the hydrological simulations.

Hay et al. (2002) used the output from RCM RegCM2 driven at 52 km for the continental United States as input to a distributed hydrological model for one rainfall dominated basin and three snowmelt dominated basins along with the station data as the other input. They found that the RegCM2 output did not exhibit the day-to-day variability in rainfall and temperature even after they were bias corrected. They suggested that the systematic biases in the RCM need to be further evaluated and improved methods were needed to remove bias in order to obtain a better day-to-day variability of climate variables for use in hydrological models.

These few examples of the application of the RCM output for hydrological studies brings to a closure, the discussion of applying climate model results for hydrological impact studies. It can be realized that this method has found usefulness for impact assessments at regional/sub-regional scales and for a suite of purposes, right from large basins to catchment scale studies. The key message from these discussions is that the climate variables from RCM, derived at higher resolutions for the use of these output in hydrological studies, do find wide applications due to their credibility in the 'added value' chain in downscaling which is established alongside the dynamical downscaling method itself.

2.6 USE OF THE SWAT MODEL TO STUDY HYDROLOGICAL RESPONSES

The earlier section discussed the use of the RCM output for hydrological studies. This thesis applies one of the widely used hydrological model, (described in detail in Chapters 3 and 5), the Soil and Water Assessment Tool (SWAT) model, for the assessment of hydrological responses over a catchment area in Lower Mekong Basin. Hence, it is felt suitable at this point to cite some recent literatures that have used this SWAT model for varied hydrological applications.

Strauch et al. (2012) investigated the influence of precipitation uncertainty on both model parameters and predictive uncertainty in a data sparse region using the integrated river basin model SWAT which was calibrated against measured stream flow of the Pipiripau River in Central Brazil. Calibration was conducted using an ensemble of different precipitation data

sources, including: (1) point data from the only available rain gauge within the watershed (2) a smoothed version of the gauge data derived using a moving average (3) spatially distributed data using Thiessen Polygons (which includes rain gauges from outside the watershed) and (4) Tropical Rainfall Measuring Mission (TRMM) radar precipitation data. For each precipitation input model, the best performing parameter set and their associated uncertainty ranges were determined using the common Sequential Uncertainty Fitting Procedure. This procedure and its usefulness have been documented by Abbaspour et al. (2007). Although satisfactory stream flow simulations were generated with each precipitation input model, the results of their study indicated that parameter uncertainty varied significantly depending upon the method used for precipitation data set generation. The study also showed that ensemble modelling with multiple precipitation inputs (as coming from outputs of several RCM simulations) can considerably increase the level of confidence in simulation results, particularly in data poor regions.

Wu et al. (2011) used the SWAT model to assess the effects of increased CO_2 concentration and climate change in the Upper Mississippi River Basin (UMRB). The standard SWAT model was modified to represent more mechanistic vegetation type specific responses of stomata conductance reduction and leaf area increase to elevated CO_2 based on physiological studies. For estimating the historical impacts of increased CO_2 in the recent past decades, the incremental (i.e., dynamic) rises of CO_2 concentration at a monthly time-scale were also introduced into the model. The study results indicated that about 1–4 % of the stream flow in the UMRB during 1986 through 2008 could be attributed to the elevated CO_2 concentrations. In addition to evaluating a range of future climate sensitivity scenarios, the climate projections by four GCMs under different greenhouse gas emission scenarios were used to predict the hydrological effects in the late twenty-first century (2071–2100).

In a similar study, Raneesh and Santosh (2011) applied the projections of the GCM HadCM3 for two emission scenarios A2 and B2, downscaled by the RCM PRECIS, to project future climate in a watershed in a river basin in Kerala, India. Projections for two important climate variables, rainfall and temperature, were made. These were then used as inputs to the SWAT

model in order to evaluate the effect of climate change on stream flow and vegetative growth in a humid tropical watershed. The authors reported that future stream flow exhibited a declining trend in these two scenarios but not so severe as to adversely affect agricultural production in the basin.

Park et al. (2011) evaluated hydrologic impacts of potential climate and land use changes in a mountainous watershed in South Korea. The climatic data predicted by the GCM MIROC3.2 HiRes under the emission scenario A1B for three time periods (2010-2039, 2040-2069 and 2070-2099) were prepared using a statistical downscaling change factor method. By applying the climate and land use predictions to the SWAT model, the watershed hydrologic components (including evapotranspiration, surface runoff, groundwater recharge and stream flow) were evaluated. The study reported temperature and precipitation increases, for the future period 2070-2099, by 4.8 °C and 34.4 %, respectively. The study also mentioned that a 6.2 % decrease in forest areas and 1.7 % increase in urban areas was likely and the combined land use with climate change scenario resulted in more stream flow change (55.4 %) than the single climate and single land use change scenario (39.8 % and 10.8 %), respectively.

In a river basin climate change study in Chile, Vicuna et al. (2011) applied the 25 km RCM PRECIS output over the Limari river basin. The PRECIS model was simulated under the A2 and B2 emission scenarios of the GCM HadCM3. The rainfall and temperature outputs form the model were fed to a water evaluation and planning model (WEAP) (Yates et al., 2005a, 2005b) to assess future changes over the period 2071-2100 with a baseline period 1961-1990. Their results showed that the annual mean stream flow decreased more than the projected rainfall decrease because a warmer climate enhanced water losses to evapotranspiration. The authors also reported that in the future climate, the seasonal maximum stream flow tended to occur earlier than in present day (historic) conditions because of the increase in temperature during spring/summer and the lower snow accumulation in winter. Some results from this study are shown in Figure 2-12.

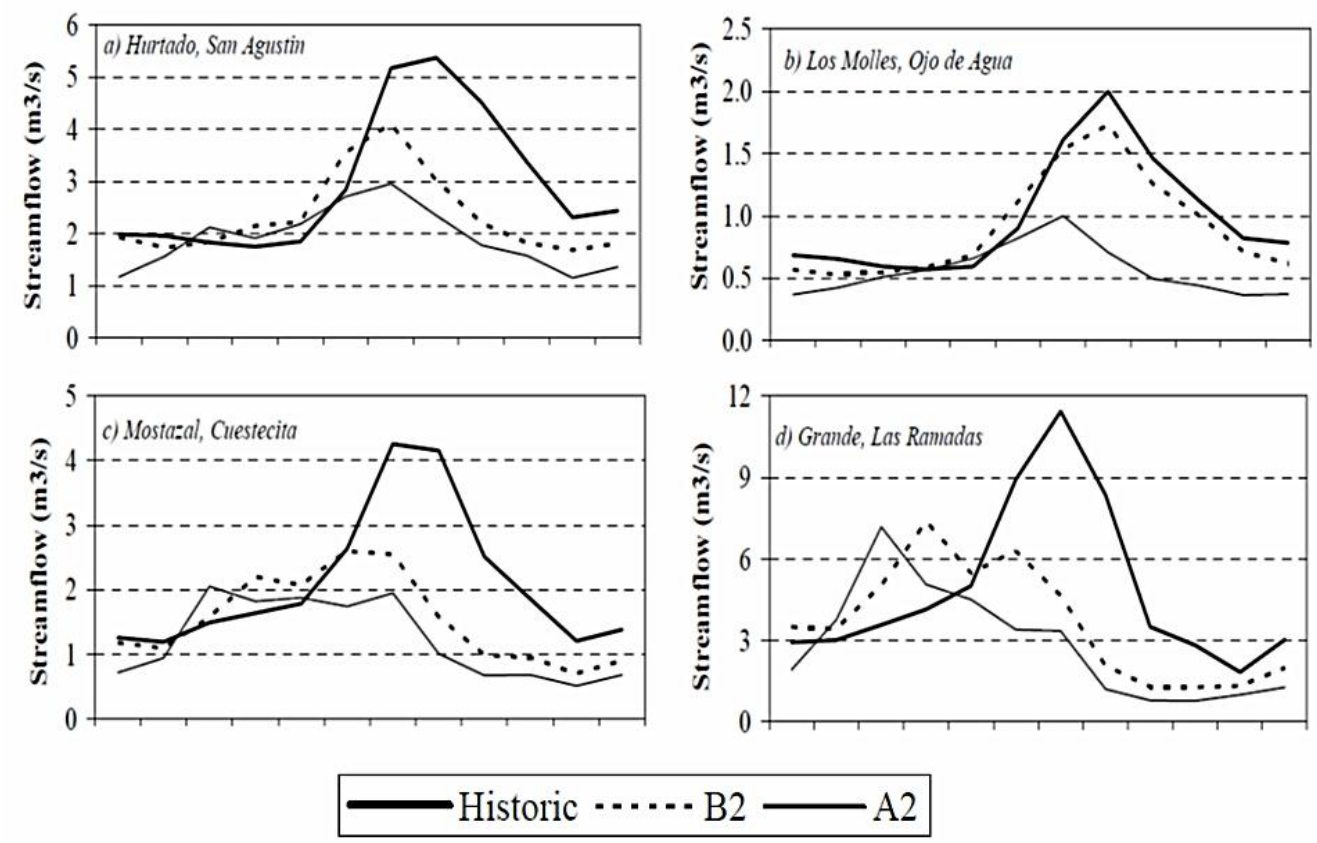

Figure 2-12: Hydrological model simulated mean monthly stream flow at four of the upper sub-basins of the Limari river basin system
[Adapted from Vicuna et al. (2011)]

In another hydrological study over Vietnam, Phan et al. (2011) applied the SWAT model to assess the impacts of climate change on stream discharge and sediment yield from Song Cau watershed in Northern Vietnam. Three climate change emission scenarios B1, B2, and A2; representing low, medium, and high levels of greenhouse gas emission, respectively, were considered in this study. It was reported that the highest changes in stream flow discharge (up to 11.4 %) and sediment load (15.3 %) could be expected during the wet season in 2050s according to the high emission scenario (A2), while for the low and medium emission scenarios, the corresponding changes were 8.8 % and 12.6 %, respectively. The results showed that the stream flow discharge was likely to increase in the future during the wet season with increasing threats of sedimentation.

2.7 SUMMARY

The different studies discussed in this chapter highlight both the importance and usefulness of applying regional climate model outputs for further hydrological impact studies. Since the GCM based outputs have been found to be too coarse for studying hydrological impacts, it is generally believed the high resolution RCM output has detailed climate information over the region of simulation. Hence, any well calibrated hydrological model is expected to yield credible simulations as long as the input to the model that comes from the RCM is of a good quality in terms of being able to represent the state of climate well enough. It is for this reason the calibration of the hydrological model is usually done using available station data and evaluated against some metrics (discussed further in Chapter 5). The uncertainties from the GCM that drives the RCM still propagates into the RCM to some extent but the RCM is expected to only improve the regional simulation owing to its higher resolution but not correct the large scale driving GCM conditions. Yet, these many studies have found the application of RCM derived outputs highly useful for hydrological impact assessments at regional and sub-regional scales. This review also supports the core theme of this research thesis that dynamical downscaling has been found to be sufficiently robust to study climate change due to their high resolution performance and for their 'added value'. In such a context, the application of the RCM outputs for hydrological impact studies in this thesis also stands justified.

Although discussing the general uncertainties in RCMs and hydrological simulations is not within the scope of this thesis, some uncertainties associated with these techniques resulting from this thesis in particular are discussed later in Chapters 4 and 5 and summarized in Chapter 6.

With this note, this chapter comes to an end. Further descriptions of different climate and hydrological models that are used in this study and some experimental methodologies that are followed in this study are given in the next chapter.

CHAPTER 3 MODELS, DATA, PERFORMANCE METRICS AND EXPERIMENTS

3.1 REGIONAL CLIMATE MODELS

An overview of the issue of climate change and of the study region has been done in Chapter 1, followed by literature reviews in Chapter 2, that have set the stage for this thesis. This chapter introduces the two regional climate models (WRF and PRECIS) and the hydrological model (SWAT) used in this study, discusses the different data used and outlines the experimental methodologies involved in the several stages of this study. The regional climate models are described first, followed by the hydrological model.

3.1.1 Weather Research and Forecasting (WRF) Model

Many previous research studies have established the skill of dynamical downscaling method as described in Chapter 1. Amongst various RCMs that are currently in use by different institutions, the WRF model, a widely used community model, has been in operation for the past few years. The effort to develop WRF has been a collaborative partnership, chiefly among NCAR, NOAA, NCEP, Forecast Systems Laboratory (FSL), Air Force Weather Agency (AFWA), Naval Research Laboratory (NRL), Oklahoma University and the Federal Aviation Administration (FAA) of the United States.

The WRF model is basically a mesoscale Numerical Weather Prediction (NWP) system designed to serve both operational forecasting and atmospheric research needs (Skamarock et al., 2008). WRF is suitable for a broad spectrum of applications across scales ranging from a few meters to thousands of kilometers and uses a three-dimensional grid to represent the atmosphere. The WRF software has a modular, hierarchical design that provides good portability and efficiency across a range of parallel computer architectures. The model incorporates advanced numerical techniques, a multiple nesting capability and numerous state-of-the-art of physics options that include user's choice of several physical atmospheric and land processes such as cumulus convection, moisture physics, planetary boundary layer,

radiation schemes and land surface hydrology. It is well suited for a wide range of applications, from operational forecasting to climate research simulations and the model also has the ability to be run at any spatial resolution as desired. The model version 3.2.1 was used in this study. The model has also the flexibility to be driven by any global climate model for climate change applications and hence WRF remains one of the widely used models in climate research as a dynamical downscaling tool. Additional information on the model can be found at: http://www.wrf-model.org/index.php.

3.1.2 Providing REgional Climates for Impacts Studies (PRECIS) Model

PRECIS is another regional climate modelling tool that can be run over any area of the globe on a relatively inexpensive, fast personal computer to provide regional climate information for impacts studies. The Hadley Centre at the UK MetOffice has configured the third-generation Hadley Centre RCM, PRECIS, which along with a software to allow display and processing of the data produced by the RCM. The RCM PRECIS is based on the atmospheric component HadAM3P of the GCM HadCM3 with substantial modifications to the model physics. Like WRF, many physical processes such as the dynamical flow, the atmospheric sulphur cycle, clouds and precipitation, radiative processes, the land surface and the deep soil are all described in the model. The model can, however, only be run at horizontal resolutions of either 0.44° (50 km) or 0.22° (25 km). Unlike WRF, the model (1) does not permit multiple nesting capabilities and (2) has fixed physics options. The PRECIS version 1.9.3 was used in this study. All data that are used to drive this model are pre-packaged by the Hadley centre and does not have the user flexibility to run with any data as such. The PRECIS model has been documented in detail by Jones et al., (2004) and is available from the PRECIS website: http://precis.metoffice.com/.

3.2 SOIL AND WATER ASSESSMENT TOOL (SWAT) Model

Rainfall runoff model is a typical hydrological modelling tool that determines the runoff from the watershed basin resulting from rainfall falling on the basin. Therefore, precipitation is an important input in deriving runoff in hydrological modelling. The SWAT model (Arnold et al.,

1998), used for rainfall runoff modelling in this study, was developed to quantify the runoff and concentration load due to the distributed precipitation, watershed topography, soil and land use conditions.

SWAT is a river basin scale model, developed by the United States Department of Agriculture (USDA) - Agriculture Research Service (ARS) in early 1990s. It has been designed to work for large river basins over a long period of time. Its purpose is to quantify the impact of land management practices on water, sediment and agriculture chemical yields with varying soil, land use and management condition. SWAT version 2005 with an ArcGIS user interface (ArcSWAT) was used in this thesis. There are two methods for estimating surface runoff in SWAT model: Green & Ampt infiltration method, which requires precipitation input in sub-daily scale (Green and Ampt, 1911) and the Soil Conservation Service (SCS) Curve Number procedure (USDA Soil Conservation Service, 1972) which uses daily precipitation. The latter was selected in this study for model simulations since daily rainfall from the climate modes was used as input to the SWAT model. Retention parameter is very important in SCS method and it is defined by Curve Number (CN) which is a function of the soil permeability, land use and antecedent soil water conditions. SWAT model offers three options for estimating potential evapotranspiration (PET). These options are: Hargreaves (Hargreaves et al., 1985), Priestley-Taylor (Priestley and Taylor, 1972) and Penman-Monteith (Monteith, 1965). Hargreaves method requires only maximum, minimum and average surface temperature. The Priestley-Taylor method needs solar radiation, surface temperature and relative humidity. The inputs for Penman-Monteith method are the same as those for Priestley-Taylor; however, it also requires the wind speed. Due to limitations in the available meteorological data for the site considered in this study, the Hargreaves method is applied. In the SWAT model, the land area in a sub-basin is divided into what are known as Hydrological Response Units (HRUs). HRUs are constructed through a unique combination of land use and soil information. One HRU is the total area of a sub-basin with a particular land use and soil characteristics. While individual fields with a specific land use and soil may be scattered throughout a sub-basin, these areas are

lumped together to form one HRU. These are used in most SWAT applications since they simplify a simulation by putting together all similar soil and land use areas into one single response unit (Neitsch et al., 2004). All processes such as surface runoff, PET, lateral flow, percolation, soil erosion, nitrogen and phosphorous are carried out in each HRU.

SWAT input requires spatial data such as the DEM (Digital Elevation Model), land use and soil map. In this study, the DEM of 250 m was obtained from the Department of Survey and Mapping (DSM), Vietnam. The land use map was obtained from the Forest Investigation and Planning Institute (FIPI) and the soil map was obtained from the Ministry of Agriculture and Rural Development (MARD), both, Vietnam. A full description of the SWAT model can be found at: http://www.swatmodel.tamu.edu. However, some essential components of the model are described in the Appendix F.

3.3 DATA

As indicated in the earlier sections, this study employs regional climate models (WRF and PRECIS) for climate simulations and then uses the output (surface temperature and precipitation) of these models as input to the SWAT hydrological model. The RCMs need to be driven by some large scale global data such as reanalyses (described in the next section) or GCM data for regional climate downscaling and then compared against available observed data for evaluating model performance. Similarly, the SWAT model needs to be calibrated against available station data to ensure good performance. These different data that are used in this study are discussed in the section ahead.

3.3.1 Global Reanalysis Data

Over the past decade, reanalyses of past multi-decadal observations have become an important and widely utilized resource for the study of atmospheric and oceanic processes. The different weather data (atmosphere, land and ocean) collected from different locations of the world are archived as a multi decadal time-series and later subject to quality control and data assimilation to produce a uniform database of several physical climate variables (such as

temperature, zonal and meridional winds, humidity, sea surface temperatures and surface pressure) in multiple atmospheric levels and surface levels at different temporal frequencies (6 hourly, daily, monthly to yearly). In short, these global observations are 'reanalysed' and hence termed 'reanalysis'. Since reanalysis are produced using the data assimilation systems, they are very suitable for use in climate studies. Two popular reanalysis datasets, widely used in climate research, that are available for long periods of multi-decadal time series are those developed at NCEP/NCAR, USA, and the European Centre for Medium range Weather Forecasting (ECMWF), UK. The former is known as the NCEP/NCAR reanalysis (available from 1948 onwards) and the latter is called as the European Reanalysis 40 years or in short, ERA40 (available from 1957-2002). The reanalysis datasets are generally termed as 'near perfect' boundary conditions as they are nothing but reanalysed observations. They are, therefore, representations of the 'true climate' of the earth.

Any regional climate model is first driven using one of these dataset to test whether the model is able to simulate the state of the climate reasonably well. It is common practice amongst climate modellers to use one of the reanalyses for testing and evaluating model performance and later drive the RCM using any GCM data for future climate projections. This study uses the ERA40 reanalysis dataset to drive the RCMs WRF and PRECIS to evaluate their performance over the 'present day' climate, the period between 1961 and 1990. It is noted here that the use of one reanalysis dataset, ERA40 (described below), is merely to test and evaluate the RCMs' performance and hence driving these two RCMs with the other NCEP/NCAR reanalyses dataset is not within the scope of this thesis. In short, driving any RCM with the reanalysis data is a sort of the calibration phase of the RCM to test its performance in being able to reproduce the 'true climate'. Once this is established, the RCM can be driven using the GCM data as the GCMs merely 'duplicate' the true climate. Nevertheless, the GCM driven simulations are important since the future climates are available only from GCMs and that the RCMs are used to downscale these future climates.

The ECMWF-ERA40 dataset

Developed at the ECMWF, UK, the ERA40 is a global atmospheric analysis of many conventional observations and satellite data available for the period 1957 - 2002. The analyses were produced 6-hourly daily at 00Z, 06Z, 12Z and 18Z hour. The atmospheric model was run with 60 levels in the vertical and spatial resolution of 2.5° × 2.5°. ERA40 has been used extensively by several climate modellers for simulating regional climates. They are also increasingly important for validating long-term model simulations, for helping develop a seasonal forecasting capability and for establishing the climate of EPS (Ensemble Prediction System) forecasts. Further details of this dataset can be obtained from their website at the address: http://www.ecmwf.int/about/overview. These datasets have also been documented by Uppala et al. (2005). This reanalyses dataset has been used in this study to evaluate the performances of RCMs WRF and PRECIS over the **present day climate, 1961-1990**.

3.3.2 Global Gridded Observation Data

As precipitation and temperature are two widely studied climate variables, there are several globally gridded observation datasets available. These datasets have been primarily developed using gauge/measured data from several station locations around the globe and subject to different interpolation techniques and quality control. These data have then been mapped at different spatial resolutions for the whole globe or for a specific region. A few of these datasets which are used in this study for evaluations of the RCM simulations are described in the following sections.

3.3.2.1 Climate Research Unit (CRU) Dataset

Developed at the Climatic Research Unit (CRU) at the University of East Anglia, UK, the CRU TS (Time-Series) version 3.0 dataset, used in this study, comprises monthly grids of observed climate, for the period 1901-2006 covering the global land surface at 0.5° of horizontal spatial resolution. This dataset is one of the most extensively used dataset by the climate modelling community. The precipitation and temperature datasets used in this study comprise data obtained from many land only locations around the globe. Data from the period 1961-1990 are used in this study for climate model evaluations. Further information on these

datasets is available at http://www.cru.uea.ac.uk/cru/data and is documented in detail by New et al. (1990, 2000) and Mitchell and Jones (2005).

3.3.2.2 Climate Prediction Center (CPC)

This global data product was developed by interpolation of gauge observations over land and by reconstruction of historical observations over ocean. This global rainfall dataset was initially developed at a 2.5° resolution and now is available at a 0.5° resolution, which is used in this thesis, for the period 1961-1990. This product has been derived from gauge observations from over 17,000 stations collected under the Global Historical Climatology Network (GHCN) and the Climate Anomaly Monitoring System (CAMS) datasets. These datasets have been documented by Chen et al. (2002) and further information is also available at ftp://ftp.cpc.ncep.noaa.gov/precip/. A 0.5° temperature dataset is also available from this source that has been used in this study for model evaluations for the 1961-1990 period.

3.3.2.3 Asian Precipitation Highly Resolved Observational Data Integration Towards the Evaluation of Water Resources dataset (APHRODITE)

APHRODITE's Water Resources project was conducted by the Research Institute for Humanity and Nature (RIHN) and the Meteorological Research Institute of Japan Meteorological Agency (MRI/JMA). The APHRODITE project developed state-of-the-art daily precipitation datasets at high-resolution grids (0.25° and 0.5°) for Asia. This study uses the 0.25° dataset of the Monsoon Asia region for the period 1961-1990. The datasets were created primarily with data obtained from a rain gauge observation network. The basic algorithm that was adopted is presented in Xie et al. (2007), with details on the methodology used. This dataset of precipitation is available on a daily scale, only for all land area covering all Asia and not available for oceanic areas. Further details can be obtained at http://www.chikyu.ac.jp/precip/ and from Yatagai et al., (2009, 2012). Surface temperature data are also now available from this product. These data, also at the same resolution of 0.25°, are used for comparisons of model simulations. This dataset is referred to as ***'APH'*** in the discussions of model results.

3.3.3 Station data

Some station data obtained from different locations in Vietnam are also used for climate model evaluations and hydrological model calibrations. For long term climatological comparisons with RCM results, 25 years of mean climatology rainfall and temperature data from 1961-1985 were taken from almost 200 stations all over Vietnam archived by the Vietnam National Hydro-Meteorological Service (VN HMS, 1989). Since most of the data are monthly values, few recorded daily precipitation and temperature data were obtained from the meteorological stations from the cities of Hanoi, Da Nang, Kon Tum and Ho Chi Minh City, which are the main popular cities in Vietnam that lie across the country spanning the broader climate zones from north to south (Figure 3-1a). These data were obtained from Institute of Meteorology Hydrology and Environment (IMHEN), Vietnam and their record lengths are shown in Table 3-1. These daily data have been used for some statistical computations and comparisons of RCM derived results of precipitation and temperature. Sufficient long records of daily and monthly data were not available from several other stations at the time of writing this thesis. Hence, statistical comparisons could not be made for any other station locations.

However, results of RCM simulations for both present day and future are discussed for the 7 climate zones of Vietnam in addition to referencing the main 4 cities for model evaluations. RCM derived future climate projections are given for these 4 cities and the 7 climate zones.

Table 3-1: Meteorological station data used

Station	**Recorded Period**	
	Precipitation	***Temperature***
Hanoi	1971-1990	1961-1990
Da Nang	1976-1990	1976-1990
Kon Tum	1964-1990	1976-1990
Ho Chi Minh City	1976-1988	1961-1987

The 4 main cities and their locations in Vietnam and the location of the Dakbla catchment with rainfall and discharge stations are shown in Figure 3-1.

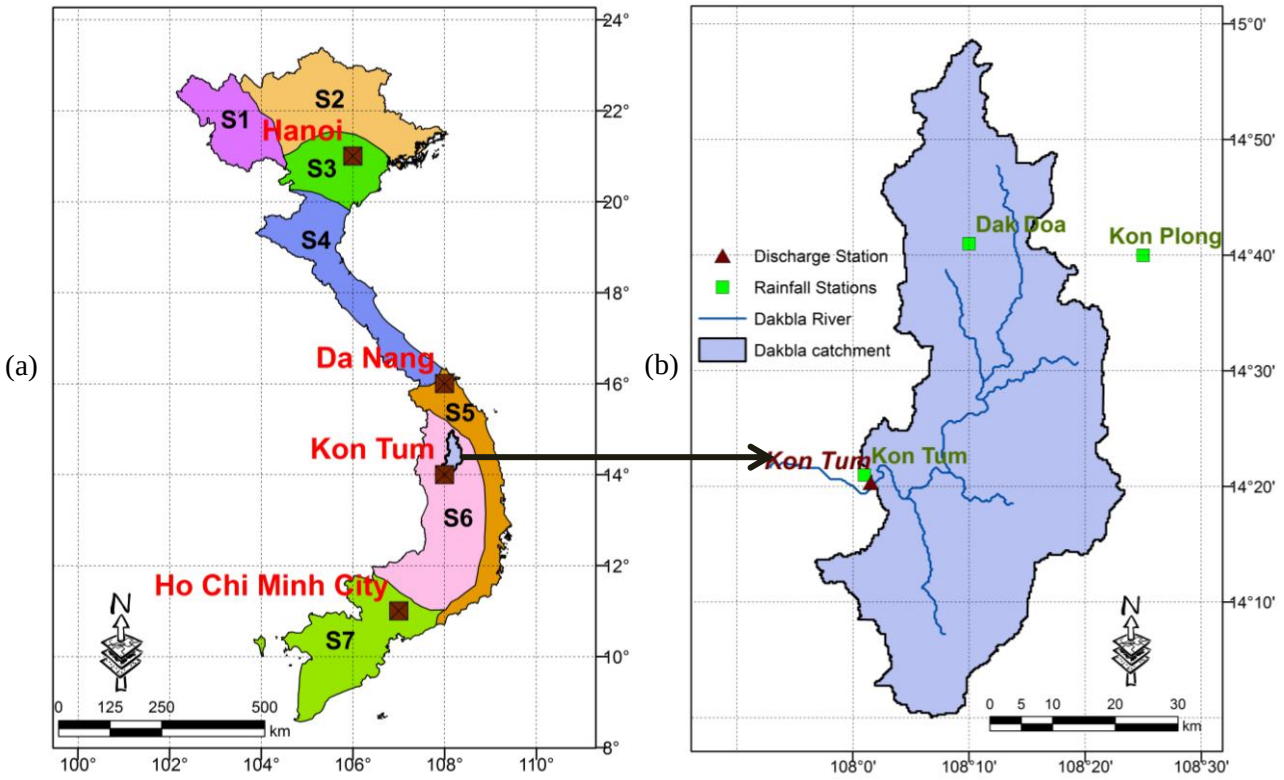

Figure 3-1: Map of Vietnam Climate Zones and Location of Dakbla catchment
(a) Different climate zones and meteorological stations used in this study (b) Dakbla catchment and its meteorological, gauging station

For hydrological simulations, daily precipitation data were obtained from three rainfall stations (Kon Plong, Kon Tum and Dak Doa) that lie outside the Dakbla catchment and daily river stream flow data were taken from the gauging station at Kon Tum, all shown in Figure 3-1b. All rainfall and discharge data have been taken for the period from 1981-2005. The widely distributed network of station locations have been tabulated (Table D-1) and shown (Figure D-1) in Appendix D.

3.3.4 GCM data

To study climate and its change, the primary information is provided by the GCMs. All GCM data used in this study have been obtained from the coupled model versions. Both present day (1961-1990) and future climate (2071-2100) information that are provided by these GCMs are used to drive the RCMs so that regional high resolution information on present day and future climates are obtained. It is customary to drive the RCM using the present day climate data from GCMs to establish credibility of RCM performance before the same GCM's future

climate data is used to drive the RCM to yield future downscaled climates. To this end, the different GCM data that were used to drive the RCMs (WRF and PRECIS) are described in the sections ahead. In this study, the lateral boundary and surface boundary conditions from the mentioned GCMs were used to drive the RCMs WRF and PRECIS at 6 hourly temporal frequencies. Future climate simulations of GCMs are usually performed under different scenarios of forcing experiments of possible changes in future emissions of greenhouse gases. (An overview of some of the IPCC TAR and AR4 climate change emission scenarios is given in the Appendix B).

3.3.4.1 Community Climate System Model (CCSM3.0) Data

The Community Climate System Model (CCSM) is a coupled (atmosphere-ocean) Global Climate Model developed by the University Corporation for Atmospheric Research (UCAR) and maintained at NCAR. The coupled components include an atmospheric model (Community Atmosphere Model), a land-surface model (Community Land Model), an ocean model (Parallel Ocean Program) and a sea ice model (Community Sea Ice Model). It has horizontal grids defined by 256×128 regular longitude and latitude divisions corresponding to a 1.4°×1.4° spatial resolution. The six hourly lateral and lower boundary conditions from version 3 (CCSM3.0) of this model are used in this study to drive the RCM WRF under present day and future climates (based on the IPCC A2 emission scenario). The present day climate conformed to the period 1961-1990 and the future period spanned 2071-2100.

3.3.4.2 European Centre Hamburg Model (ECHAM5) Data

The fifth-generation atmospheric general circulation model (ECHAM5) developed at the Max Planck Institute for Meteorology (MPIM), Hamburg, Germany, is the one in a series of ECHAM models evolving originally from the spectral weather prediction model of the ECMWF. This model has been run at a range of horizontal spatial resolutions having Gaussian grids of T21 to T159 (equivalent to longitude-latitude resolutions of 3.5° to 0.75°, respectively). A detailed description of the model has been provided by Roeckner et al. (2006). This thesis considers the 6 hourly lateral and surface boundary conditions from the T63

resolution (1.8°×1.8°) version of the GCM to drive the RCM WRF under the present day climate and future climate (based on the IPCC A2 emission scenario). Data from the present day climate for the period 1961-1990 and the future period 2071-2100 were used in this study for downscaling using the RCM WRF.

3.3.4.3 Hadley Coupled Model Version 3 (HADCM3) Data

This is one of the most popular and widely used of many GCMs available to the scientific community. Developed at the Hadley Centre, UK, it was one of the models used in the IPCC Third Assessment Report (TAR) in 2001 and the IPCC AR4 in 2007. Unlike earlier GCMs that were developed at the Hadley Centre, this version HadCM3 did not need flux adjustments (additional "artificial" heat and freshwater fluxes at the ocean surface) to produce a good simulation. The higher ocean resolution of HadCM3 has been a major factor to this end and this model is considered as one of the best among many GCMs since it was able to simulate the climates of different regions of the world reasonably well. The other factors for good performance of the model included a good match between the atmospheric and oceanic components and an improved ocean mixing scheme. This model has been run to produce simulations for periods of over a thousand years, showing little drift in its surface climate and also been run to generate future climate scenarios. The model has a horizontal resolution of 2.5°×3.75°, latitude by longitude. This model was used to drive RCM PRECIS under the present day and future climate (based on the IPCC A2 emission scenario).

It needs to be mentioned here that an ensemble method of downscaling is thus undertaken in this study as two different RCMs are driven by different GCMs under the same emission scenario A2, thereby increasing the confidence of the projected results on future climate over Vietnam, one of the first-of-its-kind dynamical downscaling studies done over this region.

3.4 PERFORMANCE METRICS

Regional Climate Model and Hydrological Model simulations need to be evaluated against observations using some statistical indices for benchmarking their performance. It is common understanding that should the model perform well over the past and present day climates, the future climate simulated by the same model is credible enough. Therefore, some performance metrics place confidence and robustness in the modelled results of the present day climate before the models can be confidently used for studying future climates. Some of such common performance metrics widely used among the climate and hydrological modelling community are discussed in the following sub-sections.

3.4.1 Bias

Bias is computed as the difference between the observed and modelled estimates. Precisely, it is a measure of the absolute magnitude of error between the observed and the modelled estimates as expressed in Equation 3-1:

$$Bias = \mu_M - \mu_O \qquad \text{(Equation 3-1)}$$

where μ_O is the domain averaged mean of the observations and μ_M is the domain averaged mean of the modelled estimates. Hence, the bias in this thesis simply refers to the difference between observations and the RCM estimates of climate variables, mainly, precipitation and temperature. Least the biases, better is the model performance.

3.4.2 Root Mean Squared Anomaly (RMSA)

Root Mean Squared Anomaly is also known as the root mean square deviation and is similar to the standard deviation, except this is used for large sample sizes, as given in Equation 3-2:

$$s_N = \sqrt{\frac{1}{N}\sum_{i=1}^{N}\left(x_i - \overline{x}\right)^2} \qquad \text{(Equation 3-2)}$$

The RMSA is calculated as above where ' $\overline{x}$ ' is the mean, ' x_i ' is each data value and 'n' is the number of observations. The term $x_i - \overline{x}$ is the anomaly or long term difference from

normal values. This index is useful to test the long term standard deviations or otherwise, the inter-annual variability of climate variables, which is a key test for climate model performance, especially precipitation.

The above two measures will be used for the evaluation of the regional climate models, WRF and PRECIS.

3.4.3 Nash-Sutcliffe Efficiency (NSE)

Proposed by Nash and Sutcliffe (1970), this index shows the skill of the estimates relative to a reference and it varies from negative infinity to 1 (perfect match). It is defined as one minus sum of the squared difference between observed and simulated normalized by the variance of the observed data (Equation 3-3):

$$NSE = 1 - \frac{\sum_{i=1}^{n}\left[\left(o_i - s_i\right)^2\right]}{\sum_{i=1}^{n}\left[\left(o_i - \bar{o}\right)^2\right]} \qquad \text{(Equation 3-3)}$$

where o_i and s_i indicate observed and simulated discharges at selected time step respectively, $\bar{o}$ is the mean of observation dataset and these indices are used for evaluating the simulations of the SWAT hydrological model. The NSE is considered to be the most appropriate relative error or goodness-of-fit measures available owing to its straightforward physical interpretation (Legates and McCabe, 1999).

3.4.4 Coefficient of Determination (R^2)

The Coefficient of Determination, R^2, is used as another benchmarking index for the simulated stream flow. R^2 is the square of correlation coefficient. The R^2 ranges from 0 to 1 of which value 0 shows no correlation whereas 1 indicates perfect match. The R^2 formula is shown in Equation 3-4.

$$R^2 = \left[\frac{\sum_{i=1}^{n} \left[(x_i - \bar{x})(y_i - \bar{y}) \right]}{\sqrt{\sum_{i=1}^{n} \left[(x_i - \bar{x})^2 \right] \sum_{i=1}^{n} \left[(y_i - \bar{y})^2 \right]}} \right]^2 \qquad \text{(Equation 3-4)}$$

where $\bar{x}$ and $\bar{y}$ are the average of the x_i and y_i time series respectively.

3.5 MODEL EXPERIMENT APPROACH

The different climate simulations that are performed using the RCMs WRF and PRECIS and the hydrological model SWAT are described in this section. The flow chart in Figure 3-2 summarizes the full experimental methodology of this research study.

3.5.1 WRF model

The regional climate model WRF was used to dynamically downscale present day (1961-1990) and future climates (2071-2100). First, the WRF model was driven by the global reanalyses ERA40 to benchmark its performance over the present day climate period of 1961-1990. This 30-year time frame is a conventionally accepted baseline climate period used by the IPCC. Since the WRF model comes with a suite of physics options or parameterizations (those essential physics that are built in the model to replicate actual atmospheric processes), a best set of physics options that well simulate the tropical climate of this region was chosen. This best set of options is shown in the Appendix C, along with some overview of what these parameterizations are. The choice of this set of options stem from (1) the WRF technical report (available at www.wrf-model.org), (2) some literatures (Fernandez et al. (2007); Venkararatnam and Cox (2006); Venkataratnam and Krishnakumar (2005); Seth and Rojas (2003); Yang and Tung (2003); Wang (2002)) that have used the model for tropical climates, and (3) the climate and weather modelling research experience from the several projects undertaken by the Tropical Marine Science Institute, National University of Singapore.

Some performance metrics were used as statistical indices to establish model performance. This step was necessary to ensure that the model was able to produce realistic results for the present day climate so that projected future climate from the same model can be deemed credible.

As the next step in generating future climate scenarios, the WRF model was driven by two GCMs: CCSM3.0 and ECHAM5, for both the present day (1961-1990) and future (2071-2100). The future climate was in accordance with the IPCC A2 emission scenario. The last 30 years of the 21st century were considered for future climate projections because a clear signal of climate change is more pronounced on a longer time scale (IPCC, 2007a). The difference between the future and present day model derived climate (precipitation and temperature) output was derived and called the 'climate response', otherwise known as the 'climate change signal'. This gives the changes in the future rainfall and temperature conditions and this information, i.e…, the outputs of RCM precipitation and temperature, were then used as an input to the SWAT hydrological model to simulate future hydrological changes over the study catchment. The SWAT hydrological simulations are described in Chapter 5.

3.5.2 PRECIS model

As mentioned earlier, since it is entirely pre-packaged as software, the user-interface allows any user to run simulations easily. The model does not have detailed options and functionalities as that of WRF, but the simulations are easy to be initialized since all model data and parameterization options are in-built and not changeable. In this study, the ERA40 reanalyses were used for the present day climate (1961-1990) simulations, but for climate scenarios, the PRECIS model was driven by the GCM HadCM3 for the period 1961-1990 and 2071-2100. Since the PRECIS model comes with its own boundary conditions, in this case the GCM HadCM3 boundary conditions, it does not have the flexibility to use other GCMs that were used to drive WRF. Hence, only one scenario for future climate from HadCM3 was performed using PRECIS. Similar to WRF outputs, the precipitation and temperature outputs derived from PRECIS were then used as inputs for hydrological simulations using the SWAT

model. It also needs to be added here that the GCM HadCM3 data were available for the PRECIS model due to being already pre-processed and packaged by the developers (Hadley Centre). At the same time, sufficient lateral boundary data from the GCM HadCM3 were not available for running the WRF model, the technical format of WRF being different than that of PRECIS.

3.5.3 Choice of emission scenarios

A2 scenario has been selected as one of the case study out of IPCC Emission scenarios. It would have been ideal to run the worst-case scenario, A1FI, so that adaptive measures can be based on that. It is common understanding that once adaptation/mitigation measures are planned for the worst-case, any 'less' severe changes can be accommodated within the policy and adaptation management issues. The primary data that are required to run RCMs (WRF, in this case) come from GCMs. Sufficient boundary conditions were not available for the A1FI scenario from the GCMs considered in this study (and others of the IPCC AR4), at the time of this research study. Hence, A2 is the second worst-case (pessimistic scenario) based on CO_2 emissions after A1FI. Since adequate boundary conditions were available from GCMs for this scenario, the A2 scenario was considered.

Further, the PRECIS model does NOT have any A1FI scenarios as data are pre-packaged by the Hadley Centre.

Also, to consider an "ENSEMBLE" approach, SAME scenario from different GCMs is ideal. Hence, for both WRF and PRECIS runs, the A2 scenario was considered from whatever GCM data available.

3.5.4 SWAT model

The SWAT model initially takes the station data rainfall for simulating stream flow, whose results can be verified using the observed stream flow/ discharge data. To ensure a good performance of the model, the initial set up of the model entails a sensitivity analysis, calibration and validation stages using station data rainfall, maximum/minimum surface

temperature and river discharge data from the gauging station. This step ensures to benchmark the model performance using the statistical metrics cited earlier. Once this stage is done, the SWAT model can be deemed suitable to be used with the rainfall outputs taken from the regional climate models for simulating stream flow. Inputs to SWAT model consist of spatial and temporal data. Spatial datasets include the Digital Elevation Model, land use and soil maps. Temporal data is a collection of time series data from different rainfall and meteorological stations. The output of the SWAT model is a daily time series of stream flow at input and output of each sub-basin and downstream end of the chosen catchment. In this thesis, the SWAT model output simulated at Kon Tum gauging station (location of the study catchment described in Chapter 2) is then compared against its observational counterpart, to evaluate the performance of the model. The rainfall and surface temperature output from the two RCMs WRF and PRECIS are bi-linearly interpolated to the nearest grid point location of the station location and then fed into SWAT model to simulate future stream flow. All these procedures are described in detail in Chapter 5.

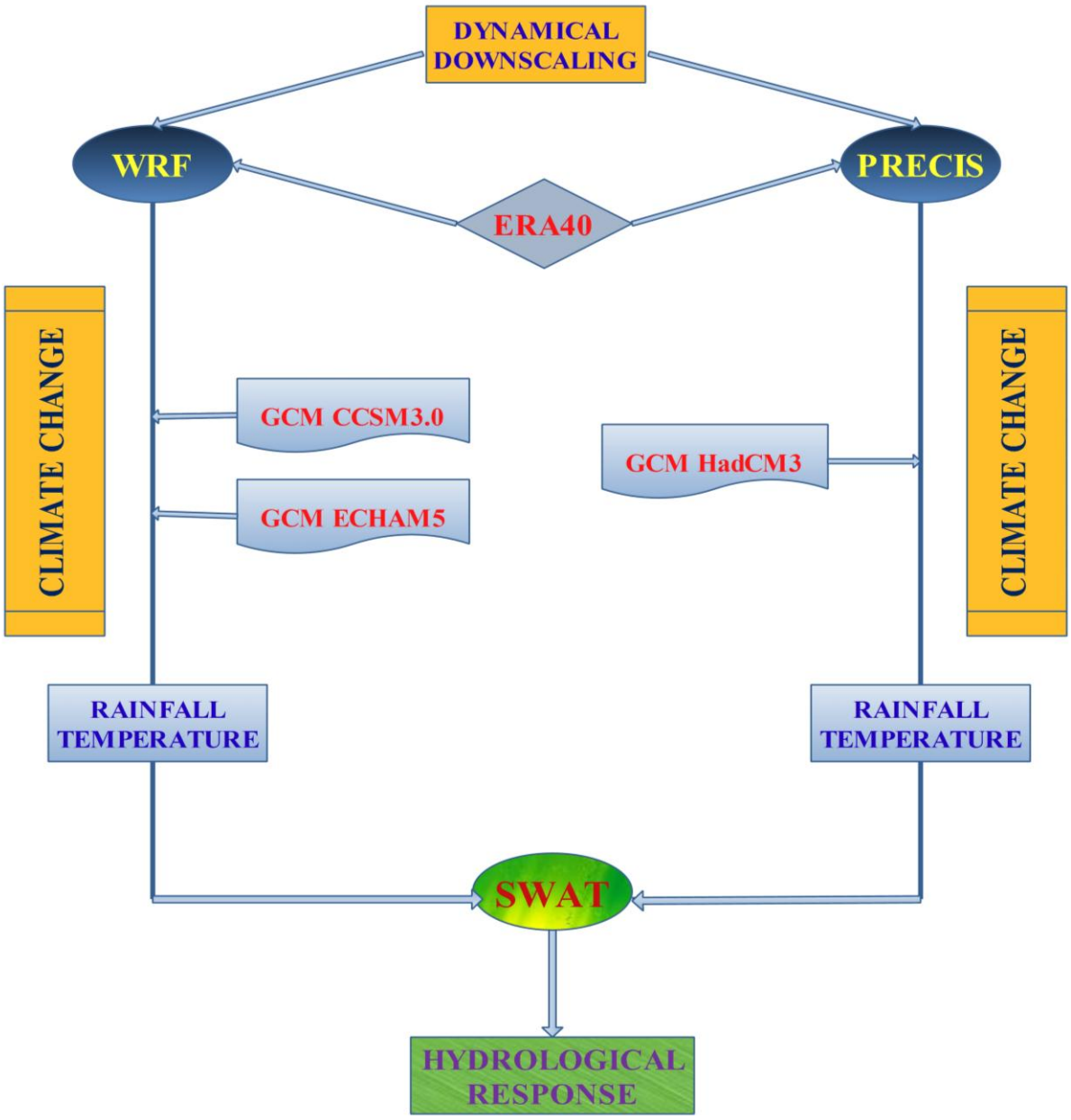

Figure 3-2: Experimental method of the use of climate models and hydrological model to assess future climate change

3.6 END REMARKS

With all these sections described above, the overview of climate and hydrological models, different data used for both simulations and comparisons of these models, performance metrics and experimental methodologies is complete. The next chapter discusses the results of the different dynamical downscaling experiments using the RCMs WRF and PRECIS.

CHAPTER 4. REGIONAL CLIMATE MODELLING OVER VIETNAM

4.1 INTRODUCTION

The regional climate models WRF and PRECIS have been used in this study to ascertain future climate change over Vietnam. Initially, both models were driven by the ERA40 reanalysis to assess the performance of the models over the present-day climate during the period 1961-1990. Later, the WRF model was driven using the GCMs CCSM3.0 and ECHAM5 to simulate the climate over the region for both present day (1961-1990) and future (2071-2100) periods. The future climate simulations were under the IPCC A2 emission scenario. The PRECIS model was also simulated for the 1961-1990 and the 2071-2100 periods using the GCM HadCM3, with the future period conforming to the A2 emission scenario. Since the PRECIS model is pre-packaged by the MetOffice, the GCM HadCM3 was the only option available to generate future scenarios under the A2 scenario, at the time of the completion of this thesis. For the same reason, the other GCMs that were used to drive the WRF model could not be used to drive the PRECIS model. Of the model output fields, rainfall, being the most important climate variable and an input to the hydrological model, is widely discussed in this chapter. The model simulations of surface temperature and wind fields are discussed first.

For clarity in reading, some abbreviated forms of model results are used for discussions. The use of 'DJF' indicates the December-January-February months of the Northeast (NE) monsoon and 'JJA', the months of June-July-August of the Southwest (SW) monsoon. Also, 'MAM' refers to the months March-April-May and 'SON' represents 'September-October-November'. For easy reading, the **model simulations of WRF driven by the ERA40 reanalyses, GCM CCSM3.0 and GCM ECHAM5 are referred to as WRF/ERA, WRF/CCSM and WRF/ECHAM, respectively, whilst the PRECIS model results driven by ERA40 and GCM HadCM3 are referred to as PRE/ERA and PRE/HAD, respectively**. These different simulations are discussed in the sections ahead. The 7 sub-climate zones, named S1 to S7, as tabulated in Table 1-2, will be referred to in the discussions of modelled results.

4.2 SIMULATIONS OF PRESENT DAY CLIMATE

Before we begin with the analyses of the RCM results, Figure 4-1a shows the entire RCM domain (encompassing a larger area of Southeast Asia to accommodate wider regional climate circulations) and Figure 4-1b shows the zoomed-in area of the Indochina region in which Vietnam is centered. The domain coordinates are indicated for clarity. As such the same coordinates hold good for all other similar spatial graphical plots shown in this chapter. Since the focus is on Vietnam, all graphical plots show the delineation of Vietnam's political boundary and climate zones within the domain and it is noted here that the model results for this smaller domain (Figure 4-1b) alone are described in this chapter, along with main discussions over Vietnam and its 7 climate zones. However, an overview of the climate simulations over the larger domain is presented in Appendix E (Figures E1 to E4).

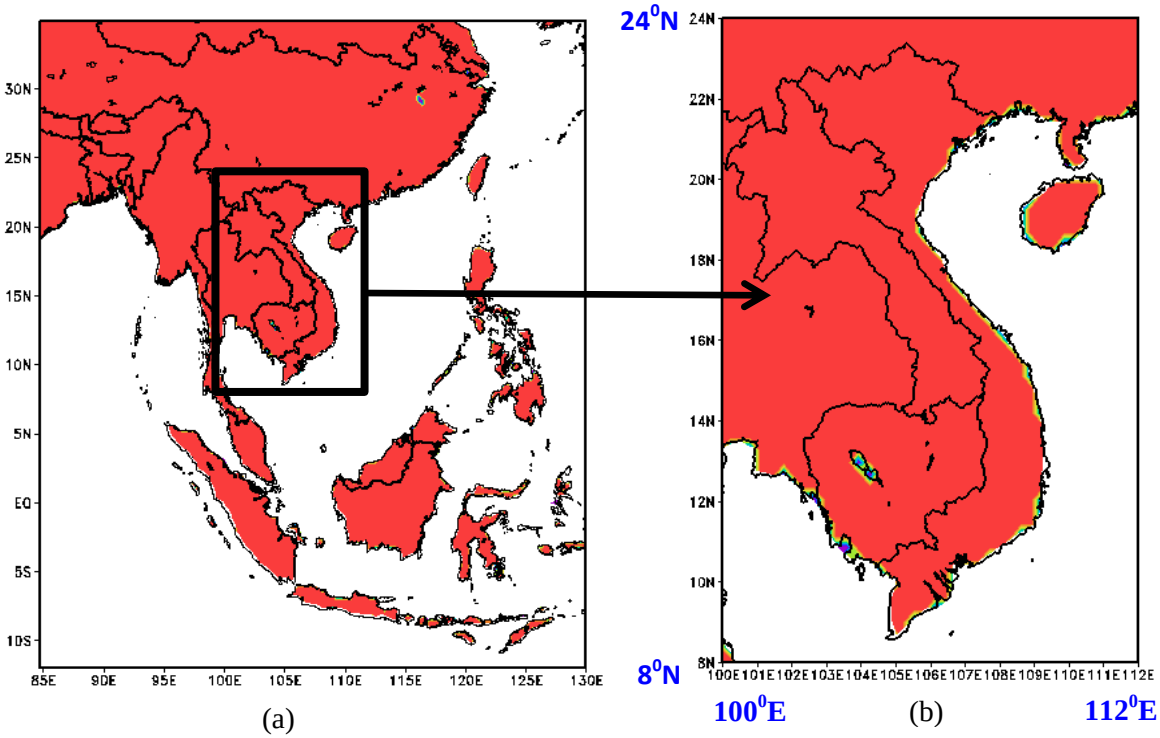

Figure 4-1: Domain configurations
(a) RCM Domain with inset showing Indochina domain (b) Indochina domain

To start with, the model simulations of mean annual, seasonal (DJF and JJA) surface temperatures for the 1961-1990 period are shown in Figure 4-2 to Figure 4-4, respectively, compared to CRU, CPC, APH and station observations. It is noted here again that the spatial

distribution of Vietnam station observed data (Figure 4-2d) and wherever shown, has been interpolated from all available meteorological station data for the period 1961-1985, as described in Section 3.3.3, also shown in Appendix D. For easy reading of discussions of results, 'S1' to 'S7' have been marked in some of the figures.

As seen in Figure 4-2 for annual average temperature, the simulations of both WRF and PRECIS models driven by ERA40 (e, f) and the different GCMs (g, h, i) show highly reasonable agreement on comparison with the different observational datasets. The gradients of high (low) temperatures over western (eastern) regions are resolved well. Lower temperatures over high terrain of S1 and S6 are also well reproduced in both the RCMs when compared against station and APH data in Figure 4-2 (c, d). Amongst all observation data, APH shows the hottest values of observations, especially over the western side of the domain. The WRF/ERA and WRF/CCSM simulations show a good agreement against APH. (All the other seasonal climatological plots (MAM, SON) (Figure E-5 and Figure E-6) and bias plots between models and observations (Figure E-7) are displayed in Appendix E, due to limitations of space in this chapter).

The winter (DJF) temperature for Vietnam is displayed in Figure 4-3. The RCMs are able to capture, very well, the distinct temperature gradients between the north regions of Vietnam (S1, S2, S3, S4) and the south (S5, S6, S7). The simulations of PRE/ERA and PRE/HAD show the characteristic temperature differences on either sides of latitude 16 °N, the border of S4 and S5. This feature is also seen in the APH and station data. The WRF results agree well against CRU and CPC observations. The summer (JJA) temperatures in Figure 4-4 clearly show the big difference between high (S1, S6) and low (S3, S7) terrain temperatures. WRF/ERA and WRF/CCSM reproduce the high temperatures over S3, S4 and S7 as found in APH, reasonably well. Simulations of WRF/ECHAM, PRE/ERA and PRE/HAD show the same pattern of temperature distributions as those of CRU, CPC and the station data.

Some model biases are shown in the Appendix E, Figure E-7 indicate that the RCM simulations of WRF & PRECIS exhibit least biases for surface temperatures when driven by both ERA40 and GCMs.

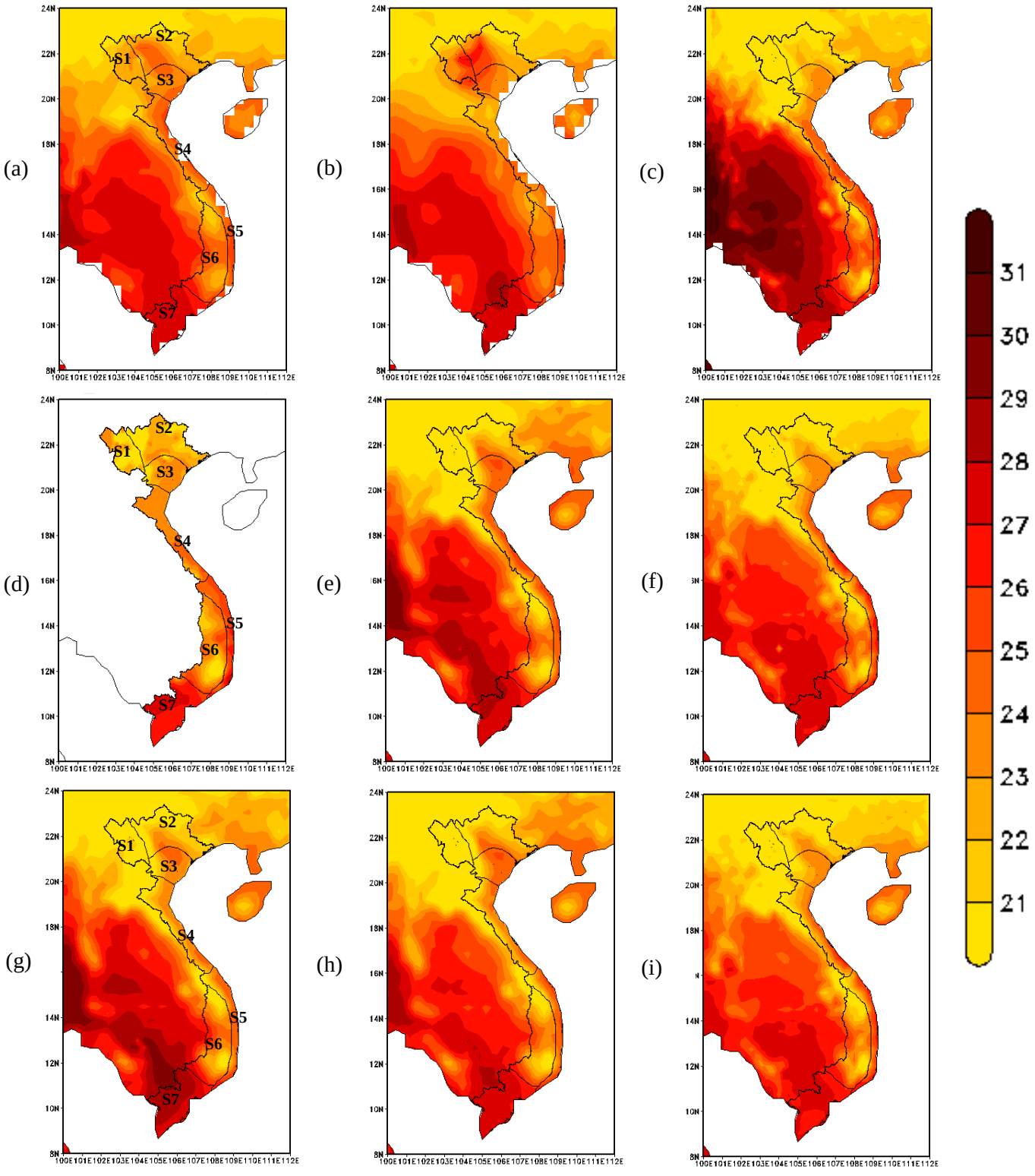

Figure 4-2: Mean Annual Surface Temperature, 1961-1990, °C
(a) CRU (b) CPC (c) APH (d) Station Data (e) WRF/ERA (f) PRE/ERA
(g) WRF/CCSM (h) WRF/ECHAM (i) PRE/HAD
NOTE: The single colour scale bar that is shown on the right is applicable for all individual plots and this is followed for other figures as necessary for effective arrangement of figures.

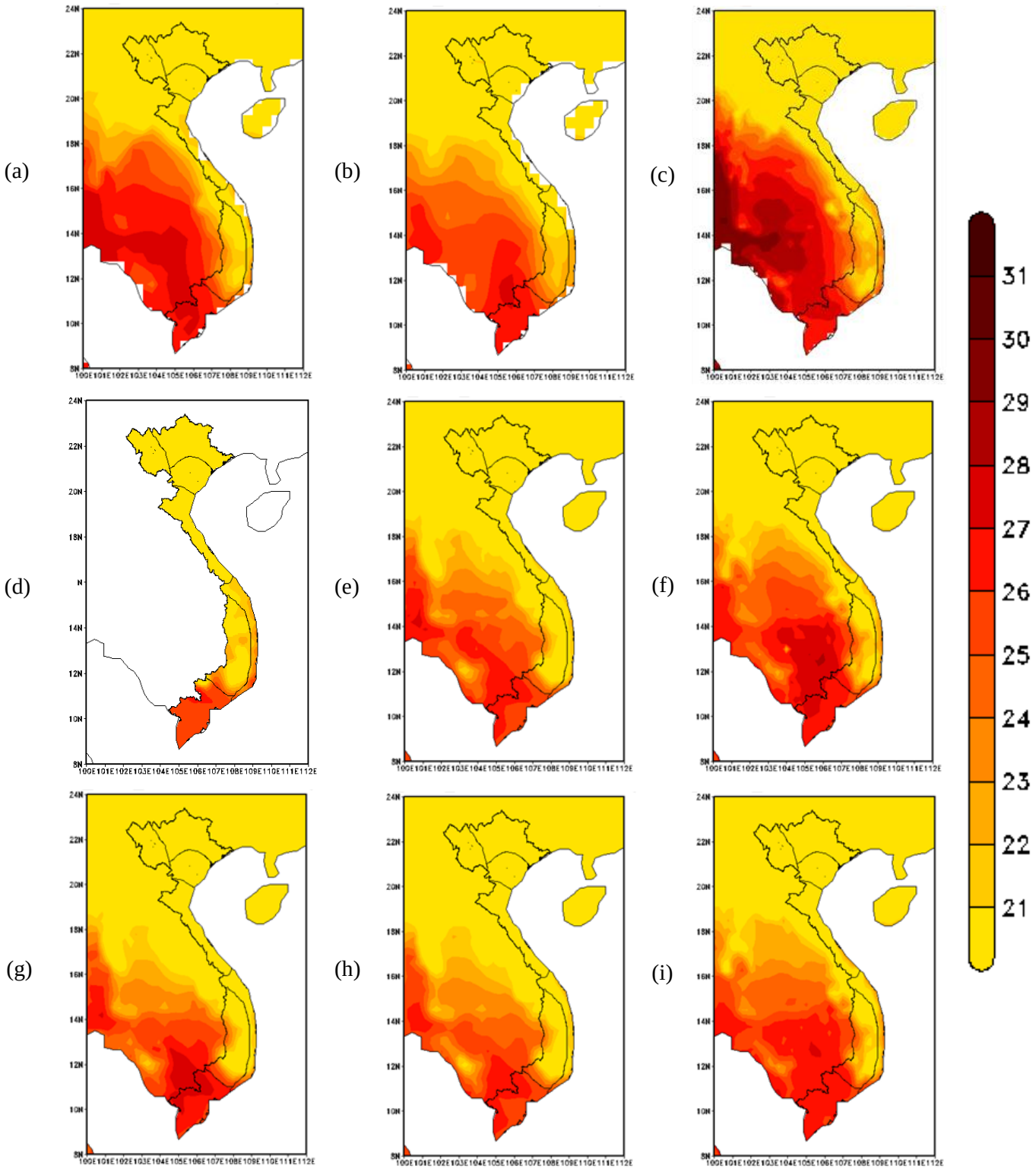

Figure 4-3: Mean Seasonal (DJF) Surface Temperature, 1961-1990, °C
(a) CRU (b) CPC (c) APH (d) Station Data (e) WRF/ERA (f) PRE/ERA
(g) WRF/CCSM (h) WRF/ECHAM (i) PRE/HAD

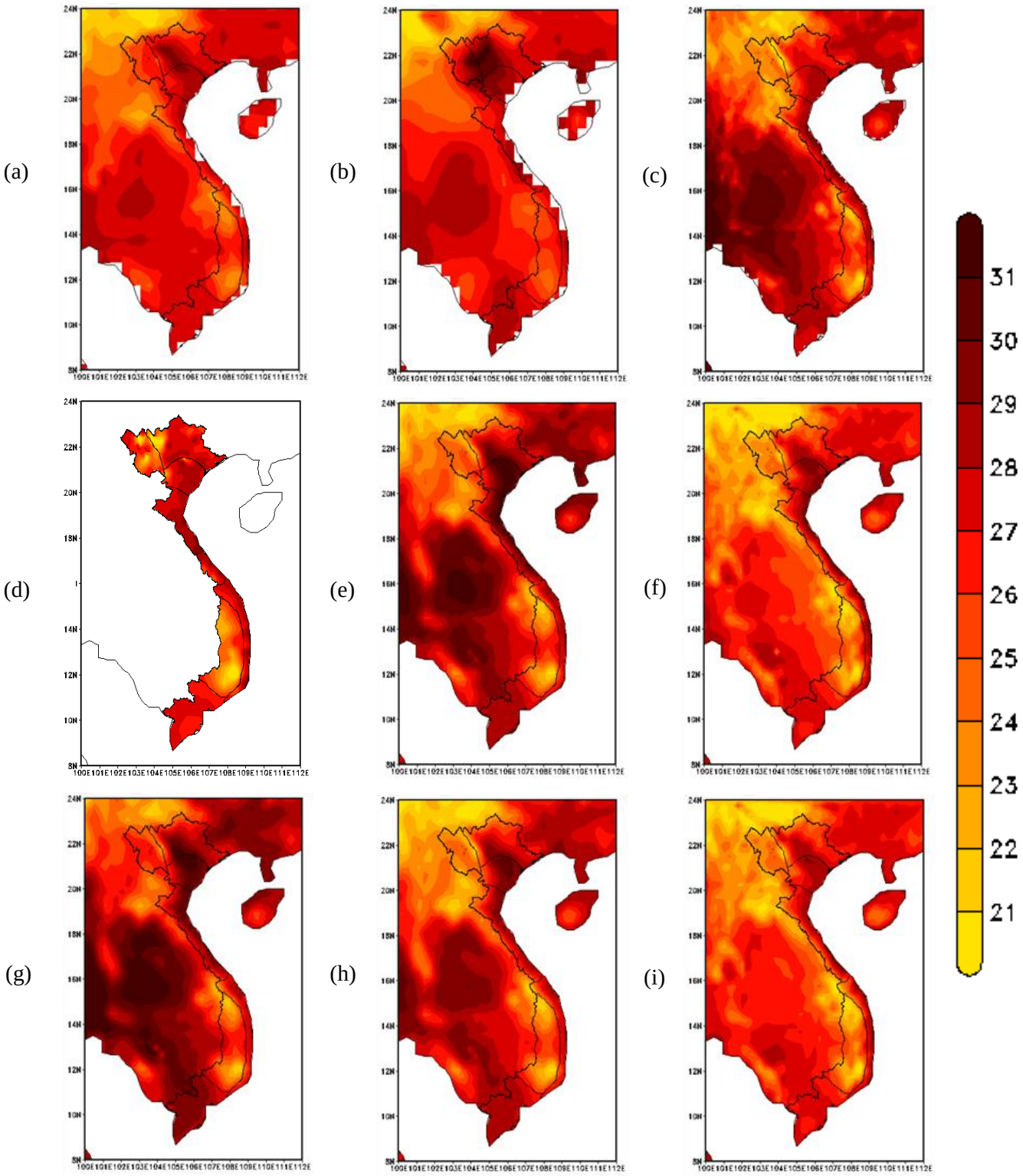

Figure 4-4: Mean Seasonal (JJA) Surface Temperature, 1961-1990, °C
(a) CRU (b) CPC (c) APH (d) Station Data (e) WRF/ERA (f) PRE/ERA
(g) WRF/CCSM (h) WRF/ECHAM (i) PRE/HAD

The annual cycles of temperature over the 4 locations (Hanoi, Da Nang, Kon Tum and Ho Chi Minh City) are shown in Figure 4-5. The cyan colour band in the figure indicates the minimum-maximum ranges of the gridded observed data from CRU, CPC and APH temperature datasets. Whilst all model simulations agree quite well against station data and gridded observations, the best profiles are simulated for Hanoi and Da Nang, although with higher values during the JJA season arising from WRF simulations and a near perfect agreement from PRECIS simulations for Hanoi. A better agreement is seen for Da Nang with nearly all simulated data falling within the observed ranges. Over Ho Chi Minh City, there is a very reasonable agreement against station data from PRECIS simulations while the WRF simulations place themselves higher than station measurements and observations. Over Kon Tum, the model simulations underestimate of about 2°C but match well with the pattern of the station data.

It is also a useful measure to evaluate how well the RCMs simulate the distribution of temperature profiles, especially in daily scale. To this endeavour, the Probability Density Functions (PDFs) of surface temperature simulations are plotted in Figure 4-6 (driven by reanalyses) and Figure 4-7 (driven by GCMs), respectively. In both cases, the profiles show good agreement against station distributions, especially over Da Nang, Ho Chi Minh City and Kon Tum stations. It needs to be mentioned here that since the PDF is plotted on a daily time step, besides station data, only the APH data is included in the plot, since daily scale data are available only from APH and not CRU and CPC. In addition, the PDFs of the surface temperature profiles simulated by the RCMs driven by GCMs are significant because it should be recalled here that the reanalysis (ERA40) driven RCM simulations are ‘true’ climate being ‘reanalysed observations’ whilst the GCMs are meant to duplicate the true climate. Since future climates are derived from GCMs and their downscaled results, it is imperative that the RCMs downscale the GCMs to a reasonable extent such as the reanalyses. From the results, it can be seen that the PDFs highlight the good performance of the RCMs.

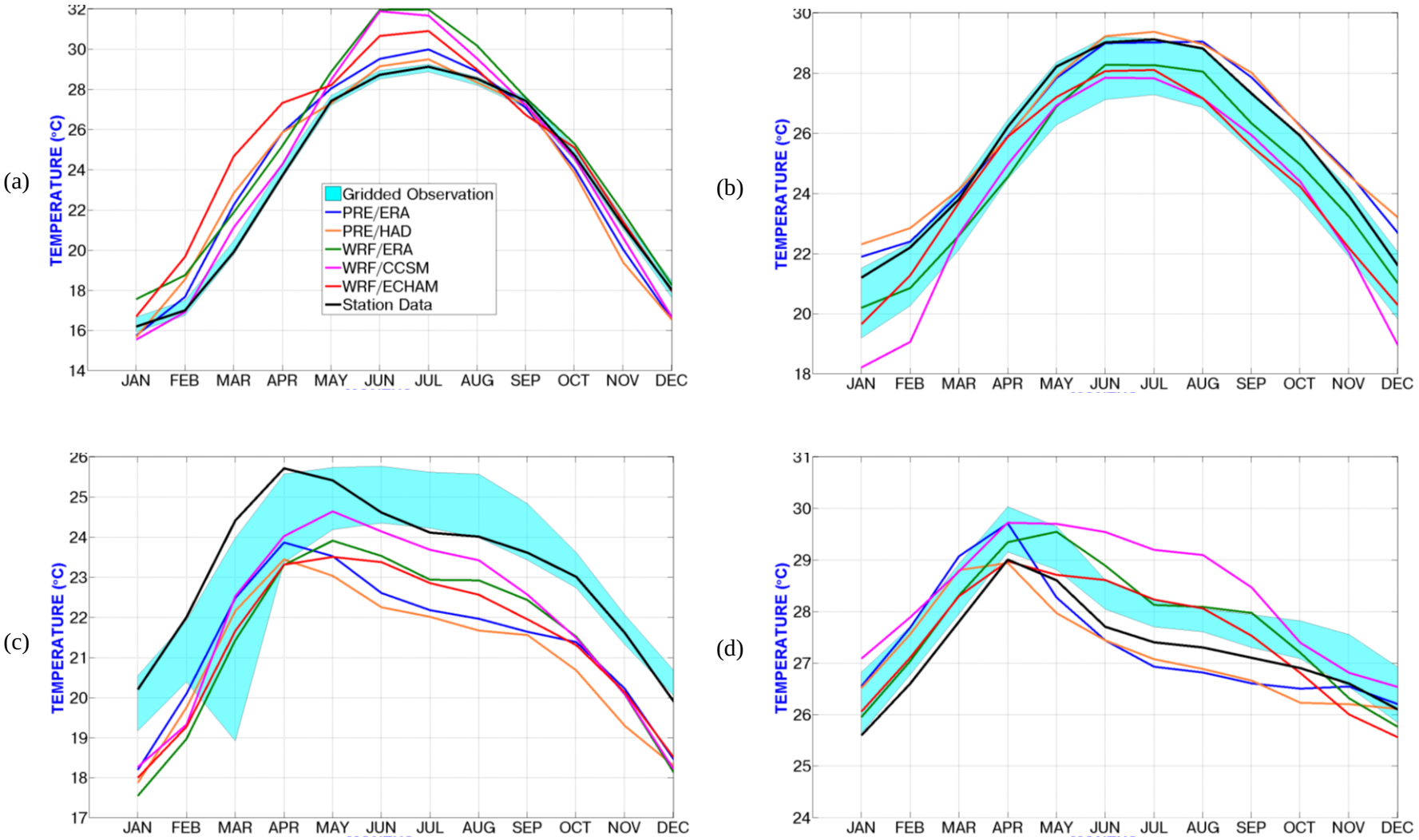

Figure 4-5: Annual Cycles of Surface Temperature, ^{o}C
(a)Hanoi (b) Da Nang (c) Kon Tum (d) Ho Chi Minh City

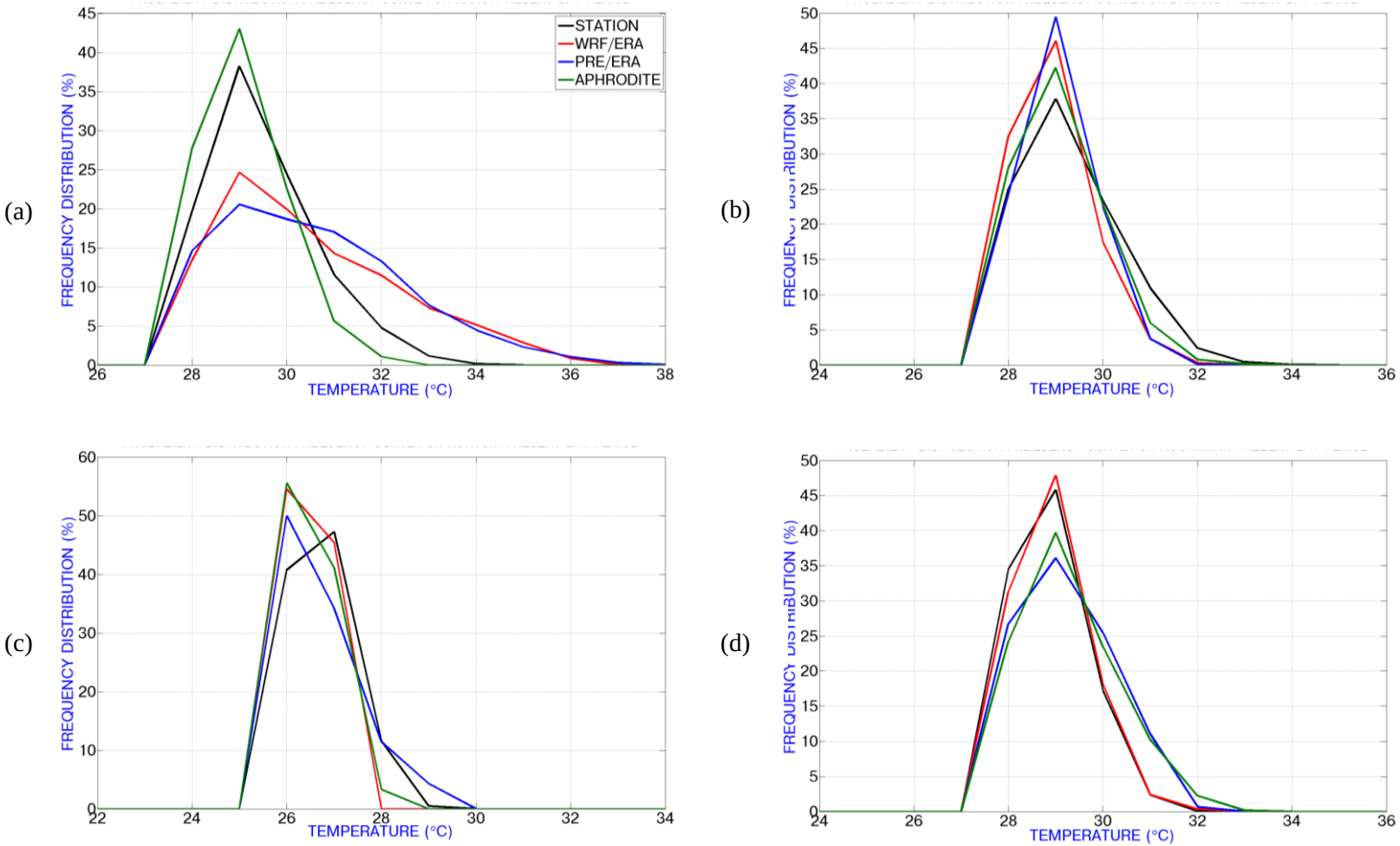

Figure 4-6: Probability Density Functions of Surface Temperature, °C, (WRF and PRECIS driven by ERA40 reanalysis)
(a) Hanoi (b) Da Nang (c) Kon Tum (d) Ho Chi Minh City

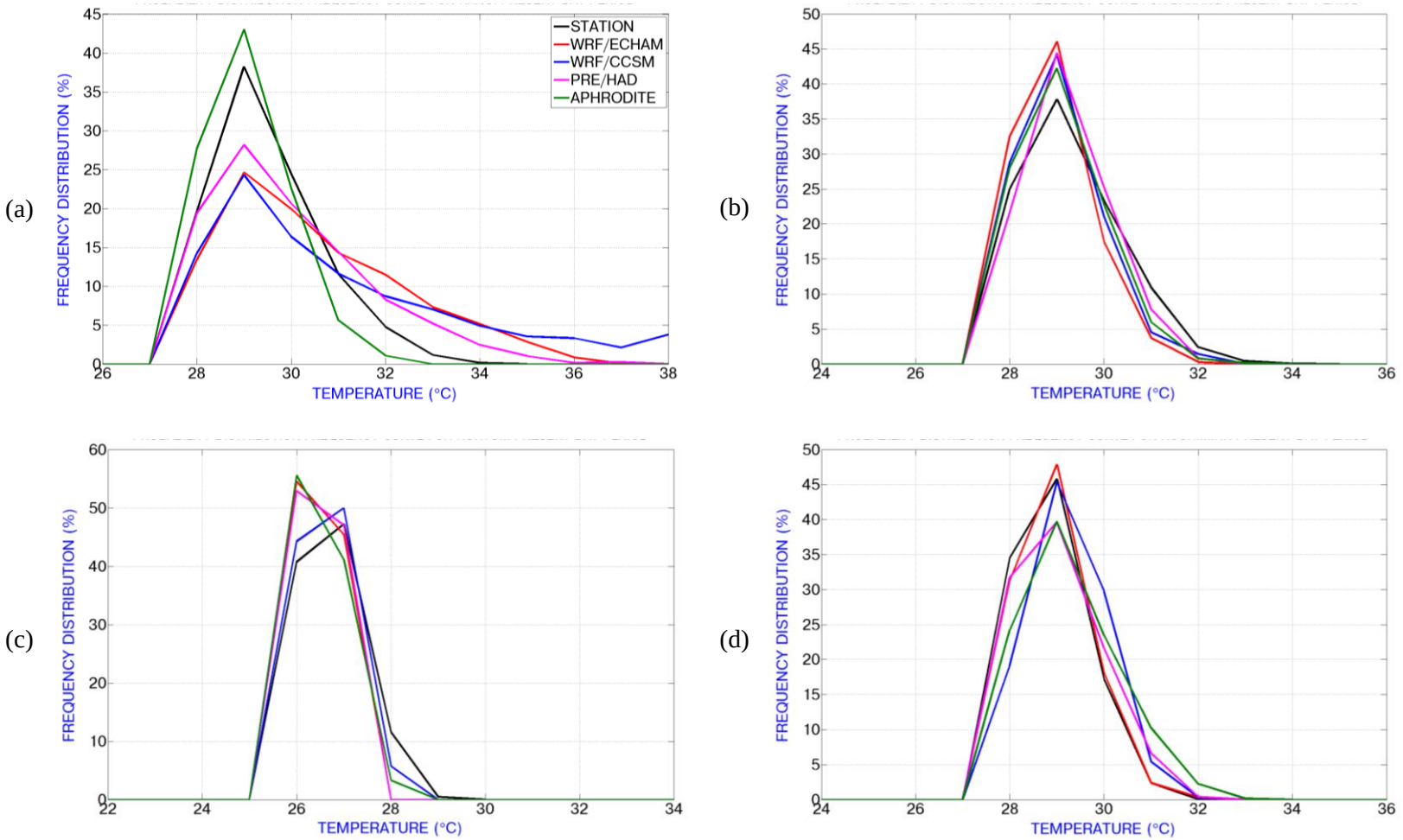

Figure 4-7: Probability Density Functions of Surface Temperature, °C, (WRF and PRECIS driven by different GCMs)
(a) Hanoi (b) Da Nang (c) Kon Tum (d) Ho Chi Minh City

Next to the surface temperature analysis, the RCMs simulations of surface winds deserve a look. The WRF and PRECIS models simulated surface wind patterns are shown in Figure 4-8 and Figure 4-9 for the Northeast Monsoon and the Southwest Monsoon seasons, respectively. These wind patterns are shown here in a qualitative perspective in evaluating model performance as a whole, although not used for any impact study in this thesis. The colour shaded distributions indicate the wind speed (m/s) and the wind vectors indicate the direction of the winds. During both seasons, both RCMs simulate the wind patterns reasonably well. The RCMs also resolve well the low wind speeds over the high terrain. As seen in Figure 4-8, the NE monsoon blowing from the north eastern side of the domain are attenuated when entering from the ocean to mainland mountainous area at latitude 16 °N at Hai Van Pass. Though there are no high resolution observations to support this feature, this circulation feature has been reported by Ho et al. (2011). The RCMs, WRF and PRECIS, clearly resolve this circulation but not seen in the coarser dataset of ERA40 (Figure 4-9). These model performances of wind circulation once again highlight the 'added value' in downscaling due to high resolution and terrain influences.

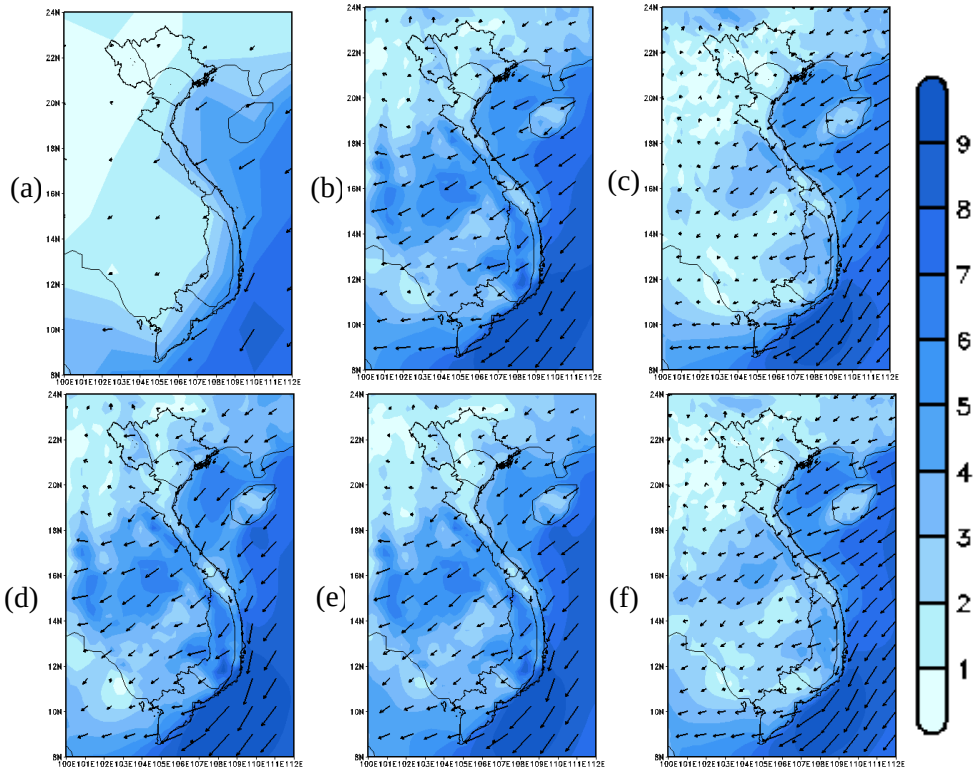

Figure 4-8: Mean Seasonal (DJF) Surface Winds, 1961-1990, m/s
(a) ERA40 (b) WRF/ERA (c) PRE/ERA (d) WRF/CCSM (e) WRF/ECHAM (f) PRE/HAD

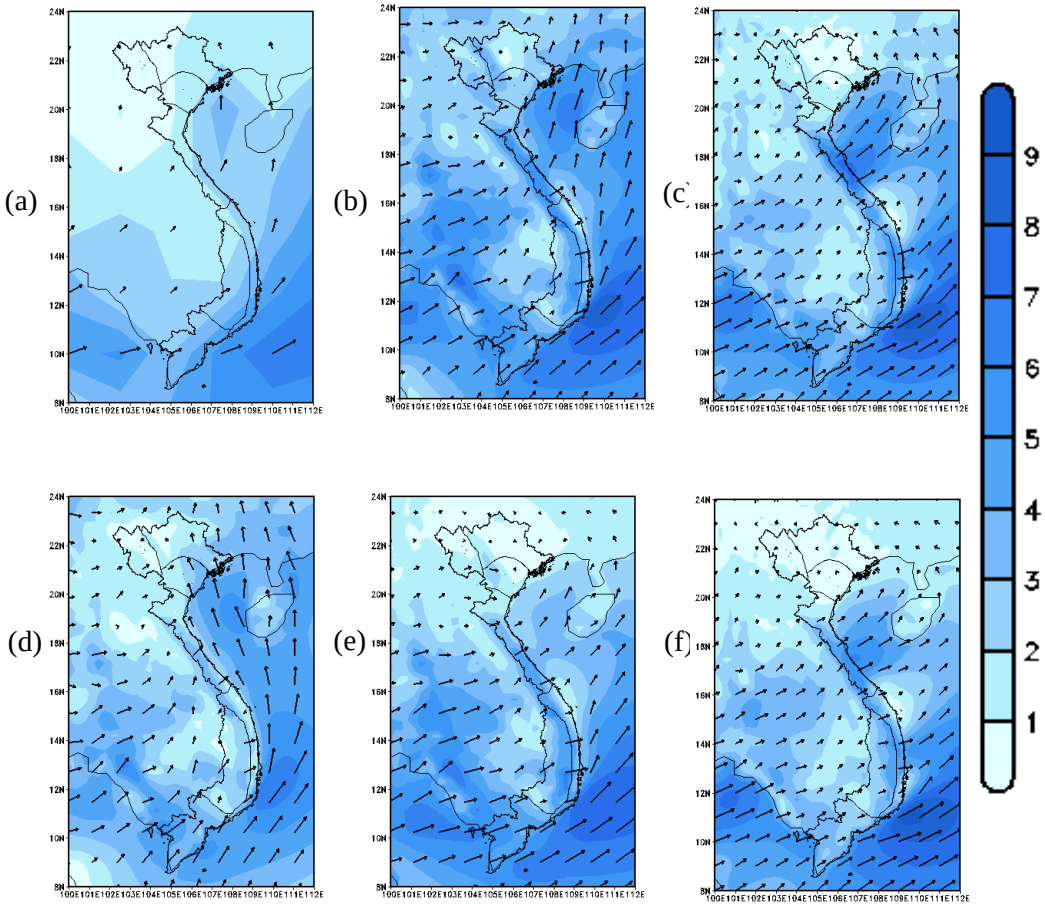

Figure 4-9: Mean Seasonal (JJA) Surface Winds, 1961-1990, m/s
(a) ERA40 (b) WRF/ERA (c) PRE/ERA
(d) WRF/CCSM (e) WRF/ECHAM (f) PRE/HAD

In a continuing discussion of model simulations, rainfall, the most sensitive and difficult variable to be simulated, is described here. The spatial distribution of mean annual average rainfall amongst observations and model simulations over the period 1961-1990, is shown in Figure 4-10. At the outset, it is clear from this figure that the observations themselves show some discrepancies. As an example, the high coastal rainfall seen over the southern west coast of Cambodia in the CRU and CPC observations is not seen in the APH dataset. Overall, the APH dataset also shows lesser rainfall than its counterparts. Similar differences are also seen in the DJF and JJA seasons (Figure 4-11 and Figure 4-12). However, high terrain rainfall is reasonably well resolved due to high resolution simulations of the RCMs. This is only to highlight that the observations, otherwise generally referred to as 'ground truth', themselves contain uncertainties. This could probably be due to inconsistent or erroneous measurements, lack of dense network of observations, different interpolation methods and number of station records accounted for, in developing these data products. The quantification or evaluation of these observational uncertainties is not within the scope of this thesis. Yet, these figures merely serve as a benchmark for comparison against model simulated results. The purpose of inclusion of more than one observed dataset for comparisons is to have a wider understanding of the performance of the model. Another source of observations, the Vietnam station data, are also shown along with these gridded observations for a detailed comparison.

It is noted here again that the common record periods for all the stations that have been used to derive this map is between the period, 1961 to 1985. Although the period 1961-1990 is in discussion, 25 years of this monthly scale station data have been used merely for a comparison of model results on a climatological perspective to have a better idea of the station recorded patterns of rainfall.

As in the case of surface temperatures, the performance of the models when driven by the reanalyses are discussed first as these simulations indicate the 'true' climate. The discussions of simulations driven by the GCMs follow after.

The comparisons of the model simulations against observations reveal an overall reasonable spatial agreement of models' simulated rainfall against observations. The high resolution simulations (25 km) of the models' also show that they are able to effectively simulate rainfall over the high terrains. This feature is seen in the models but not in the observations, possibly due to lack of gauge measurements or other observational sources over these high terrains.

The circle in Figure 4-10(e) clearly shows the effect of topography over the S6 region in WRF/ERA but it is not pronounced in the gridded observation datasets. The simulation of WRF/ERA agrees reasonably well with CRU and CPC in the overall spatial distribution of mean annual daily average rainfall at S1, S2, S3 and S7. In comparison with station data which are dense networks, WRF/ERA captures the rainfall over Hai Van pass at 16 °N, between S4 and S5, although at a lower intensity compared to the border between the S6 and S7 regions. The coastal rainfall of S4 and S5 is also resolved reasonably well. PRE/ERA simulations tend to overestimate rainfall over most of the domain and the high terrain rainfall is not as pronounced as in WRF/ERA in S6. However, it is able to capture the significant effect of precipitation around Fansipang mountain peak (Refer Chapter1, Figure 1-6b) at the border of S1 and S2 when compared against station data.

Amongst the RCM simulations driven by the GCMs, the spatial pattern of WRF/CCSM underestimates rainfall over most of the domain including Vietnam, but still captures the terrain rainfall over the S4, S5 and S6 regions. WRF/ECHAM shows a reasonable structure of rainfall compared against observations whilst PRE/HAD exhibits a similar profile to that of PRE/ERA. The model simulations of both WRF and PRECIS reproduce the seasonal gradients very well. This is also an important climate feature as Vietnam is largely influenced by a peak rainy season during JJA than DJF, although regional seasonal differences exist. This can be observed clearly in the distribution of annual cycle of rainfall over 4 stations spreading all over Vietnam in Figure 4-14.

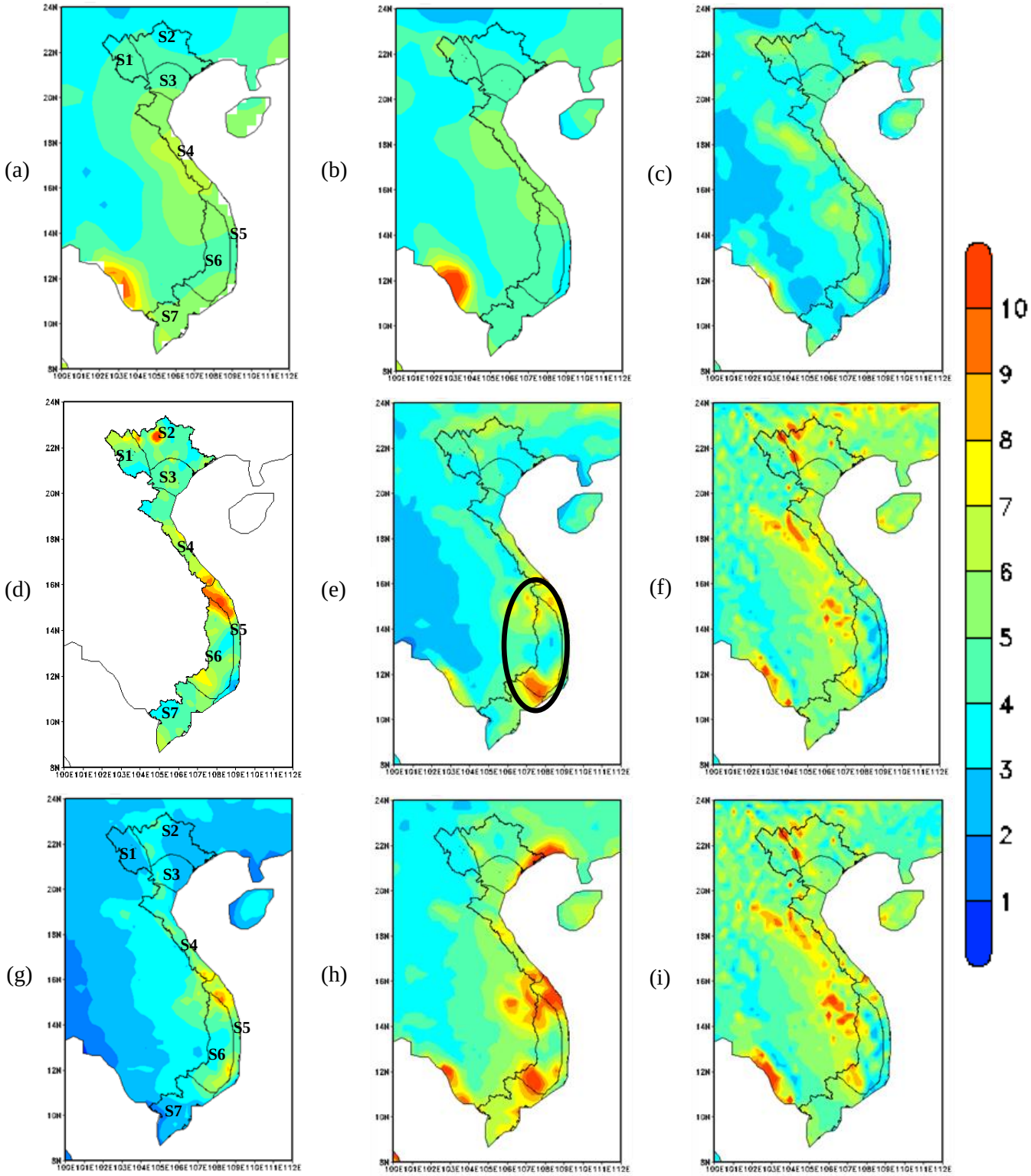

Figure 4-10: Mean Annual Rainfall, 1961-1990, mm/day
(a) CRU (b) CPC (c) APH (d) Station Data (e) WRF/ERA (f) PRE/ERA
(g) WRF/CCSM (h) WRF/ECHAM (i) PRE/HAD

The DJF rainfall is very low over the study domain as it is the dry season and its spatial distribution is well resolved by both RCMs as seen in the Figure 4-11. The heavy rainfall observed in station data (d) and RCMs (e, g, h, i) at the border of S4 and S5 is the result of the Annamite range that blocks the NE monsoon coming from China. This pattern is faintly visible in the CRU and APH observations but not in CPC. The WRF model results capture this feature effectively, especially WRF/ERA. The PRE/ERA simulations show similar distributions of rainfall as that of the APH data. The JJA season rainfall is also well reproduced by the models as seen in Figure 4-12.

In addition to the overall distribution of rainfall all over Vietnam, the gradients are also well represented by showing a wet Northern (S1, S2, S3) and Southern Vietnam (S6, S7) and a relatively dry central coastline (S4, S5). The reason for the dry central coastline of Vietnam is because the Annamite range blocks all the southwest monsoon wind coming from Laos and causes an effect called 'foehn' over sub-region S4 (Ho et al., 2011).

As a result, the monsoon rainfall is experienced over the west side of the mountains, after when the remaining air, mostly due to lack of moisture, crawls over the mountain towards the east causing dry and hot climate over the S4 region. Such a pattern is clearly resolved by WRF/ERA, PRE/ERA and PRE/HAD. The simulation of WRF/ECHAM also reproduces this pattern although to a lesser extent compared to the observations, while WRF/CCSM does not show this pattern clearly.

Away from the Vietnam domain, the very high spot of rainfall lying at the southern east coast of Cambodia, displayed as a circle in Figure 4-12(a), is seen in the observation datasets. The model simulations of PRE/ERA and PRE/HAD reproduce this feature reasonably well whilst WRF/ERA and WRF/ECHAM also simulate this pattern over that area but of lesser intensity. The simulation of WRF/CCSM, however, does not show it at all.

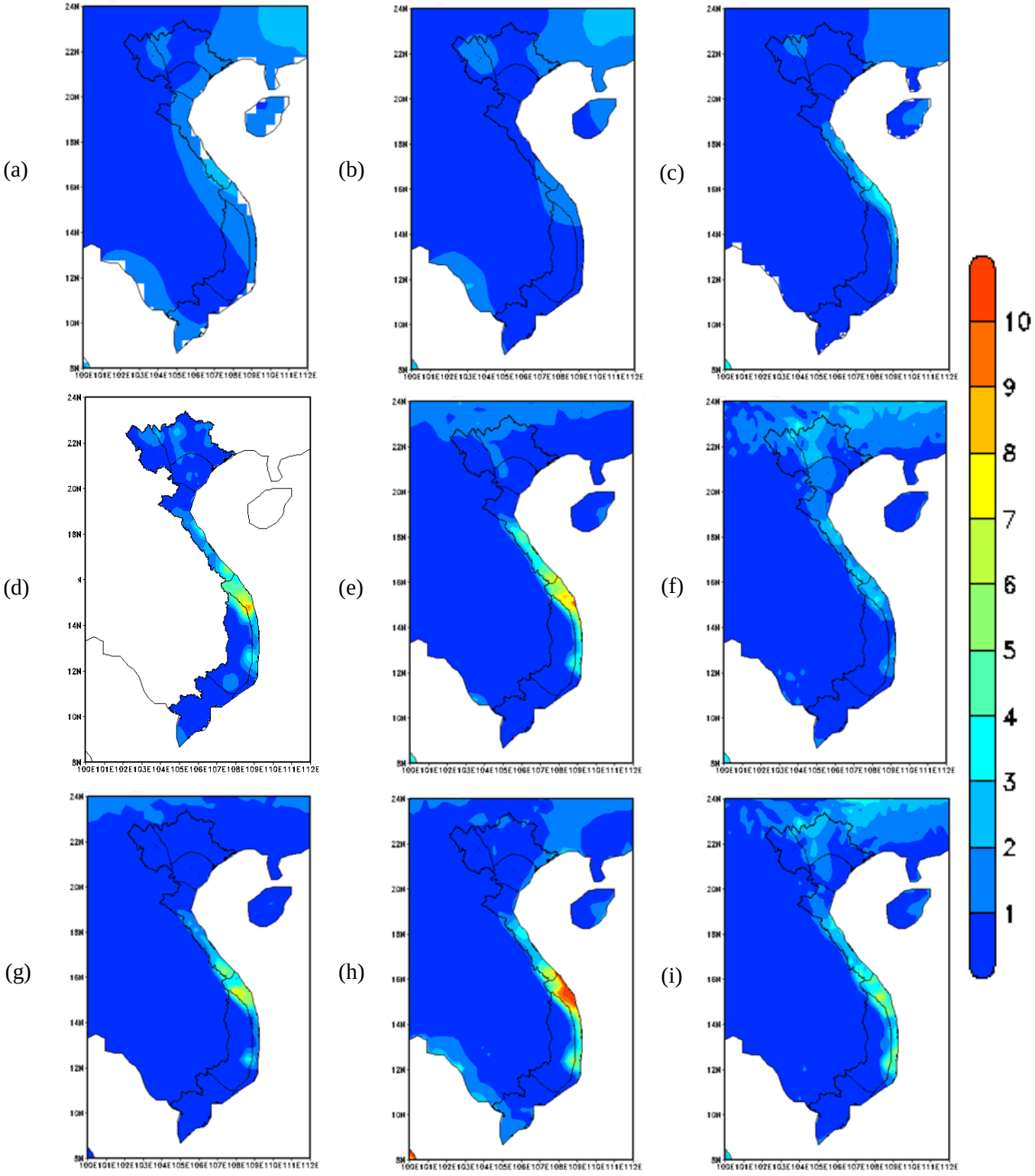

Figure 4-11: Mean Seasonal (DJF) Rainfall, 1961-1990, mm/day
(a) CRU (b) CPC (c) APH (d) Station Data (e) WRF/ERA (f) PRE/ERA
(g) WRF/CCSM (h) WRF/ECHAM (i) PRE/HAD

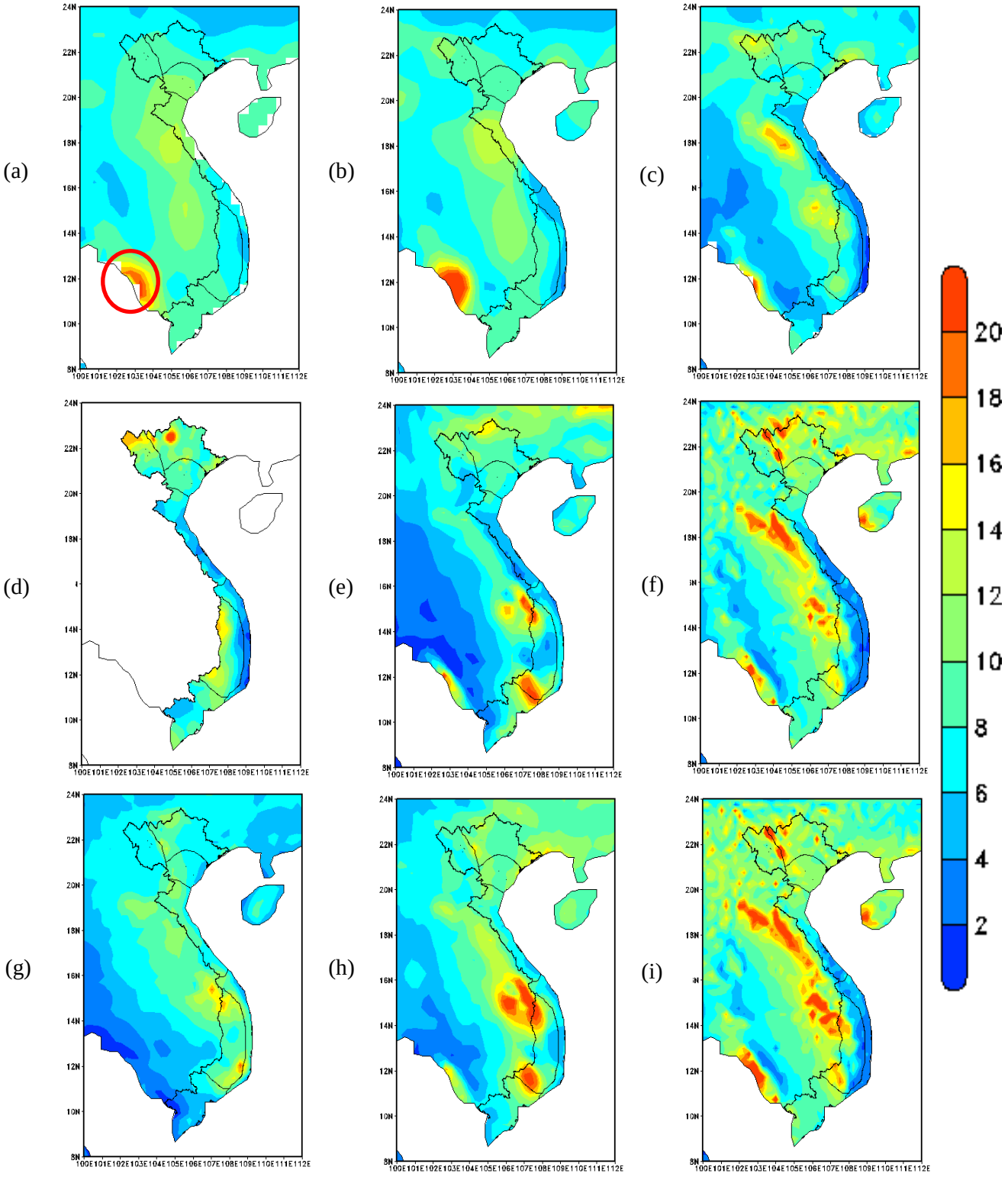

Figure 4-12: Mean Seasonal (JJA) Rainfall, 1961-1990, mm/day
(a) CRU (b) CPC (c) APH (d) Station Data (e) WRF/ERA (f) PRE/ERA
(g) WRF/CCSM (h) WRF/ECHAM (i) PRE/HAD

Additional plots for the MAM and SON season, shown in the Appendix E, Figure E-8, Figure E-9, indicate that the mean seasonal climates are well represented by the models and are in good agreement with all the observations. The terrain rainfall and rainfall over S4 and S5 region are resolved well. Some graphical plots for model biases (between both RCM vs gridded observations and RCM vs station data) are shown in Figure E-16 in Appendix E. These bias figures (Figure E-7, for temperature and Figure E-16, for rainfall) indicate that the RCM simulations of WRF & PRECIS exhibit least biases for surface temperatures using both ERA40 and GCMs. For rainfall, an overall underestimation by WRF is seen over the western regions of the domain. Although the north (S1, S2 and S3) and south (S7) regions of Vietnam show lower biases, S4 and S5 show higher biases due to the larger rainfall intensities over high terrains that are not seen in the observations. The biases from the PRECIS simulations using ERA40 indicate an overestimation of rainfall over most of the domain but relatively lower biases over the Vietnam region.

It has been mentioned that capturing the inter-annual variability of rainfall is important to validate the performance of any RCM (Tadross et al., 2006). To this end, the inter-annual variability amongst different observational records and the model simulations are depicted in Figure 4-13. These results indicate that CRU and CPC agree well between each other whilst APH underestimates this variability. The WRF/ERA is able to match this pattern better than PRE/ERA, as the latter overestimates rainfall variability over some northern regions of the domain and over Vietnam. The WRF/ECHAM shows higher variability than WRF/CCSM and PRE/HAD. The PRE/HAD is, however, reasonable in its performance by reproducing a highly variable northern Vietnam and a less variable southern Vietnam.

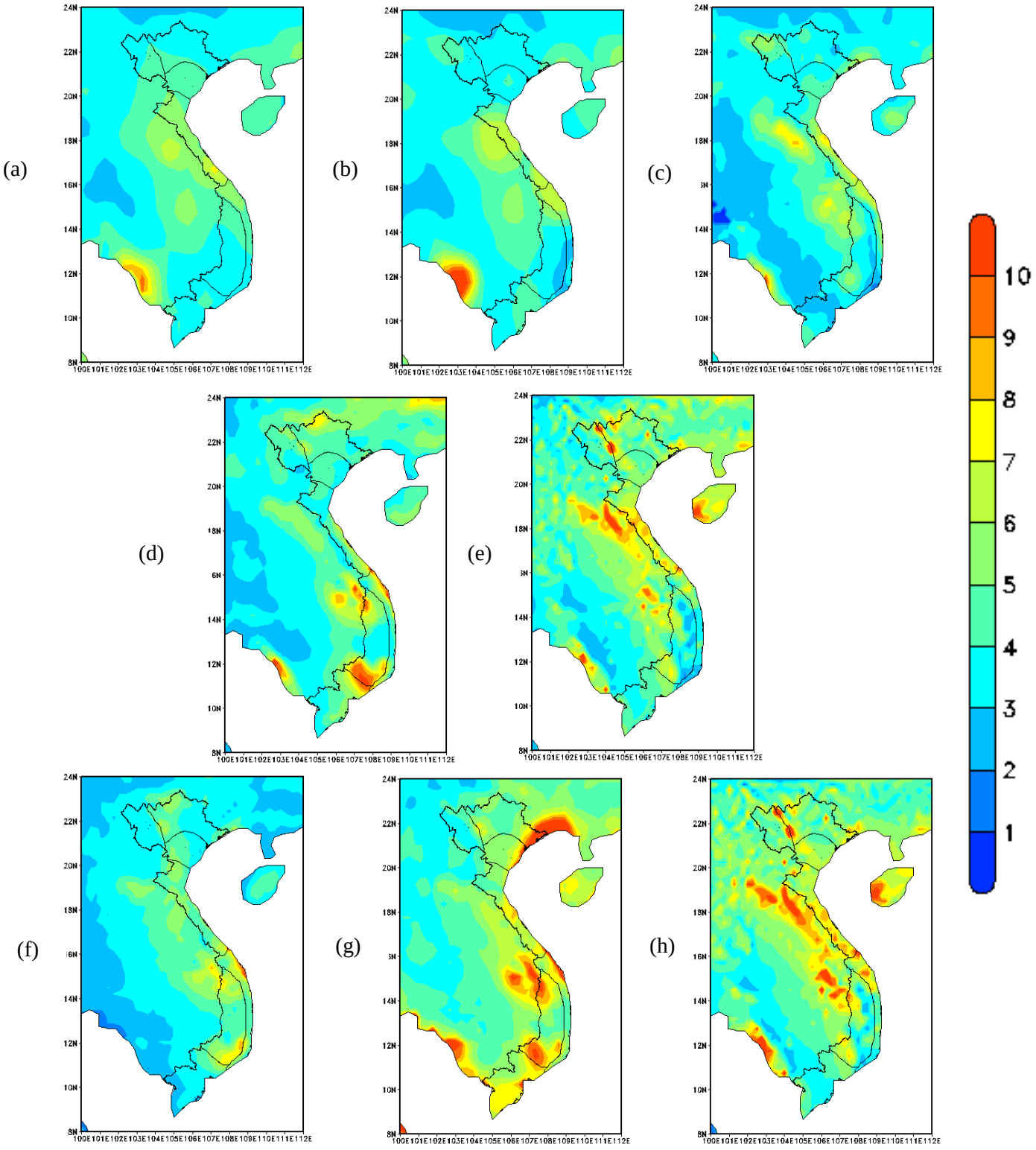

Figure 4-13: Inter-annual variability of rainfall, 1961-1990, mm/day
(a) CRU (b) CPC (c) APH (d) WRF/ERA (e) PRE/ERA
(f) WRF/CCSM (g) WRF/ECHAM (h) PRE/HAD

It is also important to assess model performance with respect to the annual cycle of precipitation over a designated area or place. This also has implications when hydrological studies are made over a chosen region or a location as rainfall is the key input for the hydrological model to simulate stream flow. Since four main cities in Vietnam: Hanoi, Da Nang, Kon Tum and Ho Chi Minh City have been chosen for model evaluations at station point, the annual cycles over these locations are compared against station data and gridded observations, as seen in Figure 4-14. The cyan band of annual cycle in the figure represents the minimum-maximum ranges of three different observations, CRU, CPC and APH. Such a band, as drawn for surface temperature plots earlier, is drawn here to showcase the range of values in rainfall amongst them and to clearly show the patterns of the station data and the model simulations.

For Hanoi, all model simulations reasonably agree on the overall pattern of the annual rainfall, especially, the peak season of rainfall in JJA months when compared against observations and station data. Some deviations in the pattern in the form of higher (lower) intensities are seen in WRF/ECHAM (WRF/CCSM). For Da Nang, all simulations agree quite well in the annual cycle pattern, but with higher intensities in the case of WRF/ERA, WRF/ECHAM and WRF/CCSM, during the months of September to December. PRE/ERA underestimates rainfall whilst PRE/HAD exhibits an excellent agreement against station data and gridded observations. The patterns of annual cycles over Ho Chi Minh City and Kon Tum are not that well resolved as compared to those of Hanoi and Da Nang. The PRE/ERA and PRE/HAD rainfall agree well with station data at Ho Chi Minh City than the other WRF simulations. Over Kon Tum station in S6 region, the PRECIS simulations show underestimation and WRF/ECHAM shows overestimation during the peak rainfall months whilst WRF/ERA and WRF/CCSM fall within the observational range.

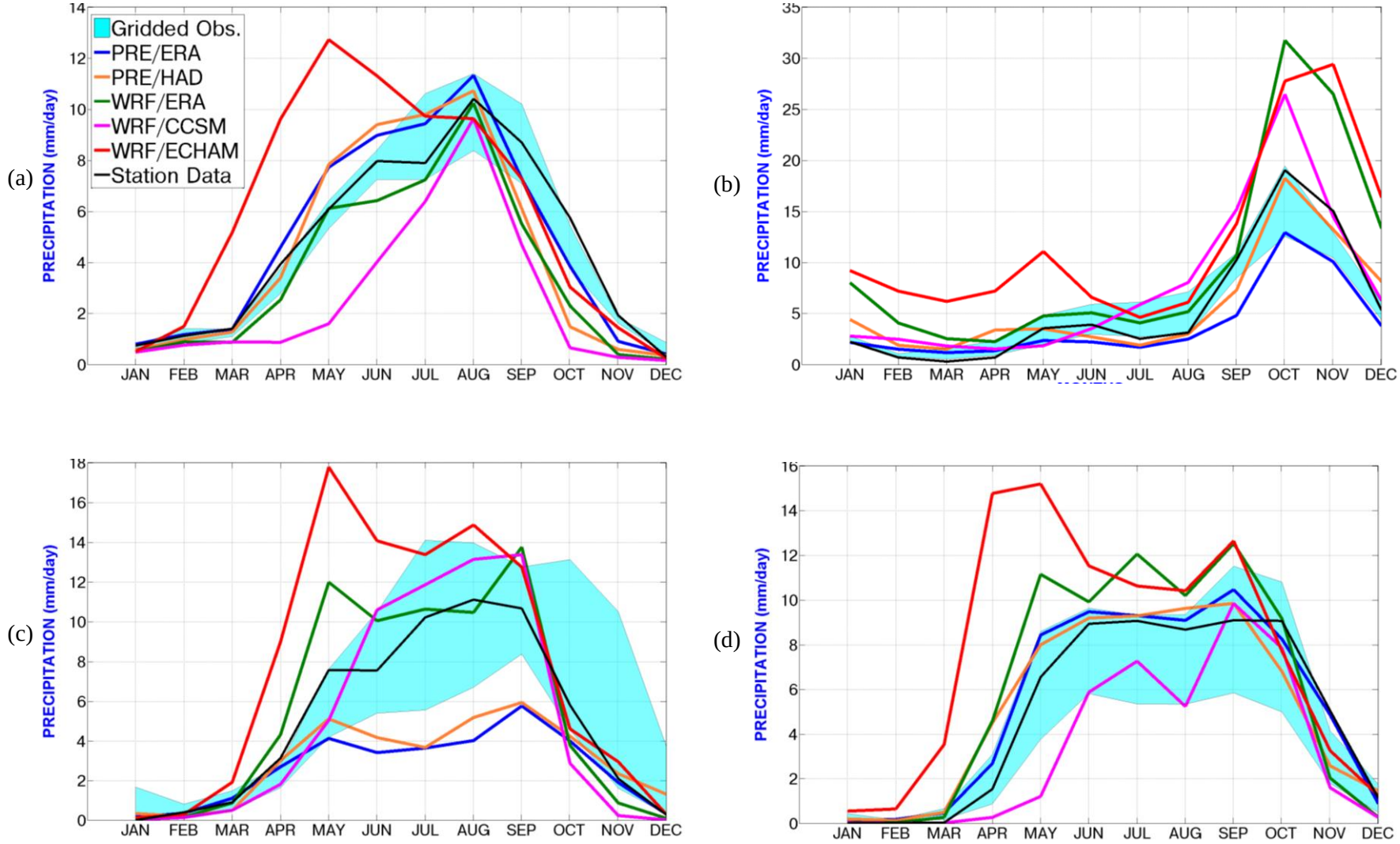

Figure 4-14: Annual Cycles of Precipitation, mm/day
(a) Hanoi (b) Da Nang (c) Kon Tum (d) Ho Chi Minh City

Not only are the mean climatologies always useful in evaluating model performance. It is also quite important that the model resolves the extreme patterns (lowest and highest rainfall) well enough. This is to ensure that the model is able to capture the distributions of rainfall reasonably well which has implications for flooding (high rain fall) and drought (low rainfall) conditions. To this end, some probability density functions are drawn to establish the model performance, both driven by the ERA40 reanalysis (Figure 4-15) and different GCMs (Figure 4-16), against station and APH dataset. It is reminded here that only the station data and APH data are used for comparisons. This is because the PDFs are drawn using daily scale rainfall time series, available only with station data and APH data, as done for the surface temperature discussed earlier. It is also reminded that since CRU and CPC are monthly time scale data, they have not been used in this analysis. Among these different simulations, WRF/ERA (Figure 4-15) was able to simulate the rainfall distributions close to the station data for all stations. Both PRE/ERA and APH profiles overestimate dry spells, however, all simulations seem to fare reasonably well in resolving higher rainfall intensities. WRF/CCSM and WRF/ECHAM (Figure 4-16), compare well in their distributions with all stations compared to PRE/HAD. As in the case of PRE/ERA and PRE/HAD, they overestimate the dry spells, whilst all WRF/GCM driven model simulations resolve higher intensities well enough. These results can be taken as a sign of reasonably good performance of the model, especially the WRF model, as the comparisons are made among three different observational sources: a point location (gauge based station), gridded observation (0.25°) and model averaged grid spacing of 25 km. The results, therefore, are strongly significant in establishing a good model performance.

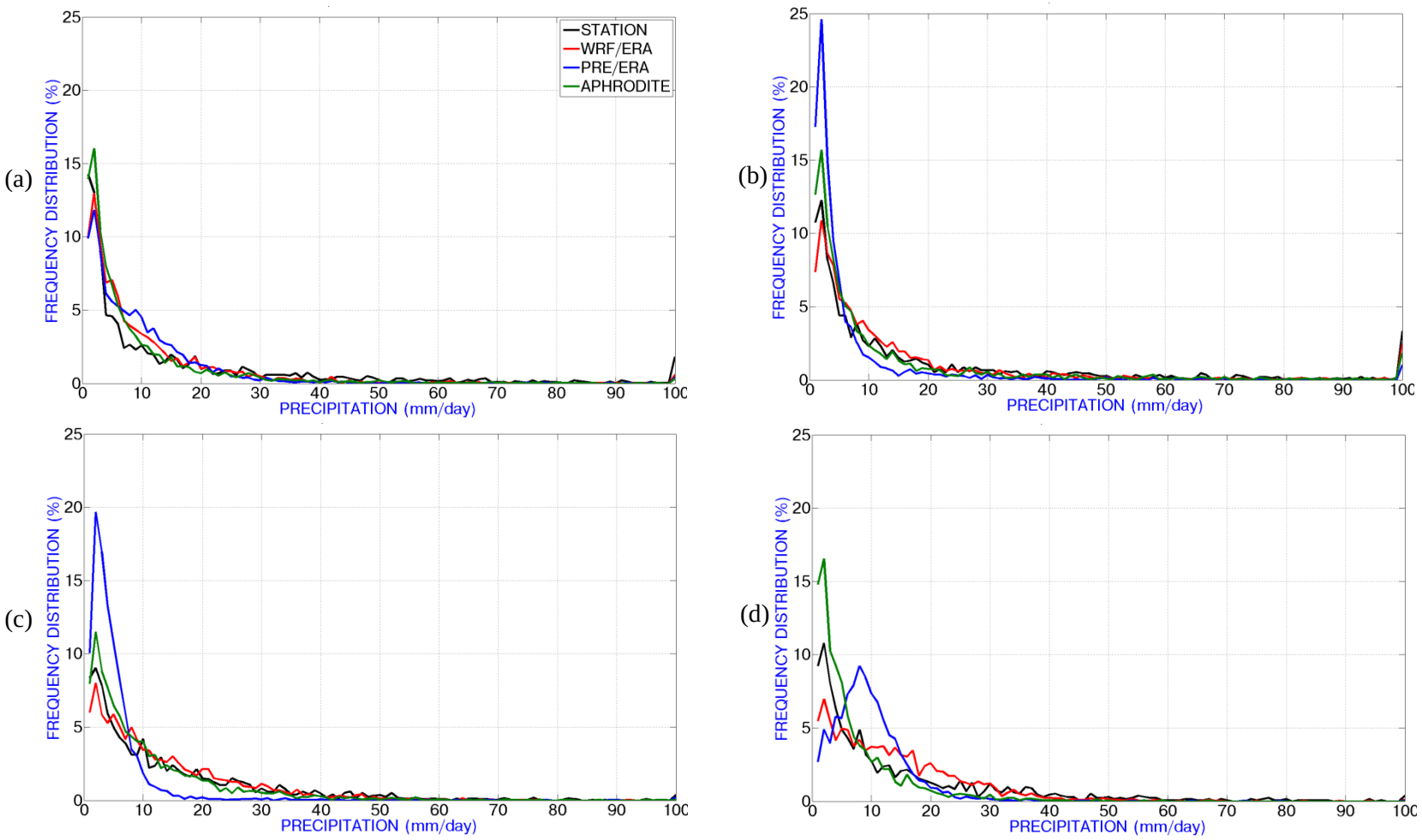

Figure 4-15: Probability Distributions of rainfall, mm/day (WRF and PRECIS driven by ERA40 reanalysis)
(a) Hanoi (b) Da Nang (c) Kon Tum (d) Ho Chi Minh City

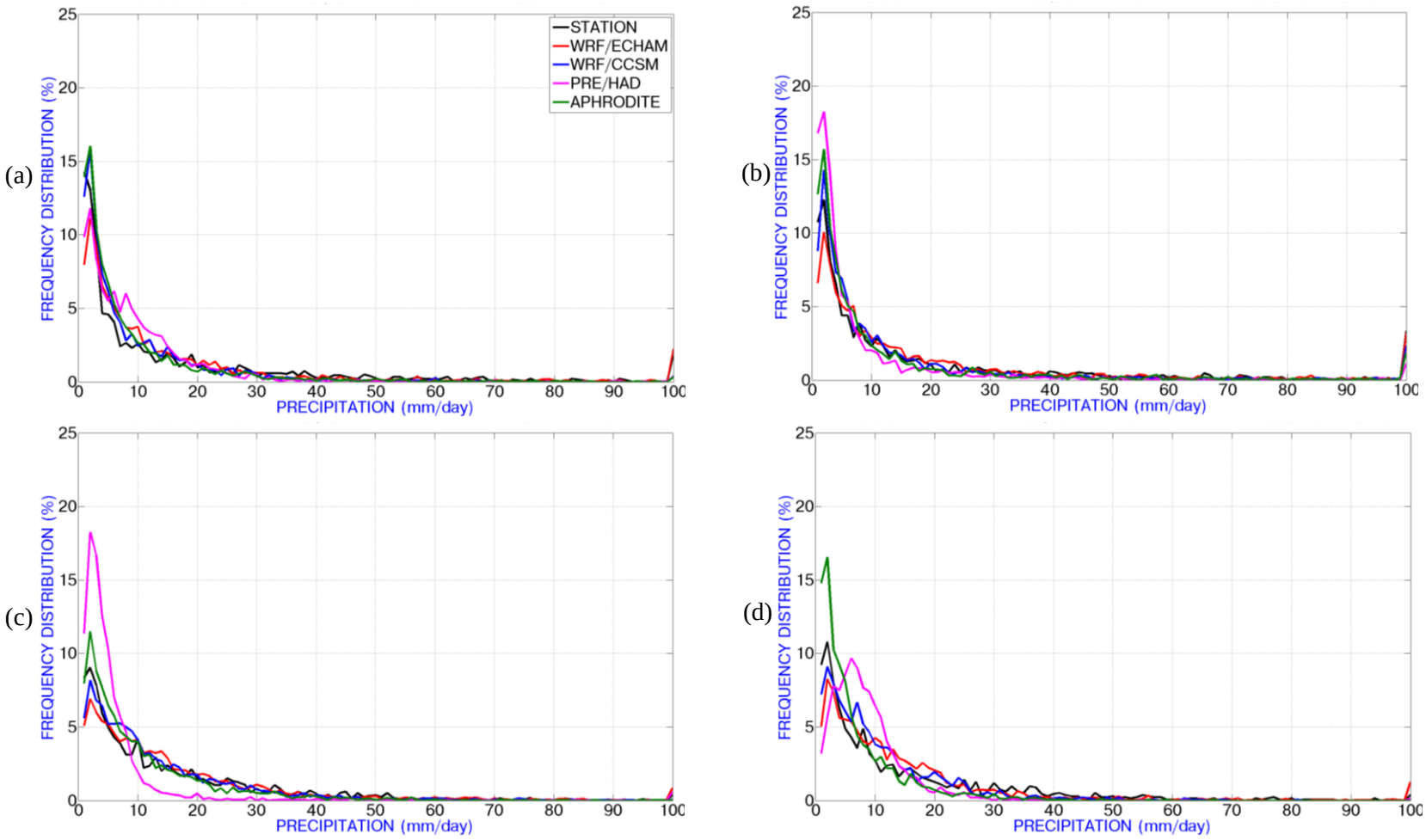

Figure 4-16: Probability Distributions of rainfall, mm/day (WRF and PRECIS driven by GCMs)
(a) Hanoi (b) Da Nang (c) Kon Tum (d) Ho Chi Minh City

Not only are the PDFs useful in evaluating model performance of simulation of precipitation, but also some statistical measures of some extreme indices. Since determining hydrological response is one of the main objectives of the impact study in this thesis, three other indices, namely, a maximum consecutive 5 day accumulated rainfall index (R5d), 90^{th} percentile of daily rainfall (P90p) and the daily rainfall intensity (SDII) are considered for evaluation. This is important as these indices are influenced by daily rainfall values, which are then used as input as a daily time series in the hydrological simulations. The R5d is shown in Figure 4-17. Although the north and south gradients and central eastern regions (S4, S5) are resolved well, WRF/ECHAM overestimates the rainfall amounts and PRE/HAD underestimates the same. The simulations of WRF/ERA, PRE/ERA and WRF/CCSM agree well with the APH data. The models simulated intensities of P90p daily rainfall are compared against APH data in Figure 4-18, which show an overall reasonable agreement of models against APH observations. The SDII plots are shown in Figure 4-19. The results indicate that the PRE/ERA and PRE/HAD simulate closer rainfall intensities to that of APH whilst the other overestimate the intensities. Except WRF/ECHAM, the other simulations show good agreement over the S1, S2, S3 and S7 regions. Overall, the WRF simulations produce more rainfall over the S4 and S5, which are seen relatively dry in APH and PRECIS simulations. Both WRF and PRECIS simulations indicate a reasonable performance showing the rainfall gradients well. A relatively wet North and a dry South over Vietnam is clearly seen in PRECIS simulations that correspond well against APH data. WRF/ECHAM simulates slightly higher amounts compared to WRF/ERA and WRF/CCSM. Nevertheless, both these indices highlight the useful of downscaling whereby the results of precipitation derived from the climate models could be effectively used as inputs for hydrological simulations. All annual scale indices have been shown here. Due to space constraints, the seasonal profiles of DJF and JJA are shown in the Appendix E as they are the main seasons of contrast, being winter and summer season, respectively.

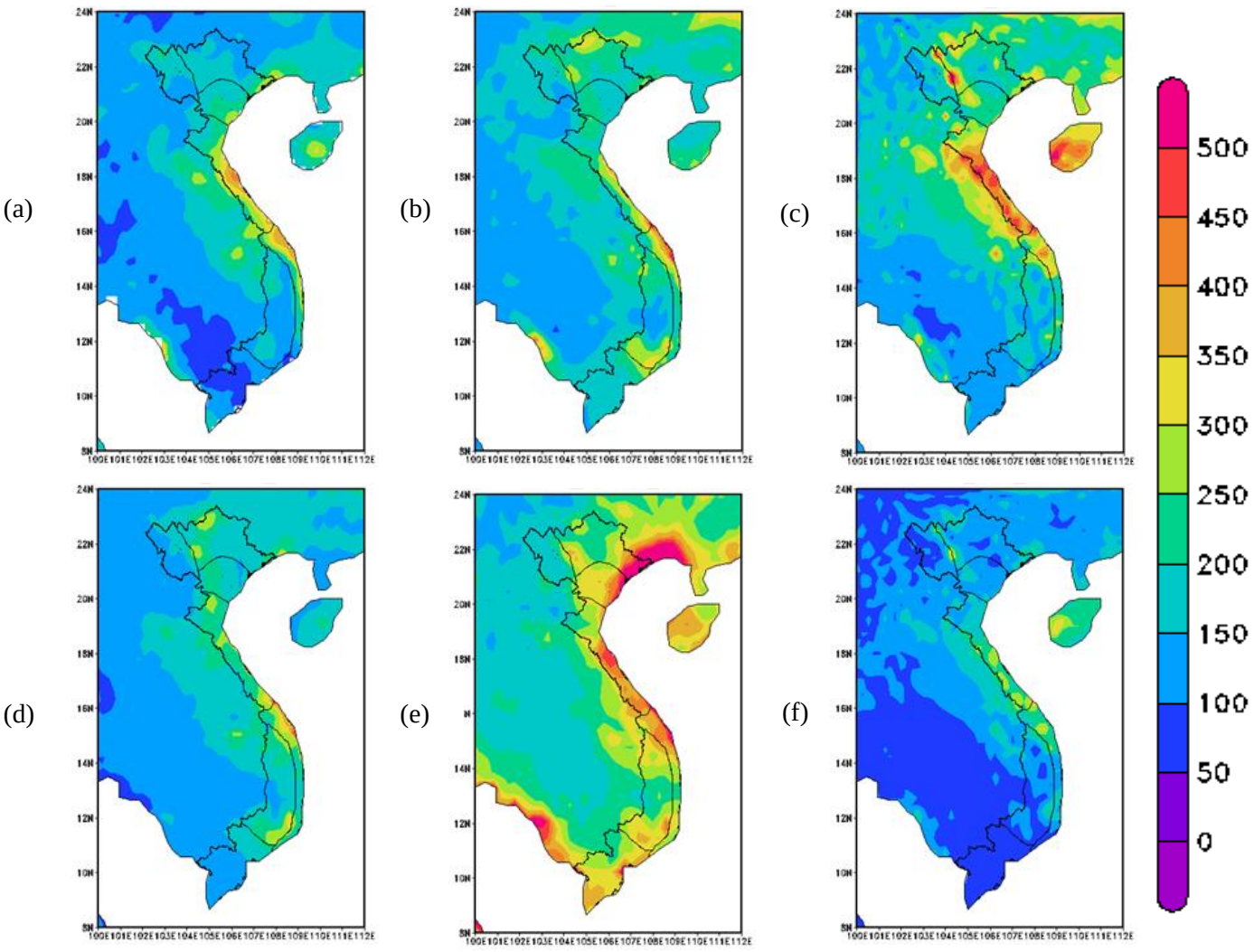

Figure 4-17: Mean Annual Maximum Consecutive 5 day Accumulated rainfall, 1961-1990, mm
(a) APH (b) WRF/ERA (c) PRE/ERA
(d) WRF/CCSM (e) WRF/ECHAM (f) PRE/HAD

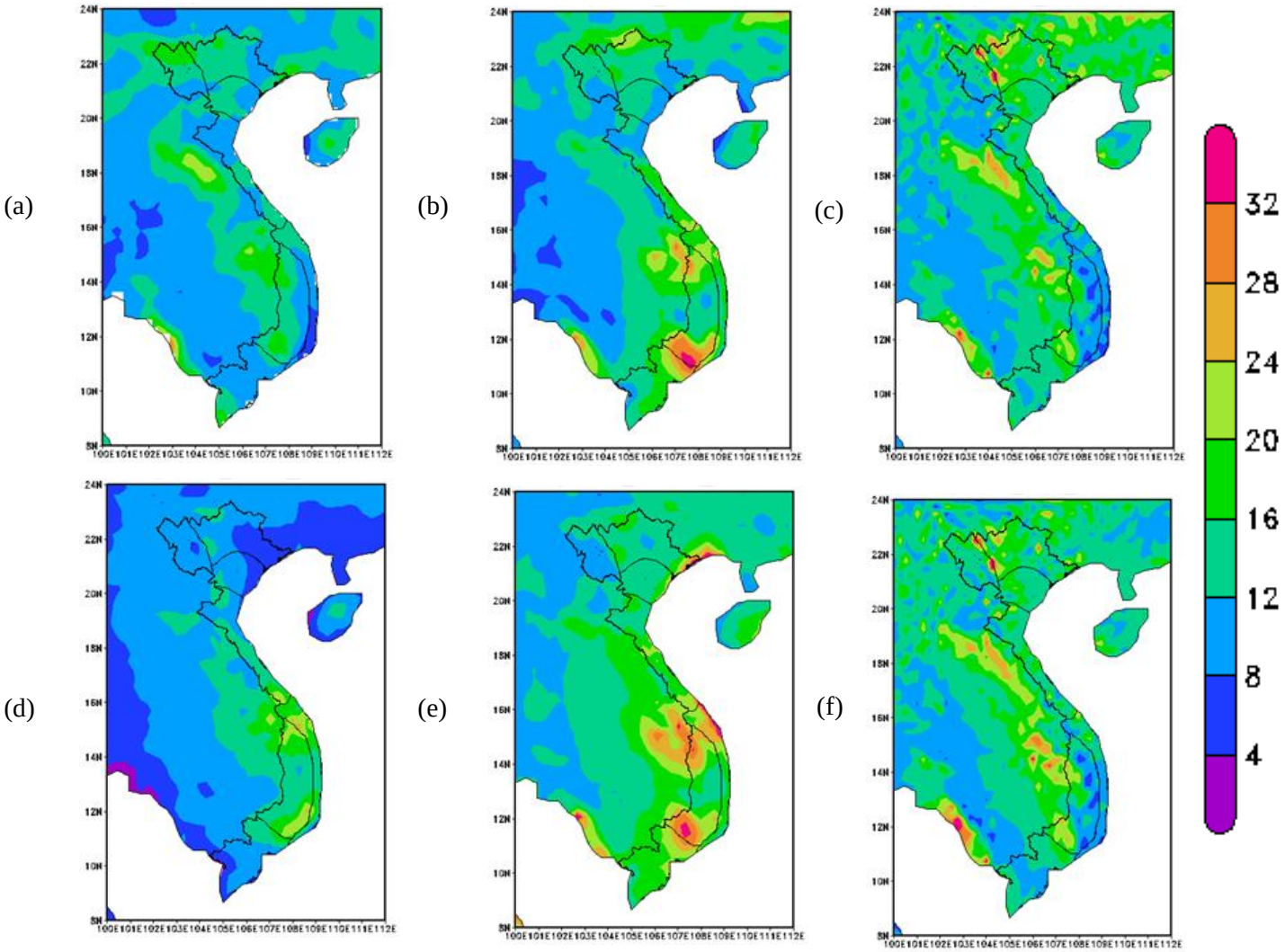

Figure 4-18: Mean Annual 90th percentile rainfall, 1961-1990, mm/day
(a) APH (b) WRF/ERA (c) PRE/ERA
(d) WRF/CCSM (e) WRF/ECHAM (f) PRE/HAD

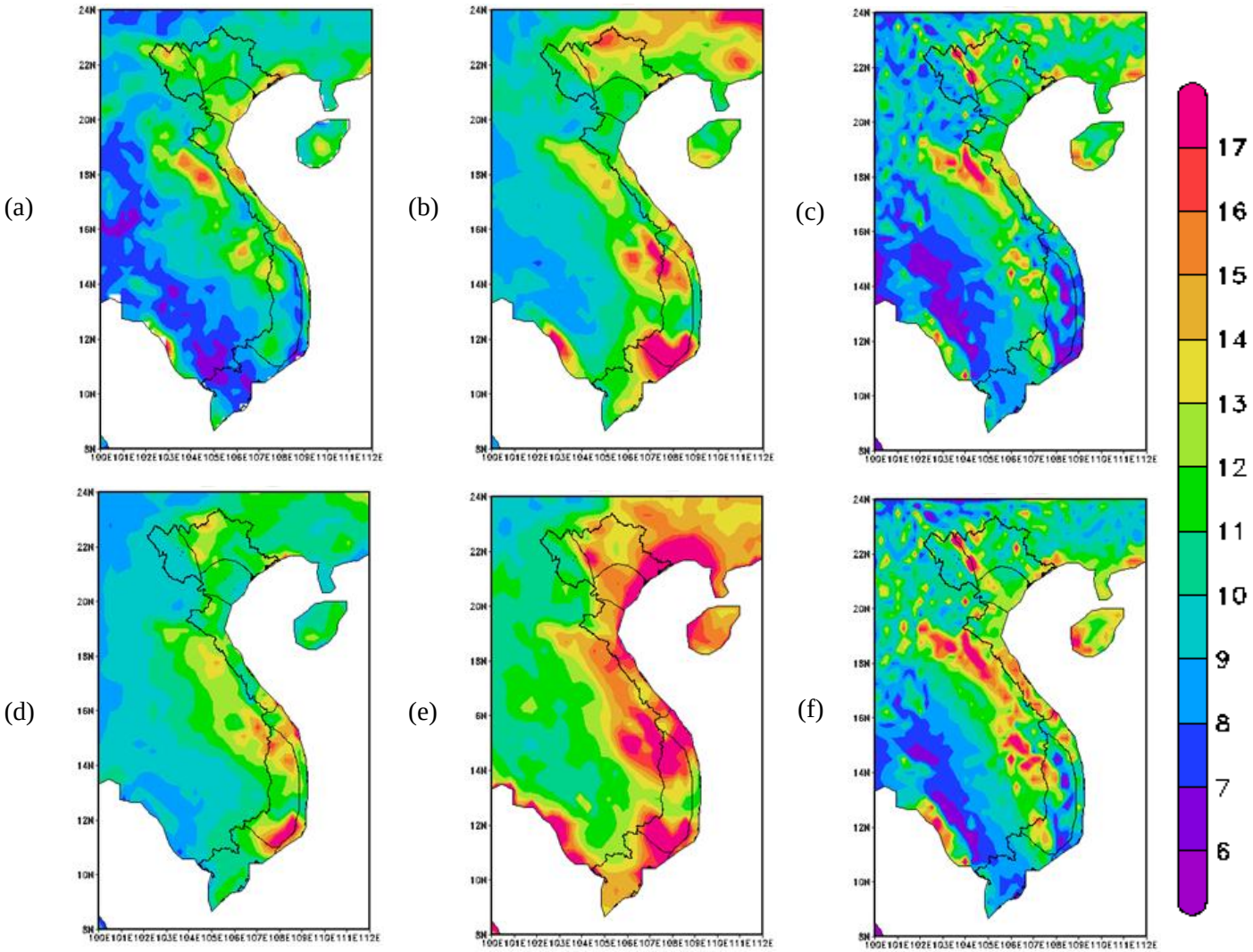

Figure 4-19: Mean Annual Rainfall Intensity, 1961-1990, mm/day
(a) APH (b) WRF/ERA (c) PRE/ERA
(d) WRF/CCSM (e) WRF/ECHAM (f) PRE/HAD

Table 4-1 and Table 4-2 show the area averaged temperature and precipitation values, respectively, over the 7 chosen climate regions: S1 to S7. These are compared to the gridded observations and station data. The area averaged values of these climate variables indicate how well the model is able to simulate the profiles at such sub-regional scale areas.

Table 4-1: Areal Average Daily Temperature (°C) over seven sub-climate zones (1961-1990)

Annual	**S1**	**S2**	**S3**	**S4**	**S5**	**S6**	**S7**
CRU	22.4	22.0	23.7	24.0	25.6	24.2	27.2
CPC	22.0	22.5	23.3	23.1	24.6	24.7	27.5
APH	19.4	20.7	22.3	23.4	24.6	24.3	27.8
STATION	21.2	21.5	22.8	23.6	25.3	23.1	26.7
WRF/ERA	**19.5**	**21.6**	**23.7**	**23.5**	**23.7**	**23.1**	**27.6**
PRE/ERA	**19.4**	**20.7**	**22.8**	**22.9**	**24.6**	**23.7**	**27.3**
WRF/CCSM	**20.2**	**21.3**	**23.0**	**22.6**	**23.6**	**23.5**	**28.2**
WRF/ECHAM	**19.4**	**21.7**	**23.6**	**22.6**	**23.5**	**22.9**	**27.4**
PRE/HAD	**19.7**	**20.8**	**22.6**	**22.7**	**24.3**	**23.4**	**27.0**

Table 4-2: Areal Average Daily Precipitation (mm/day) over seven sub-climate zones (1961-1990)

Annual	**S1**	**S2**	**S3**	**S4**	**S5**	**S6**	**S7**
CRU	4.39	3.98	4.66	5.73	5.31	5.09	5.37
CPC	4.49	4.12	4.42	5.25	4.58	4.38	4.88
APH	4.52	4.26	4.26	4.53	3.75	4.25	3.71
STATION	5.01	5.00	4.70	5.64	6.25	5.65	4.83
WRF/ERA	**4.16**	**4.51**	**3.96**	**4.90**	**6.35**	**5.76**	**5.13**
PRE/ERA	**5.69**	**6.24**	**5.76**	**6.17**	**4.11**	**4.93**	**5.51**
WRF/CCSM	**2.83**	**2.96**	**3.02**	**4.26**	**5.72**	**4.73**	**2.85**
WRF/ECHAM	**3.81**	**5.37**	**5.85**	**6.49**	**7.78**	**7.26**	**7.15**
PRE/HAD	**5.85**	**5.77**	**5.54**	**6.43**	**5.25**	**5.48**	**5.34**

The tabulated values for precipitation, Table 4-2 indicates that the model values are not strongly deviated compared to those of observations. It is also notable that observations themselves differ in their estimates by 1 or 2 mm/day. The model simulations show that, overall there is very good

agreement on area averaged values in daily precipitation with differences only between ± 1-2 mm. Compared to the small sub-regions over Vietnam that are considered in this case, these differences are relatively insignificant and hence establish a good performance of the model. A similar assessment can also be done for area averaged temperature distributions which differ only by about ± 1°C.

In a summary of these different evaluations, it can be said the climate model simulations over the present day climate period of 1961-1990 can be deemed very reasonable. It has been noted earlier that precipitation is one of the most difficult and sensitive variable to be simulated, given its nature of high variability over space and time, whilst simulation of temperature is relatively simple, given its nature of homogeneity across time and space. Precipitation is the focus in this study as it is the prime input to the hydrological models. The performance of the models on the spatial distributions of rainfall in different time scales, annual and seasonal, has been reasonable, although with some biases. Other than these mean climatological patterns, the PDFs at four main meteorological locations have shown a good agreement of model simulated rainfall distributions against station data. The interannual variability, annual cycles and area averaged values of precipitation also show reasonable agreement with observations. The extreme indices of rainfall intensity (SDII), 90^{th} percentile rainfall (P90p) and the 5 day accumulated rainfall amounts (R5d) also indicate the good performance of the models. It should also be noted that these discussions are not the complete list of evaluation metrics, but are some of the key metrics used in any climate model evaluations. It is also reminded that an exhaustive model evaluation is not the focus of this thesis, but rather to see the usefulness and robustness of the regional climate model in simulating the state of climate such that its results could be used for impact studies. Whilst the simulations of the regional climate models driven by the reanalyses shed light on the performance of the model over the present day climate, those simulations driven by the GCMs indicate that the model is also able to reproduce the present day climate well enough, given the fact that GCMs are merely representations of real

climate compared to the 'true' climate of the reanalyses. This also indicates that downscaled future climate projections from these GCMs can be taken as credible, since the present day climate has been evaluated and found reasonably satisfactory. With these results and model performances in mind, future climate simulations are described in the next section.

4.3 SIMULATIONS OF FUTURE CLIMATE

It was mentioned earlier that the present day climate simulations are for establishing how well the regional climate models simulate the state of the climate, so that there is enough credibility on the performance of the model that future climate estimates simulated by the same models can also be taken to be credible enough. Having established their performance over the present day climate in the earlier section, this section aims to assess likely changes in the future climate simulated by the RCMs WRF and PRECIS, driven by the global climate models under the A2 emission scenario (Chapter 3, Section 3.5). It is once again noted that the results from this study are one the first of its kind research done over Vietnam, giving an 'ensemble' approach of likely future changes taking account changes simulated by two different RCMs (WRF and PRECIS) that downscaled three GCMs (CCSM3.0, ECHAM5 and HadCM3), all forced under a future IPCC emission scenario A2. Since the objective of this thesis is to pronounce some estimates of changes in future climate derived from these ensemble climate simulations, this section describes the outcome of the climate change experiments, mentioned in Chapter 3, Figure 3-1. Later, the climate response or the climate change signal which is the difference between the RCM downscaled estimates of the future and present day climates, shall be ascertained.

As such, these results contribute to an outcome from ensemble climate integrations, different RCMs forced under GCMs of same scenario. This adds to the confidence in the model outcomes and also highlights the importance of using these outcomes for impact studies, keeping in mind the fact that A2 scenario corresponds to more than doubling CO_2 concentrations in the atmosphere in the future. Since harsh impacts (as discussed in earlier chapters) are expected, it would help policy

makers to prepare for adaptive measures with regard to the information gained from these model outcomes.

Future surface temperature changes are displayed in Figure 4-20, on the annual and on all seasonal scales. The results indicate steep annual increases of about 2.5° to 3.7°C towards the end of the century. Seasonal responses indicate that the MAM and JJA seasons might experience a soaring of about 4°C in the S1, S2 and S3 region Vietnam (WRF/ECHAM, PRE/HAD) while DJF is likely to experience an increase of about 2°-3°C, from all simulations. *For easy reading of the figures, it is kindly reminded to the reader that the vertical arrangement in three sets of graphical plots indicate each of the model results (WRF/CCSM (top), WRF/ECHAM (middle row) and PRE/HAD (bottom)) while the horizontal arrangement (ranging from 1 to 5) indicate the 5 different time scales (Annual, DJF, MAM, JJA and SON).*

The mean seasonal wind changes (DJF and JJA) are also shown in Figure 4-21. It can be seen that there are no significant changes in the surface wind speeds over the future.

The annual precipitation response over the future period 2071-2100 relative to the present day baseline period 1961-1990, derived from WRF and PRECIS simulations, is shown in Figure 4-22, the arrangements of figures akin to that of temperature responses mentioned earlier. On an annual scale, all WRF simulations indicate an increasing trend in precipitation over all climate zones of Vietnam of about 25 % to 50 % whilst PRECIS model simulations show a decrease in the future responses between 15 % to 20 %. It is also notable that, from all models, the SON season shows increases of up to 50 %. The other seasons show a mixed response. Since an ensemble method that combines the results from all models is considered in this study, such a result for surface temperature and precipitation is shown in Figure 4-23a and b respectively. This figure depicts the future changes which are derived by taking the model averages from all the three RCM simulations (WRF/CCSM, WRF/ECHAM and PRE/HAD).

To provide a concise view of the future changes of surface temperature and precipitation, a bandwidth of responses for annual daily averaged temperature and precipitation for the four different chosen stations are displayed in Figure 4-24.

All models indicate an increase in surface temperatures from 2.5 °C to 3.7 °C. WRF/ECHAM displays average increases of about 3 °C to 3.2 °C. WRF/CCSM has a lower sensitivity to changes in temperature than PRE/HAD, which predicts hotter temperatures than WRF/CCSM and WRF/ECHAM with the highest value of more than 3.5 °C for Hanoi. The bandwidths of responses for the other seasons are given in the Appendix E. It is likely that Hanoi might be the hottest of all stations during the JJA season, crossing a 4°C rise.

The bandwidth figures also indicate that WRF/ECHAM shows an annual average increase for all regions from 30 % to 45 % whilst PRE/HAD shows a decrease of about 5 %, for all stations. WRF/CCSM predicts higher rainfall for all cities other than Hanoi. It is notable from this that the JJA peak rainy season rainfall is relatively poised to increase more than the DJF season for all stations, while surface temperatures are also likely to be higher during the summer JJA season than DJF, as expected Additional plotted results for the future changes of extreme indices find a place in the Appendix E, Figure E-17 to Figure E-19 and for PDFs for all station data from Figure E-20 to Figure E-23.

These figures also indicate consistent increases in surface temperatures over all climate zones. Precipitation, however, is likely to show mixed trends, increasing in some regions and decrease in some locations.

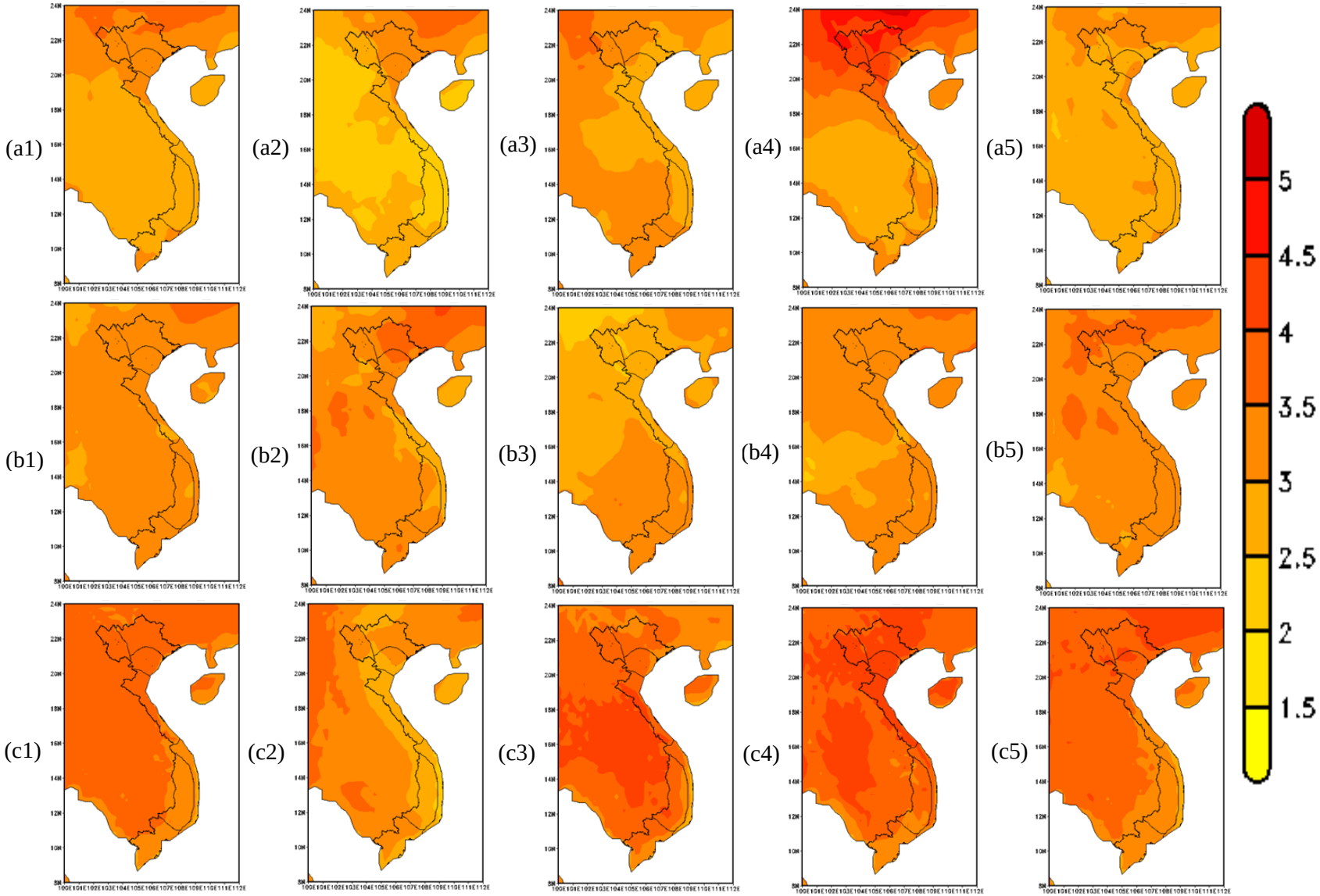

Figure 4-20: Surface Temperature Change (^{o}C), 2071-2100 relative to 1961-1990:
(a) WRF/CCSM (b) WRF/ECHAM (c) PRE/HAD
(1)Annual (2) DJF (3) MAM (4) JJA (5) SON

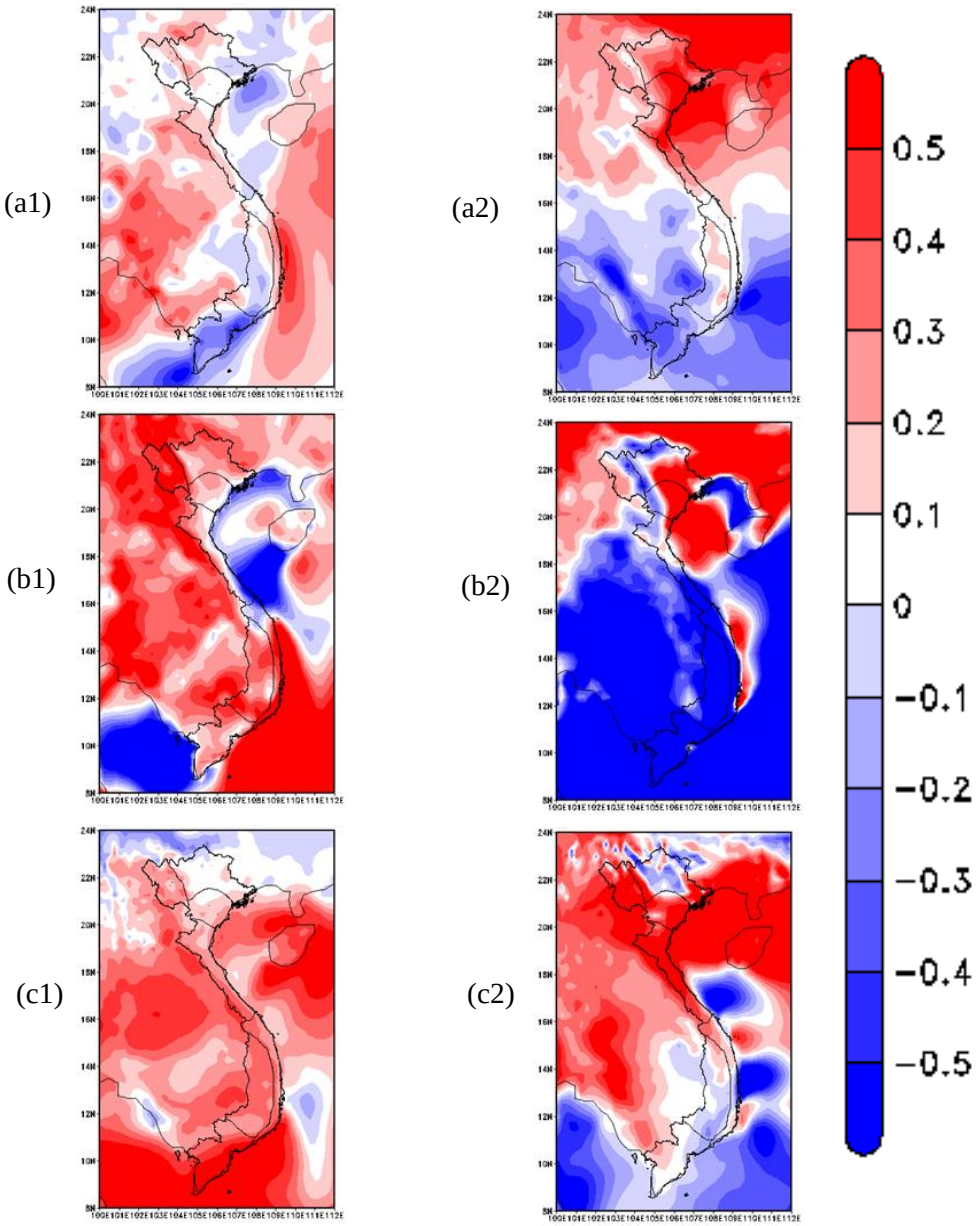

Figure 4-21: Wind speed Change (%), 2071-2100 relative to 1961-1990
(a) WRF/CCSM (b) WRF/ECHAM (c) PRE/HAD
(1) DJF (2) JJA

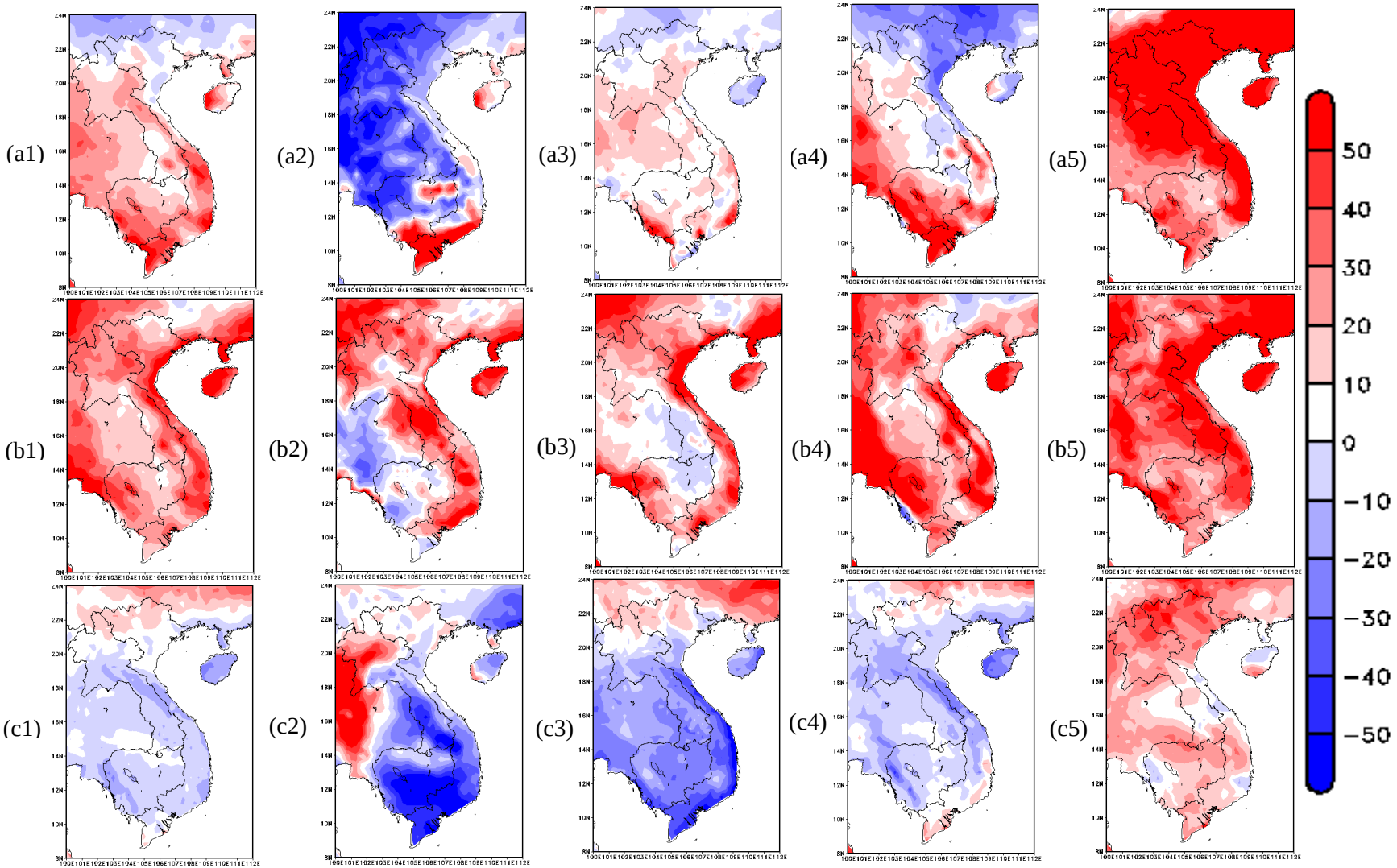

Figure 4-22: Precipitation Change (%), 2071-2100 relative to 1961-1990
(a) WRF/CCSM (b) WRF/ECHAM (c) PRE/HAD

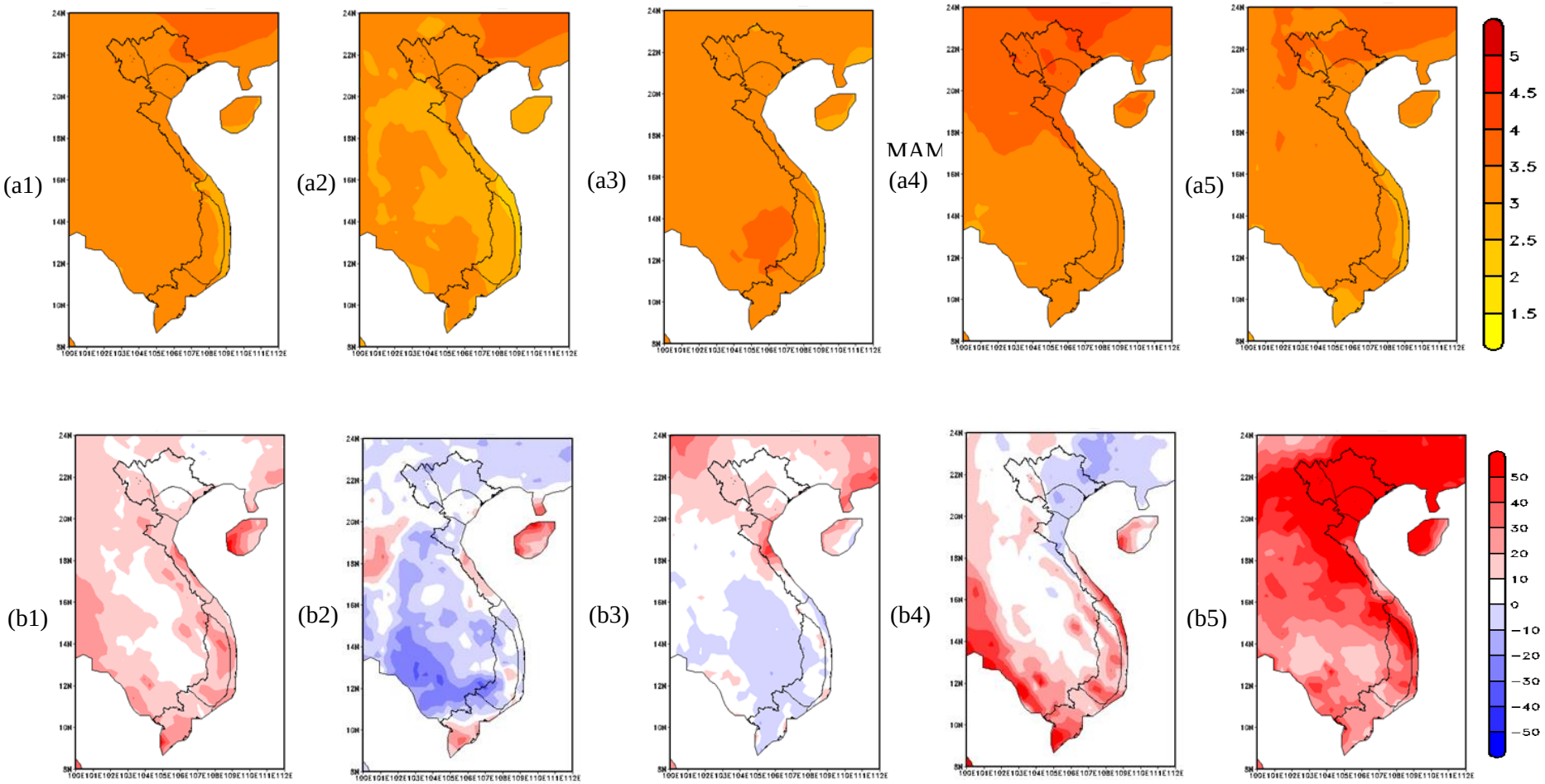

Figure 4-23: Ensemble Climate response
(a) Surface Temperature (b) Precipitation
(1)Annual (2) DJF (3) MAM (4) JJA (5) SON

(a)

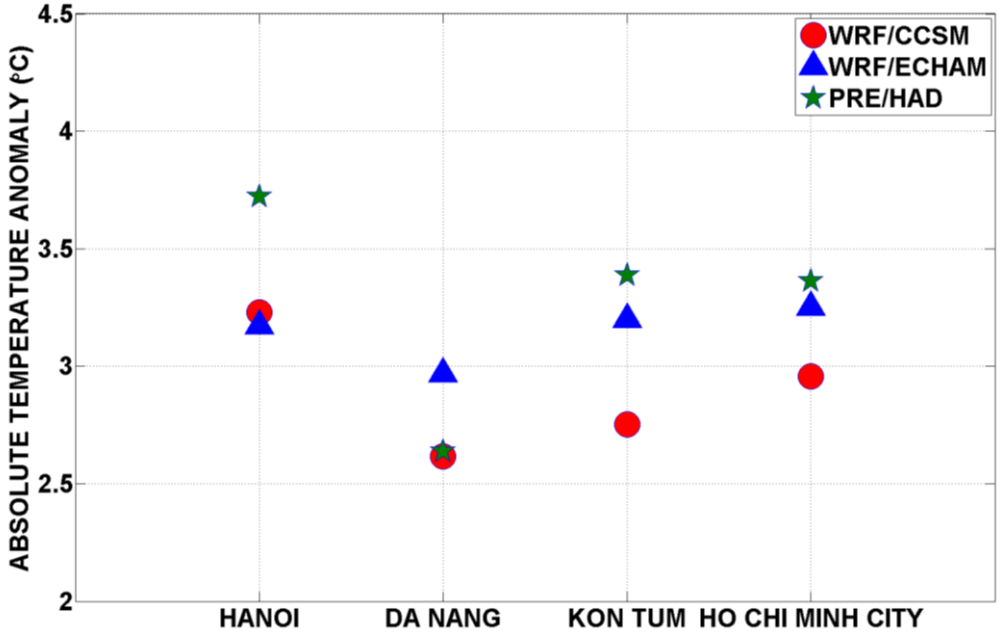

(b)

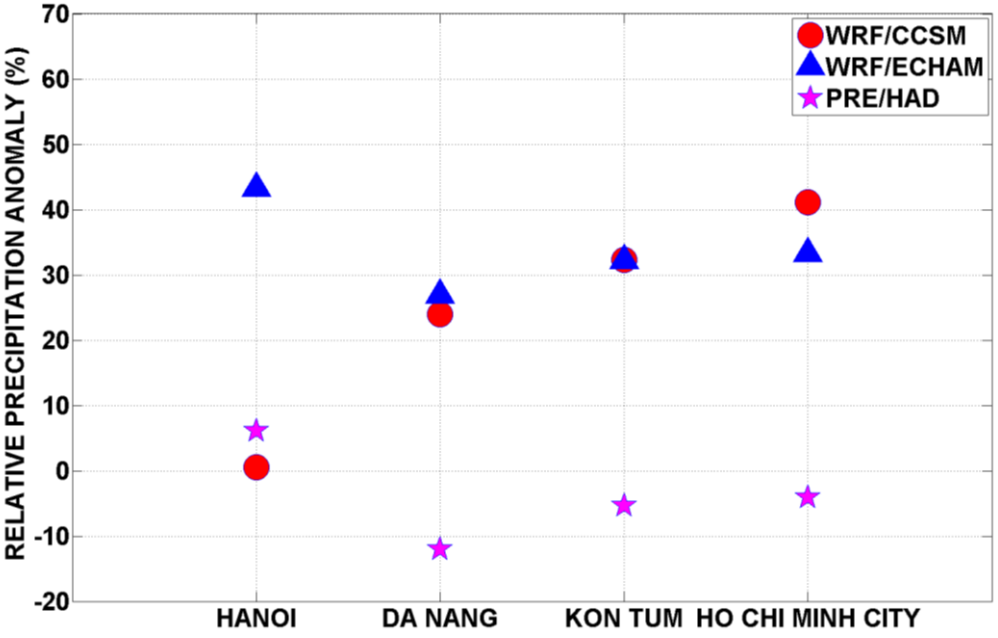

Figure 4-24: Bandwidth of Responses: 2071-2100 relative to 1961-1990
(a) Annual Surface Temperature (b) Annual Precipitation

Table 4-3 summarizes the main findings from this study. Temperature change (°C) and Precipitation change (%) are shown here for Annual and other 4 seasons (DJF, MAM, JJA and SON) for 7 climate zones derived from all 3 RCM simulations. The ensemble value is the average between 3 RCMs. For surface temperature, the 'ensemble' changes indicate at least an annual increase of about 3 °C in all zones. The summer JJA season is likely to expect more hot in the future in all season whilst the winter DJF season has the coolest change among all. Among 7 climate zones, regions S1, S2 and S3 have the highest increases in surface temperature. Region S5 has the lowest increase in temperature among all of about of 2.5 °C in winter. S6 and S7 are likely to expect a steady increase by 3 °C all year round.

An overall increase in rainfall over the seven climate zones on both annual (10 % to 20 %) and seasonal scales (-4 % to 85 %) is likely. The ensemble results also indicate that the rainy season, JJA, is likely to experience larger increases in rainfall than the DJF season, over all climatic zones, with the S7 region being the wettest and the S1, S2, the driest. The finding also points out that the transition season SON seems to have much more influence in the future with the increase in ensemble rainfall for all over the country is the highest. It refers to the shift in rainy season from JJA toward SON, especially in the S1, S2, S3 and S4 regions.

Table 4-3: Future Climate Change responses

Region	Temperature Change (°C)				Precipitation Change (%)			
	WRF/ CCSM	WRF/ ECHAM	PRE/ HAD	Ensemble	WRF/ CCSM	WRF/ ECHAM	PRE/ HAD	Ensemble
Annual								
S1	3.3	3.1	3.7	3.4	3.2	28.9	11.6	14.6
S2	3.4	3.3	3.6	3.4	-0.3	20.9	9.5	10.0
S3	3.2	3.2	3.6	3.4	2.4	42.0	2.8	15.8
S4	2.9	3.1	3.6	3.2	9.3	45.5	-5.4	16.4
S5	2.7	3.1	3.0	2.9	36.3	36.7	-10.1	20.9
S6	2.8	3.2	3.3	3.1	28.4	34.9	-5.0	19.4
S7	3.0	3.3	3.2	3.1	40.2	24.4	0.3	21.6
DJF								
S1	2.8	3.2	3.1	3.0	-38.3	32.0	6.6	0.1
S2	3.2	3.5	3.1	3.3	-28.6	27.4	6.2	1.6
S3	3.1	3.5	3.0	3.2	-18.0	35.9	0.9	6.3
S4	2.7	3.1	2.8	2.9	-8.7	29.0	-5.4	4.9
S5	2.3	2.9	2.5	2.5	22.8	27.0	-25.9	7.9
S6	2.4	3.1	2.8	2.8	9.8	39.6	-42.2	2.4
S7	2.7	3.4	3.0	3.1	86.3	17.9	-49.9	18.1
MAM								
S1	3.3	2.6	3.7	3.2	1.3	28.8	12.2	14.1
S2	3.0	2.7	3.5	3.1	-0.9	23.9	8.6	10.5
S3	2.9	2.7	3.6	3.1	10.4	53.9	-0.5	21.2
S4	2.7	2.8	3.9	3.1	10.1	56.9	-22.8	14.7
S5	2.8	3.1	3.1	3.0	20.3	37.7	-46.6	3.8
S6	3.0	3.2	3.7	3.3	10.1	23.0	-29.0	1.4
S7	3.3	3.3	3.4	3.3	10.7	23.6	-38.5	-1.4
JJA								
S1	4.4	3.3	4.1	3.9	-8.1	27.8	4.0	7.9
S2	4.2	3.3	4.0	3.9	-22.4	12.9	4.2	-1.8
S3	4.0	3.3	4.2	3.8	-27.3	20.7	-5.3	-4.0
S4	3.4	3.1	4.1	3.6	-15.0	37.5	-13.5	3.0
S5	3.0	3.2	3.5	3.2	22.6	44.7	-4.3	21.0
S6	3.0	3.2	3.6	3.3	22.2	44.3	-4.2	20.8
S7	3.0	3.2	3.3	3.2	64.0	29.5	9.5	34.3
SON								
S1	3.0	3.5	3.9	3.5	175.1	31.3	44.3	83.6
S2	3.1	3.5	3.9	3.5	172.3	47.4	35.8	85.1
S3	3.0	3.3	3.8	3.4	114.7	71.0	28.3	71.4
S4	2.9	3.3	3.5	3.2	80.4	51.0	10.4	47.3
S5	2.7	3.1	2.8	2.9	60.6	42.4	6.7	36.6
S6	2.9	3.2	3.2	3.1	48.2	40.5	15.8	34.8
S7	2.8	3.1	3.2	3.0	31.1	24.4	20.7	25.4

4.4 CONCLUSIONS

Thirty year (1961-1990) present day climate simulations have been performed using two regional climate models, WRF and PRECIS, at a horizontal spatial resolution of 25 km. The evaluation on the performance of the models on simulating the state of the climate over this baseline present day period has been discussed in Section 4.2. The results have portrayed a reasonably satisfactory performance of the climate models, further to which, another 30 year simulation of future climate (2071-2100) was undertaken to ascertain future climate change. Ensemble climate changes over seven main climate zones in Vietnam have been derived, which suggest an overall increase in rainfall and surface temperatures which have implications for climate change adaptation and mitigation. Of the two main objectives in this research study, giving ensemble high resolution regional climate projections for Vietnam is one and has thus been achieved through this chapter. The results that emanated from this study have been further used in the impact study discussed in Chapter 5, whose main findings form the second objective of this thesis. However, some analytical discussion on these model results and implications for climate change and adaptation from these derived future climate change estimates have been done in Chapter 6.

CHAPTER 5 ASSESSING FUTURE STREAM FLOW USING THE SWAT HYDROLOGICAL MODEL

5.1 INTRODUCTION

Forming the basis of the second objective of this research thesis, this chapter describes the application of ensemble regional climate model outputs that were used as input to a hydrological model to determine future hydro climatic changes. It is recalled here that these regional climate model outputs (surface temperatures and precipitation) were derived using the WRF and PRECIS models which were used to downscale the GCMs CCSM, ECHAM5 and HadCM3, under the IPCC A2 future greenhouse gas emission scenario, whose results and main findings have already been discussed in Chapter 4.

The Dakbla river basin over the Lower Mekong Basin of Vietnam has been considered for stream flow modelling using the SWAT hydrological model (Chapter 1, Section 1.6). A 20 year climatology of the past, 1981-1990 and 1996-2005, was used to calibrate and validate the model for the present day climate stream flow simulations and another 30 year climate, over the period 2071-2100, was chosen for the future climate, to assess future changes in the stream flow. The various hydrological model simulations and their results are the main contents of this chapter.

5.2 SENSITIVITY ANALYSIS, CALIBRATION AND VALIDATION OF THE SWAT MODEL

5.2.1 Model description and setup

Further to a brief introduction to the SWAT model in Chapter 3, Section 3.2, the experimental set up and detailed methodology are discussed in this section. The input for SWAT includes a spatial reference map which is a DEM having a resolution of 250 m, a land use map, a soil map (converted to raster format at the same resolution) and meteorological data (precipitation and temperature time-series of all stations in daily scale), which are displayed in Figure 5-1 (a, b, c respectively).

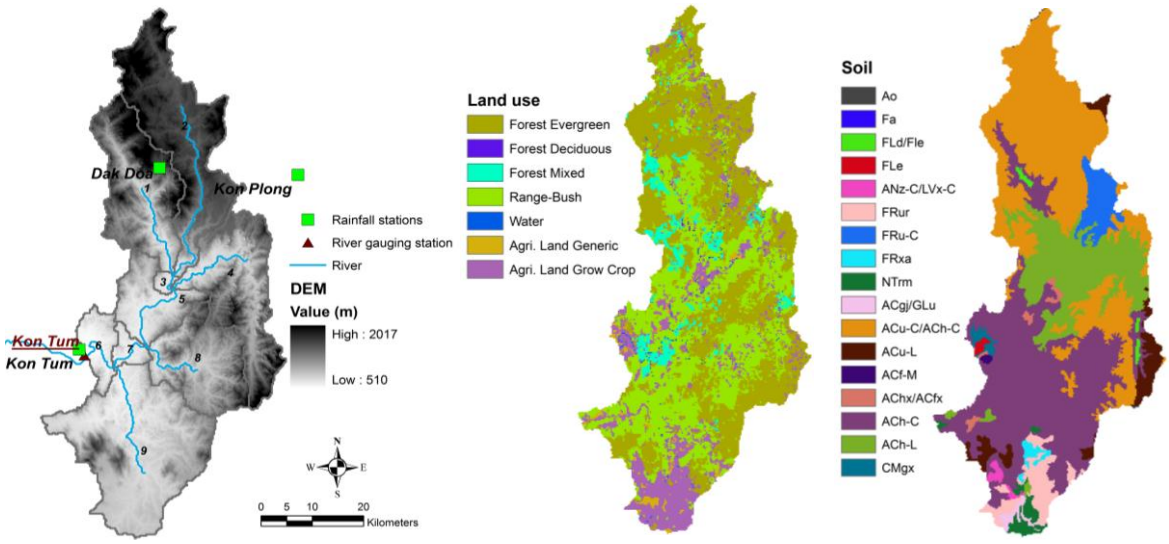

(a) (b) (c)

Figure 5-1: SWAT model spatial inputs
(a) DEM (b) Land use and (c) Soil map of Dakbla river basin

Daily scale precipitation data were obtained from 1980-1990 and 1995-2005 period for 3 rainfall stations (Kon Plong, Kon Tum and Dak Doa). Daily maximum and minimum surface temperature data were obtained from the local authority from the Kon Tum meteorological station for the same period. Daily river stream flow data at Kon Tum gauging station at the downstream end of Dakbla river were also used. These data were used for both the calibration and validation processes in the stream flow simulations of the SWAT model. In the calibration part, the SWAT model was run in a daily time step for the period of 1980-1990 using station observed rainfall and river stream flow at Kon Tum gauging station, with the first year 1980 used as the spin up period. The validation was done for another 10 year period of 1996-2005 to ensure that the model was well calibrated. The reason for choosing these 10 years periods for calibration and validation is because of the data availability as longer period data for 30 years from station sources were not available. However, a 30 year period delta factor approach (future minus present day) was applied to simulate the response in stream flow in the last 30 years of 21st century (described in Section 5.3). After the calibration and validation of the SWAT model was done, the present day climate stream flow simulations for the period 1981-1990 were undertaken using the RCM outputs to assess the models' ability to reproduce

present day stream flow conditions. Finally, future rainfall derived from different RCMs under climate change scenarios were then used to determine changes, if any, on the future stream flow over the Dakbla region with respect to the baseline period.

5.2.2 Model Sensitivity Analysis

Prior to calibrating a hydrological model, the sensitivity analysis is a method that analyzes the sensitivity of different model parameters (Table 5-1) that influence the hydrological model performance. This method serves to filter those model parameters that either have or have not any significant influence on the model results. On the other hand, it also aims to reduce the number of parameters required in the auto-calibration method. Traditional methods of sensitivity analysis have been classified by Saltelli et al., (2000). They are: (1) Local method (Melching and Yoon, 1996) (2) integration of local to global method using Random One-Factor-At-a-Time (OAT) proposed by Morris (1991) and (3) Global methods like Monte Carlo and Latin-Hypercube (LH) simulation (McKay et al., 1979; McKay, 1988). By studying the advantages and disadvantages of each of the above methods, van Griensven et al. (2006) developed the LH-OAT method which performs LH sampling followed by OAT sampling. This method samples the full range of all parameters using LH design along with the precision of OAT sampling to ensure that the changes in each model output could be attributed to the changed parameter. In this thesis study, the LH-OAT design has been coupled to the ArcSWAT 2005 (described earlier in Chapter 3, Section 3.2) model for the sensitivity analysis module. In the SWAT model, there are 25 parameters that are sensitive to stream flow, 6 parameters sensitive to sediment transport and other 9 parameters sensitive to water quality. In this study, sensitivity analysis was performed for 25 parameters of stream flow as listed in Table 5-1 from which 11 most sensitive parameters were then selected (Table 5-2) for performing the ‘auto calibration’, which is explained in the following section. Details of the LH-OAT method are given in the Appendix F2.

Table 5-1: SWAT Parameters sensitive to stream flow

Group	*Parameter*	*Description*	*Unit*
Soil	Sol_Alb	Moist soil albedo	-
	Sol_Awc	Available water capacity	mm/mm
	Sol_K	Saturated hydraulic conductivity	mm/hr
	Sol_Z	Depth to bottom of second soil layer	mm
Subbasin	Tlaps	Temperature laps rate	^{o}C/km
HRU	Epco	Soil evaporation compensation factor	-
	Esco	Plant uptake compensation factor	-
	Canmx	Maximum canopy storage	mm H_2O
	Slsubbsn	Average slope length	m
Routing	Ch_N2	Manning's "n" value for the main channel	-
	Ch_K2	Effective hydraulic conductivity in main channel alluvium	(mm/hr)
Groundwater	Alpha_Bf	Baseflow alpha factor	days
	Gw_Delay	Groundwater delay	days
	Gw_Revap	Groundwater "revap" coefficient	-
	Gwqmn	Threshold depth of water in the shallow aquifer for return flow to occur	mm H_2O
	Revapmn	Threshold depth of water in the shallow aquifer for "revap" to occur	mm H_2O
Management	Biomix	Biological mixing efficiency	-
	Cn2	Initial SCS runoff curve number for moisture condition II	-
General Data Basin	Sftmp	Snowfall temperature	^{o}C
	Smfmn	Minimum melt rate for snow during year	mm H_2O/^{o}C/day
	Surlag	Surface runoff lag time	days
	Timp	Snow pack temperature lag factor	-
	Smfmx	Maximum melt rate for snow during year	-
	Blai	Maximum potential leaf area index for land cover/plant	-
	Slope	Slope	-

5.2.3 Auto-calibration by ParaSol method (Parameter Solution)

The ArcSWAT model has the options to choose either manual or auto-calibration. Calibration is applied to those most sensitive parameters, specified in Table 5-2, to yield the optimal set of values for the model parameters which results in the minimum discrepancy between the observed and the simulated river discharge data. The auto calibration is applied to find the optimal set of parameters that give the results for the best objective function, described later in this section. Essentially, this step ensures that the best calibration is attained using a suitable set of parameters.

Table 5-2: Sensitivity analysis ranking of 11 most sensitive parameters in SWAT model to stream flow

Sensitivity Analysis Order	***Parameter***	***Description***	***Parameter range***	***Initial value***	***Optimal value***
1	Cn2	Initial SCS runoff curve number for moisture condition II	35 ~ 98	35	96.78
2	Ch_K2	Effective hydraulic conductivity in main channel alluvium	-0.01 ~ 500	0	150
3	Sol_Awc	Available water capacity	0 ~ 1	0.22	0.44
4	Sol_K	Saturated hydraulic conductivity	0 ~ 2000	1.95	1873
5	Ch_N2	Manning's "n" value for the main channel	-0.01 ~ 0.3	0.014	0.073
6	Alpha_Bf	Baseflow alpha factor	0 ~ 1	0.048	0.027
7	Surlag	Surface runoff lag time	1 ~ 24	4	1
8	Esco	Plant uptake compensation factor	0 ~ 1	0	0.66
9	Gwqmin	Threshold depth of water in the shallow aquifer for return flow to occur	0 ~ 5000	0	1107
10	Gw_Revap	Groundwater "revap" coefficient	0.02 ~ 0.2	0.02	0.17
11	Gw_Delay	Groundwater delay	0 ~ 500	31	215

Parameter Solution method (ParaSol) is a built-in auto-calibration model in the ArcSWAT 2005 version (van Griensven and Meixner, 2004). ParaSol operates by a parameter search method for model parameter optimization followed by a statistical method that was performed during the optimization to provide parameter uncertainty bounds and the corresponding uncertainty bounds on the model outputs. The ParaSol method aggregates objective functions

(OFs) into a global optimization criterion (GOC), minimizes these OFs or a GOC using the Shuffled Complex Evolution Method (SCE) (Duan et al., 1992) algorithm. A detailed description of the ParaSol method can be found in the Appendix F and it has also been documented by van Griensven and Meixner (2004). The optimal values of sensitive parameters after being calibrated by the ParaSol method are displayed in the last column of Table 5-2.

5.2.4 Results of SWAT model calibration and validation

Using the above methodology, the SWAT model was calibrated to ensure a robust performance before undertaking stream flow simulations using climate model output. The coefficient of determination (R^2) and the Nash-Sutcliffe Efficiency Index (NSE), mentioned in Chapter 3, were used as benchmarking indices to assess the goodness of fit of the SWAT hydrological model.

The calibration and validation graphical results for Dakbla river are shown in Figure 5-2 and Figure 5-3, in daily (a) and monthly (b) scales, respectively. It is clearly seen in Figure 5-2b that the simulated peak to peak discharge (on a monthly scale) and the low flow agree well with the observed data better than the agreement seen on daily scale, due to higher variability in daily scales. The validation plots, shown in Figure 5-3, indicate that the trend of observed data is being captured by the simulated flow, although some of the peak to peak discharges are underestimated compared to observed flow. The values of R^2 and NSE, shown in Table 5-3 indicate that the comparison indices in daily and monthly scale for both calibration and validation are around 0.5 and 0.7 respectively. It is considered a good performance of the SWAT model as the study focuses only on the long term period of a 10 year climatology.

These results also indicate that the hydrological model was well calibrated using the ParaSol method and that the model was able to reproduce the pattern of the observed stream flow well enough. This leads to the next stage of the application of the climate model derived rainfall data to be used for stream flow simulations, as the calibration and validation stages used only the station data rainfall and temperature.

(a)

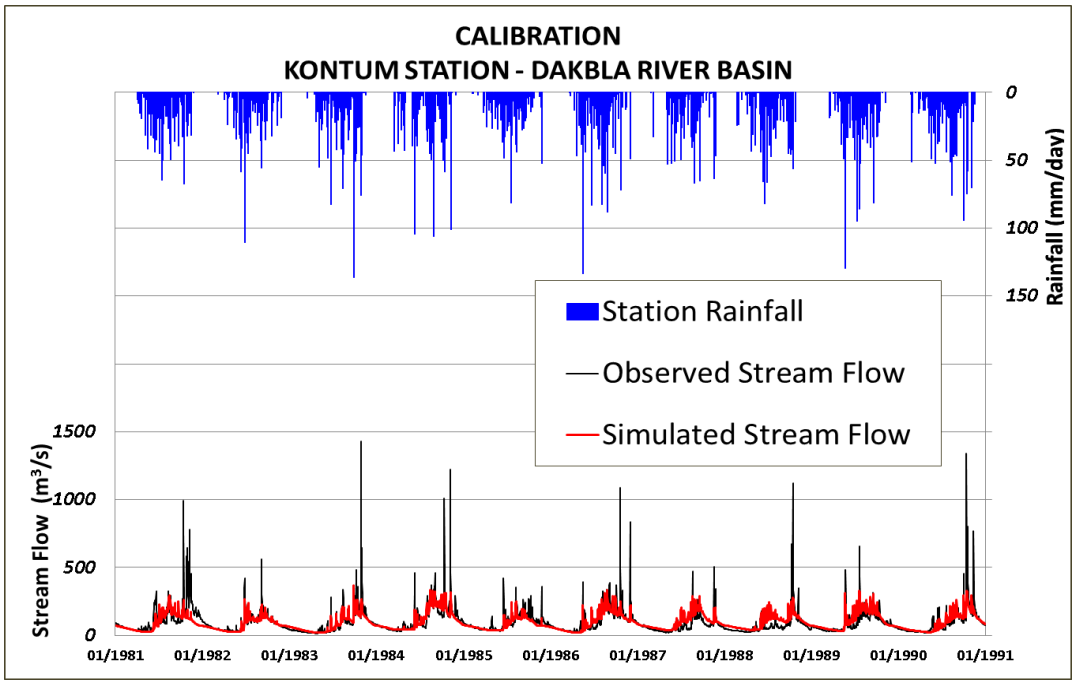

(b)

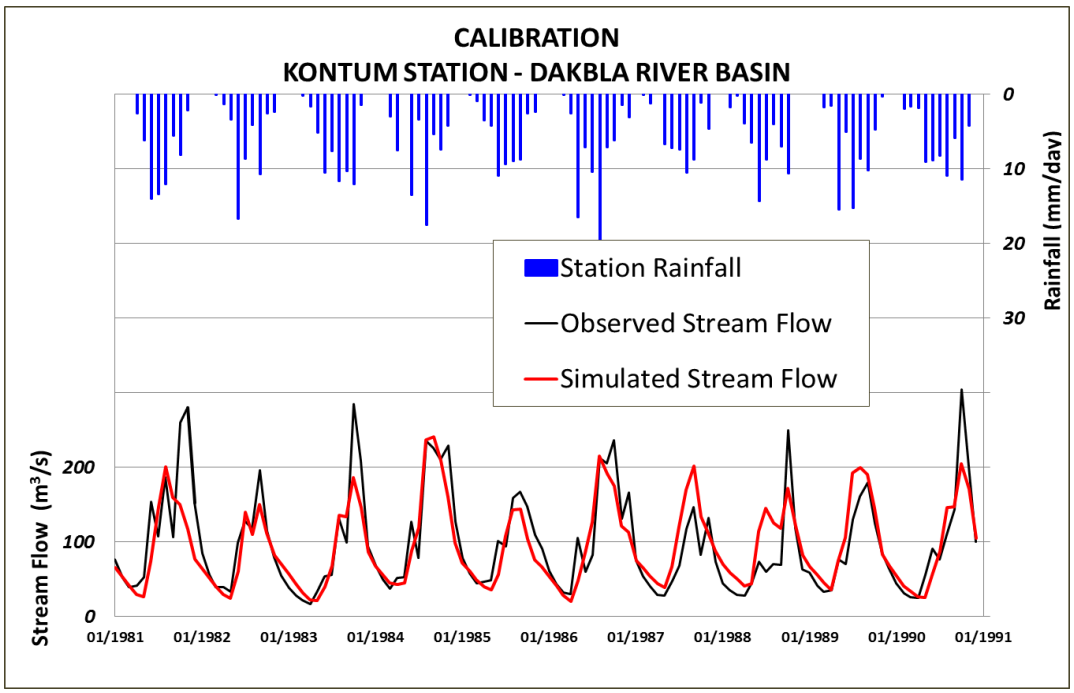

Figure 5-2: Calibration of the SWAT model
(a) daily scale (b) monthly scale

(a)

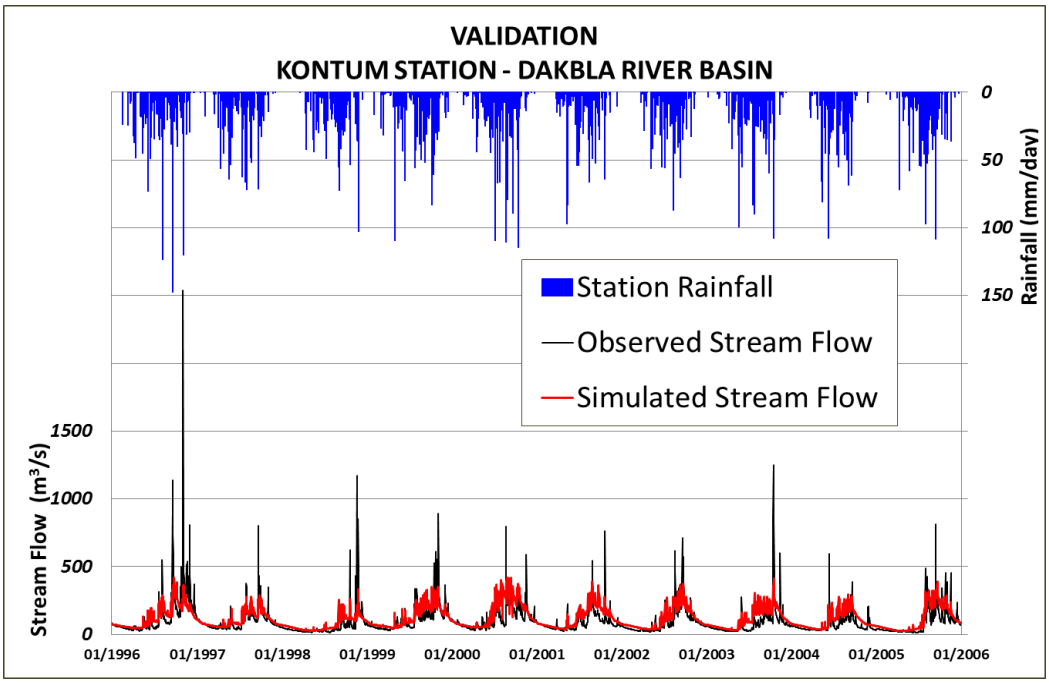

(b)

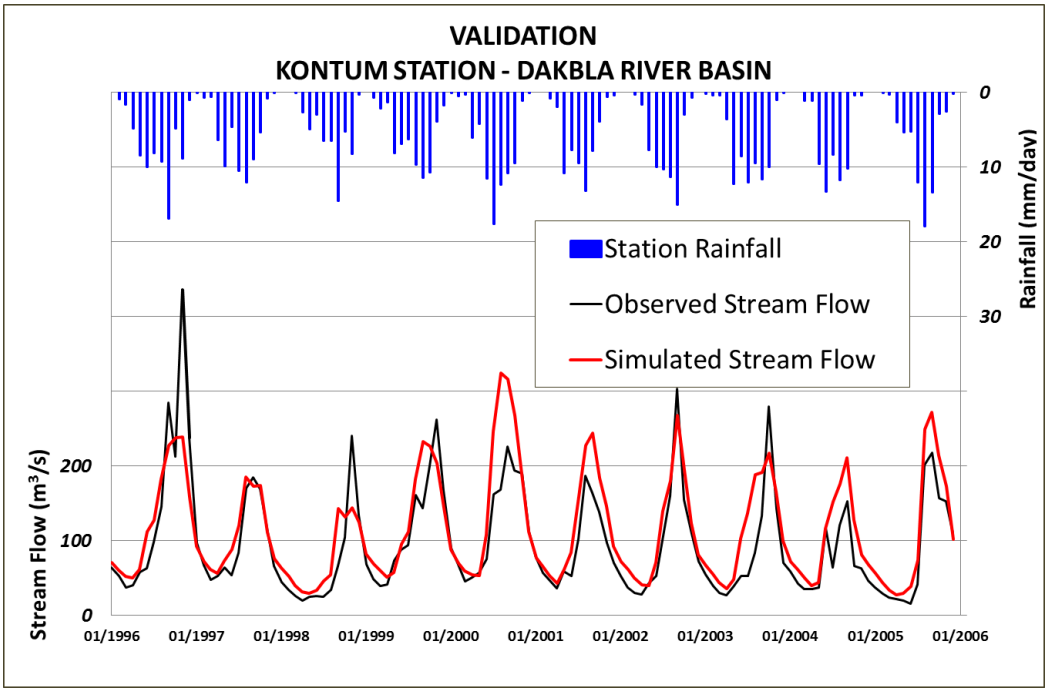

Figure 5-3: Validation of the SWAT model
(a) daily scale (b) monthly scale

Table 5-3: Statistical Indices of model calibration and validation: R^2 and NSE

River Basin	*Calibration (1981-1990)*				*Validation (1996-2005)*			
	Daily		*Monthly*		*Daily*		*Monthly*	
	R^2	*NSE*	R^2	*NSE*	R^2	*NSE*	R^2	*NSE*
DAKBLA	**0.51**	**0.53**	**0.72**	**0.74**	**0.45**	**0.43**	**0.73**	**0.66**

5.3 SIMULATION OF STREAM FLOW OVER THE STUDY REGION FOR THE PRESENT DAY CLIMATE USING REGIONAL CLIMATE MODEL OUTPUTS

Chapter 4 discussed the climate model simulations and future climate projections over Vietnam. Since the hydrological study in this thesis focuses on a catchment area in central Vietnam, the present day climate patterns and future projections derived from the climate models over this sub-region catchment alone are discussed briefly here before going into the hydrological simulations. The region of the catchment is relatively small compared to the whole Vietnam country region and it is necessary to understand how well the climate models are able to replicate the climate over a small region as the precipitation and surface temperature outputs from RCMs over this catchment area are used as input to the SWAT model simulations.

The mean climate over the present day period 1981-1990 are shown in Figure 5-4 and Figure 5-5, for temperature and precipitation, respectively. It is to be noted that the spatial maps for station data alone are not displayed here because there are not enough daily scale data available for the period 1981-1990. Hence only observation gridded data (CRU, CPC and APH) are used.

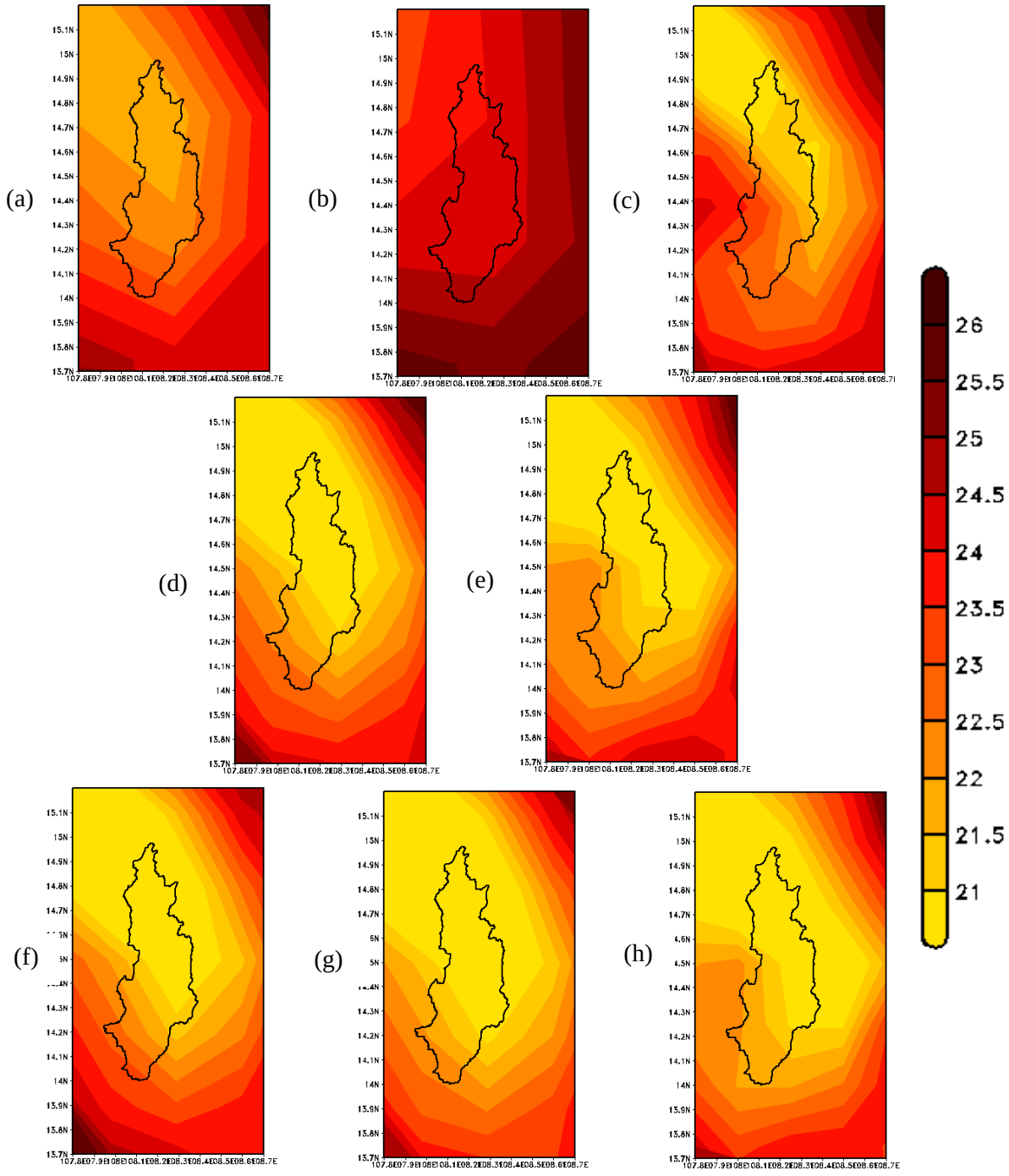

Figure 5-4: Annual Surface Temperature over Dakbla: 1981-1990, °C
(a) CRU (b) CPC (c) APH (d) WRF/ERA (e) PRE/ERA
(f) WRF/CCSM (g) WRF/ECHAM (h) PRE/HAD

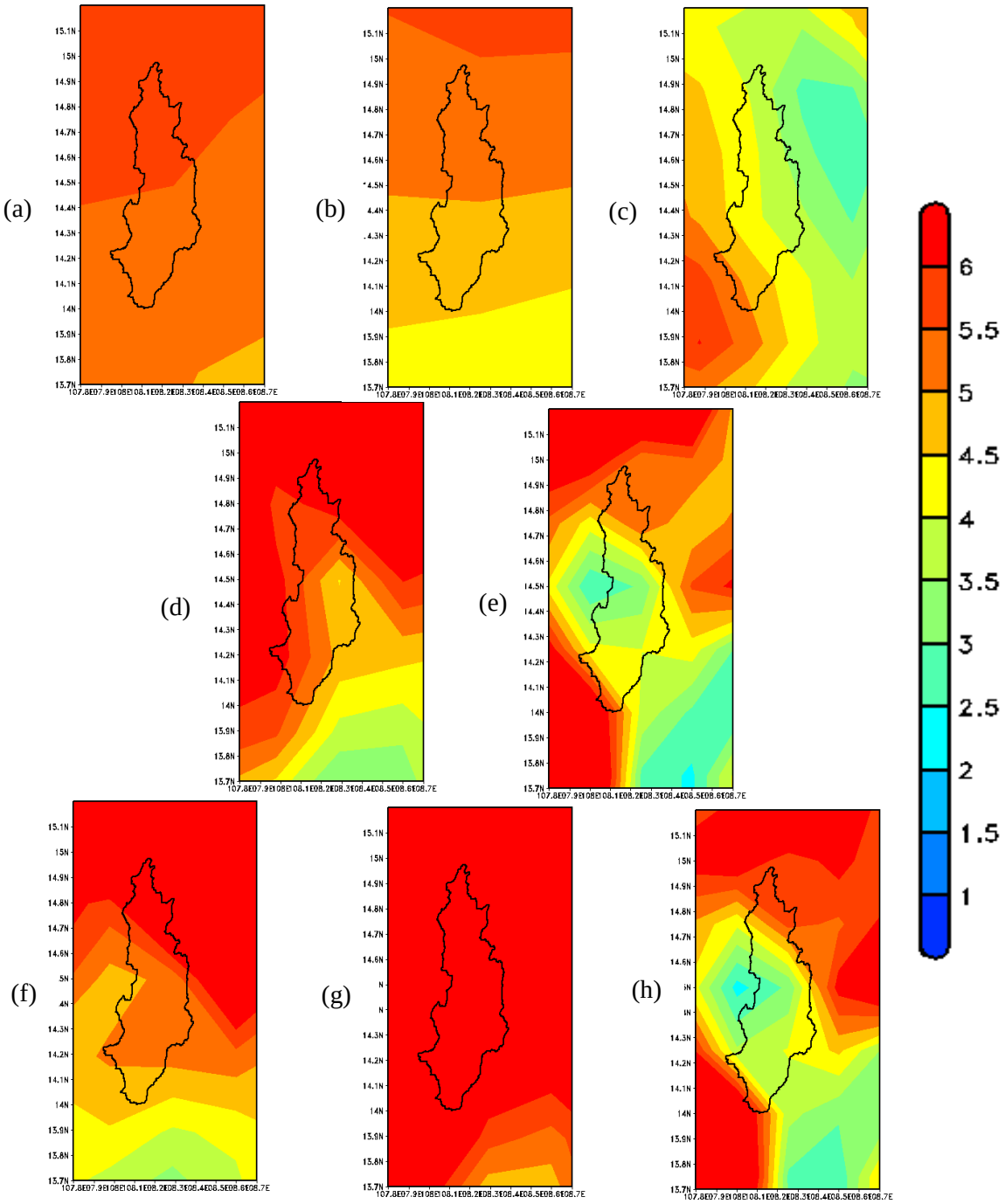

Figure 5-5: Annual daily average Precipitation over Dakbla: 1981-1990, mm/day
(a) CRU (b) CPC (c) APH (d) WRF/ERA (e) PRE/ERA (f) WRF/CCSM (g) WRF/ECHAM (h) PRE/HAD

As mentioned in Section 1.6, there are 2 distinct seasons over the Central Highland region: a wet (rainy) season (MJJASO) and a dry season (NDJFMA). The wet season is significant as it experiences 85 % of the annual rainfall and is the main source for flooding over this area. Hence, discussions of model results will largely pertain to this season. The mean rainy season (MJJASO) profiles for surface temperature and precipitation are shown in the Appendix F (Figure F-7 and Figure F-8).

As seen from the temperature distributions (Figure 5-4), both WRF and PRECIS models provide a good match against the APH dataset. CRU and CPC observations overestimate the temperature distributions in comparison with APH. The 10 year mean annual precipitation profiles of the gridded observational data, station data and the regional climate models in Figure 5-5 show some differences in the spatial distribution. It is also evident that there are strong observational uncertainties. CRU and CPC overestimate the precipitation intensities of APH. The gradient distribution is better in APH dataset compared to CRU and CPC because of its finer resolution of 0.25°. The climate model simulations indicate a reasonable replication of the gradient distribution in rainfall with WRF/ERA, PRE/ERA, PRE/HAD while WRF/CCSM follows the pattern and CRU and CPC. WRF/ECHAM overestimates the rainfall profiles. Similar inferences can be made from the seasonal profiles that are shown in the Appendix F (Figure F-7 and Figure F-8).

What these spatial results suggest is that there are higher uncertainties in both the observational dataset as well as the regional climate model simulations at sub-regional scales. This also suggests that higher resolutions (of about 5-10 km) might be necessary to improve the simulations over such smaller areas, but still remind us the need for dense observational networks against which the model performance can be further evaluated. Though further improvements might be necessary in the model simulations, the results suggest that the climate model outputs are reasonably good enough to be used for stream flow simulations. This provides a first-cut understanding of the use of these output and their usefulness for hydrological studies which have implications of assessment of changes in hydrological

responses in a future climate.

As the next step, the SWAT model was used to simulate stream flow over the present day climate period 1981-1990 using the results of the RCM (WRF and PRECIS). The precipitation and surface temperature variables from the RCM outputs of WRF/ERA and PRE/ERA were initially used for stream flow simulation, followed by the outputs of WRF/CCSM, WRF/ECHAM and PRE/HAD. The rationale for doing so is the same as that of the regional climate simulations – to test the performance of the true climate first and then that of the GCMs. The daily scale precipitation and temperature derived from the RCMs were bi-linearly interpolated to the respective rainfall stations (Kon Plong, Kon Tum, Dak Doa) and meteorological station (Kon Tum). The SWAT model usually takes as input, measured rainfall data from gauged stations then distributes its values to all of its sub-catchments. Hence, an interpolation is required to compute the station data (at a particular grid point) when using gridded data. Thus, linear interpolation is applied in this case. The bilinear interpolation method is an extension of the linear interpolation for interpolating functions of two variables on a regular grid and hence this is used to extract precipitation value for a station data, at a grid point, from the entire gridded data source derived of the RCM output. The same approach is applied for the surface temperature.

Since the parameters options were fixed in the earlier part of calibration, the SWAT model was used to simulate stream flow with the same parameter options using the RCM output described earlier. The results of this stream flow simulation for the present day climate are shown as annual cycles of stream flow in Figure 5-6. All RCM outputs show a reasonable agreement against the observed data over the dry season period from December through to April. For the main flood season (June to November) which occurs and ends one month after the rainy season, there is an increase in the intensity of stream flow simulated by the WRF model results and a decrease simulated by the PRECIS model. These correspond to the precipitation simulations of these climate models discussed earlier by analysing the 2D spatial distribution: the overestimation of rainfall by the WRF/ECHAM model and the underestimation by

PRE/HAD. The WRF/CCSM shows a close agreement with the station data whilst WRF/ECHAM simulates higher orders of stream flow intensities during peak and post flood seasons. The PRE/HAD also simulates stream flow of a lesser intensity to that of the station data. However, the stream flow simulation using the WRF/ERA and PRE/ERA gain significance since these simulations relate to the reanalysis driven 'true climate'.

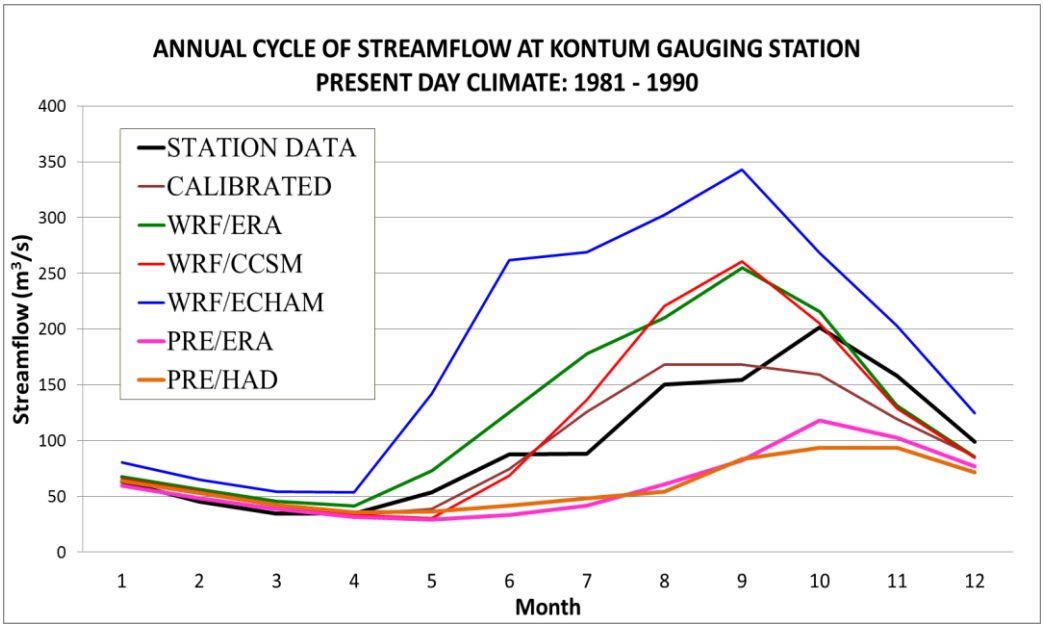

Figure 5-6: Climatological Annual Cycles of Stream flow

The differences in these model results stem from the different rainfall intensities simulated by the model and these differences, rather uncertainties, could be probably attributed to these climate model physics and dynamics, as discussed in Chapter 4. It is clear that these uncertainties in climate model simulated rainfall estimates influence stream flow simulations. This is because the uncertainties from the RCMs propagate into the hydrological model also. The RCMs improve upon the large scale or the global forcing data such as the GCMs, but do not correct any errors of these forcing data.

The improvement, in other words, the 'added value' of the RCMs comes from the fact that RCMs, at higher resolutions that incorporate detail terrain and local circulation features, provide more credible estimates of climate at such sub-regional scales. But despite these uncertainties what should be taken a good sign of model simulations is that the annual/seasonal cycle is reasonably well reproduced as this is crucial for stream flow assessments. Since the

overall present day climate patterns of the stream flow simulations were satisfactorily derived using the SWAT model, it also places confidence that the same RCM outputs can therefore be used to assess future stream flow using the changes in climate model derived future rainfall.

5.4 ASCERTAINING CLIMATE RESPONSE

The annual surface temperature and precipitation responses for Dakbla river basin over the future period 2071-2100 with baseline period 1961-1990 from the three RCM simulations discussed so far, are displayed in Figure 5-7 and Figure 5-8 respectively.

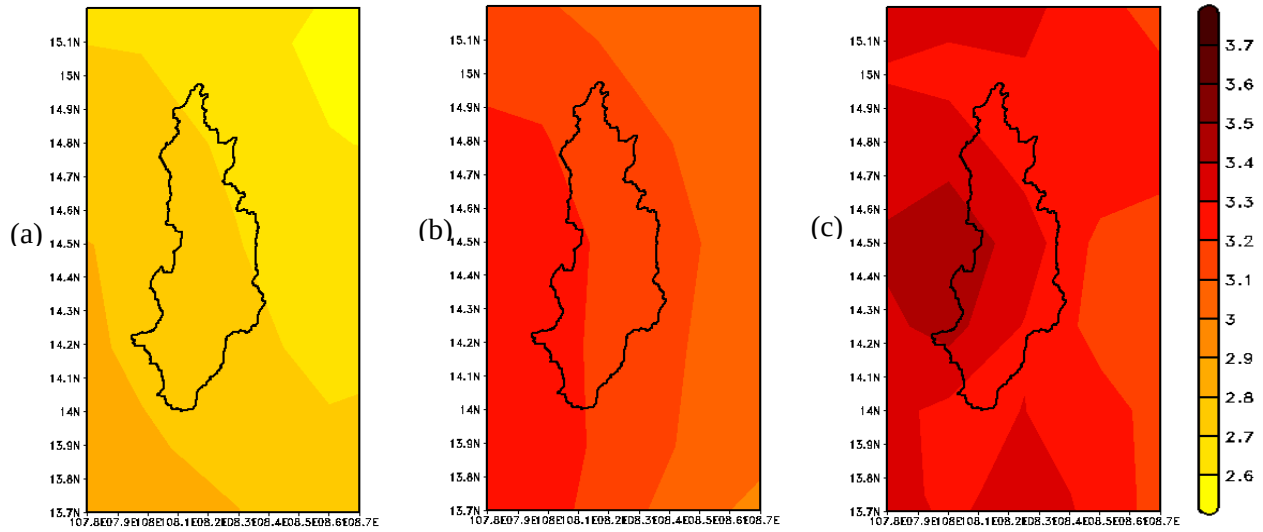

Figure 5-7: Annual Surface Temperature response (^{o}C) over Dakbla region
(a) WRF/CCSM (b) WRF/ECHAM (c) PRE/HAD

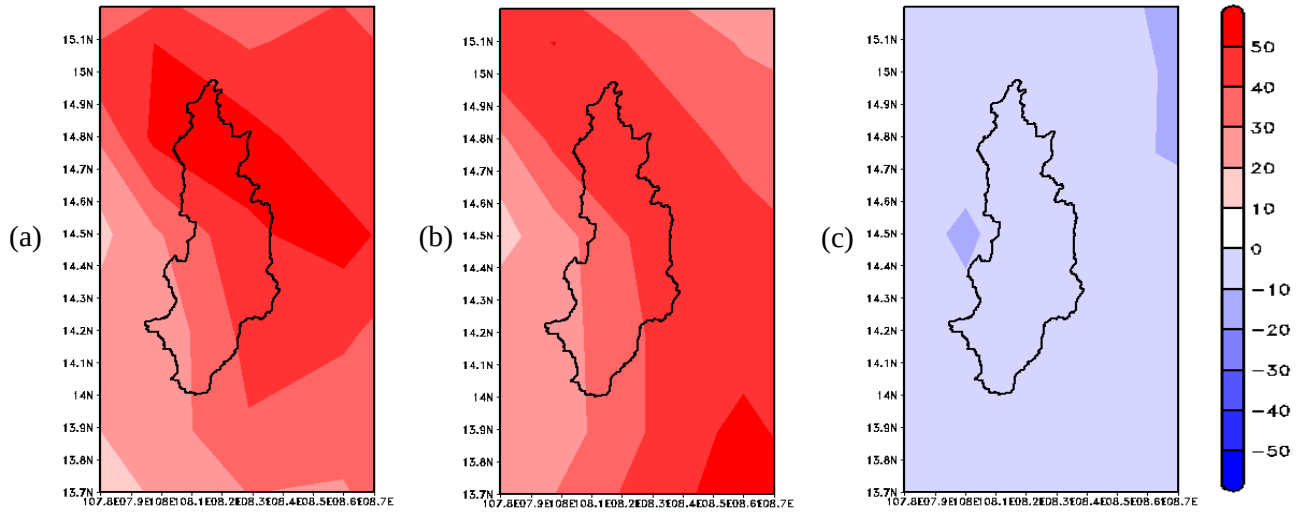

Figure 5-8: Annual Daily average Precipitation response (%) over Dakbla region
(a) WRF/CCSM (b) WRF/ECHAM (c) PRE/HAD

The surface temperature response indicates a sharp increase in this region, ranging from 2.6 °C in WRF/CCSM to 3.7 °C in PRE/HAD. The very high temperature change simulated by the PRECIS model also suggests high evapotranspiration over this area which might be affecting the stream flow results due to reduced rainfall, shown in Figure 5-9. The relatively lesser change simulated by WRF/CCSM and henceforth the differences in the warming trends is likely due to the different climate sensitivities of these global models: CCSM, ECHAM5 and HadCM3. The CCSM3.0 is considered a lower climate sensitivity model, meaning a lesser warming trend than that of the other models (IPCC, 2007a).

The WRF simulations indicate a precipitation response which shows an increase of about 10 % to 40 % whilst PRECIS simulations show a minor decrease of less than 10% over the study area. This suggests a peak discharge (increasing trend for WRF and minor decrease for PRECIS model) during rainy season as displayed in Figure 5-9. When compared to the precipitation change (increases) of the WRF/CCSM and the WRF/ECHAM models, the relatively opposite signal of change in the PRECIS model could also be attributed to the climate sensitivity of the GCM HadCM3 which was used to drive the PRECIS model. However, should the WRF model be driven with the GCM HadCM3 (data not available as mentioned in Chapter 3), this change factor in precipitation could be better corroborated. This remains as an uncertainty in rainfall projections as such.

As mentioned earlier, data availability for 20 years (for calibration and validation parts of the SWAT model) curtailed stream flow simulations to 20 year period. Such 20 year simulations are generally considered good enough for hydrological studies and similar studies have been done and documented by Hay et al, (2002) and Graham et al, (2005). However, the RCM derived precipitation and temperature climate change factor between future 2071-2100 and present day period 1961-1990 (future minus present day) is added as the **'delta factor approach'** to the precipitation and temperature data from the selected meteorological stations to calculate the future response in stream flow over Dakbla catchment. This delta factor method is usually practiced by impact modellers because the difference between the future and

present day model output cancels the biases in the model output and yields the clear signal of climate change (Sushama et al., 206, Andersson et al., 2006). Since the RCM simulations are not as perfect as the station data, this climate change delta factor information is added to the station data time series, since the best available record of precipitation and surface temperature are the station data. Since model biases in stream flows are also evident from Figure 5-6, this delta factor approach attempts to overcome the limitation of model biases propagating into the hydrological model and thus use only this 'climate change' information over the future. The addition of this climate change factor to the station data time series gives a 'new' time series of station rainfall, which incorporates the changed future conditions of climate. This change factor added station rainfall was then used as the input to the SWAT model to simulate future stream flow.

It is reminded again that the RCM outputs from WRF/CCSM, WRF/ECHAM and PRE/HAD were used for simulating future stream flow, as these are the sources of future climate information, downscaled by the two regional climate models.

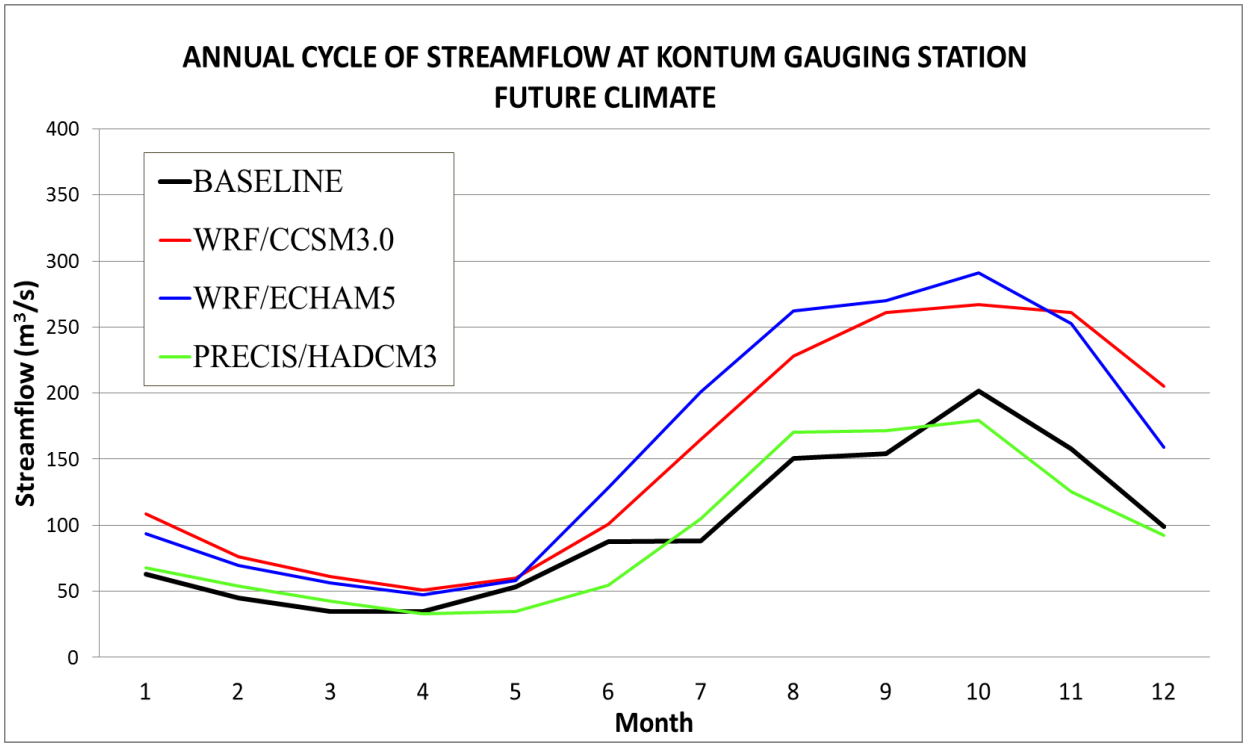

Figure 5-9: Future stream flow over Dakbla (compared to baseline stream flow)

The Figure 5-9 shows the stream flow thus derived over the river basin Dakbla using different RCMs. For clarity in comparison, the present day stream flow (shown as 'baseline') is overlain on the future estimated stream flow that used the change factor as discussed above. Results from both WRF model outputs indicate that the future stream flow is expected to increase by nearly 60 % in total annual discharge whilst it decreases by 3% using PRECIS model output. During the dry season period, the WRF/ECHAM suggests an increase of 47 % and WRF/CCSM also shows an increase, but by 70%. PRE/HAD indicates a negligible decrease. The flood season (JJASON) shows a sharp increase with WRF/ECHAM indicating an increase of about 67% and WRF/CCSM by 53% while a reduction is simulated by PRE/HAD, of 4%.

5.5 SUMMARY AND CONCLUSIONS FROM THE HYDROLOGICAL SIMULATIONS

Existing research studies indicate uncertainties in climate projections stemming from global climate models and different emission scenarios of climate change. Since global climate outputs have been found insufficient for regional and local impacts, it has been realized that adaptation measures to climate change requires high spatial resolution information and hence the use of regional climate models in climate research has become common. Impact studies are widely conducted and make use of the information derived from such regional climate models. Since hydrology is one of the most common impact studies, this chapter highlighted the importance of high resolution models in impacts research and the use of sophisticated optimization algorithms when applying hydrological models.

In this study Rainfall derived from climate model has been applied to a hydrological model (SWAT) which was calibrated with ParaSol method and its simulated discharges were compared with their observed counterparts. The performance of the model using station data rainfall has been found satisfactory and hence the model derived rainfall were also used to see assess stream flow simulation over the current and future climate. Using the RCM outputs, the present-day and future stream flows were also simulated. Results show that, over the Dakbla river basin, the future stream flow, especially during the rainy season is expected to increase,

which has implications not only for flood mitigation measures but also for water resources management, hydropower and agriculture. However, much more work is required to improve the confidence in these results.

Although the findings from the modelled results have been mentioned in the earlier section, some uncertainties in these many results also deserve a hearing. At the outset, the need for dense and robust observational networks cannot be ignored and it also needs to be stressed that better quality of station data will certainly improve the findings. Remote areas need to be equipped with more observational networks and measurements. In addition, further higher resolution simulation of the RCMs may be required to obtain more credible estimates of present day and future precipitation. Since this result has been obtained only from a few RCM simulations of future climates, it is recommended to obtain an ensemble estimate of future climate change by downscaling more GCMs or by using perturbed initial conditions to the RCM to derive multiple estimates of climate. The hydrological simulations using the results of thus derived ensemble climate simulations will add to the confidence of such a hydrological impact study. Further developments in the RCM model physics and dynamics might also help to see larger improvements in the climate simulations, yielding a better quality of RCM outputs, which in turn might improve the hydrological simulations. Yet again, the dense observations, cited earlier, will supplement the evaluations of the model performance. Therefore, it is evident that all these uncertainties are sort of inter-linked to each other and this is a clear example of a cascade of uncertainties mentioned in Chapter 1.

As to some uncertainties from the hydrological model, improved spatial data such as the DEM might help to improve the stream flow simulations since the current version was mapped a few years ago, in 2005. Other than the ParaSol method which was used for calibration, a few other auto-calibration methods which are coupled to SWAT-CUP model (SWAT Calibration Uncertainty Procedures, Abbaspour, et al., 2007) might give more possible outcomes which could help to understand a wider range of uncertainties. However, performing these methods themselves are comprehensive exercises that entail lot more sensitivity studies and

experimentations. Hence, these are as such beyond the scope of this thesis, yet possible future research work.

However, the research findings from this study are still useful as they yield some ‘new’ information that might be an inkling within wider and larger changes to come. This is because this study yet remains as one of the first detailed RCM studies undertaken over this region which provide preliminary possible future climate change information to policy makers. As these several uncertainties will be constrained down the road due to improvements in the modelling areas, those plausible wider and larger changes, probably, could be re-assuring to be used for further assessments of future changes.

CHAPTER 6 CONCLUSIONS & RECOMMENDATIONS

6.1 SUMMARY

Before concluding this thesis with a recap of the research objectives, the overall methodologies and the main findings, it is useful to recall that climate change is occurring at an alarming level. At the Cancun United Nations Climate Change Conference held on December 11, 2010, agreements were made that represented key steps forward in capturing plans to reduce greenhouse gas emissions and to help developing nations to protect themselves from climate impacts and be able to build their own sustainable futures. One of the key objectives of this meeting was to establish clear goals and a timely schedule for reducing human-generated greenhouse gas emissions over time to keep the global average temperature rise below 2 °C, because even that magnitude of increase in surface temperatures is likely to cause harsh impacts on different climate regimes and human population, leading to several changes to natural resources, bio-diversity, health and economy (http://www.unfccc.int).

The IPCC has been publishing its assessment reports every 5-6 years since 1990, but its Fourth Assessment Report, which won the Nobel Peace Prize in 2007, brought to the world's centre stage the hot issue of climate change and the necessity to combat climate change and its impacts in a war-footing. There has been a long debate on how this should be done and with time running out, the developing nations are hard hit who are naturally more vulnerable to climate change and its impacts.

Climate projections using global and regional climate models have been giving us idea of future likely changes and regional climate projections are now widely considered to be more credible in their estimates of future climate changes. GCMs have proven to be useful tools for simulating and understanding the past and present global climates, but for many regional and local climate impact studies, the GCM large scale information is insufficient to provide useful information due to its coarse spatial resolution. This is because the impact models require high resolution data at regional and local scales. This problem is compounded by considerable

uncertainties in the future projections of certain crucial climate variables, notably precipitation, highly variable in space and time. Hence, the demand for higher spatial resolution regional climate information has been steadily increasing. To overcome this problem, regional climate modelling or dynamical downscaling that uses a high resolution climate model for climate simulations over a desired region has become a wide research area in the climate sciences. Chapter 1 has already outlined this method of applying regional climate models and their 'added value' in climate simulations. Banking on such an 'added value' of using RCMs, this thesis has undertaken high resolution regional climate modelling using two widely used RCMs: WRF and PRECIS.

It has also been cited earlier that Southeast Asia remains as one of the highly climate vulnerable regions in the world. Many countries within Southeast Asia suffer from dearth of scientific expertise, technical knowledge and the resources to delve more into this climate science. This in turn leads to limitations in understanding climate and its impacts at regional and sub-regional scales, thereby not being able to devise suitable adaptive measures, putting both people and eco-system in peril. The country Vietnam was chosen in this study as the focus of research, owing to its high vulnerability and its background as a developing nation limited in scientific know-how and battling a struggling economy.

The main objectives of this thesis have been two folds: (1) to provide ensemble high resolution regional climate projections and (2) to assess future hydro-climate response over a particular catchment in the Central Highland region of Vietnam. Chapter 1 has already briefed about the Vietnam region and the catchment of study. Recent studies of the ADB and EEPSEA have marked Vietnam, within Southeast Asia, as highly vulnerable owing to factors such as floods, droughts, sea level rise, risks to farming/agriculture and weakening economy. Vietnam is the second largest exporter of rice in the world, has a vast bio-diversity, is a part of the Lower Mekong basin with extensive farming and hosts the Mekong delta that is prone to impacts from sea level rise. To date, very few studies focusing climate change and its impacts on Vietnam have been done, some of them mentioned in Chapter 2.

While some technical introduction to the climate and hydrological models and the data were dealt in Chapter 3, the ensemble regional climate projections were discussed in Chapter 4 and the hydrological response study was discussed in Chapter 5. As the next section, once again, highlights the main findings from this study, it needs to strongly reminded and stressed that this study applies 3 different GCMs (CCSM3.0, ECHAM5 and HadCM3) under one particular emission scenario of future climate change, A2, that have been downscaled by two different RCMs: WRF and PRECIS. This is indeed one of the first-of-its-kind studies over Vietnam that used such an 'ensemble' approach to study climate and its change and thus remains as one of the important contribution to the climate science research in Vietnam whose findings could be useful in policy making for adaptation to climate change.

6.2 MAIN FINDINGS AND CLIMATE CHANGE IMPLICATIONS FROM THE DYNAMICAL DOWNSCALING STUDY

In a nutshell, the results can be summarized thus. A steep increase in surface temperatures of more than 3 °C over all climatic zones is likely and rainfall is also likely to increase over all climate zones in Vietnam. The S5, S6 and S7 regions are likely to be wetter than the rest of the regions, indicating inundation risks, especially over the Mekong Delta region in S7. Some areas could also experience drought conditions, especially during the DJF season over the S1 and S2 regions in the north and during the DJF/MAM seasons in the S6 region, since the rainfall changes show mixed trends. Broadly, the ensemble projections on the annual and the seasonal scales are shown in Table 6-1, for temperature (T) and precipitation (P), since Chapter 4 has already discussed the changes on both annual and seasonal scales for different models (Refer Table 4-3).

From Table 6-1, it can be seen that the annual temperature increases in all regions from S1 to S7 with about 3.4 °C over S1, S2 and S3 regions and about 2.9 °C over S5. Highest increases are during the summer JJA over S1 and S2 (3.9 °C) and lowest is during winter DJF over S5 (2.5 °C). The annual rainfall is expected to increase over all regions in Vietnam. Wet seasons (JJA and SON) have higher increases compared to the dry seasons (DJF and MAM) in all

regions. SON is the season that has the highest increase of rainfall among all regions except S7.

It is found that the North West Vietnam region S1 has a quite varied trend as it shows no change in rainfall for the winter DJF period and it is needed to be mentioned here that DJF has minor effect over this region because of the Hoang Lien Son mountain range block the monsoon wind. The result shows slight increase in rainfall during southwest monsoon JJA (8%), while the annual increase is about 15 %. This could be explained only by analysing the changes over the other seasons where it is seen that the SON season shows a steep increase of 84 %. This implies that a slight transition of the rainy season by the end of the 21st century towards the SON season rather than JJA. This important finding could alert the local authorities for planning their activity towards impacts and adaptation. Temperature in this region tends to increase about 3.4 °C all year round and the hot summer is expected to increase by nearly 4 °C.

In a similar pattern over S1, the North East region S2 also is likely to experience a temperature increase all year round with a peak (3.9 °C) during the summer JJA season. Precipitation changes indicate an annual increase by 10% and a seasonal decrease in JJA season by 1.8%; however, it soars up during the SON season by 85 %.

The Red river delta S3 region is also likely to experience similar patterns of temperature changes as compared to the S1 and S2 region. Rainfall trends are mixed showing an annual increase by about 16 %, minor decreasing trends during JJA season (4%) and an increase during the SON season by 70%. These changes indicate that there is a need to alert local people to prepare against inundation because the S3 region is located at the river mouth of Red river and hence an increasing rainfall during the SON season for S1, S2 regions will make the conditions worse.

An annual increase in rainfall over the North Centre S4 region is nearly the same as S1 and S3 (16 %) but the increase over the SON season is only about 48 %, lower than S1, S2 and S3 area. In addition, the increasing trend in rainfall is likely in all seasons implying wet conditions all year round over this region. Historically, the Central region of Vietnam has been known

prone to flood for a very long time. People over this region have been learning to adapt to "living with flood" and they need more support from Vietnam's government during this flooding period. This study shows that this area may experience higher than normal rainfall intensity during this season. Once again, the local authority may be required to prepare for adequate adaptive measures.

The effect of southwest monsoon during the JJA season and the high topography at Hai Van pass creates huge differences in rainfall over the South Central region S5 as compared to S4. Percentage increases of 21 % in JJA and 37 % in SON contribute to the wetter conditions on an annual scale over S5. Thus, it could lead to high chances of flood exposure over this area during the rainy season. Temperature in S5 also increases with annual scale of 2.9 ℃ but with lesser magnitude compared to the north (3.4 ℃).

The Central Highland region of Vietnam S6 expects high annual temperature change (3.1 ℃) compared to its surrounding area (S5 and S7) despite its high topography. Highest change is during MAM (3.3 ℃) which is the peak of the dry season, implying probable worst conditions for drought. The S6 is currently exposed to severe drought during the dry seasons (DJF and MAM) and floods during the wet seasons (JJA and SON). The ensemble results from this study show an increase in annual rainfall by 20 % with very high increases during the rainy seasons in JJA (21 %) and SON (35%) and nearly no increase in rainfall during the dry seasons of DJF (2.4%) and MAM (1.4%). It is likely that the drought situation might not be improved by the end of 21st century whilst the flood situation may worsen.

Southern Vietnam S7 has the same characteristics as that of the S6 region with an annual rainfall increase of 21.6 % with higher increases during JJA (34.3 %) and SON (25.4 %) seasons. This area is also located at the downstream of the Lower Mekong Basin and therefore is affected from water usage from the upstream area as such during the dry season when it might face risks from drought. Besides that, flooding from heavy rainfall during the rainy season and the influences of tidal backwaters due to its low topography is typical. Hence, the increasing rainfall and any sea level rise due to climate change may contribute severely to flooding over southern Vietnam.

It is such that Vietnam is quite diverse in its climate and topography, experiencing annual and seasonal flooding in some parts while drought batters some areas. With both tropical and sub-tropical climates existing over the North and South regions and hosting high mountains, the climate over these regions, make Vietnam more difficult in its climate regime. In a concise summary, the main findings from this study show the projected changes in the future climate of temperature and precipitation from the '***ensemble'*** modelling experiments. Alongside likely impacts, some key implications due to climate change are also drawn.

Table 6-1: Summary for policy makers: VIETNAM REGION

Region	**Season**	**T (°C)**	**P (%)**	**Likely Climate Change Impacts**	**Sectors affected**
S1 NORTH WEST	Ann	3.4	14.6	• Increased annual rainfall • Highest rainfall increased during SON season • Drought during northeast monsoon • Warm winters and hot summers • Shifting in rainfall season	➢ Agriculture and Food security ➢ Hydropower ➢ Rural development ➢ Environment and biodiversity
	DJF	3.0	0.1		
	MAM	3.2	14.1		
	JJA	3.9	7.9		
	SON	3.5	83.6		
S2 NORTH EAST	Ann	3.4	10.0	• Increased annual rainfall • Highest rainfall increased during SON season • Drought during northeast monsoon • Warm winters and hot summers • Shifting in rainfall season	➢ Agriculture ➢ Forestry ➢ Rural development ➢ Environment and biodiversity
	DJF	3.3	1.6		
	MAM	3.1	10.5		
	JJA	3.9	-1.8		
	SON	3.5	85.1		

S3 RED RIVER DELTA	Ann	3.4	15.8	• Highest rainfall increased during SON season • Warm winters and hot summers • Sea level rise and saltwater intrusion in Red river delta • Shifting in rainfall season	➢ Agriculture and Food security ➢ Aquaculture ➢ Water resources ➢ Urban and Rural development ➢ Public health
	DJF	3.2	6.3		
	MAM	3.1	21.2		
	JJA	3.8	-4.0		
	SON	3.4	71.4		
S4 NORTH CENTRAL	Ann	3.2	16.4	• Increased annual rainfall • Likely massive flooding during SON season. • Likely Sea level rise and saltwater intrusion in coastal area • Landslide potential • Steep increase in temperature • Likely Drought conditions	➢ Agriculture and food security ➢ Rural development ➢ Public health ➢ Transportation
	DJF	2.9	4.9		
	MAM	3.1	14.7		
	JJA	3.6	3.0		
	SON	3.2	47.3		
S5 SOUTH CENTRAL	Ann	2.9	20.9	• Increasing rainfall all year, especially, JJA and SON • Increased flooding • Likely Sea level rise and saltwater intrusion in coastal area • Landslide potential • Mild increase in temperature • Likely Drought conditions	➢ Agriculture and food security ➢ Rural development ➢ Public health ➢ Transportation
	DJF	2.5	7.9		
	MAM	3.0	3.8		
	JJA	3.2	21.0		
	SON	2.9	36.6		

S6 CENTRAL HIGH LAND	Ann	3.1	19.4	• Increased rainfall all seasons • Increase flooding potential • Less rainfall during dry season and increases in temperature leading to severe drought.	➢ Agriculture and food security ➢ Hydropower ➢ Rural development ➢ Forestry ➢ Environment and biodiversity ➢ Water resources ➢ Public health
	DJF	2.8	2.4		
	MAM	3.3	1.4		
	JJA	3.3	20.8		
	SON	3.1	34.8		
S7 SOUTH	Ann	3.1	21.6	• Increased rainfall in all seasons • Severe flooding • Sea level rise and saltwater intrusion in Mekong delta • Highest impact from warming	➢ Agriculture and food security ➢ Aquaculture ➢ Water resources ➢ Urban and Rural development ➢ Environment and biodiversity ➢ Public health
	DJF	3.1	18.1		
	MAM	3.3	-1.4		
	JJA	3.2	34.3		
	SON	3.0	25.4		

6.3 MAIN FINDINGS AND IMPLICATIONS FROM THE HYDROLOGICAL STUDY

The Dakbla river basin, which is a small catchment located on the Central Highland region of Vietnam, is also facing similar climate change trends as discussed in the earlier section. As seen in Table 6-2, the surface temperatures (T) are likely to rise to about 3.1 °C on an annual scale, while the rest of the seasons could also see similar increases. Since catchment scale hydrology is dealt with here, the annual rainfall (P) is likely to show an increase of 30 % that leads to an increase in the annual stream flow by nearly 40 %. During the rainy MJJASO

season, rainfall increases about 36 % are likely that might result in about 44 % increase in total stream flow during the flooding season. Whilst the increase in rainfall in dry season is not much, about 12 % of that might raise the stream flow discharge (Q) to 25 %. This change also implies that the stream flow magnitude tends to increase a lot during the rainy season that may threaten the low lying areas with a flooding scenario. For simplicity, the seasons are collectively represented in the table [(May through to October) and (November through to April)] as the rainy seasons overlap between months in a year over this small region.

Table 6-2: Summary for policy makers: DAKBLA REGION

Region	Season	T (°C)	P (%)	Q (%)	Likely Climate Change Impacts	Sectors affected
DAKBLA	Annual	3.1	30.0	38.7	• Increased annual and seasonal rainfall • Higher increase rate during rainy season leads to severe flood • Increased temperature • Increased stream flow	➢ Agriculture & food security ➢ Hydropower ➢ Rural development ➢ Forestry ➢ Environment & biodiversity ➢ Water resources ➢ Public health
	MJJASO	3.3	36.0	43.6		
	NDJFMA	3.0	12.5	25.4		

6.4 THESIS CONTRIBUTION

As major contributions to this thesis work, the following are enumerated.

- Contributed significantly to the climate science over Vietnam where very few studies exists on climate research
- Provided a higher level of confidence to climate projections due to 'Ensemble approach'
- Improved understanding of likelihood of uncertainties in impact studies – range of possible outcomes
- Hydrological impact study over a small catchment, done for the first time over Dakbla river basin.

6.5 CONCLUSIONS AND FUTURE WORK

A systematic study of the future climate predictions using both regional climate models and a hydrological model has been thus performed. Possible climate change estimates have been pronounced for both the Vietnam region as a whole and over a small catchment in central Vietnam where the hydrological response has also been ascertained and thus the aims of this research study have been achieved.

While addressing the confidence in dynamically downscaled model results, it should be borne in mind the several uncertainties that exist in a 'long cascade of uncertainties' right from global climate models through to regional climate models and impact models. Since dynamical downscaling has been the main research methodology in this study, some uncertainties that pertain to RCMs might need to be understood, at the same time, it is once again noted here that quantification of RCM uncertainties is not within the scope of this thesis.

As cited in Chapter 3, the study begins with a strong premise that RCMs are good tools for downscaling. However, the usual uncertainties within RCMs largely come from the model physics options. Although a best set of such options have been chosen at this stage for this thesis, it cannot be denied that rooms for further improvement in the model physics and dynamics exist and it lies with the model developers and modelling community to pursue these efforts. Such developments in the future might improve model simulations close to reality to be able to pronounce even more credible results. As of now, these results remain as some new information that has come out from this comprehensive ensemble high resolution regional climate modelling study. Therefore, these findings are indeed useful for policy makers and stake holders as a first step in a longer series of future projections to come – from both a continued work of this research and from the research community.

There is also a further need for a systematic evaluation of propagation of uncertainty in the climate response through the use of hydrological models as these models take as input, the output from the RCMs. This, again, is beyond the scope of this research thesis but is essential to determine the full extent of climate impact uncertainties in the water resources sector. It is

highly useful to apply the ‘delta’ factor approach for RCM estimates in impact studies, as done in this study and the method discussed earlier in Chapter 5. This method removes the biases in the model estimations of precipitation and the determined delta factor can be taken as ‘new’ information along with the ‘added value’ information which is very appropriate for use in ensemble RCM simulations. Hence, the hydrological response determined over the Dakbla catchment is also a first step in delivering climate change responses, whose results have come from one of its first kind of studies, as done in this research. Future research could use even higher resolution RCM simulations of about 5-10 km to see improvements in spatial and temporal distributions of climate variables, especially precipitation that could see improvements in the hydrological simulations also. This, however, remains as continued work of this thesis.

Although the climate responses of the surface temperature show good agreement amongst all the three RCM simulations, rainfall has shown mixed trends. This primarily highlights the sensitivity in simulating a variable so highly variable in space and time. Of course, future RCM improvements may help to see better representation of the precipitation variable. Hence, there is higher confidence in temperature projections than is in precipitation. However, the ‘ensemble’ projections have clearly indicated increases in rainfall distributions all over Vietnam. This alone needs to be taken by policy makers as a mark of confidence. This argument is also applicable for extension to the hydrological responses as they have been derived using these RCM results. Such an analogy in taking the ‘ensemble’ results for consideration for policy makers can be seen from a similar approach of the IPCC (Refer to Appendix A, Figure A-1).

Drawing some concluding remarks, it can be said that although much of improvements in modelling and future climate scenarios are underway, it is essential to remember that climate models projections are more a likely snap shot of both possible and plausible changes in the future and are not final answers as such. Technical advancements in the coming years could augment the use of high resolution climate simulations to yield much more realistic and

credible simulations of climate. This could pave way for even realistic climate simulations due to enhanced topography at finer resolutions. Impacts studies might then be scaling even higher that a larger number of ensembles than done in this thesis could materialize easily without much of technical and time constraints. Hence, running different RCMs driven by the same number of GCMs and run the same RCM with different GCMs are likely to provide robust multiple ensembles of probabilistic scenarios of climate change in the future.

Given that many models will be used for climate projections, it stays with the modelling community to constrain uncertainties in models such as their physics and dynamics, incorporation of complex processes, inclusion of land use changes and atmospheric chemistry and simulations of extreme events, to make climate projections more reliable and useful for impact studies.

As scientific research is very much in that direction, future research work could throw light on more robust projections of climate change and its impacts. As these remain important tasks for the modelling and scientific community, the findings from this thesis serve as a tip of the ice berg in climate projections for Vietnam and the need for much more detailed research in this Southeast Asian context is very evident from this research.

****

BIBLIOGRAPHY

[1] Abbaspour, K.C., J. Yang, I. Maximov, R. Siber, K. Bogner, J. Mieleitner, J. Zobrist, R.Srinivasan. Modelling hydrology and water quality in the pre-alpine/alpine Thur watershed using SWAT. Journal of Hydrology, 333, pp. 413-430. 2007.

[2] ADB. The Economics of Climate Change in Southeast Asia: A Regional Review, Technical Report, Asian Development Bank, Manila. 2009.

[3] Akhtar M., N. Ahmad, M.J. Booij. The impact of climate change on the water resources of Hindukush-Karakorum-Himalaya region under different glacier coverage scenarios. Journal of Hydrology, 355, pp.148-163. 2008.

[4] Akhtar, M., N. Ahmad and M. Booij. Use of regional climate model simulations as input for hydrological models for the Hindukush-Karakorum-Himalaya region. Hydrology and Earth System Sciences, 13, pp.1075-1089. 2009.

[5] Allen, M.R. and W.J. Ingram. Constraints on future changes in climate and the hydrologic cycle, Nature, 419, pp.224–232. 2002.

[6] Alves, L.M. and J.A. Marengo. Assessment of regional seasonal predictability using the PRECIS regional climate modeling system over South America. Theoretical and Applied Climatology, 100, pp.337–350. 2010.

[7] Andersson, L., L. Wilk, M. Todd, D. Hughes, A. Earle, D. Kniveton, Layberry and H. Savenije. Impact of climate change and development scenarios on flow patterns in the Okavango River. Journal of Hydrology, 331 (1-2), pp.43-57. 2006.

[8] Arnell, N.W. Climate change and global water resources: SRES emissions and socio-economic scenarios. Global Environmental Change, 14, pp.31-52. 2004.

[9] Arnold, J.G. and N. Fohrer. SWAT2000: current capabilities and research opportunities in applied watershed modelling. Hydrol. Process. 19, pp.563–572, doi:10.1002/hyp.5611. 2005.

[10] Arnold, J.G., R. Srinivasan, R.S. Muttiah and J.R. Williams. Large area hydrologic modeling and assessment, part I: Model development. Journal of American Water Resources Association, 34(11), pp.73-89. 1998.

[11] Bader, D.C., C. Covey, W.J. Gutkowski, Jr. I.M. Held, K.E. Kunkel, R.L. Miller, R.T. Tokmakian and M.J. Zhang. Climate Models: An Assessment of Strengths and Limitations, U.S. Climate Change Science Program Synthesis and Assessment Product 3.1. Department of Energy, Office of Biological and Environmental Research, 124 pp. 2008.

[12] Bergström, S. Development and application of a conceptual runoff model for Scandinavian catchments, SMHI Report RHO 7, Norrköping, 134 pp. 1976.

[13] Bergström, S. The HBV model. In: Singh, V.P. (Ed.) Computer Models of Watershed Hydrology. Water Resources Publications, Highlands Ranch, CO., pp. 443-476. 1995

[14] Bloom, A., V. Kotroni and K. Lagouvardo. Climate change impact of wind energy availability in the Eastern Mediterranean using the regional climate model PRECIS. Natural Hazards and Earth System Sciences, 8, pp.1249-1257. 2008.

[15] Bosilovich, M.G. and W.Y. Sun. Numerical simulation of the 1993 Midwestern flood: Land-atmosphere interaction. Journal of Climate, 12 (2), pp.1490-1505. 1999.

[16] Bukovsky, M.S. and D.J. Karoly. A Regional Modeling Study of Climate Change Impacts on Warm-Season Precipitation in the Central United States. Journal of Climate, 24, pp.1985–2002. 2011.

[17] Buonomo, E., R. Jones, C. Huntingford and J. Hannaford. On the robustness of changes in extreme precipitation over Europe from two high resolution climate change simulations. Quarterly Journal of the Royal Meteorological Society, 133, pp.65-81. 2007.

[18] Caldwell, P., H.N. Chin, D.C. Bader and B. Govindasamy. Evaluation of a WRF dynamical downscaling simulation over California. Climatic Change, 95(3-4). 2009.

[19] Campbell, J.D., M.A. Taylor, T.S. Stephenson, R.A. Watson and F.S. Whyte. Future climate of the Caribbean from a regional climate model. International Journal of Climatology, 31(12), pp.866–1878. 2010.

[20] Chen, M., P. Xie, J. E. Janowiak and P.A. Arkin. Global land precipitation: A 50-yr monthly analysis based on gauge observations. J. Hydrometeorol., 3, pp. 249–266. 2002.

[21] Chotamonsak, C., J.P. Salathe, J. Kreasuwan, S. Chantara and K. Siriwitayakorn K. Projected climate change over Southeast Asia simulated using a WRF regional climate model. Atmospheric Science Letters, 12 (2), pp.213–219. 2011.

[22] Christensen, J.H. and O.B. Christensen. A summary of the PRUDENCE model projections of changes in European climate by the end of this century. Climatic Change, 81 (Supp.1), pp.7-30. 2007.

[23] Christensen, O.B. and J.H. Christensen. Intensification of extreme European summer precipitation in a warmer climate. Global and Planetary Change, 44, pp.107–117. 2004.

[24] Christensen, O.B. The PRUDENCE project, Description of work. Technical Report, pp.61. 2001.

[25] Christensen, O.B., M.A. Gaertner, J.A. Prego and J. Polcher. Internal variability of regional climate models. Climate Dynamics, 17 (11), pp.875-887. 2001.

[26] Dawson, B. and M. Spannagle. The Complete Guide to Climate Change. Routledge, Taylor & Francis, New York. 2009.

[27] Dickinson, R.E., R.M. Errico, F. Giorgi and G.T. Bates. A regional climate model for western United States. Climate Change, 15 (3), pp.383-422. 1989.

[28] Done, J., J.R. Leung, C.A. Davis and B. Kuo. Regional Climate Simulation using the WRF model. In WRF workshop, June 2005, Boulder, Colorado, USA.

[29] Duan, Q., S. Sorooshian and V.K. Gupta. Optimal use of the SCE-UA global optimization method for calibrating watershed models. Journal of Hydrology, 158, pp.265-284. 1994.

[30] Duan, Q., V.K. Gupta and S. Sorooshian. Effective and efficient global optimization for conceptual rainfall-runoff models. Water Resource Res., 28, pp.1015-1031. 1992.

[31] Dudek, M.P., X.Z. Liang and W. Wang. A regional climate model study of the scale dependence of cloud-radiation interaction. Journal of Climate, 9 (6), pp.1221–1234. 1996.

[32] Duffy, P.B., J. Coquard, J. Iorio, E. Zeledon, R.W. Arritt, W. Gutowski, J. Han, J. Kim, L.R. Leung and J. Roads. Simulations of Present and Future Climates in the Western United States with Four Nested Regional Climate Models. Journal of Climate, 19(6), pp.873-895. 2006.

[33] Duliere, V., Y.X. Zhang and E.P. Salathe. Extreme Precipitation and Temperature over the U.S. Pacific Northwest: A Comparison between Observations, Reanalysis Data, and Regional Models. Journal of Climate, 24, pp.1950-1964. 2011.

[34] Fernandez, J., J.P. Montavez, J. Saenz, J.F. Gonzalez-Rouco and E. Zorita. Sensitivity of the MM5 mesoscale model to physical parameterizations for regional climate studies: Annual Cycle. Journal of Geophysical Research,112, pp.1-18. 2007.

[35] Flaounas, E., S. Bastin and S. Janicot. Regional climate modelling of the 2006 West African monsoon: sensitivity to convection and planetary boundary layer parameterisation using WRF. Climate Dynamics, 36, pp.1083–1105. doi:10.1007/s00382-010-0785-3 for Portugal, Climate Dynamics, DOI 10.1007/s00382-012-1315-2. 2011.

[36] Forest, C.E., P.H. Stone, A.P. Sokolov, M.R. Allen and M.D. Webster. Quantifying uncertainties in climate system properties with the use of recent climate observations. Science, 295, pp.113-117. 2002.

[37] Fowler, H.J. and C.G. Kilsby. Using regional climate model data to simulate historical and future river flows in northwest England. Climatic Change, 80(3–4), pp.337–367. 2007.

[38] Fowler, H.J., M. Ekstrom, C.G. Kilsby and P.D. Jones. New estimates of future changes in extreme rainfall across the UK using regional climate model integrations-Assessment of control climate. Journal of Hydrology, 300 (1-4), pp.212–233. 2005a.

[39] Francisco, H.A. Adaptation to Climate Change: Needs and Opportunities in Southeast Asia. ASEAN Economic Bulletin, 25(1), pp.7-19. 2008.

[40] Frei, A., J.A. Miller and D.A. Robinson. Improved simulations of snow extent in the second phase of the Atmospheric Model Intercomparison Project (AMIP-2). Journal of Geophysical Research, 108(D12), pp.4369. 2003.

[41] Frei, C., R. Scholl, S. Fukutome, J. Schmidli and P.L. Vidale. Future change of precipitation extremes in Europe: Intercomparison of scenarios from regional climate models. Journal of Geophysical Research, 111, D06105. 2006.

[42] Giorgi, F. Simulations of Regional Climate using a Limited Area Model Nested in a General Circulation Model. Journal of Climate, 3 (9), pp.941-963. 1990.

[43] Gonz´alez-Zeas, D., L. Garrote, A. Iglesias and A. Sordo-Ward. Improving runoff estimates from regional climate models:a performance analysis in Spain. Hydrological Earth System Sciences Discussions, 9, pp.175-214. 2012.

[44] Graham, L.P., S. Hagemann, S. Jaun and M. Beniston. On interpreting hydrological change from regional climate models. Climatic change, 81, pp.97-122. 2007.

[45] Green, W.H. and G.A. Ampt. Studies on soil physics, Journal of Agri. Scie., 4, pp.11-24. 1911.

[46] Grell, G.A., J. Dudhia and D.R. Stauffer. A description of the fifth-generation Penn State/NCAR mesoscale model (MM5), NCAR Technical Note, NCAR/TN-398+STR, 117. 1994.

[47] Gyalistras, D., H. von Storch, A. Fischlin and M. Benitson. Linking GCM-simulated climatic changes to ecosystem models: Case studies of statistical downscaling in the Alps. Climate Research, 4, pp.167-189. 1994.

[48] Ha, D.T. and G. Shively. Coffee boom, Coffee Bust and Smallholder Response in Vietnam's Central Highlands, Review of Development Economics (Online Early Articles). 2007.

[49] Hargreaves, G.L., G.H. Hargreaves and J.P. Riley. Agriculture benefits for Senegal River basin. Journal of Irrig. and drain. Engr., 111(2), pp.113-124, 1985.

[50] Hay, L.E., M.P. Clark, R.L. Wilby, W.J. Gutowski, G.H. Leavesley, Z. Pan, R.W. Arritt and E.S. Takle. Use of regional climate model output for hydrological simulations. Journal of Hydrometeorology, 3, pp.571–590. 2002.

[51] Heikkila, U., A. Sandvik and A. Sorteberg. Dynamical downscaling of ERA-40 in complex terrain using the WRF regional climate model. Climate dynamics, 37(7-8), pp.1551-1564. 2010.

[52] Hewitson, B.C. and R.G. Crane. Climate downscaling: techniques and application. Climate Research, 7, pp.85-95. 1996.

[53] Ho, T.M.H, V.T. Phan, N.Q. Le and Q.T. Nguyen. Extreme climatic events over Vietnam from observational data and RegCM3 projections. Climate research, 49, pp.87-100.2011.

[54] Hong, S.Y., N.K. Moon, K.S. Lim and J.W. Kim. Future Climate Change Scenarios over Korea Using a Multi-Nested Downscaling System: A Pilot Study. Asia-Pacific Journal of Atmospheric Science, 46(4), pp.425-435, 2010.

[55] Hooghoudt, S.B. General consideration of the problem of field drainage by parallel drains, ditches, watercourses, and channels. Publ. No.7 in the series Contribution to the knowledge of some physical parameters of the soil (titles translated from Dutch). Bodemkundig Instituut, Groningen, The Netherlands. 1940.

[56] Im, E.S., I.W. Jung, H. Chang, D.H. Bae and W.T. Kwon. Hydroclimatological response to dynamically downscaled climate change simulations for Korean basins. Climatic Change, 100, pp.485–508. 2010.

[57] IPCC 2007a The Physical Science Basis. Contribution of Working Group I to the Fourth Assessment Report of the Intergovernmental Panel on Climate Change, S. Solomon, D. Qin,M.Manning, Z. Chen,M.Marquis, K.B.Averyt,M. Tignor and H.L.Miller, Eds., Cambridge University Press,Cambridge, 996 pp. 2007a.

[58] IPCC 2007b Impacts, Adaptation and Vulnerability Contribution of Working Group II to the Fourth Assessment Report of the Intergovernmental Panel on Climate Change, 2007 M.L. Parry, O.F. Canziani, J.P. Palutikof, P.J. van der Linden and C.E. Hanson (eds) Cambridge University Press, Cambridge, United Kingdom and New York, NY, USA. 976 pp.

[59] IPCC. Climate Change 2001: The Scientific Basis. Contribution of Working Group I to the Third Assessment Report of the Intergovernmental Panel on Climate Change [Houghton, J.T.,Y. Ding, D.J. Griggs, M. Noguer, P.J. van der Linden, X. Dai, K. Maskell and C.A. Johnson (eds.)]. Cambridge University Press, Cambridge, United Kingdom and New York, NY, USA, 881 pp. 2001.

[60] Islam, S.U, N. Rehman and M.M. Sheikh. Future change in the frequency of warm and cold spells over Pakistan simulated by the PRECIS regional climate model. Climatic Change, 94, pp.35-45. 2009.

[61] Jones, R.G., M. Noguer, D. C. Hassell, D. Hudson, S. S. Wilson, G. J. Jenkins and J.F.B. Mitchell. Generating high resolution climate change scenarios using PRECIS. Technical Report, 40 pp., Hadley Centre, UK MetOffice. 2004.

[62] Karmalkar, A.V., R.S. Bradley and H.F. Diaz. Climate change in Central America and Mexico: regional climate model validation and climate change projections. Climate Dynamics, 37, pp.605-629. 2011.

[63] Kotlarski, S., A. Block, D. Jacob, K. Keuler, R. Knoche, D. Rechid and A. Walter. Regional climate model simulations as input for hydrological applications: evaluation of uncertainties. Advances in Geosciences, 5, pp.119–125, 2005.

[64] Kumar, K.K., S.K. Patwardhan, A. Kulkarni, K. Kamala, K.K. Rao and R. Jones. Simulated projections for summer monsoon climate over India by a high-resolution regional climate model (PRECIS). Current Science, 101, pp.312-326. 2011b

[65] Kumar, K.R., A.K. SahaI, K.K. Kumar, S.K. Patwardhan, P.K. Mishra, J.V. Revadekar., K. Kamala and G.B. Pant. High-resolution climate change scenarios for India for the 21st century. Current Science, 90, 334-345. 2006.

[66] Leung, L.R. and S.J. Ghan. Pacific Northwest climate sensitivity simulated by a regional climate model driven by GCM I: Control Simulations. Journal of Climate, 12 (7), 2010-2030. 1999.

[67] Leung, L.R. and Y. Qian. Atmospheric rivers induced heavy precipitation and flooding in the western U.S. simulated by the WRF regional climate model. Geophysical Research Letters, 36, L03820. doi: 10.1029/2008GL036445. 2009

[68] Leung, L.R., Y. Qian and X. Bian, W.M. Washington, J. Han and J.O. Roads. Mid-century ensemble regional climate change scenarios for the western United States. Climate Change, 62 (1-3), pp.75–113. 2004.

[69] Leung, L.R., Y. Qian and X. Bian. Hydroclimate of the western United States based on observations and regional climate simulation of 1981–2000. Part I: Seasonal statistics. Journal of Climate, 16 (12), pp.1892–1911. 2003a.

[70] Liang, X.Z., H.I. Choi, K.E. Kunkel, Y. Dai, E. Joseph and J.X.L. Wang. Surface boundary conditions for mesoscale regional climate models. Earth Interactions, 9, paper 18. 2005.

[71] Liang, X.Z., L. Li, A. Dai and K.E. Kunkel. Regional climate model simulation of summer precipitation diurnal cycle over the United States. Geophysical Research Letters, 31, L24208, doi: 10.1029/2004GL021054. 2004a.

[72] Lo, J.C.F., Yang, Z.L. and Roger A. Pielke Sr. Assessment of three dynamical climate downscaling methods using the Weather Research and Forecasting (WRF) model. Journal of Geophysical Research, 113, D09112, doi:10.1029/2007JD009216. 2008.

[73] Ma, X. and Fukushima, Y.: Numerical model of river flow formation from small to large scale river basins. In: Singh, V.P., Frevert, D.K. (eds) Mathematical model of large watershed hydrology. Water resources publications. 891, LLC, Englewood, Colorado, USA. pg 433-470

[74] Ma, X., T. Yoshikane, M. Hara, Y. Wakazuki, H.G. Takahashi and F. Kimura. Hydrological response to future climate change in the Agano River basin, Japan. Hydrological Research Letters, 4, pp.25–29. 2010.

[75] Marengo, J.A, R. Jones, L.M. Alves and M.C. Valverde. Future change of temperature and precipitation extremes in South America as derived from the PRECIS regional climate modeling system. International Journal of Climatology, 29, pp.2241–2255. 2009.

[76] McKay, M.D. In: Ronen, Y (Ed), Sensitivity and Uncertainty Analysis Using a Statistical Sample of Input Values CRC Press, Boca Raton, FL, pp.145–186. 1988.

[77] McKay, M.D., R.J. Beckman and W.J. Conover. A comparison of three methods for selecting values of input variables in the analysis of output from a computer code. Technometrics, 21 (2), pp.239–245. 1979.

[78] Mearns, L.O., M. Hulme, T.R. Carter, R. Leemans, M. Lal and P. Whetton. Climate Scenario Development. Pp.583-638. In J.T. Houghton et al. (eds.), Climate Change 2001: The Scientific Basis, Contribution of Working I to the Third Assessment Report of the IPCC, Chapter 13. Cambridge U. Press: Cambridge. 2001.

[79] Meehl, G.A., T. Stocker et al. Global climate projection. pp.901-945. In Solomon et al. (eds.), IPCC, 2007b: Climate Change, 2007: The Physical Science Basis. Contribution of Working Group I to the Fourth Assessment Report of the Intergovernmental Panel on Climate Change. Cambridge U. Press: Cambridge UK. 2007.

[80] Melching, C.S. and C.G. Yoon. Key sources of uncertainty in QUAL2E model of Passaic river. Journal of Water Resources Planning and Management, ASCE, 122 (2), pp.105–113. 1996.

[81] Mileham, L., R.G. Taylor, M. Todd, C. Tindimugaya and J. Thompson. The impact of climate change on groundwater recharge and runoff in a humid, equatorial catchment: sensitivity of projections to rainfall intensity. Hydrological Sciences Journal-Journal Des Sciences Hydrologiques, 54, pp.727-738. 2009.

[82] Mitchell, T.D. and P.D. Jones. An improved method of constructing a database of monthly climate observations and associated high-resolution grids. Int. J. Climatology, 25, pp.693-712, Doi: 10.1002/joc.1181. 2005.

[83] MONRE, Ministry of Natural Resources and Environment, Vietnam. Climate Change, Sea Level rise scenarios for Vietnam, pp.9-16, Technical Report, Hanoi. 2009.

[84] Monteith J.L. Evaporation and the environment. Symposia of the society for Experiemental Biology. Cambridge Univ. Press, 1965, London, UK, pp.205-234.

[85] Morris, M.D. Factorial sampling plans for preliminary computation experiments, Technometrics, 33, pp.161-174. 1991.

[86] Murphy, J.M. An evaluation of statistical and dynamical techniques for downscaling local climate. Journal of Climate, 12 (8), pp.2256–2284. 1999.

[87] Murphy, J.M. Predictions of climate change over Europe using statistical and dynamical downscaling techniques. International Journal of Climatology, 20 (5), pp.489-501. 2000.

[88] Nash, J.E. and J.V. Sutcliffe, River flow forecasting through conceptual models, Part 1 – A discussion of principles. Journal of Hydrology, 10(3), pp.282-290. 1970.

[89] Neitsch, S.L., J.G. Arnold, J.R. Kiniry, R. Srinivatsan and J.R. Williams. Soil and Water Assessment Tool Input/Output File Documentation, Version 2005. Grassland, Soil and Water Research Laboratory, Agricultural Research Service, Temple, Texas 76502. 541pp.

[90] New, M., M. Hulme and P.D. Jones. Representing twentieth century space-time climate variability. Part 1: development of a 1961-90 mean monthly terrestrial climatology. Journal of Climate, 12, pp.829-856. 1990.

[91] New, M., M. Hulme and P.D. Jones. Representing twentieth century space-time climate variability. Part 2: development of 1901-96 monthly grids of terrestrial surface climate. Journal of Climate, 13, pp.2217-2238. 2000.

[92] Nguyen, D.N and T.H. Nguyen. Climate and Climate resource of Vietnam. Hanoi Agriculture Publisher. 2004. (in Vietnamese)

[93] Paegle, J., K.C. Mo and J.N. Paegle. Dependence of simulated precipitation on surface evaporation during the 1993 United States summer floods, Monthly Weather Review, 124 (3), pp.345–361. 1996.

[94] Pan Z., M. Segal, R. Turner and E. Takle. Model simulation of impacts of transient surface wetness on summer rainfall in the United States Midwest during drought and flood years, Monthly Weather Review, 123 (5), pp.1575–1581. 1995.

[95] Park, J.Y., M.J. Park, H.K. Joh, H.J. Shin, H.J. Kwon, R. Srinivasan and S.J. Kim, Assessment of MIROC3.2 HiRes climate and CLUE-s land use change impacts on

watershed hydrology using SWAT, Transactions of the ASABE , 54(5), pp.1713-1724, 2011.

[96] Phan, D.B., C.C Wu and S.C. Hsieh. Impact of climate change on stream discharge and sediment yield in Northern Viet Nam, Water Resources, 38(6), pp.827-836. 2011.

[97] Phan, V.T., Thanh, N.D and Ho, T.M.H. Seasonal and interannual variations of surface climate elements over Vietnam. Climate Research, 40, pp.49-60. 2009.

[98] Pitman, W.V. A Mathematical Model for Generating Monthly River Flows from Meteorological Data in South Africa. Report No. 2.73, Hydrological Research Unit, University of Witwatersrand, Johannesburg, South Africa. 1973.

[99] Praskievicz, S. and H. Chang. A review of hydrological modelling of basin-scale climate change and urban development impacts. Progress in Physical Geography, 33 (5), pp.650-671. 2009.

[100] Priestley, C.H.B and R.J. Taylor. On the assessment of surface heat flux and evaporation using large scale parameters, Mon. Weather Rev., 100, pp.81-92, 1972.

[101] Raneesh, K.Y. and G.T. Santosh. A study on the impact of climate change on stream flow at the watershed scale in the humid tropics. Hydrology Science Journal, 56(6), pp.946–965. 2011.

[102] Ritchie, J.T., Model for predicting evaporation from a row crop with incomplete cover. Water Resource Research, 8, pp.1204-1213. 1972.

[103] Roeckner, E., R. Brokopf, M. Esch, M. Giorgetta, S. Hagemann, L. Kornblueh, E. Manzini, U. Schlese and U. Schulzweida. Sensitivity of simulated climate to horizontal and vertical resolution in the ECHAM5 atmosphere model. Journal of Climate, 19(16), pp.3771-3791. 2006.

[104] Salathé, E.P Jr, R. Steed, C.F. Mass and P.H. Zahn, A High-Resolution Climate Model for the U.S. Pacific Northwest: Mesoscale Feedbacks and Local Responses to Climate Change, Journal of Climate, 21, pp.5708–5726. 2008.

[105] Salathé, E.P. Jr., Downscaling simulations of future global climate with application to hydrologic modelling. International Journal of Climatology, 25, pp.419-436. 2005.

[106] Saltelli A., K. Chan and E.M. Scott (Ed). Senstivity Analysis. Wiley, New York. 2000.

[107] Schär, C., D. Luethi and U. Beyerle. The soil precipitation feedback: A process study with a regional climate model. Journal of Climate, 12 (3), pp.722–741. 1999.

[108] Schmidli J., C. Frei and P.L. Vidale. Downscaling from GCM Precipitation: A Benchmark for Dynamical and Statistical Downscaling Methods. International Journal of Climatology, 26 (5), pp.679-689. 2006.

[109] Sen O.L., Y. Wang and B. Wang. Impact of Indochina deforestation on the East-Asian summer monsoon. Journal of Climate, 17 (6), pp.1366–1380. 2004.

[110] Seth, A. and M. Rojas. Simulation and sensitivity in a nested modeling system for South America, Part I: Reanalyses boundary forcing. Journal of Climate, 16(15), pp.2437-2453. 2003.

[111] Skamarock, W.C., J.B. Klemp, J. Dudhia, D.O. Gill, D.M. Baker, M.G. Duda, X.Y. Hwang, W. Wang and J.G. Powers. A description of the advanced research WRF version 3. Technical Note 475+STR, National Centre for Atmospheric Research, Boulder, CO. 2008.

[112] Sloan, P.G., I. D. Moore, G.B. Coltharp, and J.D. Eigel, Modeling surface and subsurface stormflow on steeply-sloping forested watersheds. Water Resources Institute Report, No. 142, University of Kentucky, Lexington, Ky. 1983.

[113] Soares, M.M.P., R.M. Cardoso, P.A.A. Miranda, J. de Medeiros, M. Belo-Pereira and F. Espirito-Santo. WRF high resolution dynamical downscaling of ERA-Interim. Climate Dynamics, DOI 10.1007/s00382-012-1315-2. 2012.

[114] Sushama, L., Laprise, R., Caya, D., Frigon, A. and Slivitzky, M. Canadian RCM projected climate-change signal and its sensitivity to model errors, International Journal of Climatology, 26 (15), 2141-2159.2006

[115] Stainforth D.A., T. Aina, C. Christensen, M. Collins, N. Faull, D.J. Frame, J.A. Kettleborough, S. Knight, A. Martin, J.M. Murphy, C. Piani, D. Sexton, L.A. Smith, R.A. Spicer, A.J. Thorpe and M.R. Allen. Uncertainty in predictions of the climate response to rising levels of greenhouse gases. Nature, 433, pp.403-406. 2005.

[116] Strauch, M.C., B.S. Koide, M. Volk, C. Lorz and F. Makeschin. Using precipitation data ensemble for uncertainty analysis in SWAT stream flow simulation. Journal of Hydrology, 414-415, pp.413-424. 2012.

[117] Tadross, M., W.J. Gutowski, B.C. Hewitson, C. Jack and M. New. MM5 simulations of interannual change and the diurnal cycle of southern African regional climate. Theoretical and Applied Climatology, 86 (1-4), 63–80. 2006.

[118] Takahashi, H.G., T. Yoshikane, M. Hara, T. Yasunari. High resolution modelling of the impact of land surface conditions on regional climate over Indochina associated with the diurnal precipitation cycle. International Journal of Climatology, 30(13), pp.2004-2020. 2010.

[119] Takahashi, H.G., T. Yoshikane, M. Hara, T. Yasunari. High resolution regional climate simulations of the long term decrease in September rainfall over Indochina. Atmospheric Science Letters, 10, pp.14-18. 2009.

[120] Tapiador, F.J. A Joint Estimate of the Precipitation Climate Signal in Europe Using Eight Regional Models and Five Observational Datasets. Journal of Climate, 23, pp.1719–1738. 2010.

[121] Teutschbein, C. and J. Seibert. Regional Climate Models for Hydrological Impact Studies at the Catchment Scale: A Review of Recent Modeling Strategies. Geography Compass, 4/7, pp.834-860. 2010.

[122] Uppala, S.M., P.W. Kållberg, A.J. Simmons, U. Andrae, V. da Costa Bechtold, M. Fiorino, J.K. Gibson, J. Haseler, A. Hernandez, G.A. Kelly, X. Li, K. Onogi, S. Saarinen, N. Sokka, R.P. Allan, E. Andersson, K. Arpe, M.A. Balmaseda, A.C.M. Beljaars, L. van de Berg, J. Bidlot, N. Bormann, S. Caires, F. Chevallier, A. Dethof, M. Dragosavac, M. Fisher, M. Fuentes, S. Hagemann, E. Hólm, B.J. Hoskins, L. Isaksen, P.A.E.M. Janssen, R. Jenne, A.P. McNally, J.F. Mahfouf, J.J. Morcrette, N.A. Rayner, R.W. Saunders, P. Simon, A. Sterl, K.E. Trenberth, A. Untch, D. Vasiljevic, P. Viterbo and J. Woollen. The ERA-40 re-analysis. Q. Journal Royal Meteorological Society, 131, pp.2961-3012. 2005.

[123] USDA Soil Conservation Service. SCS National Engineering Handbook, Section 4: Hydrology, Washington DC, 1972.

[124] van Griensven, A. and T. Meixne. ParaSol (Parameter Solutions), PUB-IAHS Workshop Uncertainty Analysis in Environmental Modelling. 2004.

[125] van Griensven, A. and T. Meixner. Methods to quantify and identify the sources of uncertainty for river basin water quality models. Water Science and Technology, 53(1), pp.51-59. 2006.

[126] Venkataratnam, J. and E.A. Cox. Simulation of monsoon depressions using MM5: sensitivity to cumulus parameterization schemes. Meteorology and Atmospheric Physics, 93 (1-2), pp.53-78. 2006

[127] Venkataratnam, J. and K. Krishnakumar. Sensitivity of the Simulated Monsoons of 1987 and 1988 to Convective Parameterization Schemes in MM5. Journal of Climate, 18 (14), pp.2724-2743. 2005.

[128] Vicuna, S., R.D. Garreaud and J. McPhee. Climate change impacts on the hydrology of a snowmelt driven basin in semiarid Chile. Climatic Change, 105, pp.469-488. 2011.

[129] VN HMS (Vietnam National Hydro-Meteorological Service). Vietnam Hydrology and Meteorology database, period 1961-1985. Hanoi, 1989. (In Vietnames)

[130] von Storch, H. Inconsistencies at the interface of climate impact studies and global climate research. Meteorologische Zeitschrift, 4, pp.72–80. 1995.

[131] Wang, Y. An explicit simulation of tropical cyclones with a triply nested movable mesh primitive equation model: TCM3, Part II: model refinements and sensitivity to cloud microphysics parameterization. Monthly Weather Review, 130, pp. 3022–3036. 2002.

[132] Wang, Y., L.R. Leung, J. L. McGregor, D. K. Lee, W. C. Wang, Y. H. Ding and F. Kimura. Regional Climate Modeling: Progress, Challenges and Prospects. Journal of the Meteorological Society of Japan, 82, pp.1599-1628. 2004.

[133] Widmann, M. and C.S. Bretherton. Validation of mesoscale precipitation in the NCEP reanalysis using a new grid cell dataset for the northwestern United States. Journal of Climate, 13(11), pp.1936-1950. 2000.

[134] Wigley, T.M.L. MAGICC/SCENGEN 5.3: User Manual. Boulder, CO., USA. 2008

[135] Wilby, R.L. and T.M.L. Wigley. Downscaling general circulation model output: a review of methods and limitations. Progress in Physical Geography, 21, pp.530-548. 1997.

[136] Williams J.R. and Hann R.W. HYMO: Problem-Oriented Language for Hydrologic Modeling - User's Manual. USDA: ARS-S-9. 1973.

[137] Wood, A.W., R.L. Leung, V. Sridhar and D.P. Lettenmaier. Hydrologic implications of dynamical and statistical approaches to downscaling climate model outputs. Climatic Change, 62, pp.189–216. 2004.

[138] Wu, Y., S. Liu and O.I. Abdul-Aziz. Hydrological effects of the increased CO_2 and climate change in the Upper Mississippi River Basin using a modified SWAT. Climatic Change, 110(3-4), pp.977-1003. 2011.

[139] Xie, P., A. Yatagai, M. Chen, T. Hayasaka, Y. Fukushima, C. Liu and S. Yang. A Gauge-Based Analysis of Daily Precipitation over East Asia. J. Hydrometeor., 8, pp.607-627. 2007.

[140] Yadav, R.K., K.R. Kumar and M. Rajeevan. Climate change scenarios for Northwest India winter season. Quaternary International, 213, pp.12-19. 2010.

[141] Yang, M. and Q. Tung. Evaluation of Rainfall Forecasts over Taiwan by Four Cumulus Parameterization Schemes. Journal of the Meteorological Society of Japan, 81(5), pp.1163-1183. 2003.

[142] Yatagai, A., K. Kamiguchi, O. Arakawa, A. Hamada, N. Yasutomi and A. Kitoh. APHRODITE: Constructing a Long-term Daily Gridded Precipitation Dataset for Asia based on a Dense Network of Rain Gauges. Bulletin of American Meteorological Society (in press), doi:10.1175/BAMS-D-11-00122.1. 2012.

[143] Yatagai, A., O. Arakawa, K. Kamiguchi, H. Kawamoto, M. I. Nodzu and A. Hamada. A 44-year daily gridded precipitation dataset for Asia based on a dense network of rain gauges, SOLA , 5, pp.137-140, DOI:10.2151/sola.2009-035. 2009.

[144] Yates, D., J. Sieber, D. Purkey and A. Huber-Lee. WEAP21: A demand, priority and preference driven water planning model: Part1, model characteristics. Water International, 30 (4), pp.501-512. 2005b.

[145] Yates, D., J. Sieber, D. Purkey, A. Huber-Lee and H. Galbraith. WEAP21: A demand, priority and preference driven water planning model: Part2, Aiding freshwater ecosystem service evaluation. Water International, 30(4), pp.487-500. 2005a.

[146] Yusuf, A.A. and H.A. Francisco. Climate Change: Vulnerability Mapping for Southeast Asia. EEPSEA Special and Technical Paper, Economy and Environment Program for Southeast Asia (EEPSEA). 2009.

[147] Zhang, Y., V. Duliere, P. Mote and E.P. Salathe Jr. Evaluation of WRF and HadRM mesoscale climate simulations over the United States Pacific Northwest. Journal of Climate, 22, pp.5511–5526. 2009.

[148] Zorita, E. and H. von Storch. A survey of statistical downscaling techniques. GKSS report 97/E/20. 1997.

APPENDIX A LIST OF GCMs OF THE IPCC AR4 MMD

Table A-1: List of the GCMs used in IPCC AR4 MMD

No	*Model*	*Sponsor(s)/Country*	*Atmosphere Resolution*	*Ocean Resolution*
1	BCC-CM1 (2005)	Beijing Climate Center, China	T63 (1.9° × 1.9°) L16	1.9° × 1.9° L30
2	BCCR-BCM2.0 (2005)	Bjerknes Centre for Climate Research, Norway	T63 (1.9° × 1.9°) L31	1.5° × 1.5° L35
3	CCSM3 (2005)	NCAR,USA	T85 (1.4° × 1.4°) L26	1.0° × 1.0° L40
4	CGM3.1 (2005)	CCCMA, Canada	T47 (2.8° × 2.8°) L31	1.9° × 1.9° L29
5	CGM3.1 (2005)	CCCMA, Canada	T63 (1.9° × 1.9°) L31	0.9° × 1.4° L29
6	CNRM-CM3 (2004)	Meteo-France/CNRM, France	T63 (1.9° × 1.9°) L45	2.0° × 2.0° L31
7	CSIRO MK3.0 (2001)	CSIRO, Australia	T63 (1.9° × 1.9°) L18	0.8° × 1.9° L31
8	ECHAM/MPI-OM (2005)	Max Planck Institute for Meteorology, Germany	T63 (1.9° × 1.9°) L31	1.5° × 1.5° L40
9	ECHO-G (1999)	Meteorological Institute of Bonn, Meteorological Research Institute of Korean Met Agency	T30 (3.9° × 3.9°) L19	2.8° × 2.8° L20
10	FGOALS-g1.0 (2004)	National Key Laboratory of Numerical Modelling for Atmospheric Sciences and Geophysical Fluid Dynamics (LASG)/ Institute of Atmospheric Physics, China	T47 (2.8° × 2.8°) L26	1.0° × 1.0° L16
11	GFDL-CM2.0 (2005)	US Dept. of Commerce/NOAA/GFDL, USA	2.0° × 2.5° L24	1.0° × 1.0°
12	GFDL-CM2.1 (2005)	US Dept. of Commerce/NOAA/GFDL, USA (with semi-Lagrangian transport)	2.0° × 2.5° L24	1.0° × 1.0°

Continued…				
13	GISS-AOM (2004)	NASA/GISS,USA	3.0° × 4.0° L12	3.0° × 4.0° L16
14	GISS-EH (2004)	NASA/GISS,USA	4.0° × 5.0° L20	2.0° × 2.0° L16
15	GISS-ER (2004)	NASA/GISS,USA	4.0° × 5.0° L20	4.0° × 5.0° L13
16	INM-CM3.0 (2004)	Institute of Numerical Mathematics, Russia	4.0° × 5.0° L21	2.0° × 2.5° L33
17	IPSL-CM4 (2005)	Institut Pierre Simon Laplace, France	2.5° × 3.75° L19	2.0° × 2°.0 L31
18	MIROC3.2 high resolution (2004)	Center for Climate System Research/ National Institute for Environmental Studies, (CCSR/NIES), Japan	T106 (1.1° × 1.1°) L56	0.2° × 0.3° L47
19	MIROC3.2 medium resolution (2004)	CCSR/NIES, Japan	T42 (2.8° × 2.8°) L20	1.4° × 1.4° L43
20	MRI-CGCM2.3.2 (2003)	Meterological Research Institute, Japan	T42 (2.8° × 2.8°) L30	2° × 2.5° L23
21	PCM (1998)	NCAR/USA	T42 (2.8° × 2.8°) L26	0.7° × 1.1° L40
22	UKMO-HadCM3.0 (1997)	Hadley Centre for Climate Prediction and Research, Metoffice, UK	2.5° × 3.75° L19	1.25° × 1.25° L20
23	UKMO-HadGEM1 (2004)	Hadley Centre for Climate Prediction and Research, Metoffice, UK	1.3° × 1.9° L38	1.0° × 1.0° L40

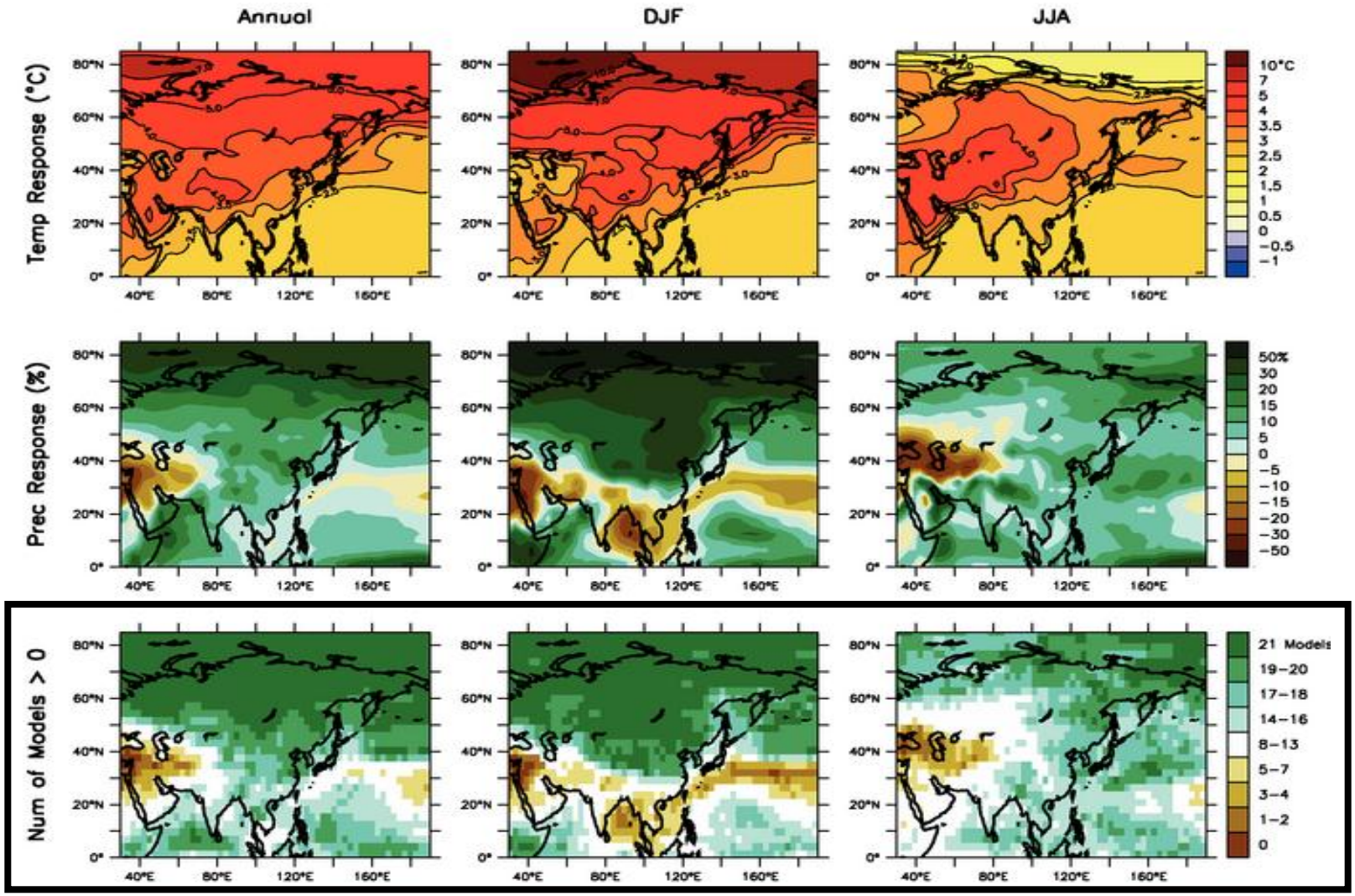

Figure A-1: Temperature and precipitation changes over Asia from the MMD-A1B simulations.
Top row: Annual mean, DJF and JJA temperature change between 1980 to 1999 and 2080 to 2099, averaged over 21 models. Middle row: same as top, but for fractional change in precipitation. Bottom row: number of models out of 21 that project increases in precipitation. Black Box indicates ensemble model results.
[Adapted from the IPCC, 2007]

APPENDIX B IPCC EMISSION SCENARIOS

[Source: IPCC, 2001]

The IPCC has developed multiple scenario families to explore the uncertainties behind potential trends in global developments and GHG emissions. The IPCC decided that narrative storylines, based on the futures and scenario literature would be the most coherent way to describe their scenarios, for the following reasons:

- To help the team to think more coherently about the complex interplay between scenario driving forces within and across alternative scenarios and to enhance the consistency in assumptions for different parameters.
- To make it easier to explain the scenarios to the various user communities by providing a narrative description of alternative futures that goes beyond quantitative scenario features.
- To make the scenarios more useful, in particular, to analysts contributing to IPCC Working Groups II (Climate Impacts, Adaptation and Vulnerability) and III (Mitigation of Climate Change). The demographic, social, political and technological contexts described in the scenario storylines are all important in the analysis of the effects of policies to either adapt to climate change or to reduce GHG emissions.
- To provide a guide for additional assumptions to be made in detailed climate impact and mitigation analyses because at present no model or scenario can possibly respond to the wide variety of informational and data needs of the different user communities of long-term emissions scenarios.

The different story lines developed by the IPCC are described in brief below.

A1 - The A1 storyline and scenario family describes a future world of very rapid economic growth, global population that peaks in mid-century and declines thereafter and the rapid introduction of new and more efficient technologies. Major underlying themes are

convergence among regions, capacity building and increased cultural and social interactions with a substantial reduction in regional differences in per capita income. This family develops into three groups that describe alternative directions of technological change in the energy system. The three A1 groups are distinguished by their technological emphasis: fossil-intensive (A1FI), non-fossil energy sources (A1T) or a balance across all sources (A1B) (where balanced is defined as not relying too heavily on one particular energy source, on the assumption that similar improvement rates apply to all energy supply and end use technologies).

A2 - The A2 storyline and scenario family describes a very heterogeneous world. The underlying theme is self- reliance and preservation of local identities. Fertility patterns across regions converge very slowly, which results in continuously increasing population. Economic development is primarily regionally oriented and per capita economic growth and technological change more fragmented and slower than other storylines.

B1 - The B1 storyline and scenario family describes a convergent world with the same global population that peaks in mid-century and declines thereafter, as in the A1 storyline, but with rapid change in economic structures toward a service and information economy, with reductions in material intensity and the introduction of clean and resource-efficient technologies. The emphasis is on global solutions to economic, social and environmental sustainability, including improved equity, but without additional climate initiatives.

B2 - The B2 storyline and scenario family describes a world in which the emphasis is on local solutions to economic, social and environmental sustainability. It is a world with continuously increasing global population, at a rate lower than A2, intermediate levels of economic development and less rapid and more diverse technological change than in the B1 and A1 storylines. While the scenario is also oriented towards environmental protection and social equity, it focuses on local and regional levels.

APPENDIX C PHYSICS PARAMETERIZATIONS IN RCMs AND COMPUTATIONAL RESOURCES

The various physics options or otherwise, parameterizations, are described briefly below and the choices of such parameterizations used for the two regional climate models WRF and PRECIS are tabulated in Table C-1. Detailed documentations of all the parameterizations of WRF and PRECIS can be obtained from their respective websites cited in Chapter 3.

Precipitation Physics

1. ***Cumulus Convection Schemes***

   Cumulus Convection in the atmosphere is an important physical process that is responsible for precipitation as well as vertical transport of heat and moisture and needs to be realistically represented in the model. The horizontal scale of cumulus clouds are of the order of 0.1-10 km. Therefore, models whose grid sizes are of the same order can directly resolve the cumulus clouds without the need for cumulus parameterizations. On the other hand, the grid spacing of synoptic forecast models such as WRF and PRECIS are greater than the sizes of cumulus clouds. Therefore, it becomes totally impracticable to resolve them in any numerical model of large-scale circulation. Instead, the collective influence of clouds within a larger area is formulated or parameterized in terms of the large scale environmental variables. This is called as the cumulus parameterization more often referred to as cumulus convection parameterization or cumulus convection schemes.

2. ***Explicit Moisture Physics Schemes***

   These schemes are activated when grid-scale saturation is reached in model simulations. In simple terms they remove super saturation as precipitation and add latent heat to the atmosphere. While the convection scheme represents the subgrid-scale transports by updrafts and downdrafts and produces convective rainfall, the explicit moisture scheme acts on the grid-scale averaged mesoscale clouds produced

by the air which is detrained by the parameterized convection and produces the mesoscale or the non-convective precipitation.

3. Land Surface Schemes

An important option available in WRF and PRECIS, land surface models govern the land and atmosphere interactions and simulate the land surface and soil variables of moisture (both liquid and frozen), soil temperature, skin temperature, snow pack depth, snow pack water equivalent (and hence snow pack density), canopy water content and the energy flux and water flux terms of the surface energy balance and surface water balance. Many of these variables are important to assess soil and hydrologic properties. The ground temperature, which is a key parameter amongst land surface variables, is based on heat budget using radiative fluxes and surface-layer properties.

4. Planetary boundary Layer

It is the lowest part of the atmosphere and its behaviour is influenced by its contact with the ground surface. It responds to surface forcings in a timescale of an hour or less. In this layer, physical quantities such as flow velocity, temperature and moisture exhibit rapid fluctuations (turbulence) and vertical mixing in the atmosphere is strong. Physical laws and equations of motions, which govern the planetary boundary layer dynamics and microphysics are strongly non-linear and are strongly influenced by properties of the earth's surface and evolution of the processes in the free atmosphere. Clouds in the boundary layer influence trade winds, the hydrological cycle, and energy exchange.

5. Radiation schemes

The radiation schemes govern the different fluxes in the atmosphere, namely, the short wave and long wave, downward and upward. Since the earth’s radiation budget is defined by physical laws, the incorporation of appropriate radiation equations and their

interactions with the ground surface, atmosphere, clouds and other physical features of the climate system is important.

Table C-1: Physical Parameterizations for WRF and PRECIS models

Parameterizations	**Physics options used in WRF**	**Physics options used in PRECIS**
Cumulus Physics	Grell	Gregory and Rowntree
Explicit Moisture Physics	Thomson	Smith
Planetary Boundary Layer	Yonsei University	Smith
Radiation (Shortwave and Longwave)	RRTMG	Martin and Jones
Land Surface Model	NOAH	MOSES

The table above indicate what options were chosen for WRF and PRECIS models from similar many other options available. It is also reminded here that unlike WRF, PRECIS has a fixed set of parameterizations (as cited in the table) that cannot be changed. The references and additional information for these schemes are described in detail in their technical manuals available from their websites.

Table C-2: Detailed description of the computer resources

Model	Computer system	Details of processors	Time for 1 year simulation	Number of years	Storage
WRF	NUS HPC	12 nodes, 96 CPUs	2.0 days	150	108 gb/year
PRECIS	Work station	16 CPUs	1.2 days	90	30 gb/year
SWAT	PC	4 CPUs	fast	80	-

Parallel has been applied using MPICH (Message Passing Interface CH). Linux based supercomputer environment. Sun Grid Engine (SGE) and also Load Scheduler Facility (LSF) used for job submissions and cluster programming.

APPENDIX D VIETNAM STATION DATA

The table below is a list of stations distributed over Vietnam from where observed precipitation and temperature data were taken for comparison of model results discussed in Chapter 4 and Figure D-1 is the same as that shown in Chapter 3 and reproduced here for easy reference to see these station locations over Vietnam.

Table D-1: Vietnam station data

ID	Station name	ID	Station name	ID	Station name	ID	Station name
001	Bình Lư	061	Thái Nguyên	142	Hồi Xuân	208	Ayunpa
002	Điện Biên	062	Võ Nhai	146	Như Xuân	209	P-lây Cu
003	Lai Châu	063	Minh Đài	150	Thanh Hoá	211	B-mê Thuột
005	Mường Tè	065	Phú Thọ	151	Tĩnh Gia	212	Buôn Hồ
006	Pha Đin	066	Thanh Sơn	153	Yên Định	213	Đắc Nông
007	Phong Thổ	067	Việt Trì	156	Đô Lương	218	M'drắc
008	Sìn Hồ	069	Tam Đảo	158	Hòn Ngư	219	Bảo Lộc
009	Tam Đường	071	Vĩnh Yên	160	Quỳ Châu	220	Đà Lạt
010	Tủa Chùa	072	Bảo Lạc	161	Quỳ Hợp	221	Liên Khương
011	Tuần Giáo	073	Cao Bằng	162	Quỳnh Lưu	222	Biên Hoà
012	Bắc Yên	074	Hà Quảng	163	Tây Hiếu	226	Đồng Phú
013	Cò Nòi	075	Nguyên Bình	164	Tương Dương	228	Phước Long
014	Mộc Châu	077	Trùng Khánh	165	Vinh	229	Sở Sao
016	Phù Yên	078	Bắc Sơn	166	Hà Tĩnh	230	Tây Ninh
017	Quỳnh Nhai	079	Đình Lập	167	Hương Khê	231	Côn Đảo
018	Sơn La	080	Hữu Lũng	169	Kỳ Anh	233	Vũng Tàu
019	Sông Mã	081	Lạng Sơn	170	Ba Đồn	234	Tân S. Nhất
023	Yên Châu	084	Thất Khê	172	Đồng Hới	235	Mộc Hoá
024	Chi Nê	085	Bắc Giang	175	Tuyên Hoá	237	Mỹ Tho
025	Chợ Bờ	087	Hiệp Hoà	176	Cồn Cỏ	238	Cao Lãnh
026	Hoà Bình	088	Lục Ngạn	177	Đông Hà	242	Càng Long
027	Kim Bôi	089	Sơn Động	178	Khe Sanh	243	Châu Đốc
028	Lạc Sơn	090	Tân Yên	180	A Lưới	244	Cần Thơ
029	Mai Châu	093	Cô Tô	181	Huế	246	Phú Quốc
030	Bắc Mê	094	Cửa Ông	182	Nam Đông	247	Rạch Giá
031	Bắc Quang	096	Móng Cái	184	Đà Nẵng	250	Cà Mau
032	Hoàng Su Phì	098	Tiên Yên	185	Hoàng Sa		
033	Hà Giang	099	Uông Bí	186	Tam Kỳ		
036	Bắc Hà	100	Bạch Long Vĩ	187	Trà My		
037	H.liên Sơn	106	Hòn Dấu	188	Ba Tơ		
038	Lào Cai	107	Phù Liễn	190	Quảng Ngãi		
039	Mường Khương	109	Ba Vì	191	Hoài Nhơn		

040	Phố Ràng	111	Hà Đông	192	Quy Nhơn
041	Sa Pa	112	Mỹ Đức	193	Miền Tây
043	Than Uyên	113	Sơn Tây	194	Sơn Hoà
045	Lục Yên	118	Hà Nội A	195	Tuy Hoà
046	Mù Căng Chải	121	Chí Linh	196	Cam Ranh
048	Văn Chấn	122	Hải Dương	197	Nha Trang
049	Yên Bái	123	Hưng Yên	199	Trường Sa
050	Chiêm Hoá	129	Nam Định	200	Nha Hố
051	Hàm Yên	130	Văn Lý	202	Hàm Tân
052	Na Hang	131	Thái Bình	203	Phan Thiết
053	Tuyên Quang	137	Kim Sơn (BM)	204	Phú Quý
054	Bắc Cạn	138	Nho Quan	205	Đăk Tô
058	Đại Từ	139	Ninh Bình	206	Kon Tum
059	Định Hoá	140	Bái Thượng	207	An Khê

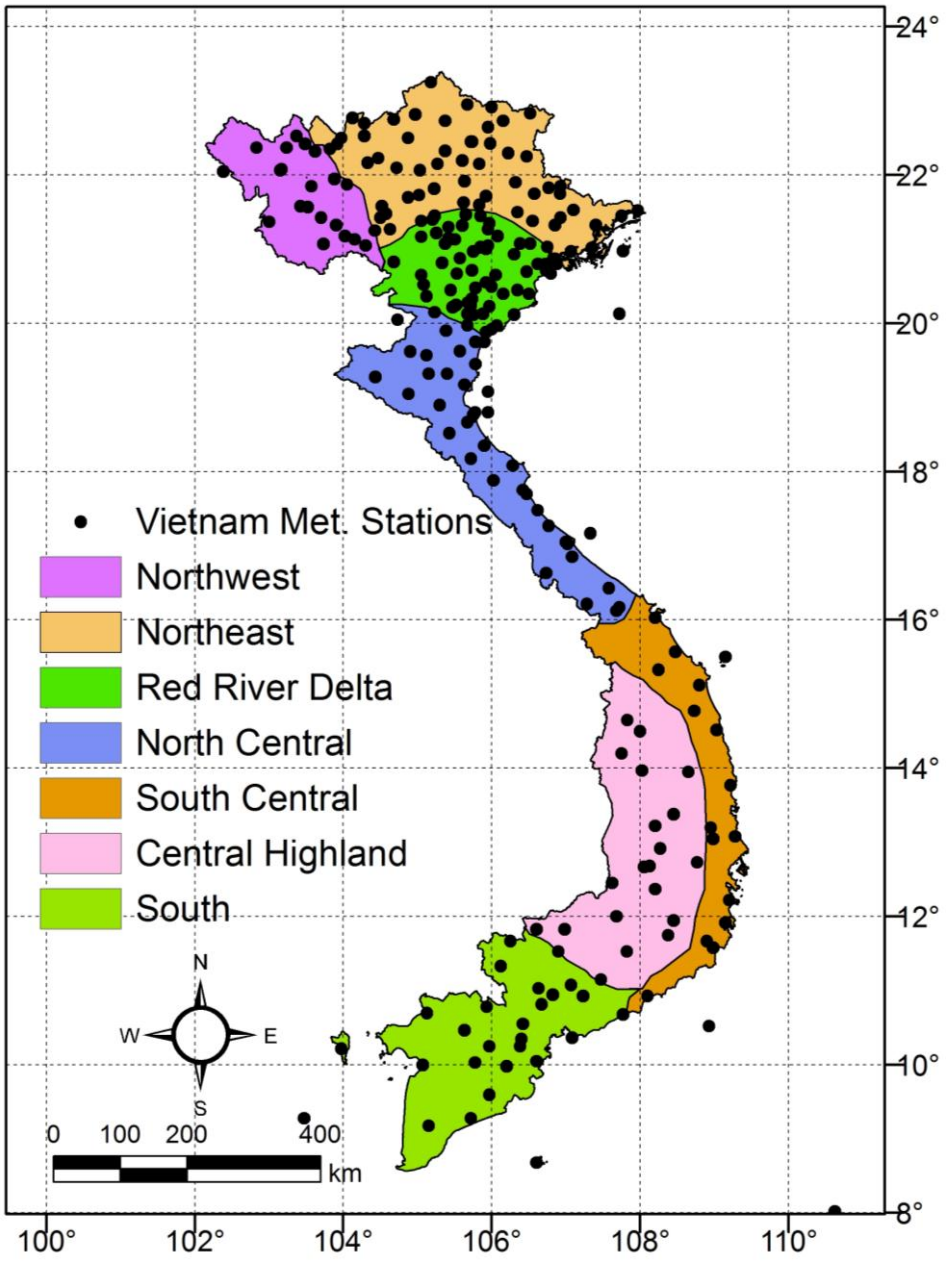

Figure D-1: Locations of Vietnam Meteorology Stations

APPENDIX E REGIONAL CLIMATE MODEL RESULTS

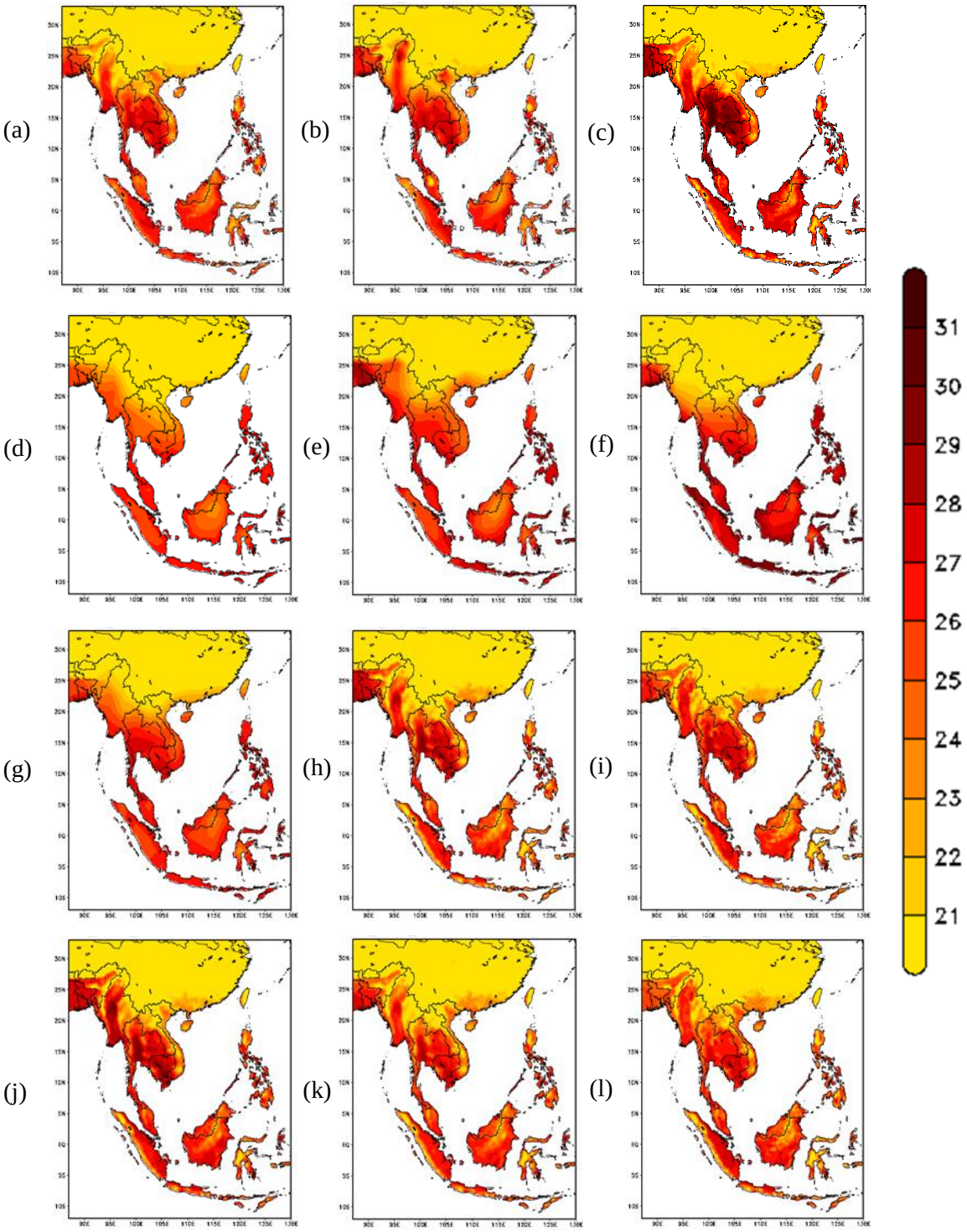

Figure E-1: Annual temperature Model domain 1961-1990, °C
(a) CRU (b) CPC (c) APH (d) CCSM3 (e) ECHAM5 (f) HADCM3 (g) ERA40
(h) WRF/ERA (i) PRE/ERA (j) WRF/CCSM (k) WRF/ECHAM (l) PRE/HAD

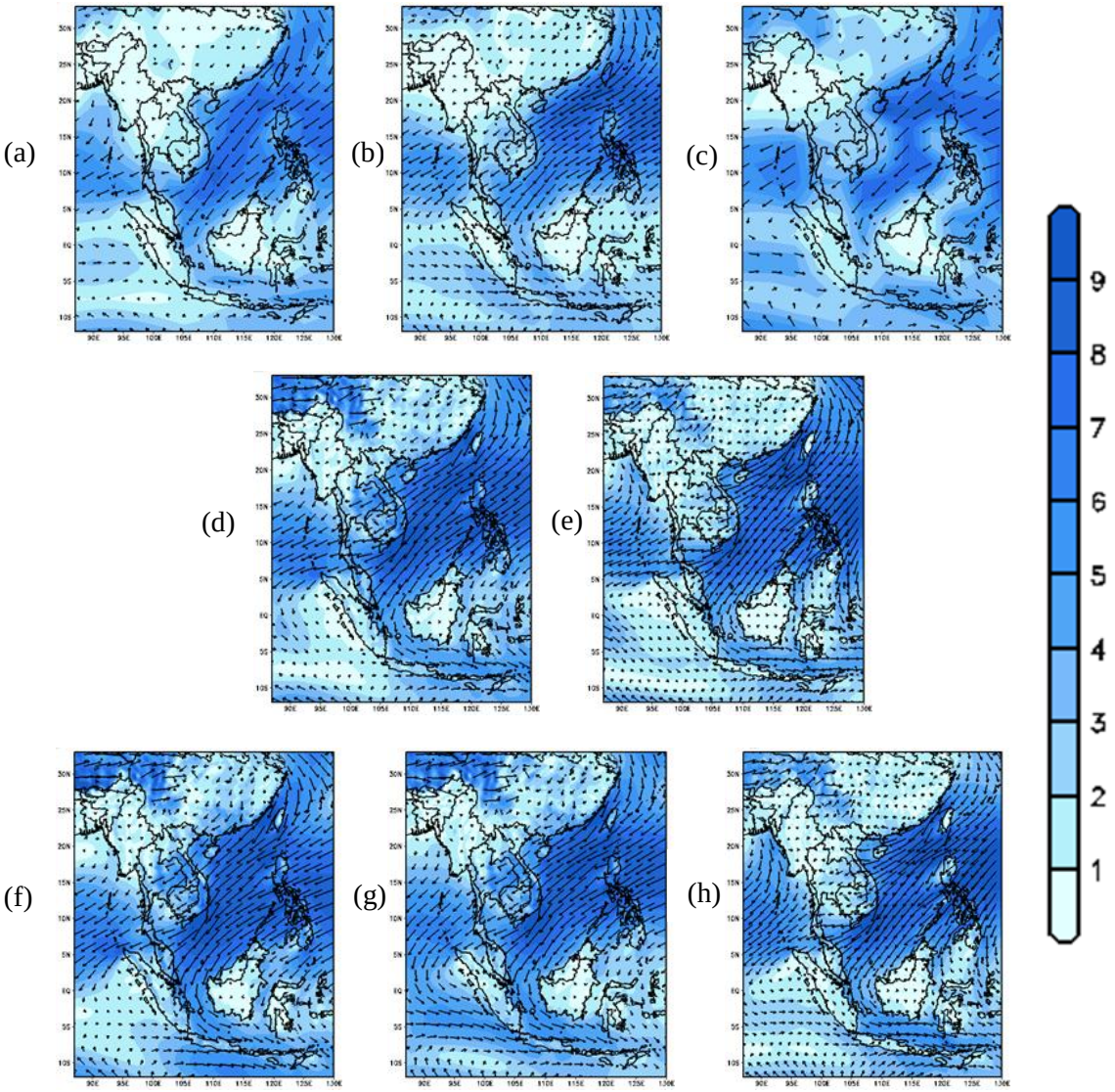

Figure E-2: Northeast monsoon wind (DJF) Model domain 1961-1990, m/s
(a) ERA40 (b) ECHAM5 (c) HADCM3 (d) WRF/ERA (e) PRE/ERA (f) WRF/CCSM
(g) WRF/ECHAM (h) PRE/HAD

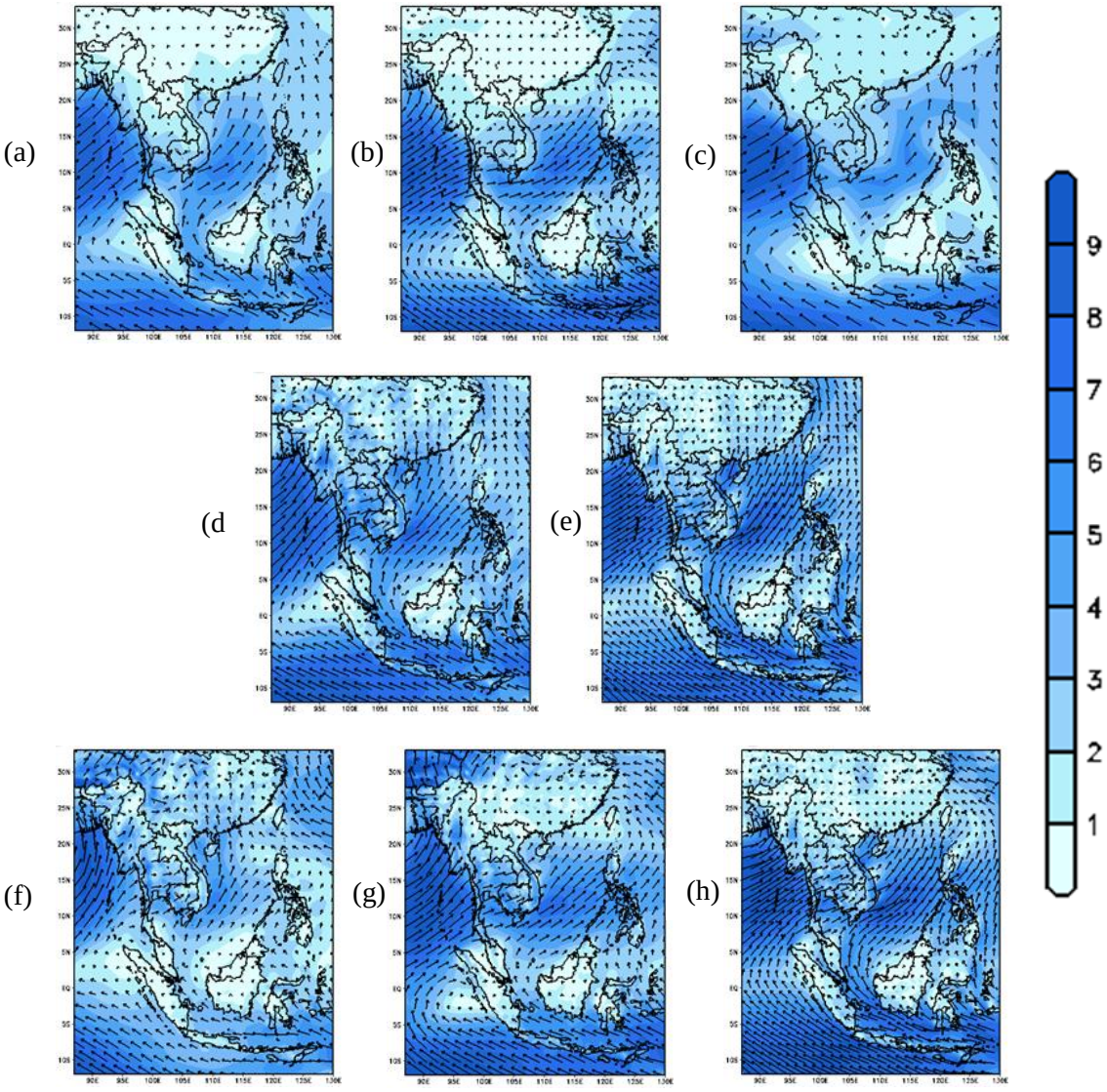

Figure E-3: Southwest monsoon wind (JJA) Model domain 1961-1990, m/s
(a) ERA40 (b) ECHAM5 (c) HADCM3 (d) WRF/ERA (e) PRE/ERA
(f) WRF/CCSM (g) WRF/ECHAM (h) PRE/HAD

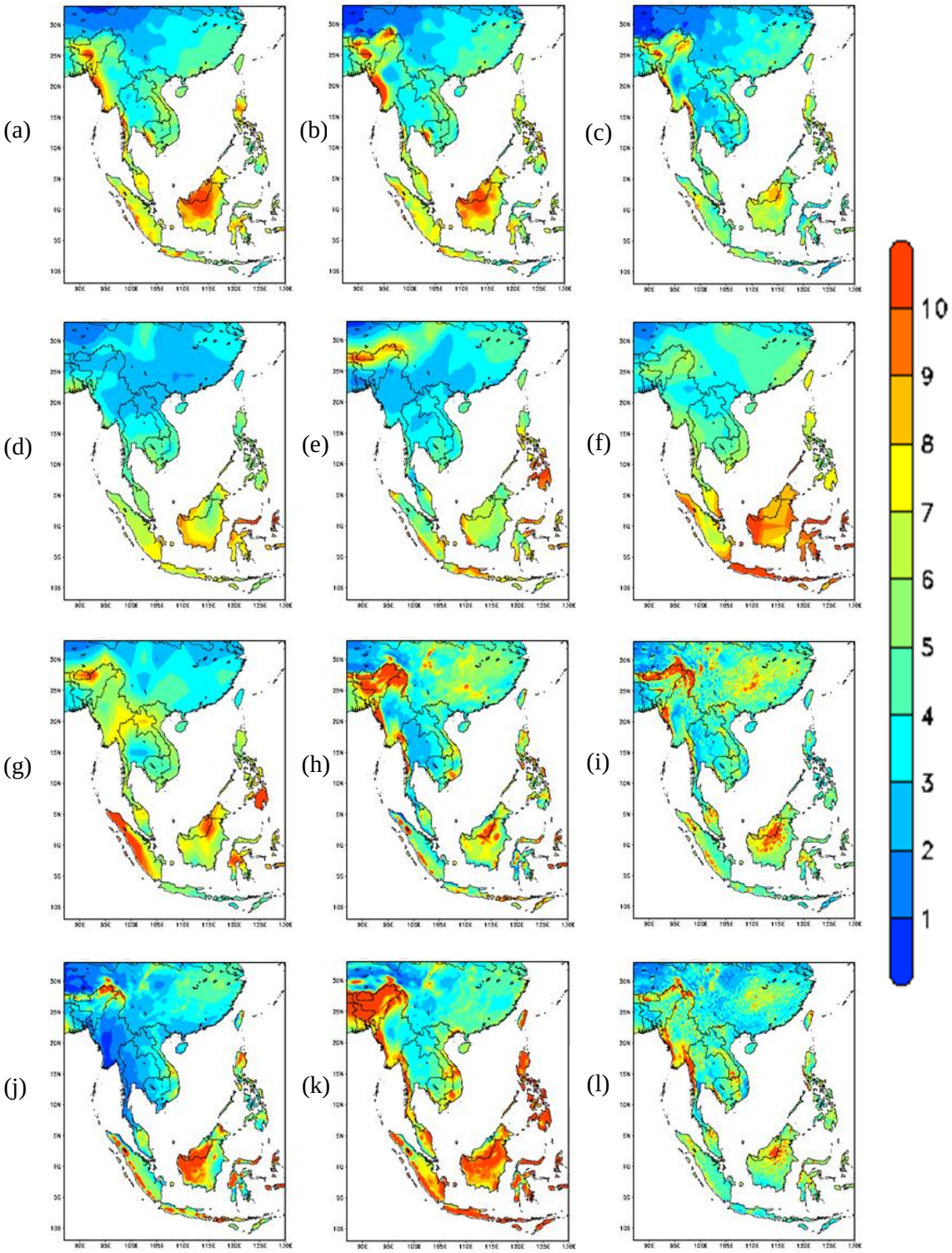

Figure E-4: Annual Precipitation Model domain 1961-1990, mm/day
(a) CRU (b) CPC (c) APH (d) CCSM3 (e) ECHAM5 (f) HADCM3 (g) ERA40
(h) WRF/ERA (i) PRE/ERA (j) WRF/CCSM (k) WRF/ECHAM (l) PRE/HAD

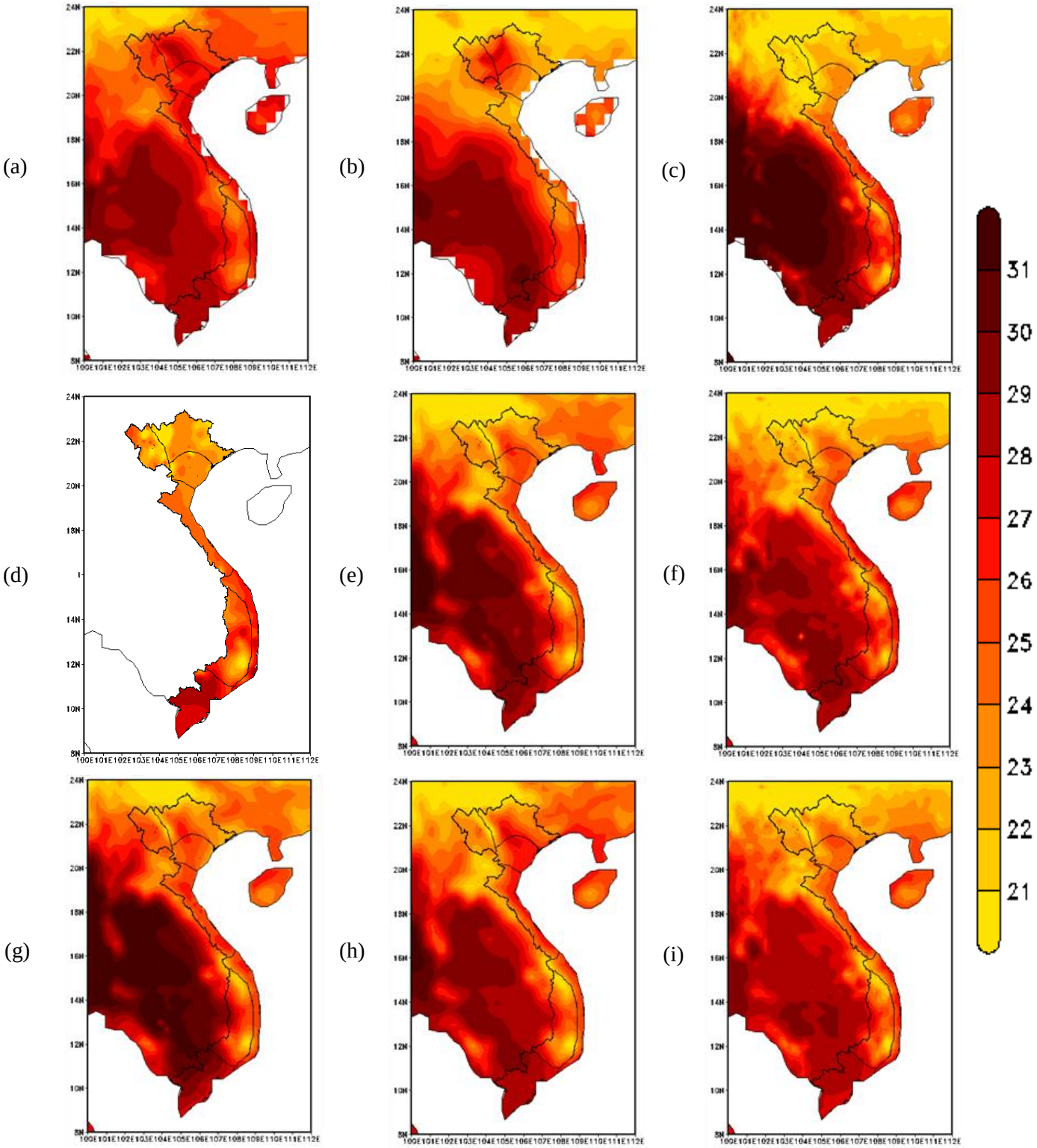

Figure E-5: Mean Seasonal (MAM) Surface Temperature, 1961-1990, °C
(a) CRU (b) CPC (c) APH (d) Station Data (e) WRF/ERA (f) PRE/ERA
(g) WRF/CCSM (h) WRF/ECHAM (i) PRE/HAD

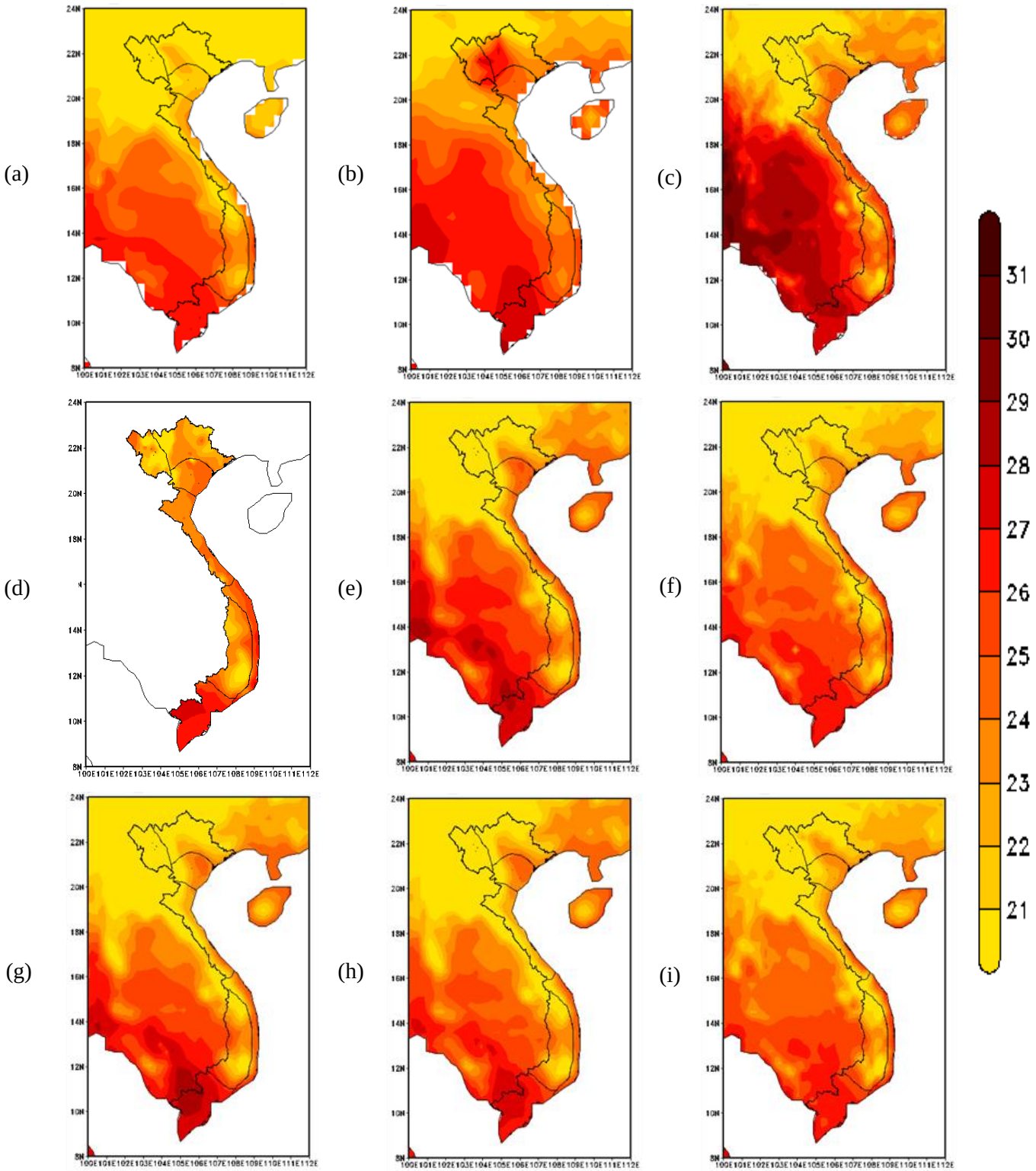

Figure E-6: Mean Seasonal (SON) Surface Temperature, 1961-1990, °C
(a) CRU (b) CPC (c) APH (d) Station Data (e) WRF/ERA (f) PRE/ERA
(g) WRF/CCSM (h) WRF/ECHAM (i) PRE/HAD

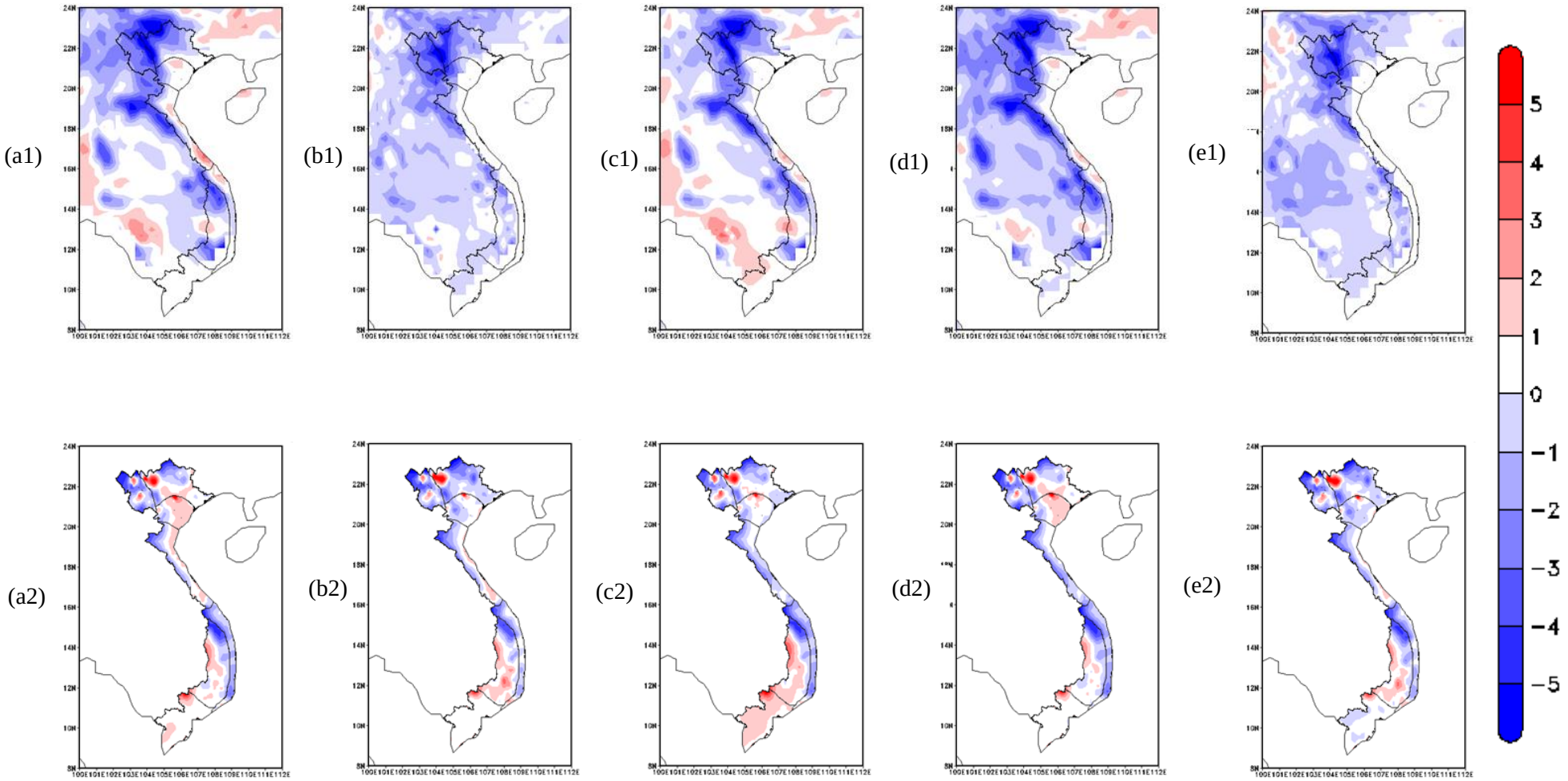

Figure E-7: RCM Temperature bias vs Gridded Observations and Station data, 1961-1990, °C
(a) WRF/ERA (b) PRE/ERA (c) WRF/CCSM (d) WRF/ECHAM (e) PRE/HAD
(1) RCMs minus Average Gridded Observation data (2) RCMs minus Station data

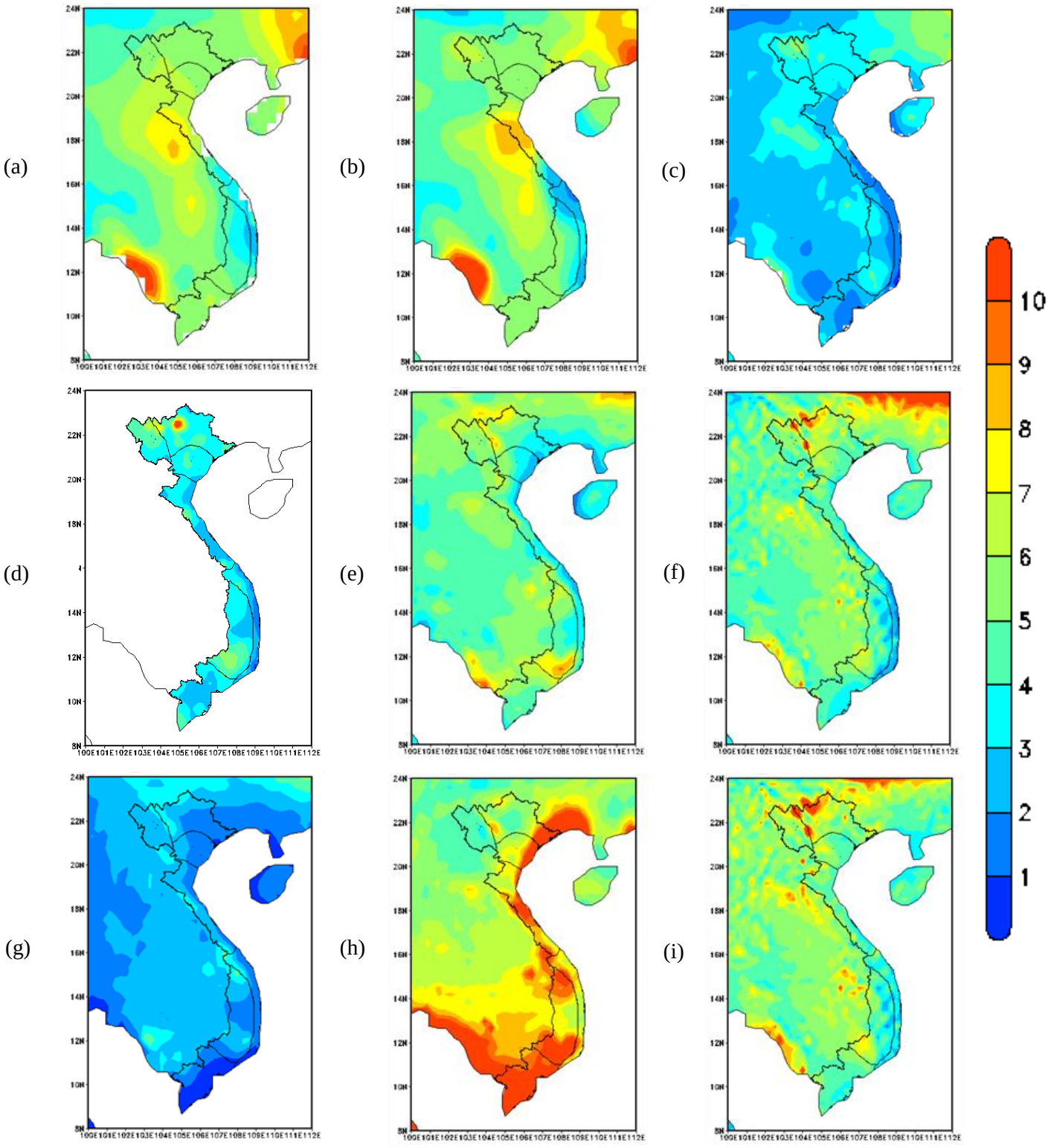

Figure E-8: Mean Seasonal (MAM) Rainfall, 1961-1990, mm/day
(a) CRU (b) CPC (c) APH (d) Station Data (e) WRF/ERA (f) PRE/ERA
(g) WRF/CCSM (h) WRF/ECHAM (i) PRE/HAD

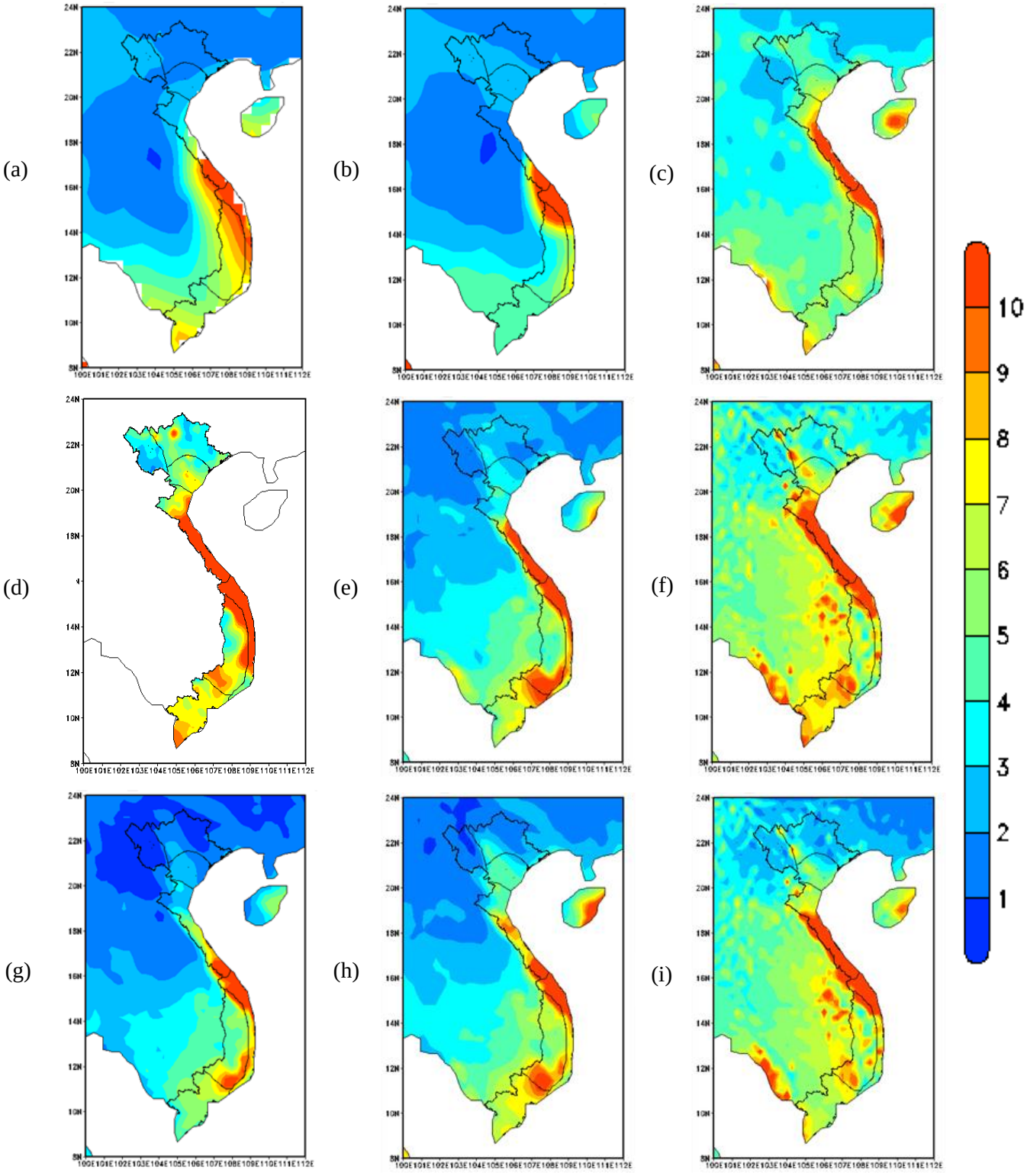

Figure E-9: Mean Seasonal (SON) Rainfall, 1961-1990, mm/day
(a) CRU (b) CPC (c) APH (d) Station Data (e) WRF/ERA (f) PRE/ERA
(g) WRF/CCSM (h) WRF/ECHAM (i) PRE/HAD

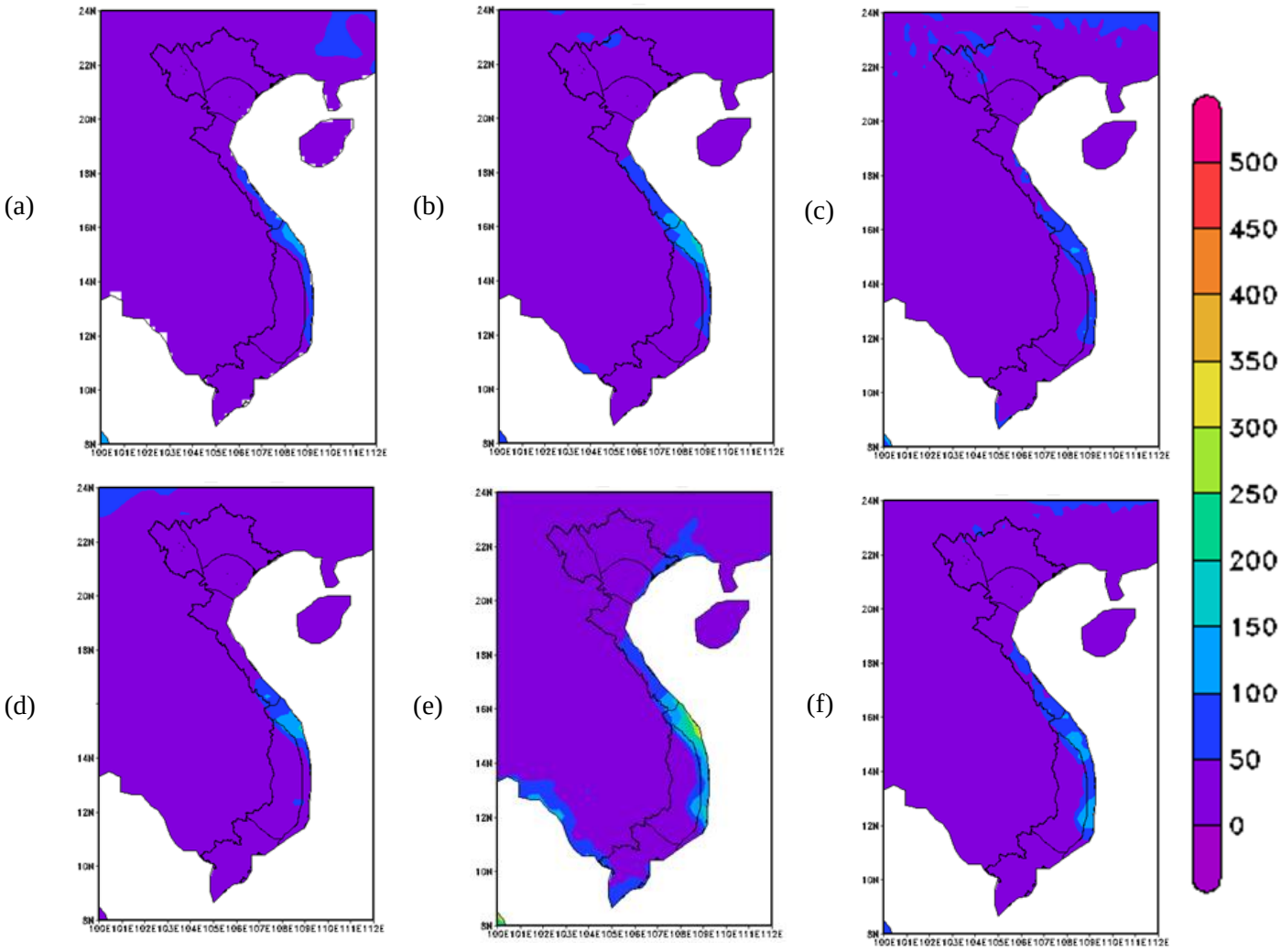

Figure E-10: Mean Seasonal (DJF) R5d, 1961-1990, mm
(a) APH (b) WRF/ERA (c) PRE/ERA
(d) WRF/CCSM (e) WRF/ECHAM (f) PRE/HAD

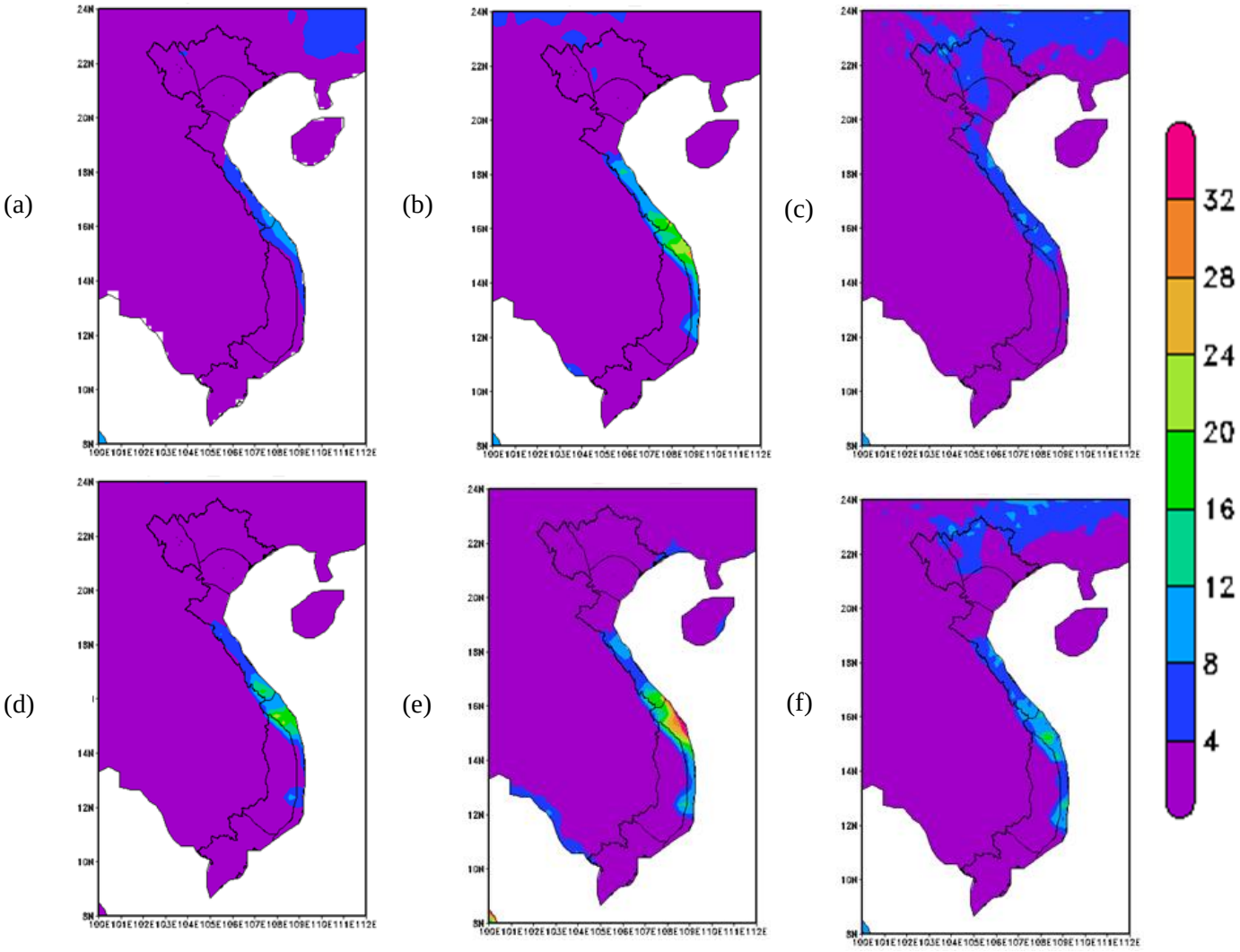

Figure E-11: Mean Seasonal (DJF) P90p, 1961-1990, mm/day
(a) APH (b) WRF/ERA (c) PRE/ERA
(d) WRF/CCSM (e) WRF/ECHAM (f) PRE/HAD

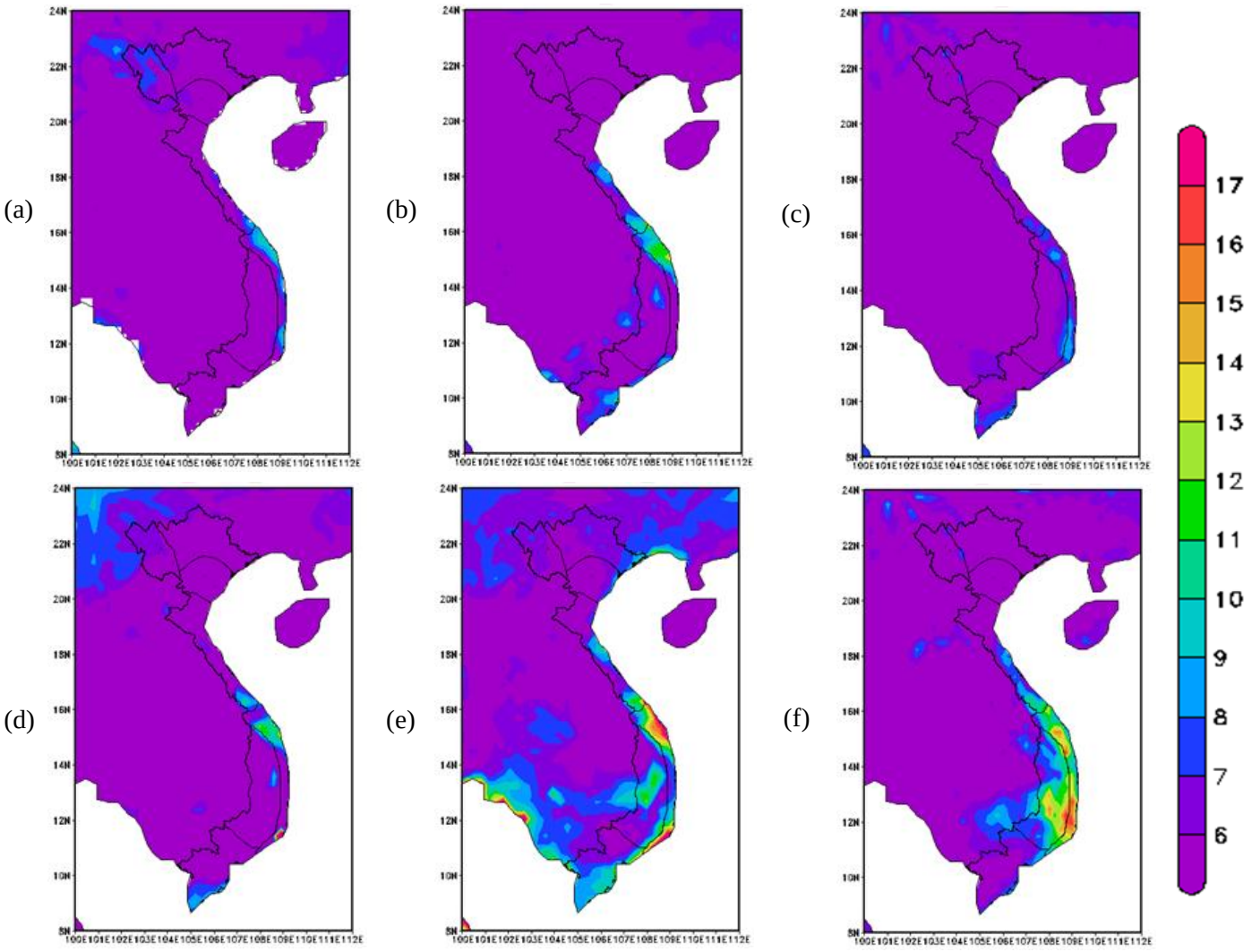

Figure E-12: Mean Seasonal (DJF) SDII, 1961-1990, mm/day
(a) APH (b) WRF/ERA (c) PRE/ERA
(d) WRF/CCSM (e) WRF/ECHAM (f) PRE/HAD

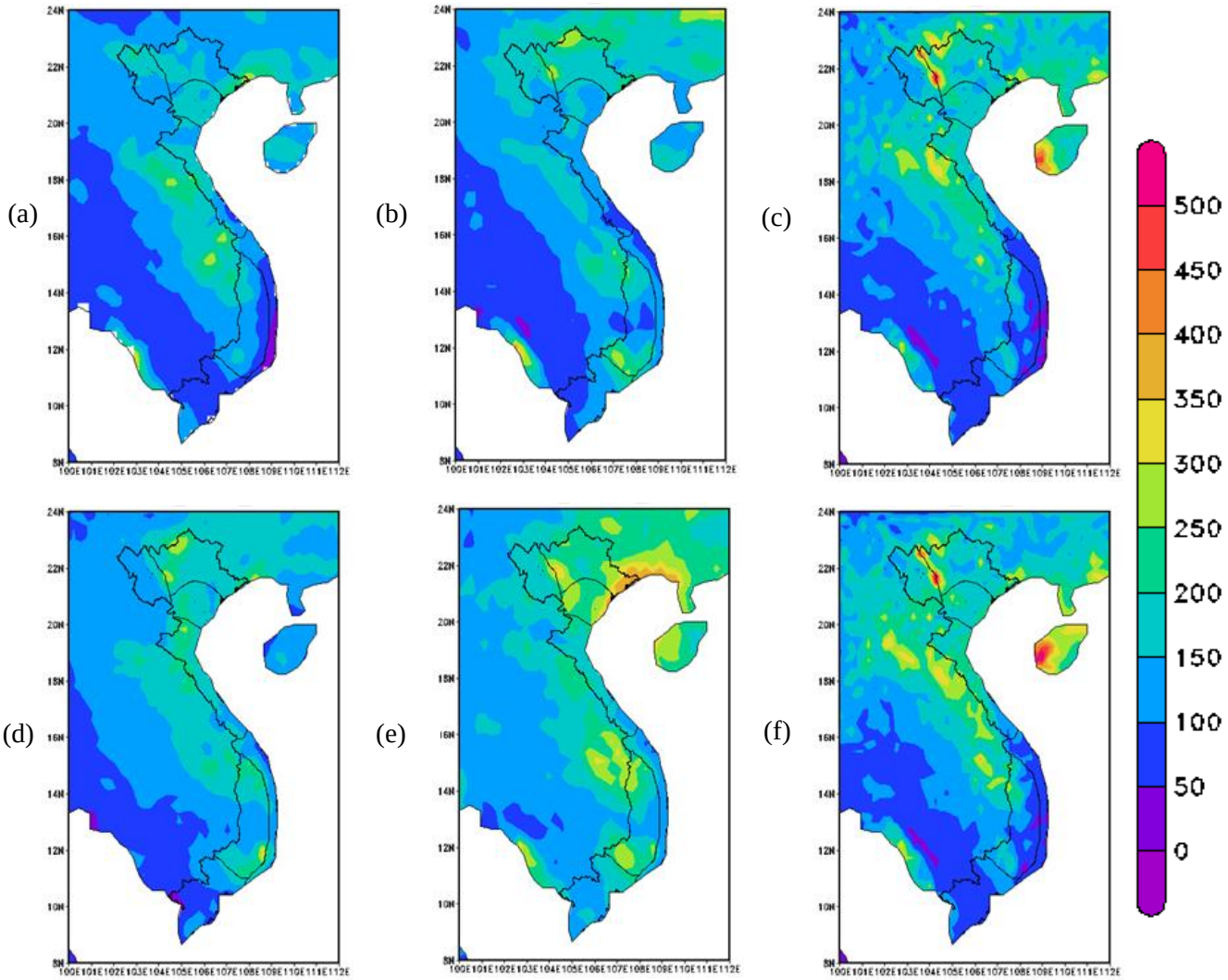

Figure E-13: Mean Seasonal (JJA) R5d, 1961-1990, mm
(a) APH (b) WRF/ERA (c) PRE/ERA
(d) WRF/CCSM (e) WRF/ECHAM (f) PRE/HAD

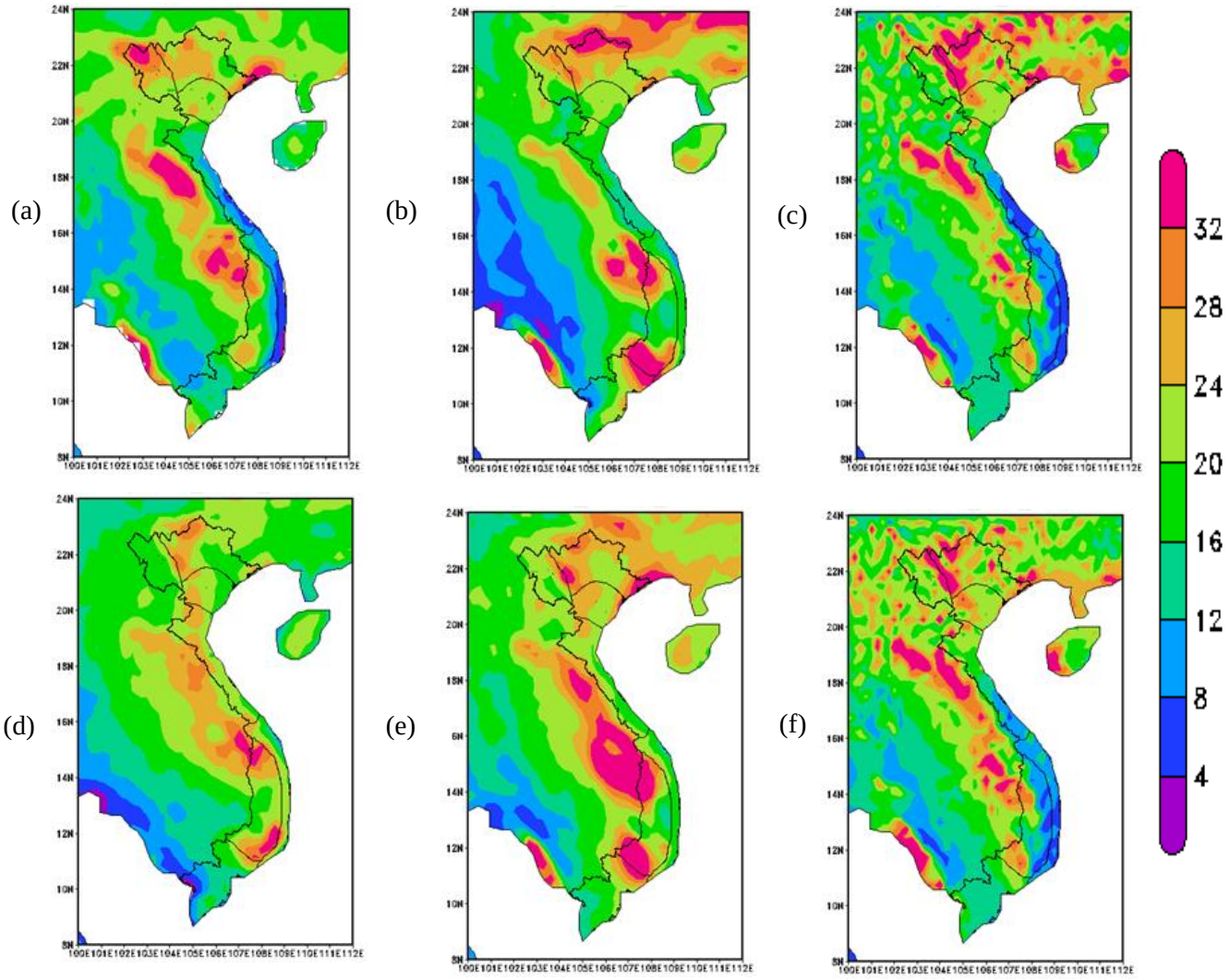

Figure E-14: Mean Seasonal (JJA) P90p, 1961-1990, mm/day
(a) APH (b) WRF/ERA (c) PRE/ERA
(d) WRF/CCSM (e) WRF/ECHAM (f) PRE/HAD

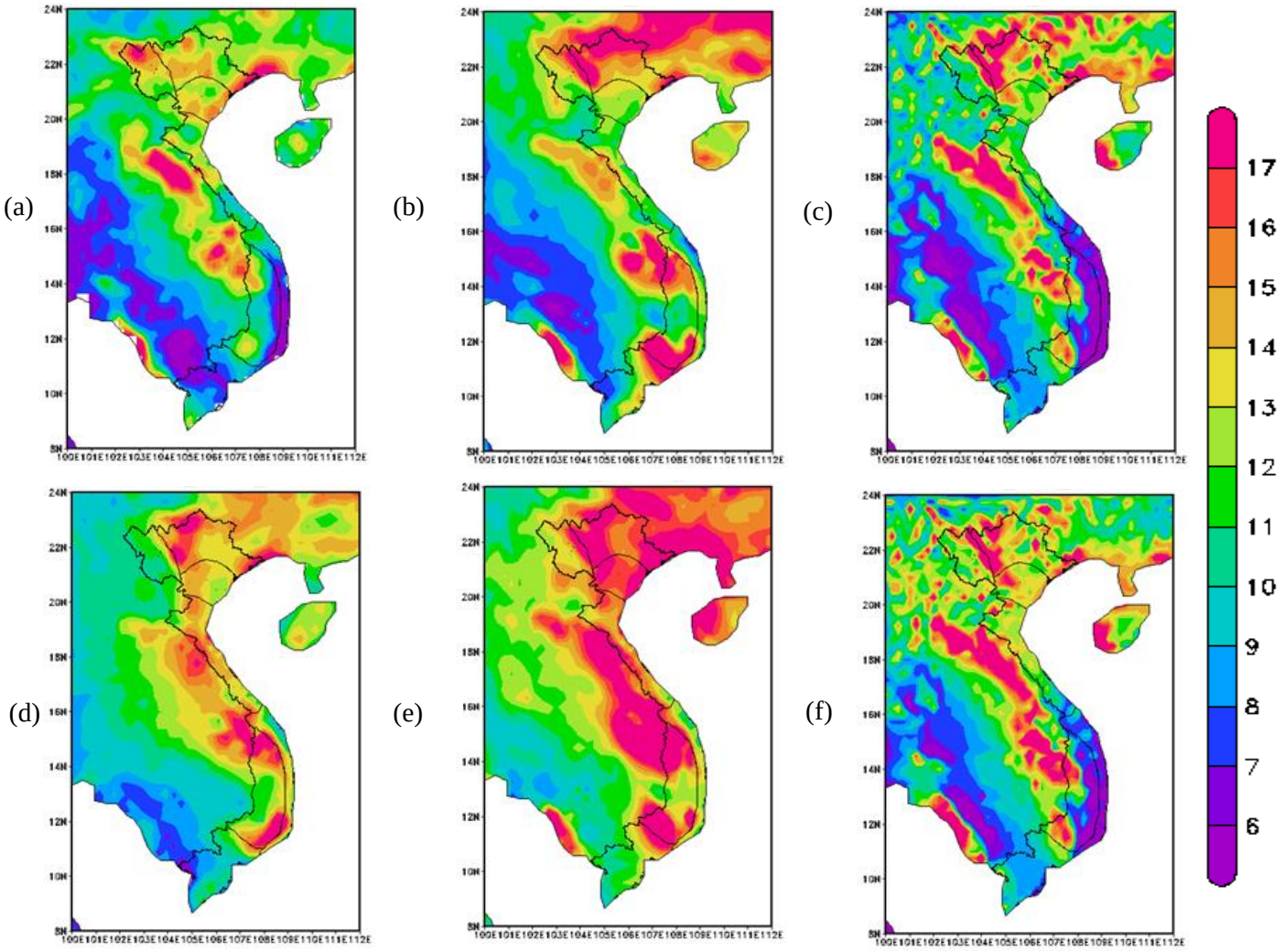

Figure E-15: Mean Seasonal (JJA) SDII, 1961-1990, mm/day
(a) APH (b) WRF/ERA (c) PRE/ERA
(d) WRF/CCSM (e) WRF/ECHAM (f) PRE/HAD

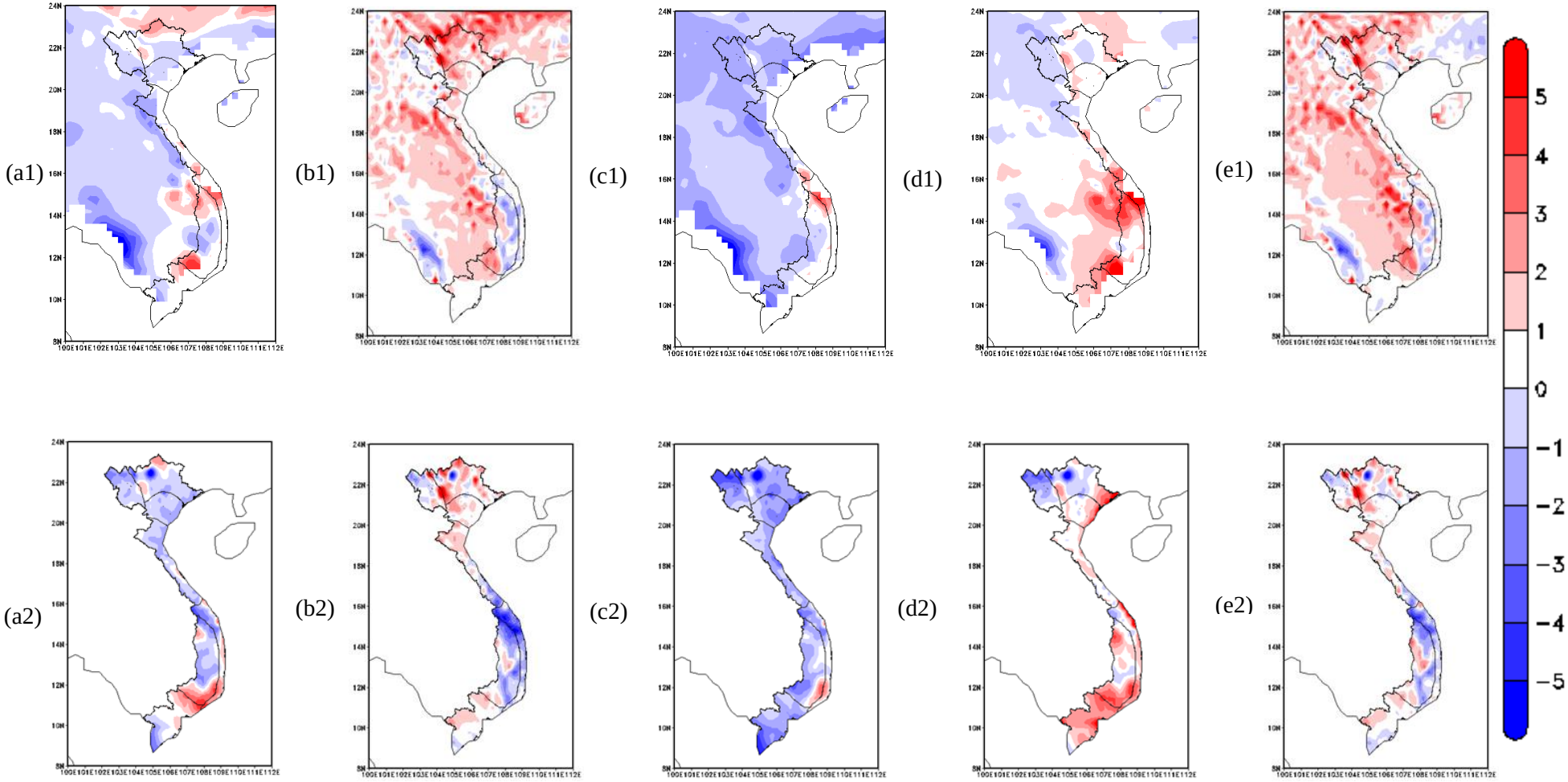

Figure E-16: RCM Precipitation bias vs Gridded Observations and Station data, 1961-1990, mm/day
(a) WRF/ERA (b) PRE/ERA (c) WRF/CCSM (d) WRF/ECHAM (e) PRE/HAD
(1) RCMs minus Average Gridded Observation data (2) RCMs minus Station data

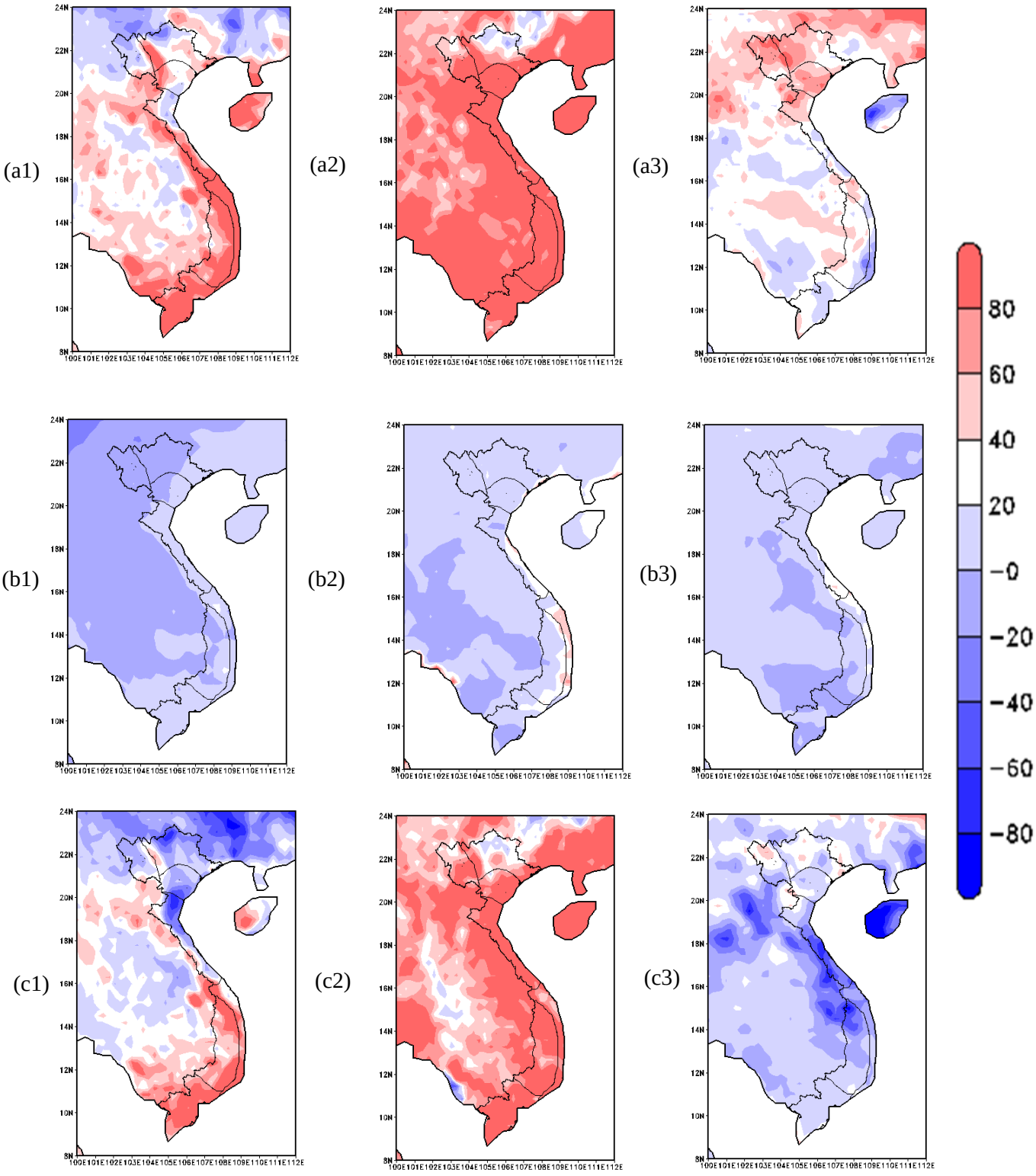

Figure E-17: R5d Change (%), 2071-2100 relative to 1961-1990
(a) WRF/CCSM (b) WRF/ECHAM (c) PRE/HAD
(1) Annual (2) DJF (3) JJA

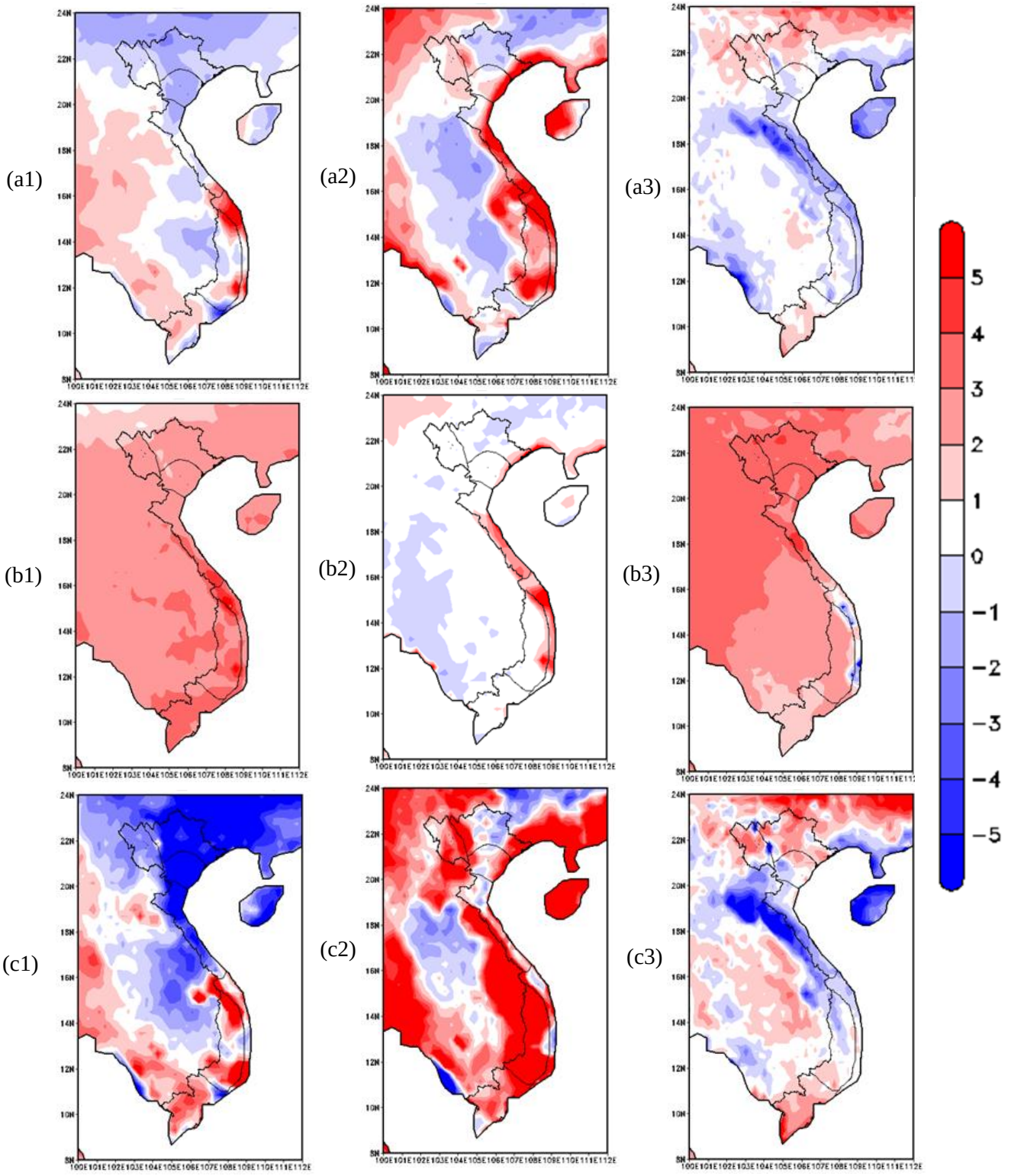

Figure E-18: P90p Change (%), 2071-2100 relative to 1961-1990
(a) WRF/CCSM (b) WRF/ECHAM (c) PRE/HAD
(1) Annual (2) DJF (3) JJA

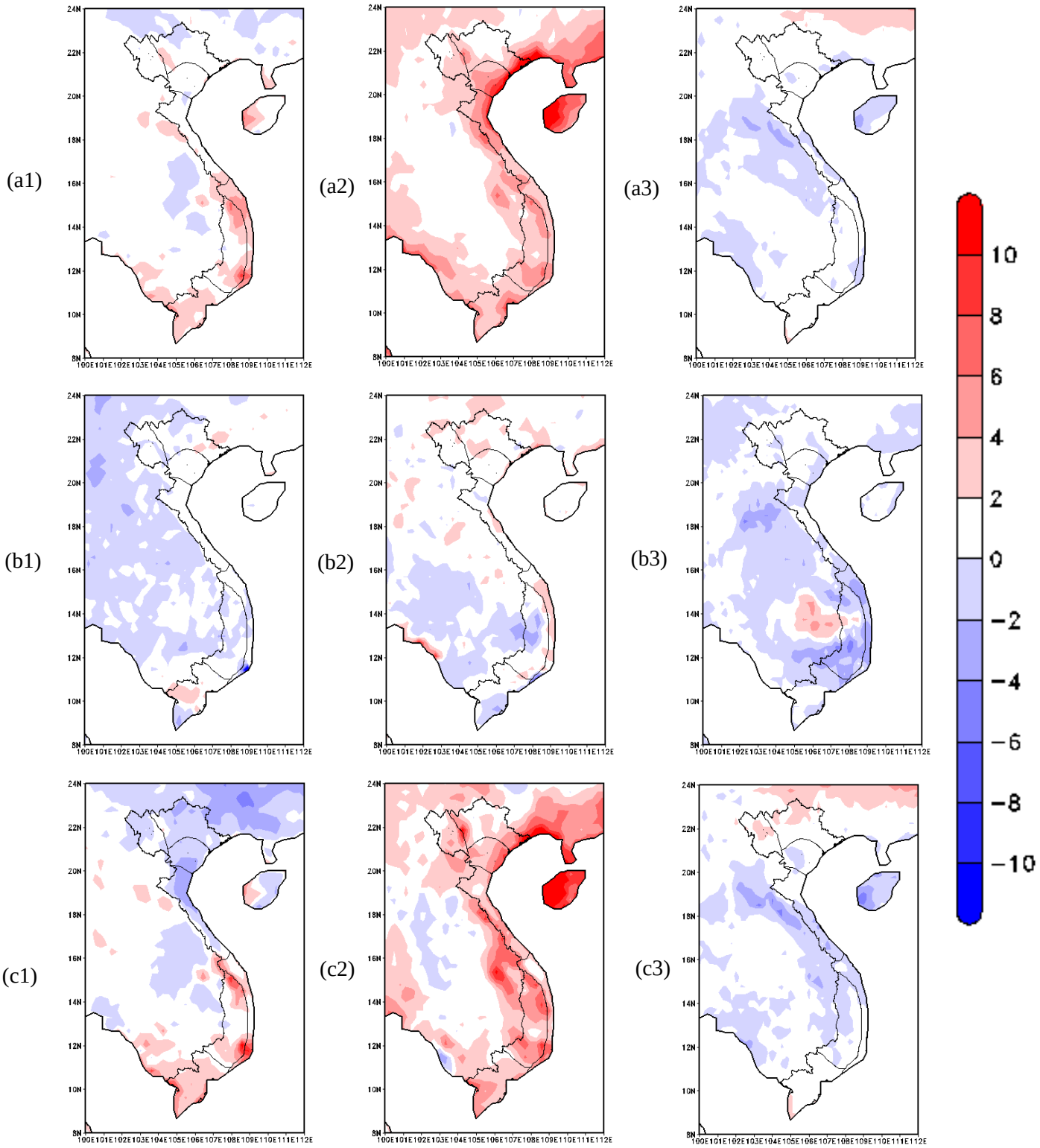

Figure E-19: SDII Change (%), 2071-2100 relative to 1961-1990
(a) WRF/CCSM (b) WRF/ECHAM (c) PRE/HAD
(1) Annual (2) DJF (3) JJA

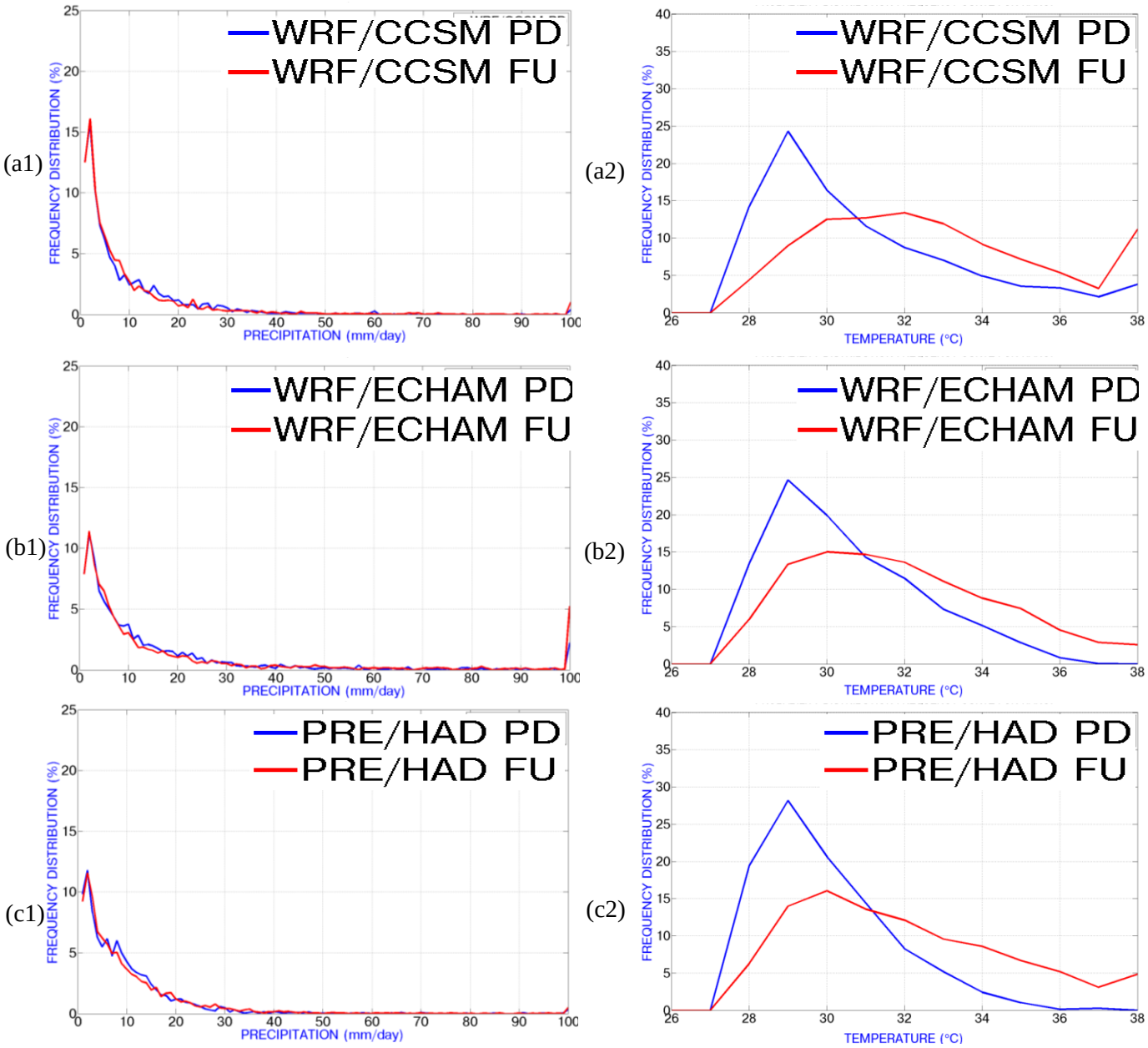

Figure E-20: Probability Distributions Frequency of Hanoi 2071-2100
(1)Precipitation (mm/day) (2) Surface Temperature (^{o}C)
(a) WRF/CCSM (b) WRF/ECHAM (c) PRE/HAD

*** PD = Present Day (1961-1990)**

FU = Future (2071-2100)

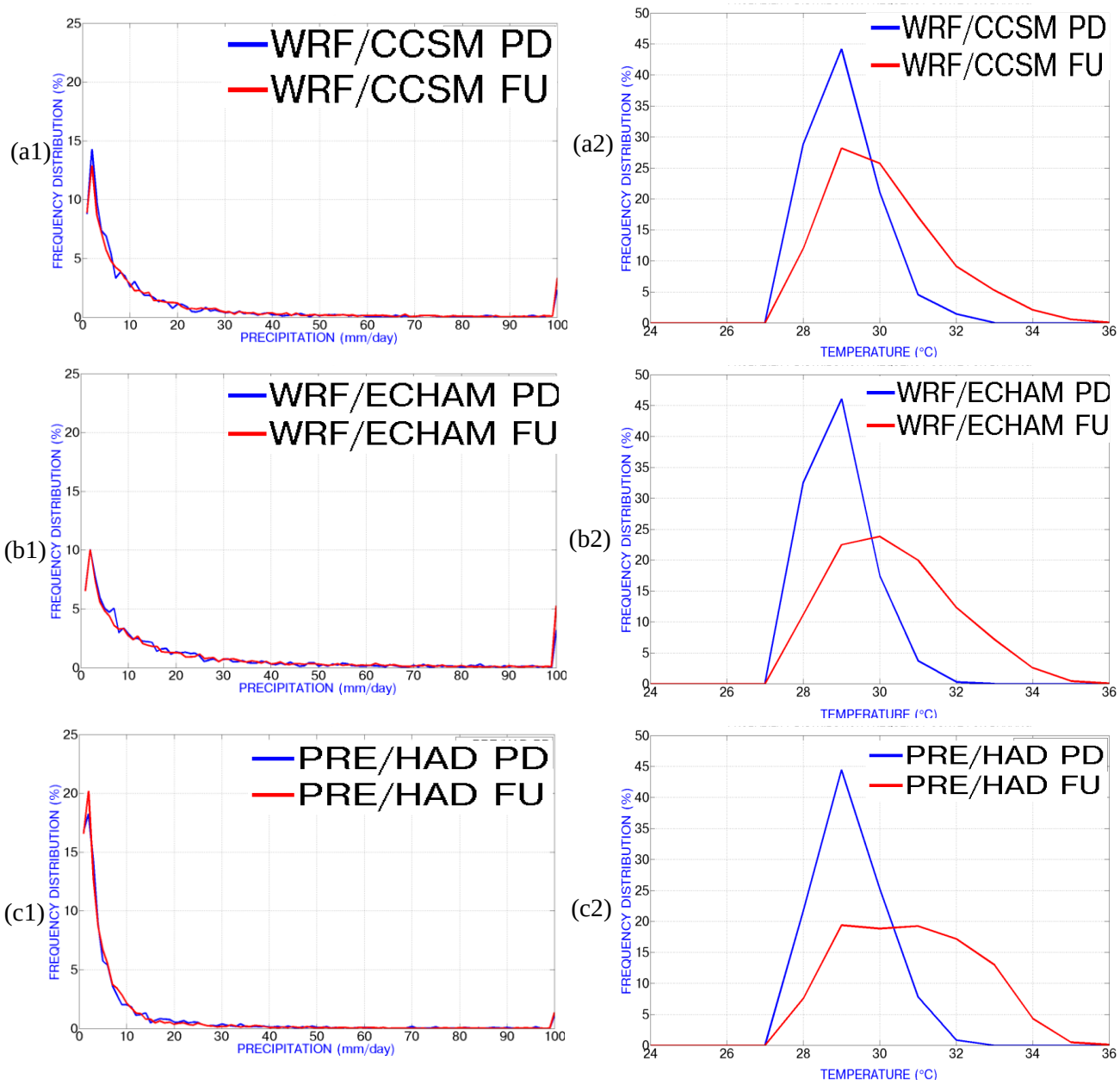

Figure E-21: Probability Distributions Frequency of Da Nang 2071-2100
(1)Precipitation (mm/day) (2) Surface Temperature (^{o}C)
(a) WRF/CCSM (b) WRF/ECHAM (c) PRE/HAD

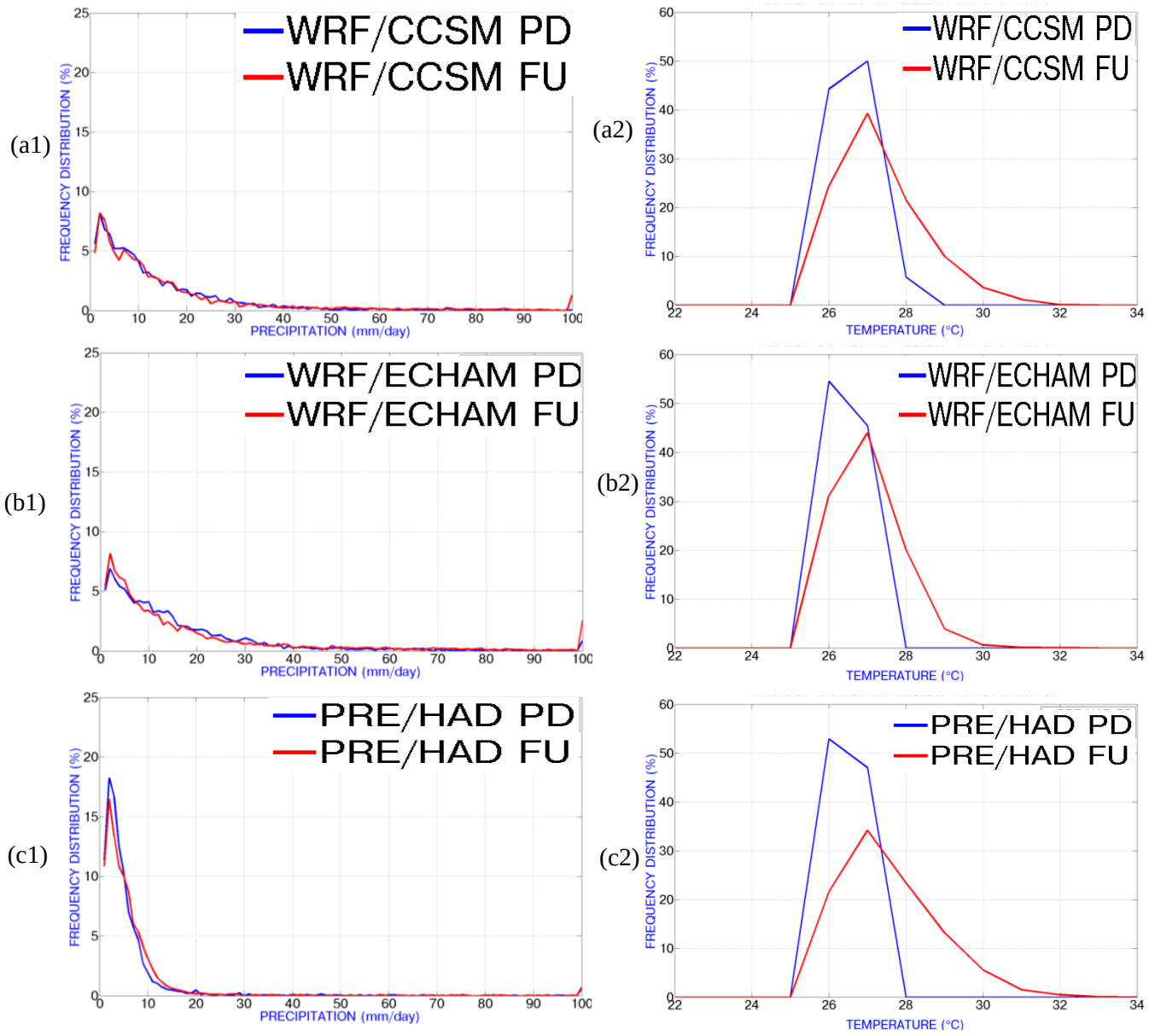

Figure E-22: Probability Distributions Frequency of Kon Tum 2071-2100
(1)Precipitation (mm/day) (2) Surface Temperature (^{o}C)
(a) WRF/CCSM (b) WRF/ECHAM (c) PRE/HAD

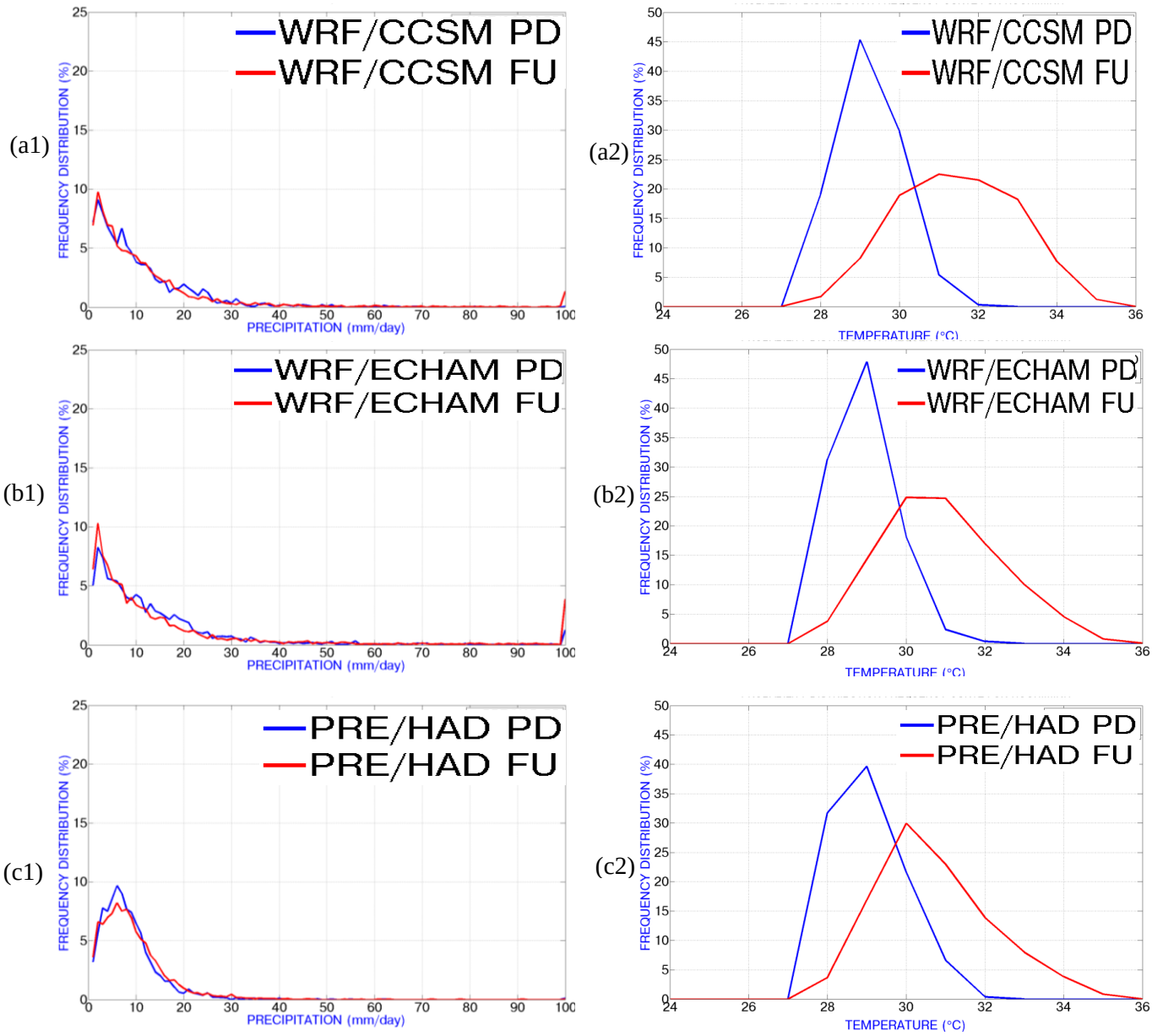

Figure E-23: Probability Distributions Frequency of Ho Chi Minh City 2071-2100
(1)Precipitation (mm/day) (2) Surface Temperature (^{o}C)
(a) WRF/CCSM (b) WRF/ECHAM (c) PRE/HAD

(a)

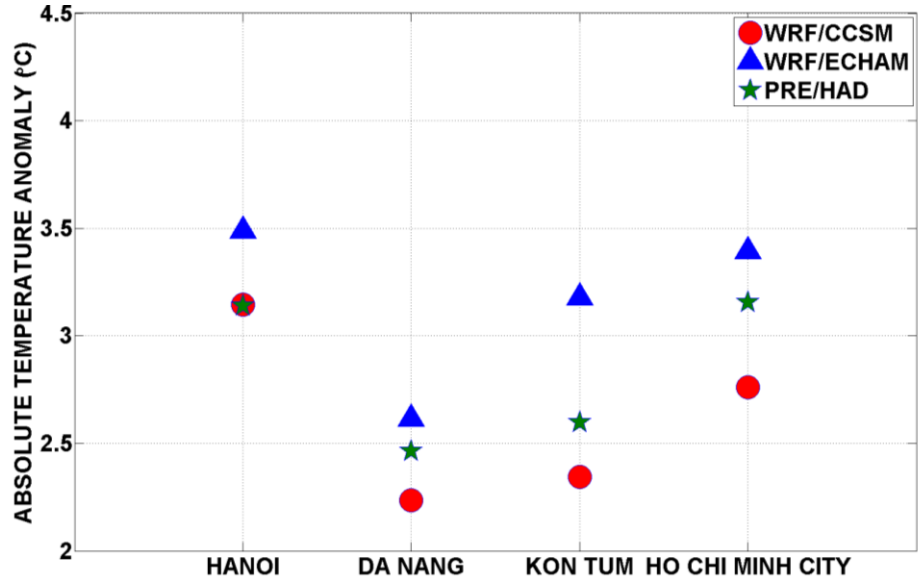

(b)

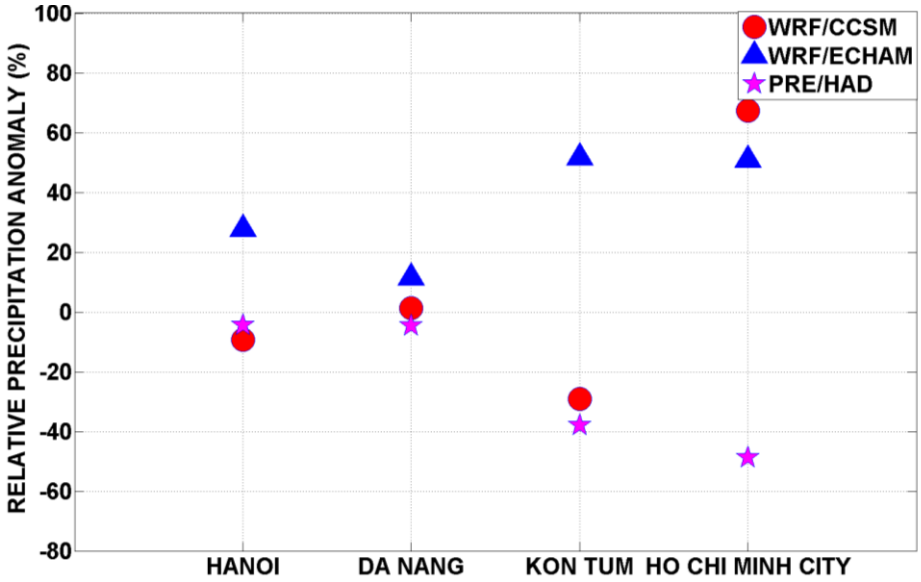

Figure E-24: Bandwidth of Response: 2071-2100 relative to 1961-1990
(a) DJF Surface Temperature (b) DJF Precipitation

(a)

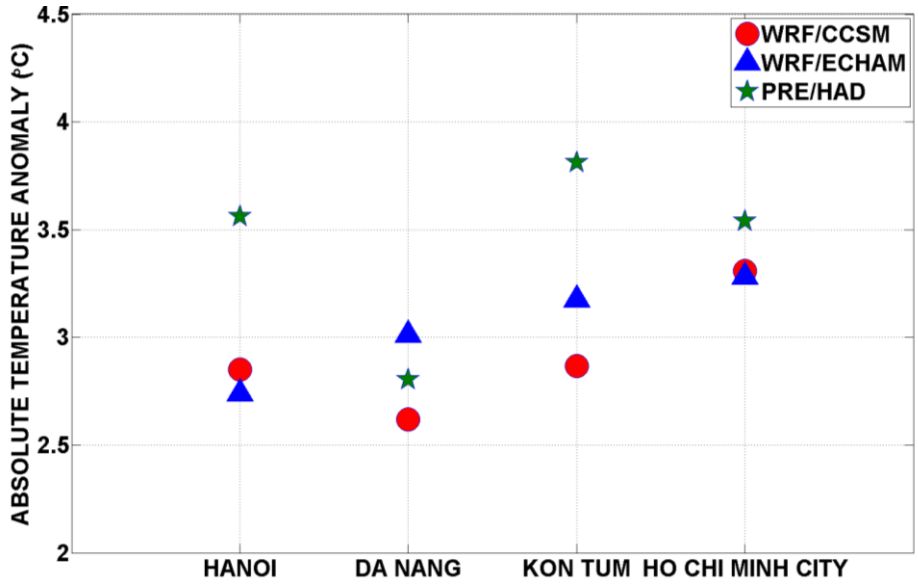

(b)

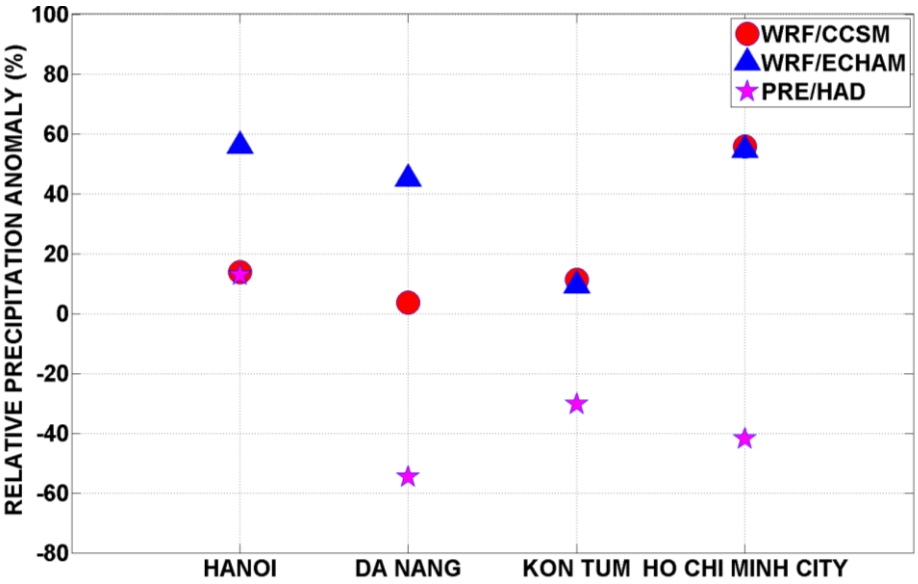

Figure E-25: Bandwidth of Response: 2071-2100 relative to 1961-1990
(a) MAM Surface Temperature (b) MAM Precipitation

(a)

(b)

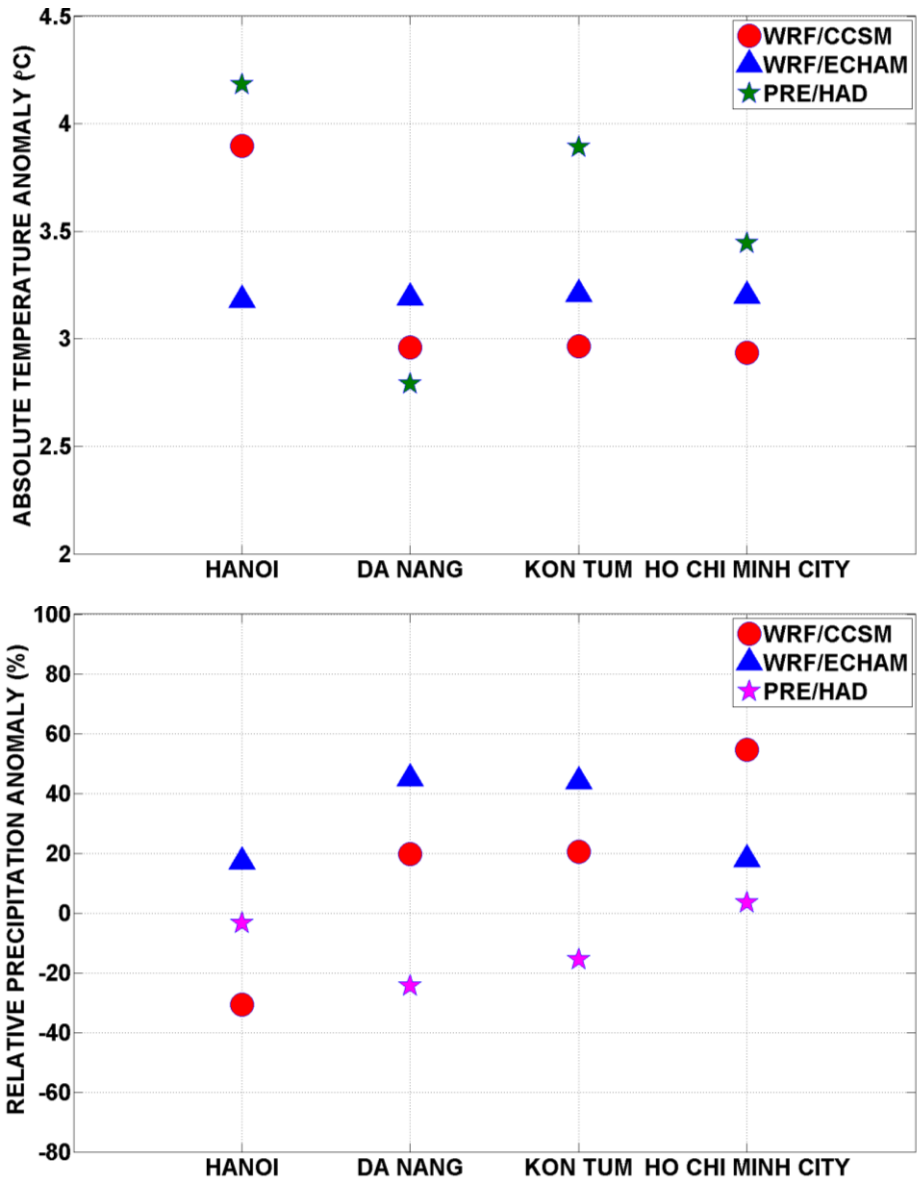

Figure E- 26: Bandwidth of Response: 2071-2100 relative to 1961-1990
(a) JJA Surface Temperature (b) JJA Precipitation

(a)

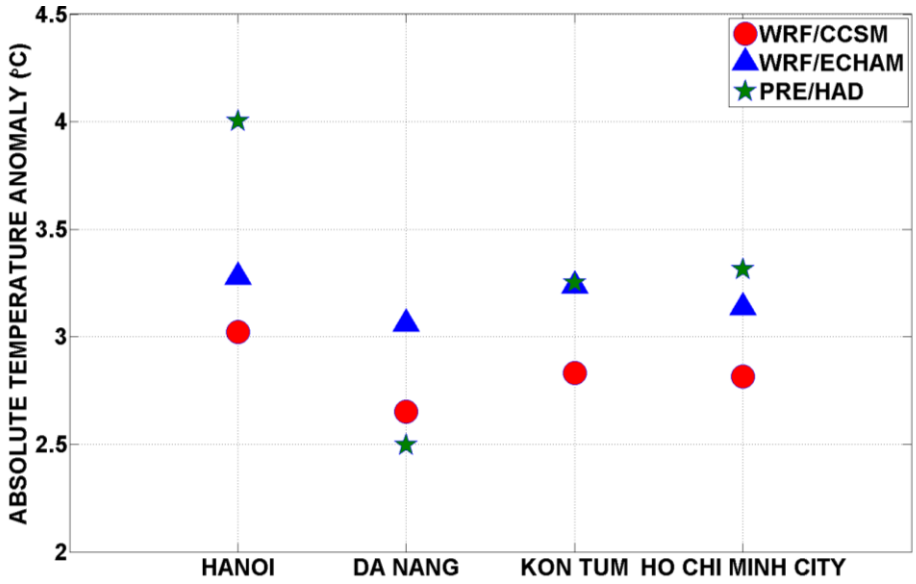

(b)

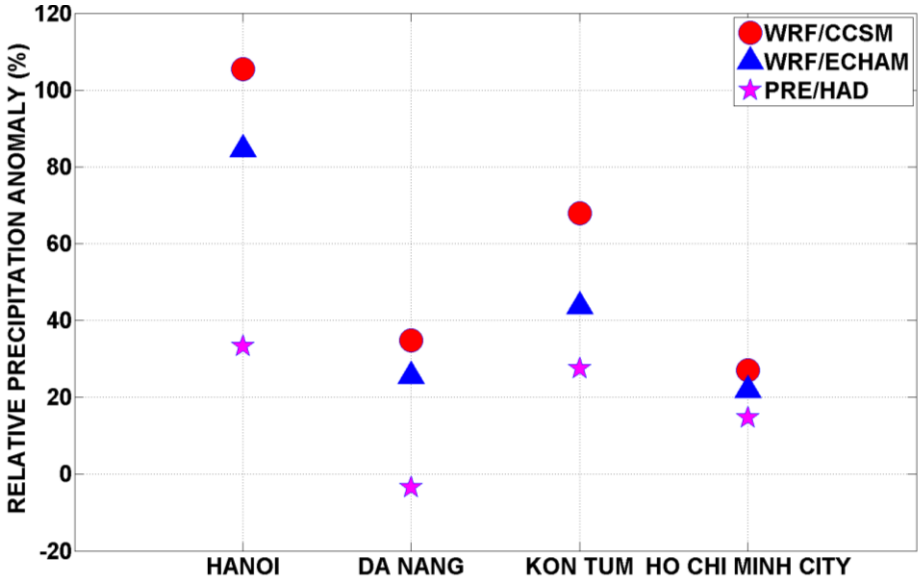

Figure E- 27: Bandwidth of Response: 2071-2100 relative to 1961-1990
(a) SON Surface Temperature (b) SON Precipitation

APPENDIX F SWAT MODEL, SENSITIVITY ANALYSIS AND AUTO-CALIBRATION PARASOL METHOD

F1. SWAT MODEL

Water balance

The water quantity processes simulated by SWAT consists of precipitation, evapotranspiration, surface runoff, lateral sub-surface flow, groundwater flow and river flow. The water balance equation is as following:

$$SW_t = SW_0 + \sum_{i=1}^{t}\left(R_{day} - Q_{surf} - E_a - w_{seep} - Q_{gw}\right)$$

t: time in day

SW_t: the final soil water content (mm)

SW_0: initial soil water content (mm)

R_{day}: daily precipitation

Q_{surf}: runoff

E_a: evapotranspiration

w_{seep}: percolation

Q_{gw}: groundwater and return flow

The SWAT hydrologic cycle is shown in Figure F-1

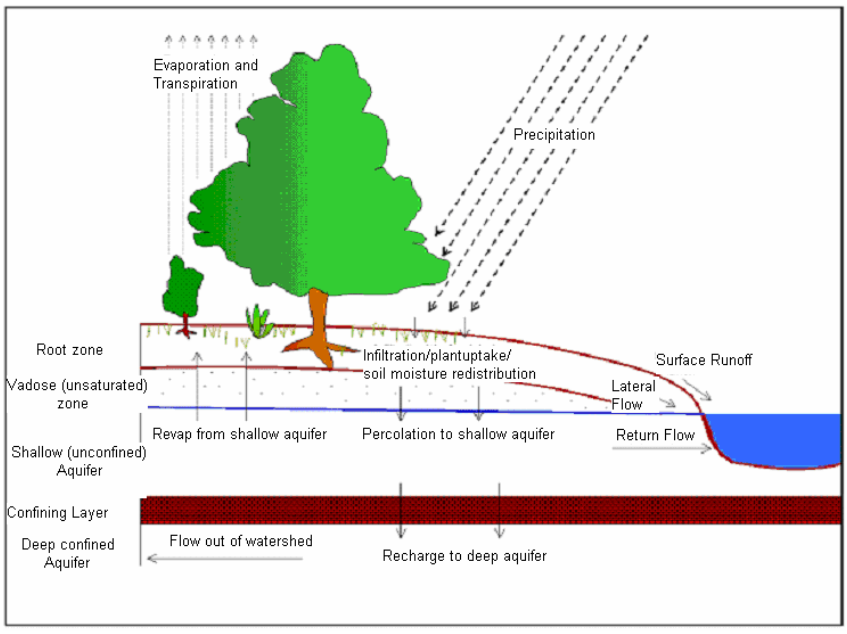

Figure F-1: Schematic representation of the hydrologic cycle in SWAT
[Adapted from Neitsch et al., 2004]

F2. THE LH-OAT SENSITIVITY ANALYSIS

The LH-OAT is the combination of One factor At a Time (OAT) design with Latin Hypercube (LH) sampling by taking the LH samples as initial points for an OAT design (Figure F-2)

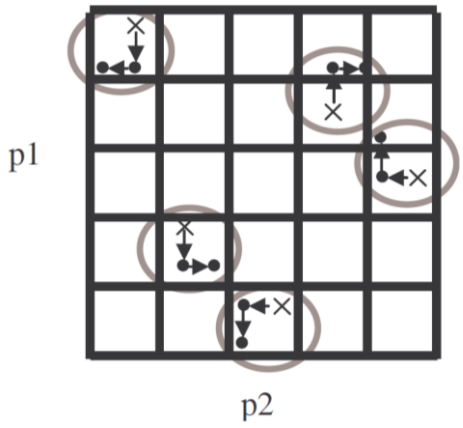

Figure F-2: Illustration of LH-OAT sampling of values for a two parameters model where × represent the Monte-Carlo points and • the OAT points
[Adapter from van Griensven et al., 2006].

Latin-Hypercube sampling (McKay, 1988) is a sophisticated way to perform random sampling such as Monte-Carlo sampling, resulting in a robust analysis requiring not too many runs (Saltelli et al. 2000). It subdivides the distribution of each parameter into m ranges, each with a probability of occurrence equal to 1/m. Random values of the parameters are generated, such that each range is sampled only once. For each of the m random combinations of the parameters an OAT loop is performed.

In the OAT design (Morris, 1991), only one input parameter is modified between two successive runs of the model. Therefore, the change in model output (e.g. SSE of the surface runoff) can then be unambiguously attributed to such a parameter modification by means of an elementary partial effect Si,j defined by equation:

$$S_{i,j} = \left[\frac{SSE(\Phi_1,...,\Phi_i * (1+f),...,\Phi_p) - SSE(\Phi_1,...,\Phi_i,...,\Phi_p)}{f} \right]$$

$S_{i,j}$: is a partial effect for parameter, Φ_i around an LH point j, *f* is the fraction by which the parameter Φ_i is changed (a predefined constant) and SSE is the Sum of Squared Errors. In

equation, the parameter is randomly increased or decreased with the fraction *f*. Considering *p* parameters, one loop involves performing *p*+1 model runs to obtain one partial effect for each parameter. As the influence of a parameter may depend on the values chosen for the remaining parameters, the experiment is repeated for all the *m* LH samples. The final effect will then be calculated as the average of a set of the *m* partial effects.

As a result, the LH-OAT sensitivity analysis method is a robust and efficient method: for *m* intervals in the LH-method, a total of $m\times(p+1)$ runs is required. The LH-OAT provides ranking of parameter sensitivity based on the final effects. Using the LH-OAT techniques in unison means that the sensitivity of model output to a given parameter is assessed across the entire feasible range for that parameter and across a number of different values for other parameters in the model, thus incorporating a limited amount of parameter interaction.

F3. AUTO-CALIBRATION BY PARASOL METHOD USING SCE-UA ALGORITHM

ArcSWAT model has the options to choose either manual or auto-calibration. Calibration is applied to those most sensitive parameters specified in Table 5-2 to yield the optimal set of values for the model parameters which results in the minimum discrepancy between the observed and the simulated river discharge data. While manual calibration can be used by trained, experienced users who are familiar with the model and the catchment under consideration, auto-calibration is recommended especially for the new user in the lengthy calibration processes.

Parameter Solution method (ParaSol) is a built-in auto-calibration model since the ArcSWAT 2005 version was implemented (van Griensven and Meixner, 2004). ParaSol operates by a parameter search method for model parameter optimization followed by a statistical method that is performed during the optimization to provide parameter uncertainty bounds and the corresponding uncertainty bounds on the model outputs. The ParaSol method aggregates objective functions (OFs) into a global optimization criterion (GOC), minimizes these OFs or a GOC using the Shuffled Complex Evolution Method (SCE) algorithm with a choice between 2

statistical concepts. The SCE-UA (Dual et al., 1992) method is based on a synthesis of all the best functions from many other existing methods consisting of the Genetic Algorithm (GA), simplex method (Nelder and Mead, 1965), controlled random search (Price, 1987), competitive evolution (Holland, 1975) and the newly developed concept of complex shuffling. SCE-UA conducts a global minimization of a single function for up to 16 parameters. This method is also capable for non-linear optimization problems.

In SCE-UA, the initial set of parameters (first step) is chosen randomly throughout the feasible parameters space for p parameters to be optimized. Then the set is partitioned to several "complexes" that have 2p+1 points in which each complex evolves independently using the simplex algorithm. The complexes are then shuffled to form new complexes in order to share information between the complexes. SCE-UA method can be illustrated in Figure F-3. SCE-UA has been used widely in watershed model calibration and other areas like soil erosion, subsurface hydrology, land surface modelling. There are 2 objective functions which can be used in the model calibration using SCE-UA. They are (1) the sum of the squares of the residuals (SSQ) and (2) the sum of the squares of the difference of the measured and simulated values after ranking (SQQR). In this study the SSQ objective function is used. The SSQ, used to target at matching the simulated with the observed data, is expressed as in equation:

$$SSQ = \sum_{i=1,n} \left[TF\left(x_{i,obs}\right) - TF\left(x_{i,sim}\right) \right]^2$$

where, n is the number of pairs of observed and simulated variable and 'TF' is a user defined transformation function. Detailed description of ParaSol method can be found in van Griensven and Meixner (2004).

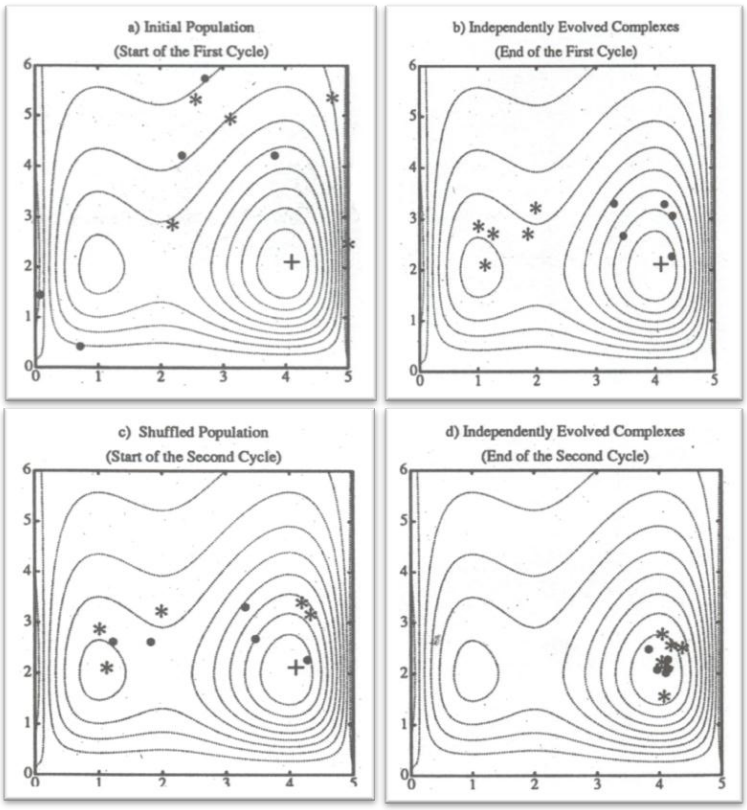

Figure F-3: Illustration of the SCE-UA method
[Adopted from Duan et al., 1994]

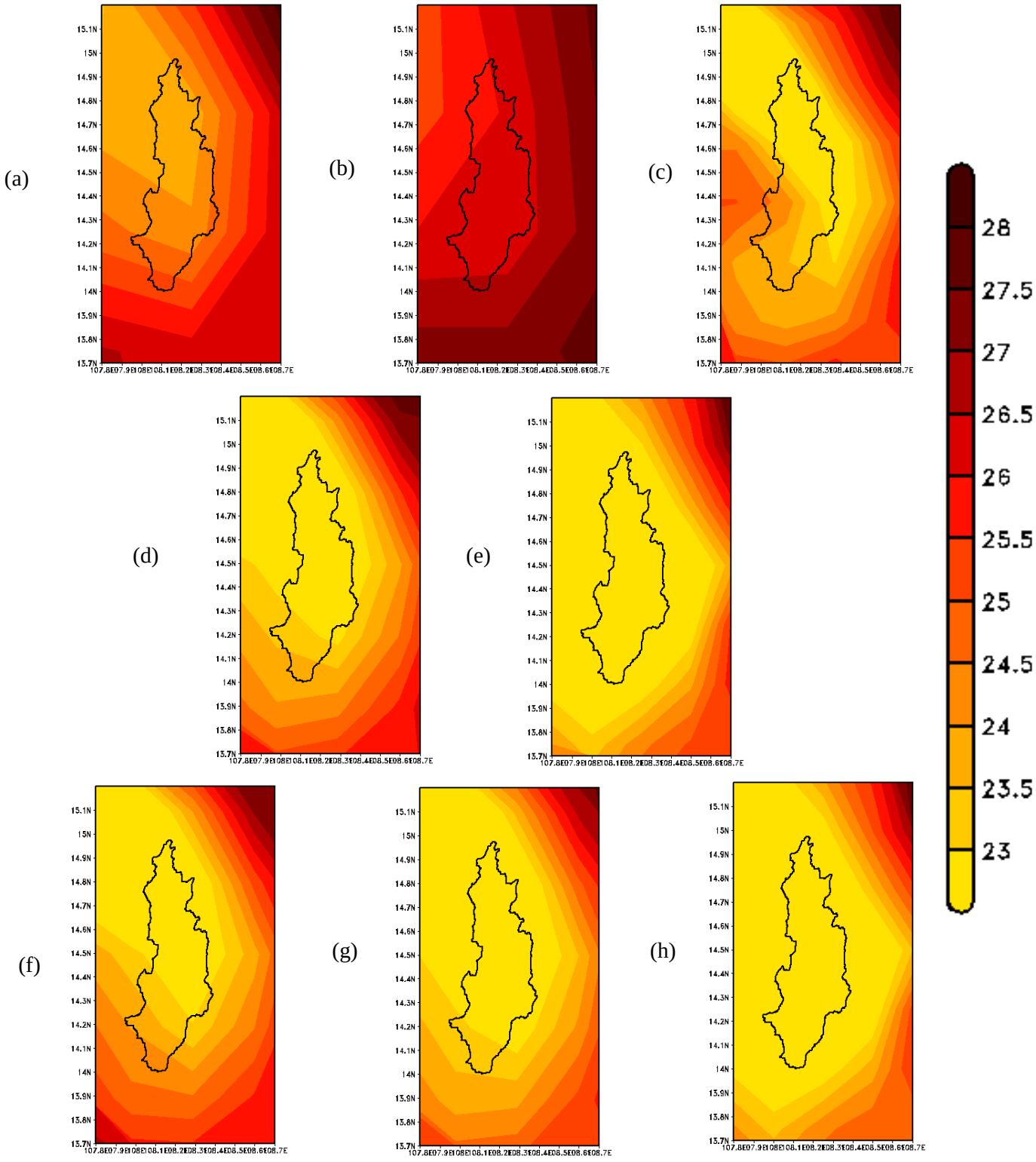

Figure F-4: Rainy season (MJJASO) Surface Temperature over Dakbla: 1981-1990, ^{o}C
(a) CRU (b) CPC (c) APH (d) WRF/ERA (e) PRE/ERA
(f) WRF/CCSM (g) WRF/ECHAM (h) PRE/HAD

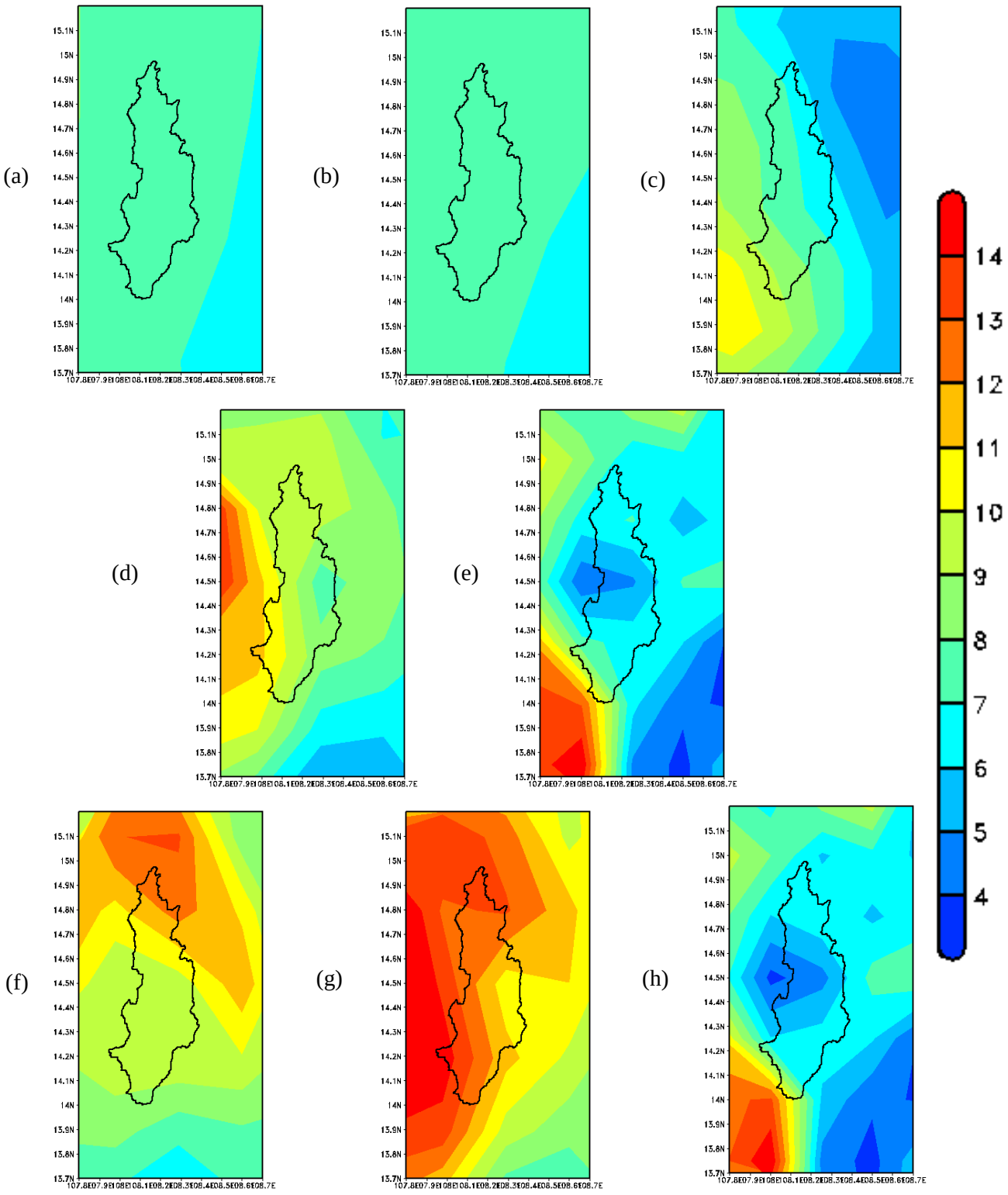

Figure F-5: Rainy season (MJJASO) Precipitation over Dakbla: 1981-1990, mm/day
(a) CRU (b) CPC (c) APH (d) WRF/ERA (e) PRE/ERA
(f) WRF/CCSM (g) WRF/ECHAM (h) PRE/HAD